Author:
Marcolino De Assis Junior, Eudmar

Title:
The regulation of PRH/HHEX by transforming growth factor

The regulation of PRH/*HHEX* by transforming growth factor β

By

Eudmar Marcolino de Assis Junior

A thesis submitted to the University of Bristol, School of Biochemistry, for the degree of Doctor of Philosophy

Word count: 56,442

ABSTRACT

The transcription factor PRH/*HHEX* (Proline-Rich Homeodomain/Haematopoietically Expressed Homeobox) controls cell proliferation, cell differentiation and cell migration/invasion in a diverse range of cell types. Here I show that the gene encoding PRH is deleted in around 4% of sequenced samples from patients with prostate cancer. Additionally, I show that there is increased CpG DNA methylation at this gene in prostate cancer samples compared to samples from normal prostate and that PRH mRNA levels are reduced in prostate cancer. Using immunohistochemistry to stain 96 samples of prostate neoplasia, I show that PRH expression is negatively correlated to tumour differentiation in prostate cancer.

Recent published work has shown that the down-regulation of PRH expression in breast and prostate cancer cells results in increased cell proliferation and increased cancer cell invasion. Moreover, PRH inhibits breast and prostate cancer cell migration and invasion in part at least by activating the transcription of Endoglin, a Transforming Growth Factor β (TGF-β) co-receptor. Here I show that the treatment of immortalised prostate epithelial (PNT2-C2) cells and prostate adenocarcinoma (PC3) cells with TGF-β increases cell migration and induces an epithelial to mesenchymal transition (EMT), with up-regulation of the EMT transcription factor Snail and down-regulation of the epithelial marker E-Cadherin. TGF-β treatment down-regulates the expression of PRH/*HHEX* in prostate cell lines at both the protein and mRNA level. Moreover, chromatin immunoprecipitation (ChIP) experiments show that the regulation of PRH/*HHEX* by TGF-β may be via the direct binding of the TGF-β effector pSmad3 at the PRH promoter. I also investigate the effects of PRH over-expression on PC3 cells. PRH expression in these cells re-activates the expression of E-cadherin, reduces the migratory ability of these cells and inhibits cell proliferation.

PRH over-expression also down-regulates the expression of multiple genes involved in the TGF-β signalling pathway including *TGFB2* and *TGFBR2*. ChIP shows that PRH binds to both the *TGFB2* and *TGFBR2* gene bodies, suggesting a direct effect of PRH on the expression of these genes. Prostate cancer cells are exposed to TGF-β from multiple sources in vivo and blood platelets were tested as a possible source of TGF-β using this model. Platelet treatment was able to increase cell migration, trigger EMT and down-regulate PRH expression in a similar way to TGF-β treatment. Platelets treatment resulted in the up-regulation of pSmad3 and the effect of platelets on cell migration were abolished when TGF-β signalling was blocked.

In summary, the work described in this Thesis shows that TGF-β increases prostate cell migration in part at least by the down-regulation of PRH expression. PRH up-regulates E-cadherin expression and down-regulates cell migration suggesting that TGF-β alters E-cadherin levels and increases cell migration via its effects on PRH. Since PRH also regulates several genes important in TGF-β signalling this creates a feedback loop that enables a more precise control of cell behaviour. Changes in PRH levels or activity are likely to disrupt this control mechanism and to contribute to tumour progression.

Acknowledgements

I would like to say thank you,

To mother, Sandra, for the unconditional love and support, without her I would not be here.

To my family, especially my father and my siblings, Emanuel and Cinthya for the love and patience, I would not have the strength to carry on without them.

To my supervisor, Prof. Kevin Gaston, for the guidance, patience, support and wisdom for these past four years. I learned so much from you I cannot thank you enough.

To Dr. Sheela Jayaraman and her group, especially Dr. Philip Kitchen, who welcomed me into their group to learn new techniques that were essential to my thesis.

To the D40 laboratory, you were an amazing support network, and were always there when I needed. I learned a lot from you.

To my friends, Gabriel, Grace, Caitriona, Emma, Fruzsina, Lucy, Gemma, Jack, Alex, Anisha, Adriene, Jenifer, Gabriella, Emmanuelle, David and Andrew. You were like my family away from home. You love me and helped me when thing got very difficult. I truly love you all. Specially to Andrew and Adriene that helped me edit this thesis, I do not think I could had done without your help.

To my friend in Brazil, Bruno, Gleyciane, Camila, Pedro, Debora, Evelin, Thayanne and my lovely god son Guilherme, who supported me coming to the UK, and who are there missing me and wishing great things for my future. I feel you close to my heart.

To my previous supervisor, Prof. Roberto Cesar, thanks for introducing me to science and being a mentor to me.

To the Conselho Nacional de Desenvolvimento Científico e Tecnológico (CNPq) through the Sciences Without Borders program, for the financial support for the project and for the scholarship.

This is dedicated to my mother,

whom is my everything.

"It is our choices that show what we truly are, far more than our abilities."

Albus Dumbledore

AUTHOR'S DECLARATION

I declare that the work in this dissertation was carried out in accordance with the requirements of the University's regulations and Code of Practice for Research Degree Programmes and that it has not been submitted for any other academic award. Except where indicated by specific reference in the text, the work is the candidate's own work. Work done in collaboration with, or with the assistance of, others, is indicated as such. Any views expressed in the dissertation are those of the author.

SIGNED:……DATE:……

Table of contents

List of figures

List of tables

Abbreviation List

Abbreviation	Name
3D	Three Dimension
ACS	American Cancer Society
ADT	Androgen Deprivation Therapy
AJ	Adherent Junction
ALK1	Activin Receptor-Like Kinase 1
ALK2	Activin Receptor-Like Kinase 2
ALK5	Activin Receptor-Like Kinase 5
α-SMA	Smooth Muscle Actin α
ANOVA	Analysis of Variance
APS	Ammonium Persulfate
AR	Androgen Receptor
BFU-MK	Burst-Forming Unit–Megakaryocyte
BMP	Bone Morphogenic Protein
BPH	Benign Prostate Hyperplasia
BSA	Bovine serum albumin
CAFs	Cancer Associated Fibroblasts
Calcein-AM	Calcein-acetoxymethyl
CDKs	Cyclin-dependent kinases
cDNA	Complementary deoxyribonucleic acid
CFU-GEMM	Colony Forming Unit - Granulocyte, Erythrocyte, Monocyte, Megakaryocyte
CFU-Meg	Colony Forming Unit – Megakaryocyte
CH18	Chromosome 18
ChIP	Chromatin immunoprecipitation
ChIP-qPCR	Chromatin Immunoprecipitation – quantitative Polymerase Chain Reaction
ChIPseq	Chromatin Immunoprecipitation – sequencing
CK2	Casein Kinase 2
CMV	Cytomegalovirus
CTLs	Cytotoxic T Cell

CycD	Cyclin D
DAPI	4′,6-diamidino-2-phenylindole
DMSO	Dimethyl Sulfoxide
DNA	Deoxyribonucleic Acid
Doxy	Doxycycline
DRE	Digital Rectal Examination
ECM	Extracellular matrix
EDTA	Ethylenediaminetetraacetic acid
EdU	5-Ethynyl-2'-deoxyuridine
EGF	Epidermal growth factor
EGTA	Ethylene glycol-bis(β-aminoethyl ether)-N,N,N′,N′-tetraacetic acid
EMT	Epithelial to Mesenchymal Transition
EMT-TFs	Epithelial to Mesenchymal Transition – Transcription factors
ESM-1	Endothelial Cell-Specific Molecule
FBS	Foetal Bovine Serum
FDR	False discovery rate
FGF	Fibroblast growth factor
G1	Gap 1 phase
GAPDH	Glyceraldehyde 3-phosphate dehydrogenase
GFP	Green fluorescent protein
GLOBOCAN	Global Cancer Observatory
GS	Gleason Score
HCC	Hepatocellular Carcinomas
HD	Homeodomain
HDAC	recruitment of histone deacetylase complexes
HEPES	4-(2-hydroxyethyl)-1-piperazineethanesulfonic acid
HHEX	Haematopoietically Expressed Homeobox
HNF3β	Hepatocyte Nuclear Factor 3 β
HPP-CFU-MK	High Proliferative Potential–Colony-Forming Unit–Megakaryocyte
IgG	Immunoglobulin G

IL	Interleukin
INCA	Instituto Nacional de Cancer (*National Institute of Cancer*)
I-Smad	Inhibitor Smad
ISUP	International Society of Urological Pathology
KD	Knockdown
KO	Knockout
LB	Lysogeny Broth
LV	Lentivirus
MET	Mesenchymal to Epithelial Transition
mRNA	Messenger Ribonucleic Acid
MTT	3-(4,5-dimethylthiazol-2-yl)-2,5-diphenyltetrazolium bromide
NADPH	Nicotinamide adenine dinucleotide phosphate
NK	Natural Killer
Notch	Neurogenic locus notch homolog protein
NSCLC	Non-Small-Cell Lung Cancer
NTCP	Sodium-Dependent Bile Acid Co-Transporter
OE	Overexpression
PBS	Phosphate buffered saline
PDGF	Platelet-Derived Growth Factor
PDH	Pyruvate Dehydrogenase
PEI	Polyethylenimine
PMSF	Phenylmethanesulfonyl fluoride
pPRH	Phosphorylated Proline Rich homeodomain
PRH	Proline Rich homeodomain
PSA	Prostate-Specific Antigen
PVDF	Polyvinylidene Fluoride or Polyvinylidene Difluoride
qPCR	quantitative Polymerase Chain Reaction
RB	Retinoblastoma-Associated
RNAseq	Ribonucleic acid sequencing
RPM	Revolutions Per Minute
RPMI	Roswell Park Memorial Institute
R-Smad	Receptor Smad

qRT-PCR	quantitative Reverse Transcriptase-Polymerase Chain Reaction
SDS	Sodium dodecyl sulphate
SDS-PAGE	Sodium dodecyl sulphate-polyacrylamide gel electrophoresis
SEM	Standard Error of The Mean
TBB	2-ethylhexyl 2,3,4,5-tetrabromobenzoate
TBS-T	Tris-buffered saline
TE	Tris-EDTA
TEMED	Tetramethylethylenediamine
TERT	Telomerase Reverse Transcriptase
TFs	Transcription Factors
TGFB	Transforming growth factor beta
TGF-β	Transforming Growth Factor β
TJ	Tight junction
Tris-Gly	Tris Glycine Buffer
TSG	Tumour Suppressor Gene
TβRI	Transforming Growth Factor β Receptor 1
TβRII	Transforming Growth Factor β Receptor 2
UV	Ultraviolet
VEGF	Vascular Endothelial Growth Factor
VEGFA	Vascular Endothelial Growth Factor A
WHO	World Health Organization
ZO-1	Zonula Occludens-1

Chapter 1: Introduction

Cancer

The World Health Organization defines cancer as a generic term for a large group of diseases that can affect any part of the body. One of its features is the fast and uncontrolled proliferation of abnormal cells, which can then invade adjoining parts of the body and spread to other organs. This particular ability is the major cause of death by cancer, and it is called metastasis (WHO 2014).

The development of novel technologies has allowed studies which utilize molecular biology to investigate the several kinds of cancer, aiming to understand its biology. These studies have helped to modernize cancer treatment enabling health professionals to customize treatment to individual patients. However, this disease is far from being defeated and research to understand cancer at a molecular level is the lead driving force in the development of effective therapies.

According to the World Health Organization, cancer is the leading cause of death worldwide: 14 million cases and 8.2 million cancer deaths occurred in 2012 (WHO 2014), causing an economic loss of $216.6 billion dollars in 2009 (ACS 2014). Prostate cancer is the fourth most common cancer in humans, and the second most common cancer in men. With an estimated 1 276 106 (7.1% of total cancer cases in both sexes) new cases and 358 989 (3.8% of total cancer deaths in both sexes) deaths in 2018, prostate cancer is the fifth leading cause of death from cancer in men (7.6% of the total men deaths) (Globocan 2018). An estimated 1.1 million men worldwide were diagnosed with prostate cancer in 2012, accounting for 15% of the cancers diagnosed in men, with almost 70% of the cases (759,000) occurring in more developed regions (Globocan 2018). In Brazil alone, in 2018 there were 68.220 new prostate cancer cases with approximately 2800 deaths per year. That means that in every 100 000 men we expect about 70 new cases (INCA 2018). These statistics show that a greater Ratio of diagnosis/death in Brazil when compared to the global statistics. This discrepancy could be a reflection of a lower life expectancy observed in Brazil when compared to other countries like the United Kingdom.

Hallmarks of cancer

Uncontrolled tumour growth is only one of the characteristics of cancer. The hallmarks of cancer: The next generation (Hanahan & Weinberg 2011) listed the main ten capabilities of all cancers that make them such a dangerous set of diseases. These are: sustaining proliferative signalling, evading growth suppressors, avoiding immune destruction, enabling replicative immortality, promoting inflammation, activating invasion and metastasis, inducing angiogenesis, inducing genome instability mutations, resisting cell death and dysregulating cell energetics (figure 1.1).

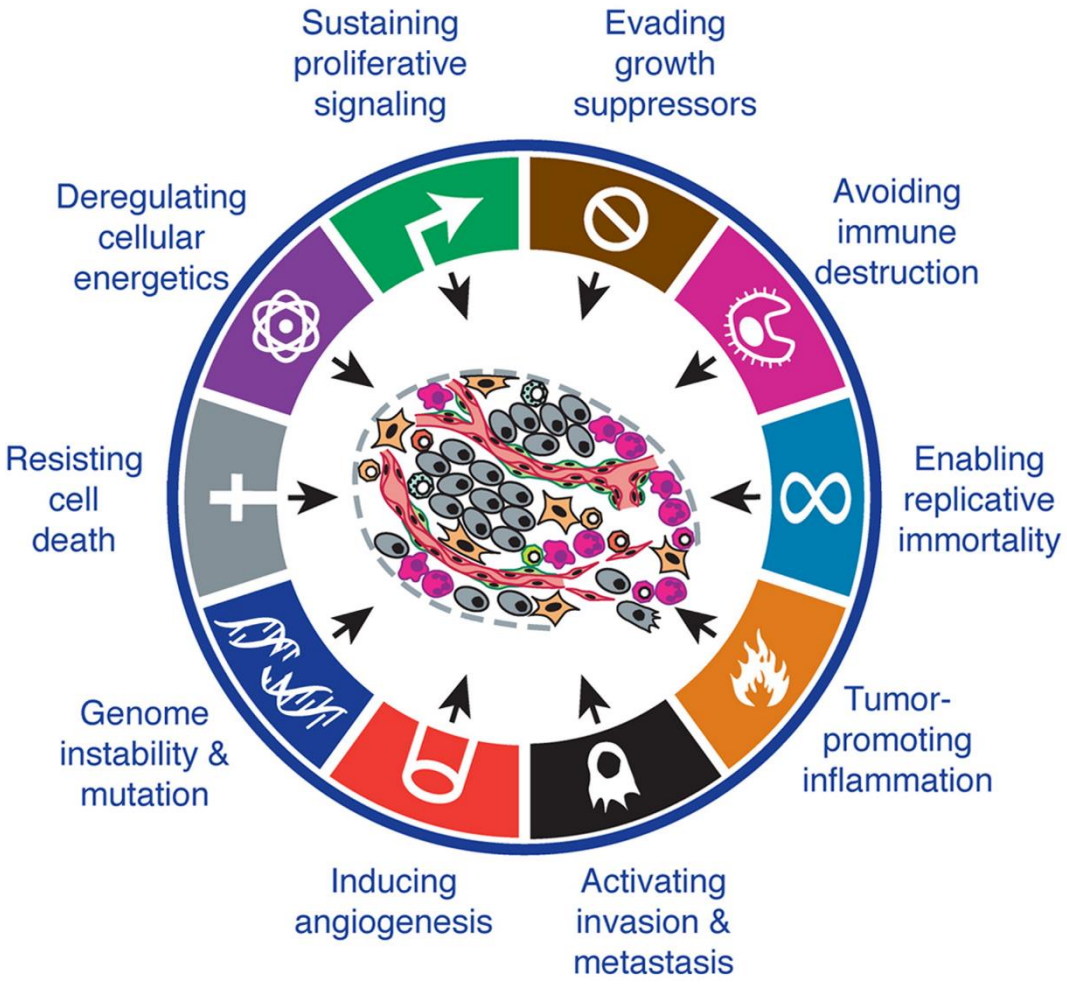

Figure 1.1. Hallmarks of cancer. source: (Hanahan & Weinberg 2011)

Unlike normal cells, cancer cells sustain a continuous proliferating stimulus. This cellular signalling can come from different sources: they can produce their own growth factors in an autocrine stimulation (Witsch et al. 2010); they can educate the stroma (surrounding non-cancerous cells and proteins associated with the tumour) to produce growth factors that activate growth stimuli in cancer cells (Bhowmick et al. 2004); they can become hypersensitive to growth factors by augmenting the number of receptors in their cell surface (Korc et al. 1992; Rusch et al. 1997); they can constitutively activate the subcellular signals triggered when growth factors bind to their receptors (Huang et al. 2009); and finally they can disrupt negative feed-back mechanisms placed to control such growth signals (Amit et al. 2007; Jiang & Liu 2009; Yuan & Cantley 2008). Cancer cells can benefit from one or more of these mechanisms, however, excessive growth factor stimulation can trigger intrinsic cellular defence mechanisms that lead to senescence and cell death (Hanahan & Weinberg 2011). For that reason, to survive and continue unrestricted proliferation cancer cells must develop mechanisms to resist cell death.

There are several mechanisms through which cancer cells avoid senescence (a state in which cells cease to divide and become enlarged) and crisis-induced cell death. The most common adaptation is the deactivation of growth suppressor proteins like retinoblastoma-associated (RB) protein and the TP53 protein (Hanahan & Weinberg 2011). These two systems are activated by different stimuli, RB is regulated mainly by external signalling, (as reviewed by Zheng & Lee 2001) and is mainly activated by anti-proliferative signals such as TGF-β signalling. TGF-β prevents the phosphorylation of RB (Massagué & Polyak 1995), and hypo-phosphorylated RB sequesters members of the E2F family of transcription factors inhibiting E2F function and arresting the cell cycle in G1 phase. RB can also repress transcription by recruitment of histone deacetylase (HDAC) complexes, (as reviewed by Burkhart & Sage 2008); the deacetylation of histones by HDAC leads to chromatin remodelling and transcription repression. *RB* is the prototype tumour suppressor gene (TSG) as it was the first to be discovered. Another important TSG is *TP53*. *TP53* acts as a sensor in the cell responding mainly to crises situations, for example DNA damage or DNA replication error. The protein encoded by the gene *TP53*, P53, can recruit DNA repair proteins in the case of DNA damage, but its cell cycle arrest function is mediated by the transcription activation of several genes, for

example the gene encoding p21, a protein that binds to cyclin-dependent kinases (CDKs) that are important to the transition from the G1 phase to S phase (He et al. 2005). In cases where the DNA damage is irreversible or extensive, P53 can activate apoptosis (a form of programmed cell death). The mechanisms underlying this activation are not fully understood, but the apoptosis repressor with caspase recruitment domain (ARC) is involved, as P53 can repress the transcription of ARC and thereby abrogate its anti-apoptotic activity (Li et al. 2008). Besides being activated by different signalling systems, both, P53 and RB, can regulate cell proliferation.

Another important factor in the inhibition of cell proliferation is the effect of cellular contacts. The loss of contact inhibition present in normal cells by cancer cells allows them to continuously proliferate to the point of forming macroscopic nodes (Hanahan & Weinberg 2011). Uncontrolled proliferation, metabolic changes, constant DNA damage and mutations creates a chaotic environment in the cancer cell that can potentially trigger intrinsic defence mechanisms that lead to cell death. TGF-β is an important tumour suppressor molecule, however, tumours can evolve in a fashion to corrupt the TGF-β signal in such a way that it starts to stimulate cancer cell proliferation and genome instability through a process known as epithelial to mesenchymal transition (EMT) (Massagué 2008b). The role of TGF-β in cancer progression and the process of EMT are further discussed in the following sections.

To survive, cancer must avoid triggering apoptosis and autophagy (a cellular process used to disassemble cellular organelles that are dysfunctional or during cell starvation) (Hanahan & Weinberg 2011). The most common dysregulation that cancer cells adopt to avoid such mechanisms is the loss of TP53 function. As explained above, TP53 is an important DNA damage sensor that is central in activating the apoptotic circuit in cells (Hanahan & Weinberg 2011).Autophagy signalling has been shown to have contradictory implications when it comes to cancer (White & DiPaola 2009). When one of the Beclin-1 alleles (encoding an autophagy activator) is deleted in mice, they are more susceptible to cancer (Qu et al. 2003). However, it has been demonstrated that some cancer cells activate autophagy to shrink and reach a state of reversible dormancy (a state where cell growth is stopped) during stress and this process can protect the cancer cell from death, inflammation, and immunosurveillance (Degenhardt et al. 2006).

This contradictory effect of an apparently anti-cancer cellular system is also observed in the event of cellular necrosis. The main difference between necrosis and apoptosis is that necrotic cells burst and release cellular components, which does not happen in apoptotic events (Hanahan & Weinberg 2011; Vakkila & Lotze 2004). The release of cellular contents triggers a systemic inflammatory response. Inflammatory cells make their way to the tumour site where they can release factors intended to destroy cancer cells, however, inflammation can also promote cancer progression (O'Byrne & Dalgleish 2001; Ammirante et al. 2010). Therefore, tumours can benefit from a moderate degree of necrosis that attracts tumour promoting inflammatory cells that trigger vasculature genesis and promote genomic evolution (Hanahan & Weinberg 2011).

As aforementioned, the excess growth factor stimulatory signals, often experienced by cancer cells, can lead to a senescent or apoptotic state (that acts as to block proliferation in response to stress). In general terms, cells possess a limited number of times that they can undergo cell division (Hanahan & Weinberg 2011; Shay & Wright 2000). This limitation is associated with the presence of multiple tandem hexanucleotide repeats known as telomeres at the end of the chromosomes (Blasco 2005). Telomeres protect chromosomes against end-to-end fusions helping to maintain chromosomal integrity and avoiding the triggering of cellular crisis signalling (Blasco 2005; Hanahan & Weinberg 2011). However, in each cell division cycle the telomeres get shortened. The expression of a specialised polymerase complex called telomerase is associated an immortalised phenotype and cancer progression (Hanahan & Weinberg 2011). Telomerase also presents some telomere-independent effects, for example, the telomerase subunit telomerase reverse transcriptase (TERT) can modulate the expression of the Wnt/β-catenin pathway. Additionally, TERT is commonly mutated in several human cancers (Vinagre et al. 2013). TERT is the gene that codifies the catalytic subunit of telomerase. Two mutations in a non-coding region of TERT promoter were discovered to be present in 71% of melanoma cancers and, the mutations were usually heterozygous (Horn et al 2013; Huang et al 2013). They created a new binding site for transcription factors like the ones in the ETS family. The mutations were further identified in high frequency in several other types of cancer (reviewed by Bell et al 2016). A study in bladder cancer

demonstrated that promoter mutations were associated with increased telomerase activity and stable telomere length (Borah et al 2015).

However, the role of telomeres and telomerases seems to be much more complicated than that. Cells that reached a senescent state can be revitalised by the epigenetic changes that induce telomerase expression in the senescence cell (Hanahan & Weinberg 2011; Chin et al. 2004). Furthermore, cancer cells can benefit from the mutations induced by chromosomal aberrations acquired during the senescence state before cell reactivation by telomerase expression (Karlseder et al. 1999; Chin et al. 1999). This creates aggressive metastatic cancers with aberrant number and arrangement of chromosomes.

Another essential event in cancer survival is the acquisition of nutrition for the tumour (Hanahan & Weinberg 2011). This happens by the advancement of tumour vascularisation. In normal tissues vascularisation is regulated by a balance of pro- and anti-angiogenic stimuli. The vascularisation switch that is activated during body growth is only reactivated transiently in the adult during specific events like wound healing (Roberts et al. 1986) and the oestrous cycle/pregnancy (Hobson & Denekamp 1984). However, in advanced tumours the vascularisation switch seems to be always turned on (Hanahan & Folkman 1996). In contrast, there are reports of cancers that present vast avascular stroma regions in earlier stages, followed by a variable intensity of ongoing neovascular formation (Olive et al. 2009; Hanahan & Weinberg 2011). This avascular state can have an impact on the metabolic changes that cancer cells undergo (discussed further below) and can induce, latter on, vascularisation. Hypoxic states can induce the expression of *VEGFA* (Vascular endothelial growth factor A) in tissues, therefore, the transient avascular environment can lead VEFG induced vasculature sprouting in cancer (Shweiki et al. 1992) bringing access to nutrition, evacuation and immune cells. VEGF signal transduction is a complex network of ligands, receptors and signal transductors that orchestrate not only angiogenesis but is also involved in proliferation, migration and cell survival. (reviewed by Koch and Claesson-Welsh 2012). Cancer cells can also can go through genomic evolution to overexpress the *VEGFA* gene and other genes that induce vascularisation (Hervé et al. 2008). VEGF has been used as a target to treat colorectal carcinoma, Figure 1.2 shows a diagram of VEGF signalling and its common therapeutic targets in cancer treatment. (reviewed by Lopez et al. 2019).

The inflammatory component of the cancer can be exacerbated by neovascular formation and vice versa. The neovascularization in tumours is often marked by precocious capillary growth, excessive branching and distorted vessels resulting in microhaemorrhage and inflammation. On the other hand, peritumoral inflammatory cells can trigger an angiogenesis switch and facilitate local invasion (Hanahan & Weinberg 2011)

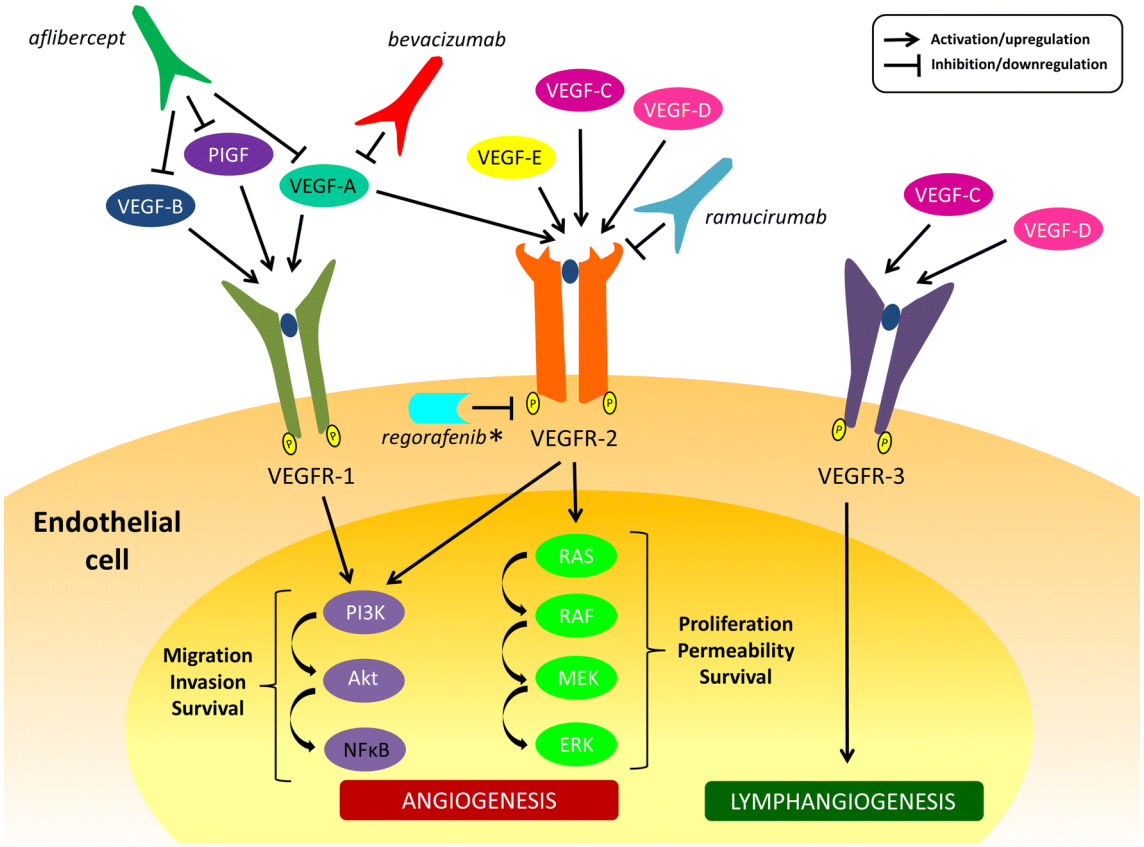

Figure 1.2. Vascular endothelial growth factor (VEGF) pathway and targeted therapies. *PIGF* placental growth factor, *VEGFR* vascular endothelial growth factor receptor, *PI3K*phosphoinositide 3-kinase, *Akt* protein kinase B, *NFκB* nuclear factor kappa-light-chain-enhancer of activated B cells, *RAS* rat sarcoma, *RAF* rapidly accelerated fibrosarcoma, *MEK* mitogen-activated protein kinase, *ERK* extracellular signal-regulated kinases. *Regorafenib also inhibits multiple targets in addition to VEGFR-2, not shown in this figure: PDGFR, FGF, KIT, RET, RAF1, B-RAF, and B-RAF-V600E (Lopez et al. 2019).

The next step in cancer progression involves the activation of an invasion and metastasis programme. The most often observed alteration in these processes is the loss of E-cadherin and proteins associated with adhesion in epithelial cells in general (Hanahan & Weinberg 2011; Hoover et al. 1998; van Roy 2014). E-cadherin loss is associated with malignant behaviour (Birchmeier & Behrens 1994). Conversely, adhesion proteins associated with cell migration and transfer of cells through the endothelial barriers (diapedesis) are constantly up-regulated (Wheelock et al. 2008). Although, the invasion/metastasis process is complex, it involves a series of discrete

events described as follows: local invasion of the surrounding tissue, intravasation of the cancer cells into local vessels, transportation of the cancer cell via lymphatic or hematologic streams, diapedesis of the cancer cell to a different tissue, the formation of micronodules and finally growth into macroscopic lesions (Hanahan & Weinberg 2011).

The regulatory programme referred as epithelial to mesenchymal transition (EMT) is intimately associated with the invasion and metastasis process (Krebs et al. 2017; Takeyama, Sato, Horio, Hase, Yoshida, Yokoyama, Nakashima, Hashimoto, Sekido, Adi F. Gazdar, et al. 2010; Brabletz et al. 2018; Heldin et al. 2012a; Shibue & Weinberg 2017). The activation of EMT can lead to increased ability to invade, to resist apoptosis and metastasise (Hanahan & Weinberg 2011). Interestingly, the EMT program is often only partially and/or transiently activated by cancer cells during the course of metastasis (Brabletz et al. 2018). This feature is thought to maintain phenotypic plasticity and adaptability, often helping the metastatic cells to adapt to the new environments where they have taken residence (Brabletz et al. 2018).

Besides the loss of E-cadherin the EMT program confers a series of other characteristics to the cancer cells, including: conversion from polygonal epithelial cells to spindle-shaped fibroblastic morphology, higher expression of matrix degrading enzymes, increased motility and increased resistance to apoptotic signals (Hanahan & Weinberg 2011). The conversation between cancer cells and elements of the tumour microenvironment such as inflammatory cells and blood platelets, among others, can play an important role in the activation of this programme, by supplying matrix degrading enzymes and molecules such as growth factors (Karnoub & Weinberg 2007; Brabletz et al. 2001; Labelle et al. 2011).

It is well known that tumours present heterogeneity at a molecular and cellular level (Roerink et al. 2018). The main components of the tumour microenvironment are fibroblasts, neuroendocrine cells, adipose cells, immunological and inflammatory cells, vasculature networks and the extracellular matrix (ECM). Cancer-associated fibroblasts (CAFs) are activated by several factors that can be released in response to injury such as TGF-β, epidermal growth factor (EGF), platelet-derived growth factor (PDGF) and fibroblast growth factor 2 (FGF2), reviewed by (Kalluri & Zeisberg

2006). The activated fibroblasts secrete an increased level of smooth muscle α-actin (α-SMA) and metalloproteases that degrade the ECM inducing alterations in the composition of the ECM. CAFs also secrete a range of growth factors that induce proliferative signals in epithelial cells (Bhowmick et al. 2004) and factors that attracts and modulate inflammation, induce angiogenesis and promote an invasive phenotype (as reviewed by Kalluri & Zeisberg 2006).

In prostate cancer CAFs seem to play an important role, It was demonstrated that the non-tumorigenic prostate cell line BPH-1, when recombined with CAFs, went through transformation and became tumorigenic. New cell lines established from the tumours formed by CAFs activated BHP-1 inherited the tumorigenic ability (Hayward et al. 2001). Furthermore, heterogenetic mix of CAFs can influence the tumorigenic conditioning of the epithelial cells by CAFs. The heterogenic expression of the TGF-β receptor 2 (TGFβRII) in CAFs cell populations induced dysregulation on the expression of several factors including TGF-β1, and these changes induced epithelial proliferations and tumorigenesis (Franco et al. 2011).

Inflammatory and immunological cells in the tumour microenvironment, provide immune surveillance and attempt to remove emerging tumour cells (Hanahan & Weinberg 2011). However, the role played by the immune system is complex. Communication between cancer cells and immune system can be divided into three phases: elimination, equilibrium and escape (Dunn et al. 2004). In the elimination phase, inflammatory and immunological responses can eliminate the nascent cancer cells. In the equilibrium phase, the immune cells can no longer completely clear the cancer cells, instead they contain cancer growth, the surviving cells are then selected and a number of them can develop immune evading characteristics through mutations or through disrupted EMT signals. Such cells will eventually enter the escape phase where the cancer cells can modulate the immuno-response and form solid tumours (Dunn et al. 2004). A component of the inflammatory system that is often overlooked are blood platelets. Platelets have been frequently implicated in cancer progression by supply of growth factors, cytokines and helping with immune evasion (Labelle et al. 2011; Carr et al. 2014; Im et al. 2004), this topic is further discussed in later sections.

Several other cell populations are reported to contribute to the creation of the tumour microenvironment and to aid cancer progression, among them are the blood and lymphatic vasculatures, which are important to tumour nutrition, secretion of metabolic waste and evasion of immune surveillance. Adipocytes can be a major source of energy to a tumour, plus they interact with the immune system recruiting immune cells and promote vasculogenesis (as reviewed by Wang et al. 2017).

Many of the hallmarks acquired by cancer cells depend largely on genome alterations. These alterations arise from mutations or failure to repair DNA damage. However, intrinsic defence mechanisms of DNA surveillance can trigger apoptotic signals when mutations are detected. Cancer cells can benefit from genome instability and mutations if these signals are lost (Hanahan & Weinberg 2011). One of the main events seen in several cancers is deactivation of the TP53 DNA surveillance. TP53 is often referred to as the genome guardian. TP53 can detect DNA damage and arrest cell growth, and if the damage is irreversible, it can trigger apoptosis by repression of the anti-apoptotic protein ARC, as explained above (Hanahan & Weinberg 2011). P53 also has a role in the response to short telomeres; reduced numbers of telomere repeats triggers cellular growth arrest by destabilisation of P53 (Milyavsky et al. 2001). Deactivations of other proteins involved in DNA damage detection and repair can also enable genome instability in cancer cells (Hanahan & Weinberg 2011).

As discussed, one of the main traits of cancer is the ability to continuously grow powered by growth signalling, avoidance of anti-proliferative signals and evasion of the intrinsic defence mechanism that can trigger cell death. However, the uncontrolled proliferation observed in cancer cells also involves adjustments of energy metabolism (Hanahan & Weinberg 2011). First observed in 1930, cancer cells fuel their cell divisions mostly by glycolysis, even in the presence of oxygen. Respiration still occurs in cancer cells, however, the respiration is not sufficient for these cells; measurements show that the glycolysis and glycolytic routes produce similar amounts of energy in cancer cells (Warburg 1956a; Warburg 1956b). This process is known as aerobic glycolysis and is thought to be used by the cancer cells because this metabolic route avoids the engagement of the metabolic products into ‘low flux’ (slower metabolic processes like mitochondrial pyruvate importation) biosynthetic pathways naturally undertaken in the glycolytic route (DeBerardinis et al.

2008). The glycolytic route requires importation of pyruvate to the mitochondrial matrix and the next steps of the processing are carried by highly regulated enzymes, like pyruvate dehydrogenase (PDH), which overall may reduce the reaction speed (DeBerardinis et al. 2008). Indeed, the Vmax flux of glycolysis is much greater than the Vmax of PDH in highly proliferative cells (Curi et al. 1988). Instead, in cancer cells, the products of glycolysis are used as intermediates to biosynthetic pathways, for example, ribose sugars for nucleotides; glycerol and citrate for lipids; production of nonessential amino acids; and, through the oxidative pentose phosphate pathway, NADPH (DeBerardinis et al. 2008). Therefore, even though glycolysis produces less energy per sugar molecule, if the reaction is rapid enough and the availability of sugar is unlimited, the energy supply would not be a limitation for cancer cells. With this, aerobic glycolysis seems to supply the cancer cells with most of its biogenetic and biosynthetic needs. However, glycolysis is approximately eighteen folds less efficient than the glycolytic route. Because of the less efficient metabolic pathway used, cancer cells must up-regulate the expression of glucose transporters like GLUT1 augmenting the cellular glucose intake (Hanahan & Weinberg 2011). Interestingly tumours often present a mixed population of cells regarding energy production. Some of the cells in a tumour can use the lactate secreted by cells in aerobic glycolysis (Feron 2009). In these cells, the lactate is incorporated into the citric acid cycle to produce energy (Kennedy & Dewhirst 2010), creating a symbiotic relationship between the two cell populations, this feature is observed in tumours with large avascular regions (Feron 2009; Hanahan & Weinberg 2011).

The inflammatory component of the cancer was already mentioned here as supporting the installation of other cancer hallmarks, therefore they were described as an enabling hallmark of cancer (Hanahan & Weinberg 2011). Inflammation can contribute to the tumour microenvironment by supplying bioactive molecules, including growth factors, pro angiogenic stimulation, metalloproteinases and signals that induce EMT (DeNardo et al. 2010; Qian & Pollard 2010). Inflammation can also provide reactive oxygen species that actively damage DNA, potentially accelerating genomic evolution of the tumour (Grivennikov et al. 2010).

Finally, the attraction of inflammatory cells to the tumour site also represents an attempt by the immune system to clear the neoplastic lesion. There are compelling data demonstrating that mice deficient in components of the innate and the adaptive

immune response are more susceptible to cancer (Smyth et al. 2000; Dighe et al. 1994). Transplantation experiments showed that tumours grown in immunodeficient mice were not competent to grow in immunocompetent mice after transplantation, but the reverse was not true, suggesting that inflammatory cells can destroy immunogenic cancer cells (Svane et al. 1996; Engel et al. 1997). This suggests that a mixed population of cells in the tumour presents different levels of immunogenicity, in immunocompetent mice a less immunogenic strain of cells is selected (Hanahan & Weinberg 2011; Syverton et al. 1950). Examples of immune cells from the innate and adaptive system that presents anti-tumoral activity are natural killer (NK) (Wu & Lanier 2003) and cytotoxic T cell (CTLs) (Martinez-Lostao et al. 2015). On the other hand, cancer cells can avoid immune detection by secreting factors that paralyse infiltration of CTLs and NK cells, for example, TGF-β (Yang et al. 2010; Murakami et al. 2002), and immunosuppressive cytokines (Shields et al. 2010) and by recruiting a population of regulatory lymphocytes to the tumour site (Takeuchi & Nishikawa 2016; Murakami et al. 2002). Therefore, the presence of inflammatory infiltrate in the tumour can be both beneficial or not to the patient depending on the context in which it happens, and the inflammatory cell population recruited (Hanahan & Weinberg 2011).

Epithelial to mesenchymal transition

Epithelial tissue

The body of mammalian animals is composed of four basic tissues: connective, epithelial, muscular and nervous. Epithelial tissue is found on the inner and/or outer surface of many organs in the body, for example the epithelium covering the inner surface of the gastro-intestinal tract. Epithelial cells can be classified in three morphologies, observed in different organs: squamous, columnar and cuboidal (Eurell et al. 2006). The epithelium can also be classified by the number of layers of cells stacked on top of each other. If the only one layer is present it is called simple epithelium and with two or more layers the epithelium is termed stratified. In some rare cases a simple columnar epithelium can be mistook for stratified epithelium due a lack of alignment of the nuclei, and this type of epithelium is called pseudo-stratified (Eurell et al. 2006).

The cells in an epithelium tissue are closely attached to each other by specialised adhesion proteins (Eurell et al. 2006). One of the main proteins responsible for cell adhesion in epithelial tissues is E-cadherin. E-Cadherin is a member of the Cadherin superfamily encoded by the *CDH1* gene; it is a calcium-dependent cell-to-cell adhesion glycoprotein composed of five extracellular cadherin repeats, a transmembrane region and a conserved cytoplasmic region (Geiger and Ayalon, 1992). The extracellular domain links to other adhesion proteins in adjacent cells, holding the two cells together.

Another important feature of epithelial cells is the presence of specialised regions in their cellular membrane. This creates a polarisation on the cellular membrane allowing specialisation to develop. For example, the apical surface commonly develops a structure known as primary cilia, that increases the contact surface of the epithelial barrier. The formation of the primary cilia depends on the defined existence of an apical surface, and it is only observed in the luminal side of the cells (Adams et al 2008). The lateral surfaces of the cells is the region that impermeably separates the apical and basal surface of the cellular membrane. It does that through adhesion proteins that strong binds to adhesion proteins in the neighbouring epithelial cells. Dysfunctions of this barrier can be involved in pathological diseases (Lee at all

2018). The lateral surface presents agglomerates of adhesion proteins in structures called tight junctions (TJ) and adherent junctions (AJ) (Turner et al 2009; Adams et al 2008). TJs are usually formed by transmembrane Claudins and Occludins. In the intracellular portion of the proteins they interact with ZO-1 that anchor the adhesion proteins to fibres of F-actin and Myosin in the cytoskeleton (Lee et al 2018). In AJ the adhesion is less tight than at the TJ and the cytoplasmic termini of the adhesion proteins at the AJ are linked to the actin belt of the cells by β and α catenin proteins (Lee et al 2018) (Figure 1.3).

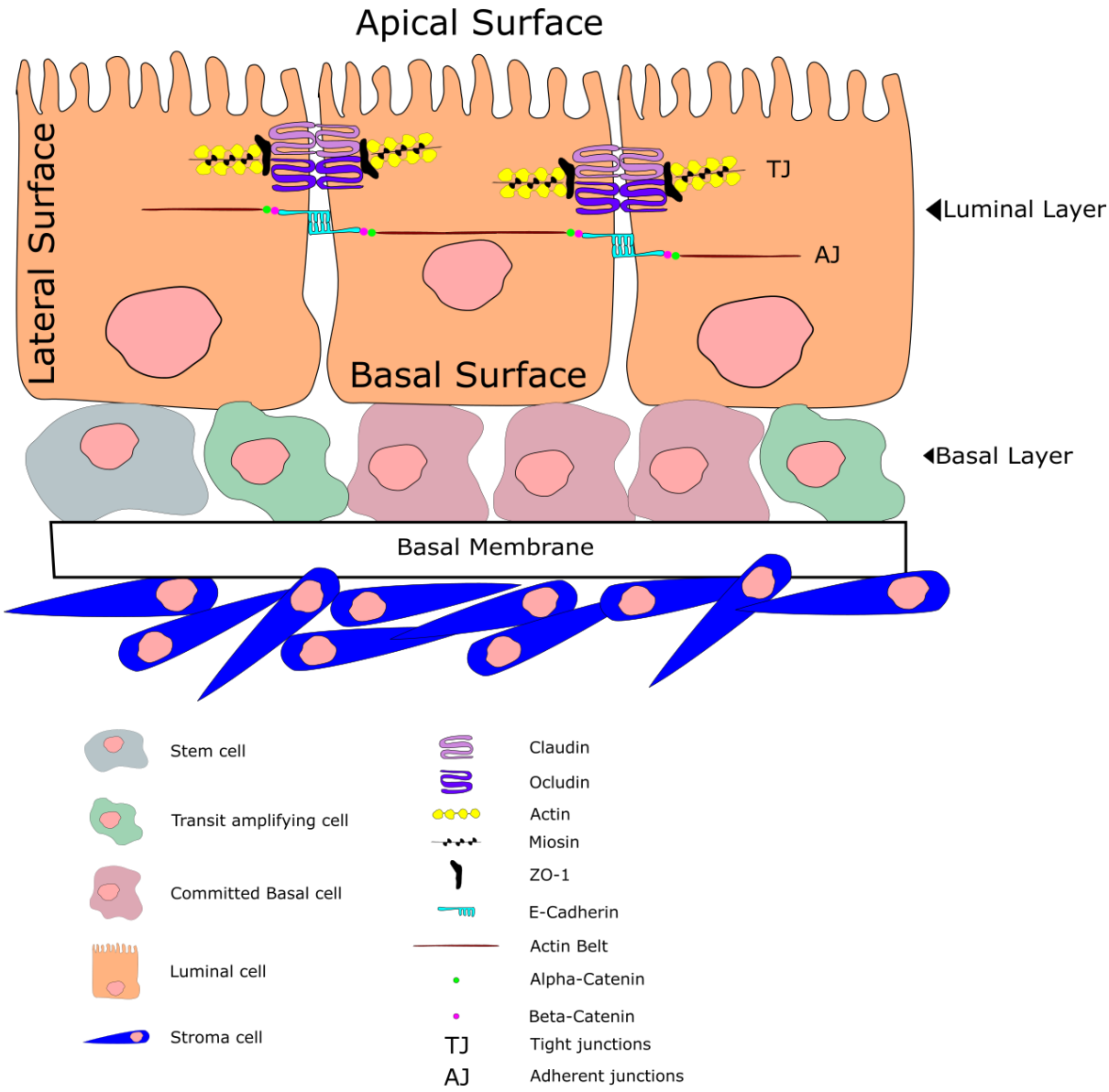

Figure 1.3 Cell polarity in human prostate epithelium. The epithelium is composed of a double layer of cells (Luminal and Basal). The luminal layer is composer of secretory luminal cells. The Basal layer is composed of 3 different types of cells: Stem cells (capable of self-renew and differentiate), transient Basal cells (an intermediate progenitor line) and committed basal cell which originates the luminal population of cells. The luminal cells present a complex network or adhesion proteins that confers polarity to the epithelium. In tight junctions (TJ) Claudin and Occludinforms an impermeable junction between the epithelial cells, in the intracellular side these proteins interact with Actin and Myosin fibres from the cytoskeleton of the cell. Adherent junctions (AJ) are form by interactions between E-cadherin from neighbouring cells. B-catenin interacts with the intracellular domain of the E-cadherin and throught interactions with α-catenin anchors the E-cadherin to the cellular actin belt. The TJ and AJ separate the cellular epithelial cellular membrane in 3 specialised surfaces: Apical, Basal and Lateral.

The apical membrane of an epithelium varies with the type of surface it is covering (Eurell et al. 2006). In epithelium covering the lumen of hollow organs it is not uncommon to find epithelial cells specialised in secreting substances, for example, the parietal cells that secrete acids into the stomach (Schubert 2012). Of note, some entire epithelial tissues also can specialise in secreting substances necessary to the maintenance of bodily function. These specialised epithelia are called glands. Glands are folds of specialised epithelial tissue that synthesise substances like hormones, like the pituitary gland (Vankelecom and Gremeaux 2010), or digestive, like the pancreas (Seo et al 2018) for example. They are classified by the histological appearance of the epithelium using the same epithelium classification described above. Glands can also be classified by the destination of the substances it produces. Endocrine glands secrete substances that are released into the bloodstream and that will have systemic effects. Exocrine glands secret substances on an epithelial surface, having most of its effects locally, some glands present both endocrine and exocrine functions (Yatchenko et al 2019).

Another important classification of glands sorts them by the glandular morphology. If the gland has only one draining duct and presents no branching it is termed a simple gland. If the gland presents several branching ducts that terminate into a main secretory duct it is termed a compound gland. The histologic appearance of the whole gland is also used to group glands. Glands that shows tubular formation in histological observations are termed tubular glands. The second type of histological observations of glands is the acinar morphology. This term refers to morphologies resembling lobed-berries. Both acinar and tubular glands can be simple or compound, and cases where one gland presents both morphologies are not uncommon, in this cases the gland is called tubuloascinar (Eurell et al. 2006).

All epithelia in the body rest on a basal membrane. The basal membrane is composed of ECM, giving architectural support to the epithelium (Eurell et al. 2006). The basal membrane is the connection between the epithelium and the underlying tissue. Since the epithelium is not vascularised itself, the nutrients, oxygen, growth factors and other molecules necessary for the basic functions of epithelial cells are provided by diffusion through the ECM, however, more recent research shows an active role of the ECM on regulating stimulation on the surrounding tissue, being able to transport factors like BMP enabling long distance interaction (Sedlmeier and

Sleeman 2017). In fact, the ECM in the basal membrane regulates cell metabolism, survival and differentiation. Epithelial cells rest on their basal membrane and, except in extraordinary occasions, never leave. In culture, epithelial cells present a round, poorly-spread morphology, with intermediated states of spreading associated with cell movement. With proliferation and movement the cells make contact with other cells, recovering polarization and forming cellular sheets (Brown & Middleton 1985).

EMT

The extraordinary occasions where epithelial cells leave their basal membrane is called EMT (Nieto et al. 2016). EMT is seen during the early development and embryogenesis. EMT plays an important role on the differentiation of the embryologic tissues that later on form all the organs in an animal's body (Nieto 2001; Shook & Keller 2003). In fully developed bodies EMT plays an important role in wound healing and fibrotic processes (Kalluri & Neilson 2003). After the inflammation process of wound healing, endothelial cells undergo EMT to promote re-epithelialisation (Kalluri & Neilson 2003). The EMT program in this case allow cells to become motile and resolve the wound. However, when epithelial cells become cancerous, they can initiate the EMT program present in these cells resulting in malignancy (Brabletz et al. 2018). EMT is thought to play a role in several cellular events involved with cancer progression. It can be involved not only in invasion and metastasis but also in immune evasion and avoidance of apoptosis/senescence (Terry et al 2017; Robson et al 2006). Published data describes TGF-β as a potent promoter of EMT in cancer cells (Li, et al, 2014; Katsuno et al 2013). This effect has been described in several cancers, such as colorectal, pancreatic and prostate cancer, and it is associated with a malignant phenotype.

During EMT, one of the most notable changes is the down-regulation of adhesion proteins associated with epithelial phenotype like E-Cadherin, ZO-1, Lamin-1 (among others). A cadherin switch is also commonly observed, during EMT levels of E-cadherin decrease and the levels of N-cadherin increases. N-cadherin can interact with surface proteins of the endothelium and aid cell extravasation (Zeisberg and Neilson 2009). EMT put cells through a series of morphological and biochemical changes culminating with the expression of end stage EMT markers (like Vimentin, smooth muscle actin α (α-SMA), N-cadherin, fibronectin, among others) and the

detachment of the epithelial cells from the basal membrane (Kalluri & Weinberg 2009). However, E-cadherin loss seems to be heterogeneous; some tumours present separate areas of positive or negative E-cadherin expressing cells (Yang & Weinberg 2008). The detection of E-cadherin in distant metastases also indicates that the activation of the EMT program is, in most of the cases, partial or reversible (Bukholm et al. 2000).

The concept of Epithelial to mesenchymal plasticity (EMP) offers a better explanation of the heterogeneity observed in cancer related EMT. Researchers observed that the EMT/EMP changes occurs in a spectrum due to the observation that cancer cells phenotype can be put somewhere between an epithelial and a mesenchymal state. On that context, the cells can change towards either way on a complete or partial alteration depending on tissue of origin, genetic and epigenetic evolutions and environment inputs, that characteristic seems to be advantageous to cancer cells from an adaptable point of view (Tam and Weinberg 2013; Lamouille et al 2014; Nieto et al 2016).

Apart from the loss of epithelial markers and the gain of mesenchymal markers, cells undergoing EMT present specific characteristics like spindle-shape morphology, increased cell migration, ability of cells to invade other tissues, and the reorganization of the ECM (Kalluri & Weinberg 2009). In these steps, degradation of the ECM from the basal membrane allows the cancer cells to invade the surrounding tissue (Kalluri & Weinberg 2009). The cytoskeleton rearrangement redistributes the acting stress fibres and confers different morphology to the cell, making the cells more motile. The expression of proteins like vimentin, confers resistance to tensile stress, facilitating the movement through tight spaced like between endothelial cells (Mendez et al. 2010). And finally, the cell expresses different adhesion proteins that are displayed on the cell surface. Commonly E-cadherin is substituted by N-cadherin (this is called a Cadherin switch) (Li, et al, 2014). The N-cadherin allows the cancer cell to interact with endothelial cell adhesion proteins enabling the cancer cell to move through the endothelium and in and out of the bloodstream (Li et al, 2001).

Cells that undergo EMT in the primary tumour are considered to be the cells that enter the later stages of invasion and metastasis (Fidler & Poste 2008). However, histologic observations of metastases show resemblance to the original tumour. This

indicates that the new environment where the cancer cell arrives does not provide the cells with the factors that initiated the EMT or that maintain the mesenchymal state (Fidler & Poste 2008). Therefore, the cell starts a process of reversion of EMT known as mesenchymal to epithelial transition (MET). Many studies indicate that activation of EMT and MET programmes in the context of cancer is rarely complete, this confers plasticity and adaptability to the cancer cell (Brabletz et al. 2018). Table 1.1 shows a list of different criteria used to identify EMT (Zeisberg and Neilson 2009).

Table 1.1. Major criteria for EMT in vitro – Modified from Zeisberg and Neilson (2009)

Cadherin switch.
Increase expression of HSP47, Collagen I (α1), Collagen 2 (α2), or Vimentin.
New expression of FSP1 and possibly DDR2.
Nuclear relocation of CBF-A or β-catenin/LEF or new expression of one of the following transcription factors: Snail, Slug, or Twist.
Absence of epithelial markers; loss of cytokeratin or ZO-1.
Spindle shape morphology with redistribution of stress fibres and loss of polarity.
Resistance to apoptotic stimuli.
Increased migratory capacity.
Stable phenotype upon removal of inducing stimuli.

EMT transcription factors

EMT can be induced and regulated by a number of signalling pathways, depending on the contextual genetic, epigenetic and environmental inputs. TGF-β is a classic inducer of EMT, however, a number of other signals can activate the EMT program. Tyrosine kinase receptor pathway can initiate EMT through the PI3K-AKT and ERK-MAPK signalling (Lotz-Jenne et al 2016). Wnt signalling activation of EMT seems to be through the inhibition of β-catenin degradation which upregulates Slug, downregulating E-cadherin and contributing to the accumulation and nucleus translocation of β-catenin (as discussed in the next paragraph) (Gasior et al 2017). Several other possibilities of EMT activations are reported on Notch-signalling, Hedgehog signalling, and a number of inflammatory pathways (Lamouille et al 2014).

The expression modifications caused by the activation of these pathways are carried by transcription factors that are classically correlated to EMT, like Snail, Slug, Twist and β-catenin.

The intracellular domain of the E-cadherin protein presents phosphorylated regions where β-catenin binds. β-catenin bound to the intracellular portion of the E-Cadherin links the cytoskeleton to the adhesion junction (Stockinger et al. 2001). However, β-catenin also plays an important role in regulating the expression of several genes related to the cell proliferation and evading apoptosis, such as Cyclin D1 (CCND1) and Transcription Factor 7 (TCF/LEF) (Marrs and Nelson, 1996). The upregulation of Dishevelled (Dvl) by the Wnt signaling inhibits the degradation of β-catenin, which accumulates in the cytoplasm and eventually gets translocated to the nucleus. β-catenin helps the expression of EMT-TF Slug, which supress E-cadherin expression, in absence of E-cadherin, β-catenin is not sequestered at the cellular membrane, exacerbating the accumulation of β-catenin (Stockinger et al. 2001).

The β-catenin expression effects on the cell can also be activated by silencing of the E-cadherin gene CDH1. In prostate cancer, the hyper-methylation of the CDH1 gene was reported to occur in 70% of the high grade tumours (reviewed by Chin et al 2011).

Several transcription factors are known to regulate EMT, they are known as EMT-TFs. The transcription factors Snail, Slug, *ZEB1* and *TWIST1* can all reduce the expression of E-cadherin leading to EMT (Zeisberg and Neilson, 2009). Most of invasive cancer cell lines express one or more of these transcription factors (Yang & Weinberg 2008). Slug was shown to repress E-cadherin expression in breast cancer (Hajra et al. 2002) and this EMT-TF is related to the EMT program in several different cancers (Medici et al. 2008; Villarejo et al. 2014; Heldin et al. 2012a; Brabletz et al. 2018).

ZEB1 is implicated in the initiation of EMT programs in prostate cancer (Graham et al. 2008), lung cancer (Takeyama et al. 2010) and pancreatic cancer (Krebs et al. 2017). The use of tumour-cell-specific *TWIST1* knockout mice in a oncogene-induced spontaneous breast tumour model showed that *TWIST1* causes EMT and tumour-cell-specific *TWIST1* knockout reduced appearance of lung metastasis (Xu et al. 2017). Cooperation between *TWIST1* and the oncogenic transcription factors c-

Myc can inhibit the intrinsic cellular defence mechanism that activates cell death in case of cellular crises (Valsesia-Wittmann et al. 2004) indicating that EMT program helps with death evasion in this model. Myc is a gene family that encodes transcription factors that are commonly dysregulated in human cancers, and Myc over-expression drives increased in cellular proliferation facilitating several aspects of tumour initiation and progression (Venkateswaran & Conacci-Sorrell 2017).

Snail, is part of the zinc-finger transcriptional repressor complex that binds to two E-boxes located in the E-cadherin promoter, down-regulating E-cadherin expression (Thiery 2002). Snail is reported to participate in EMT programs in several cancers (Wang et al. 2013). For example, Snail was reported to be necessary to lymph node metastasis of breast cancer cells in *in vivo* models using BALB/c immunocompromised mice (Olmeda et al. 2007). Notch is a transmembrane protein family that receives signals from close cell to cell contact or from ECM components (juxtracrine signalling). Its activation triggers gene regulation through Notch activated transcription factors (Pursglove & Mackay 2005). Notch is reported to activate Snail expression in ovarian cancer cells mediating EMT and invasion (Sahlgren et al. 2008).

It has been reported that the induction of EMT by overexpression of EMT-TF or treatment with TGF-β in immortalized human mammary epithelial cells (HMLE) stimulated the expression of cell surface stem cell markers (Sendurai et al 2008). In this study the cells overexpressing Snail or Twist, presented EMT markers like downregulation of e-cadherin gene and upregulation of vimentin genes. Concomitantly, nearly 100% of these cells presented stem cell markers ($CD44^{high}/CD24^{low}$), fact also observed with TGF-β treated cells (Sendurai et al 2008). Interestingly, the same group demonstrated that the downregulation of e-cadherin gene resulted in EMT in the same cell line (Tamer et al 2008). They used two different approaches to achieve e-cadherin downregulation, the expression of a shRNA targeting e-cadherin or the expression of truncated e-cadherin protein lacking its ectodomain, which results in a protein that cannot perform the normal adhesion observed in wield-type protein. The results showed that the downregulation of e-cadherin results in EMT, demonstrated by the loss of cellular adhesion up-regulation of vimentin and n-cadherin. The expression of the truncated protein prevented cellular adhesion, but did not induce the expression of mesenchymal markers. The

authors also showed that the translocation of β-catenin to the nucleus was important to the induction of the mesenchymal phenotype observed in the e-cadherin downregulated cells, explaining why the expression of the truncated e-cadherin was not able to induce the appearance of mesenchymal markers (Tamer et al 2008).

Additionally, several EMT-TF has been shown to be implicated in other vital processes for cancer progress. They can promote and maintain cancer cell stemness and tumorgenicity, and they can help the cell to escape from senescence and regulate both pro-inflammatory and immunosuppressive cytokines (Puisieux et al. 2014; Nieto et al. 2016), giving even more importance to the understanding of their roles. Figure 1.4 shows a diagram summarising the event on EMT.

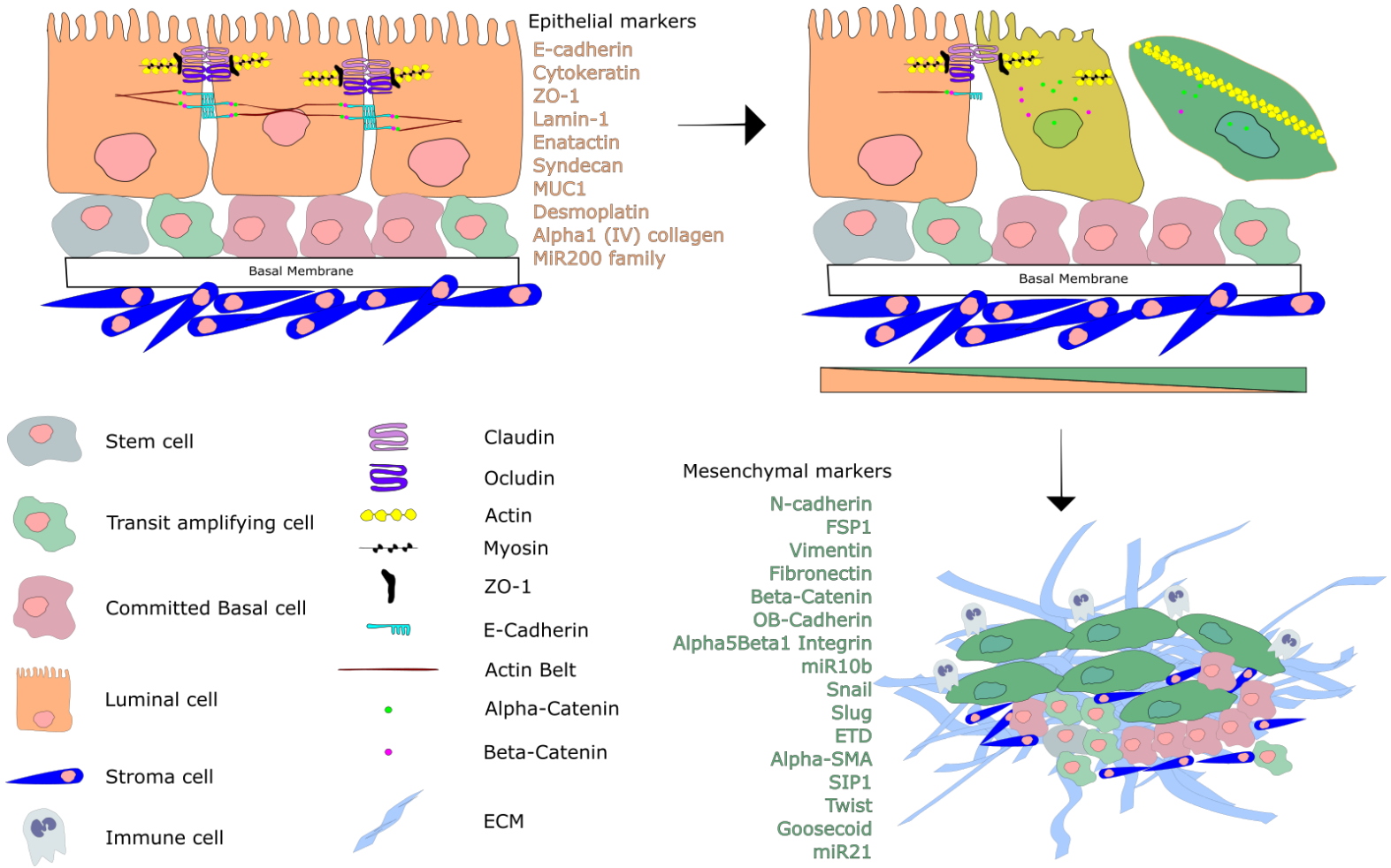

Figure 1.4. Epithelial to mesenchymal transition. A diagram of EMT and the associated markers with each stage. The transitional states presents a mixture of markers from both states. Epithelial cells express a number of proteins involves in epithelial cells adhesion. During EMT the cells lose their polarity and pass through cytoskeleton rearrangement with the appearance of actin stress fibres. Free β- catenin can translocate to the nucleus and exacerbate EMT signalling, however several transcription factors are capable of activating EMT program. The dissolution of the Basal membrane is important event in cancer related EMT because the growing tumour can invade

Prostate cancer EMT

Cancer cells use the intrinsic EMT mechanisms within the human genome to become invasive acquiring the ability form metastasis. The life quality of patients with prostate cancer drastically declines during metastasis, with nearly all prostate cancer caused death being associated with metastasis (Odero-Marah et al 2018). Different cell signalling programs are associated with EMT in prostate cancer, among them androgen receptor (AR) signalling, oestrogen signalling, TGF-β, IGF and EGF commonly flagged as activators (as reviewed by Montanari et al 2017).

The reports of the role of androgens in the prostate cancer related EMT are conflicting. Treatment with Dihydrotestosterone (DHT) caused cadherin switch in PC3 cells (Zhu and Kyprianou 2010). The castration of nude mice bearing a classic human prostate xenograft tumour (LuCaP35) caused tumour regression and expression profiles changes in the tumour tissue. Cadherin switch was observed associated with Vimentin, ZEB and TWIST upregulation (Sun et al 2012). The conflicting data is still to be clarified, but the clinical outcome of patients that undergo hormone deprivation treatment develops into catastrophic cancer progression, suggesting that the maintenance of androgen signalling would be necessary for EMT regulation.

Recent insights showed EMT in PC3 cells induced by osteoblast differentiation medium (ODM). When treated with ODM PC3 cells lost expression of E-cadherin and β-catenin, while the expression of N-cadherin, Snail and Slug were upregulated. The authors also demonstrated that ODM treatment in PC3 promotes cell migration and colony formation through the activation of the NF-κB pathway. These effects were confirmed by tumour formation and metastasis assays in nude mice (Tong et al 2018).

Oestrogen receptor (ER) signalling is reported to act through H1F1α to activate the VEGF pathway that can influence the expression of Snail in prostate cancer. EGF is reported to act through multiple signalling pathways that regulates EMT, for example the activation of Ros and ultimately expression of EMT-TF Twist. EGF can also up-regulate Snail which directly down regulates E-caderin (reviwed by Montanari et al 2017) A summary of the signalling pathways that can regulate EMT in prostate cancer is in Figure 1.5.

TGF-β is reported to play a major role on prostate cancer related EMT, plus TGF-β and AR signalling share common gene targets making this crosstalk an important element of prostate cancer EMT (reviewed by Zhu and Kyprianou 2008). It was demonstrated that the AR expression influences the prostate cancer cell response to TGF-β induced apoptosis via, at least partially, AR-Smad4 interaction (Zhu et al 2008).

The TGF-β regulation of EMT in prostate cancer seems to be important in both early and late stated of cancer. TGF-β signals in prostate cancer can be grouped in two categories: smad-dependent pathway and smad-independent ones. Some authors associate Smad-independent pathways with the pro-tumour progression and EMT effects of TGF-β (as reviewed by Montanari et al 2017). However, it is reported that TGF-β induced EMT involves MAPK, Smad and AP-1 pathways (Davies et al 2005). Details about the TGF-β signalling pathway is given on the next sections.

Inputs from stroma cells seem to be one important component of the TGF-β mediated activation of the EMT program in prostate cancer (Hu et al 2014). It was reported that heterogeneity in the expression of TGFβRII in prostatic stroma cells resulted in elevated expression and secretion of growth factors including TGF-β1, driving formation of prostatic intraepithelial neoplasia (PIN) and carcinogenesis (reviewed by Barron and Rowley 2012). This shows the context importance for the TGF-β signalling in prostate cancer EMT. TGF-β signalling can be regulated at several stages by different co-regulators and cross-talking signals. Another example is the demonstration that genetic deletion of Smad4 in PTEN-null prostate cancer mouse model developed in 100% invasive, metastatic and lethal disease (Ding et al 2011). Recently, it was shown in pancreatic ductal adenocarcinoma (PDA) that the expression of Smad4 can be decisive on the cell fate in this model (David et al 2016).

The prostate gland

Morphology and physiology

The human prostate gland is an organ formed by glandular and non-glandular components enclosed by a capsule formed of fibromuscular tissue (prostate capsule). The prostate capsule is composed of a bundle of smooth muscle cells that merges with the smooth muscle cells in the bladder neck. There are five distinguishable zones observed in the prostate gland: peripheral zone, central zone, transition zone, periurethral gland region, and anterior fibro-muscular zone. The peripheral zone forms about 70% of the prostate gland mass, with vast areas of glandular ducts that exit from the posterolateral recesses of the urethra wall. This region is the most susceptible to inflammation and it is the region where prostate cancer most commonly arises. The central zone corresponds about 25% of the glandular mass, this portion arises from the seminal colliculus region of the urethra with its ducts branching towards the base of the prostate along the course of the ejaculatory duct, and almost the whole base of the prostate is formed by the tissue from this zone. The transient zone comprises approximately 5-10% of the prostate glandular tissue, being composed of two small lobes with each duct leaving from a single point in the proximal urethra epithelium, both departing from the lower border of the prostatic sphincter and spreading around its distal border, curving around sharply towards the bladder neck. The periurethral gland region is the approximate size of the transient zone but it is formed of non-functional glandular tissue. The anterior fibro-muscular zone extends from the bladder neck to the prostate apex. The lateral sides of this zone blend with the prostatic capsule. The glandular tissue of prostate gland presents a compounded tubuloascinar morphology. As explained before, tubuloascinar glands are the ones that presents both tubular and acinar morphology in histological sections. It presents an exocrine secretion of a fluid called prostate fluid. In humans the prostate fluid composes 30% of the semen volume, being responsible for maintaining the alkaline pH in the environment and counteracting the acid pH of the female vaginal tract. This enhances the sperm cell performance and aids fertilization (McNeal 1988) (Figure 1.5). The prostatic fluid presents high contents of polyamines, which presents functions related to cellular

proliferation and secretory activities, however no clarifications are needed for the reasons for its secretion on the seminal fluid (Schipper et al 2003; Jasuja et al 2014). Some biochemical studies of seminal fluid revealed that the polyamines can serve as amine donor substrates for transglutaminases (Romijn 1990). Additionally, its expression had been associated with higher grades of prostate tumours (reviewed by Schipper et al 2003).

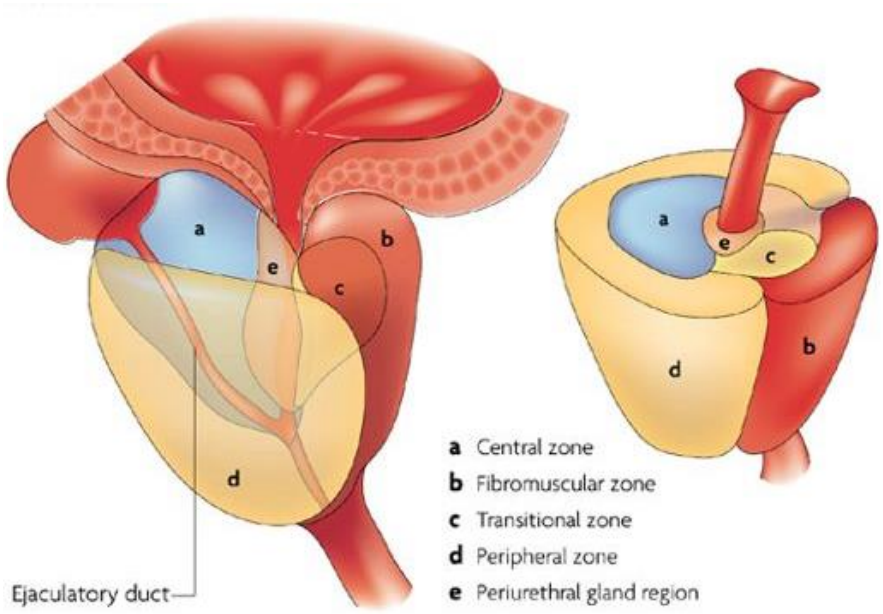

Figure 1.5. Prostate zones. Modified imaged from (De Marzo et al. 2007) shows the five zones of the prostate gland.

Histologically, the prostate epithelium is a bilayer of basal and luminal cells inserted into the fibromuscular stroma. The bilayer is composed of luminal (60%) and basal (40%) cells. There are four types of cells in the prostate epithelium, the basal portion is composed of stem cells, transient amplifying (TA) cells and committed basal (CB). The luminal portion is composed of luminal cells (reviewed by Packer and Maitland 2016). Figure 1.6 shows a diagram with the prostate epithelium organisation.

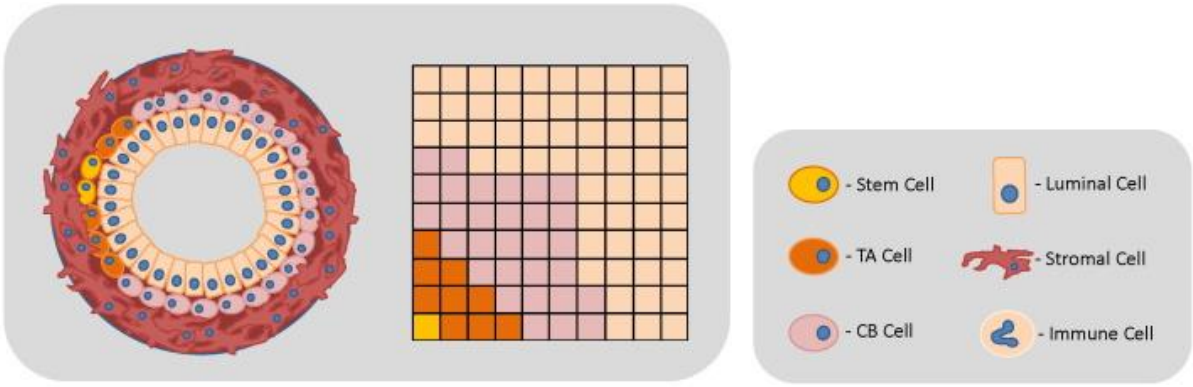

Figure 1.6. Diagrammatic representation of a normal prostatic acinus. The epithelial bilayer of basal and luminal cells, surrounded by fibromuscular stroma. The relative content of different epithelial cells in the normal prostate are summarised graphically; luminal (60%), basal (40%) with the stem cells constituting ~ 1% of total epithelia. Transient Amplifying (TA) cells and Committed Basal (CB) (Packer and Maitland 2016).

Prostate cancer

Prostate adenocarcinomas are most commonly derived from glandular epithelium neoplasia (which are tumour neo formations in the gland epithelium) (Dermer 1978). In the early stages of prostate carcinomas the most common local invasion is to the stroma tissue, and local spread into the surrounding adipose tissue, bladder neck and seminal vesicle, is also common, but more serious complications happen when the invasion develops into motile cells reaching the bloodstream and forming metastases (McNeal 1988). The High-grade prostatic intraepithelial neoplasia (PIN) is accepted as a precursor of the invasive prostate adenocarcinoma. Because PIN cells resemble invasive adenocarcinoma cell morphology, there are also compelling data from zonal co-localisation between PIN and adenocarcinoma. Furthermore both diseases share important molecular changes like ETS gene rearrangements and loss of PTEN (reviewed by De Marzo et al 2016). The most common metastasis observed in prostate adenocarcinoma are in the lymph node of the pelvis and bone marrow tissues

The origin of the prostate cancer is currently a field for debate. The heterogeneity of the organ hampers the search of origin for the cancer, additionally, there is no epidemiologic marker that supports the high frequency of the prostate malignancy (reviewed by Packer and Maitland 2016). The controversy starts on the origin of the heterogeneity of the tumour itself. There are two theories to explain this observation, firstly, the Stochastic model where a definitive driver mutation activating an

oncogene or deactivating a tumour suppressor gene happens, and the subsequent cell division generates an identical cell with equal propagating potential. In this model the heterogeneity is created by subsequent mutations on the clonal expansion. The second is the cancer stem cell (CSC) model, where only a small subpopulation of stem cells pool (capable of self-renew and differentiation) in the tumour are can initiate tumour formation. In this model the genetic variation is introduced by cellular differentiation. As it is commonly observed in prostate cancers, several cancer driver alterations in the genome are heterozygous. When stem cells differentiate the mutation is carried in one branch of the cell expansion process (reviewed by Packer and Maitland 2016).

Of course, the two theories are not mutually exclusive. Subsequent mutations could happen in a copy of the original cell and kept in a neutral evolutional fashion, enhancing furthermore the heterogeneity (reviewed by Packer and Maitland 2016). The genetic variability in the CSC pool is likely to generate progenitor cells that could be dominant in later stages upon changes in the tumour microenvironment brought by crisis inducing events like chemotherapy (Anderson et al 2011).

The origin of the progenitor CSC is also debated, if the original cell comes from a luminal or a basal cell still not 100% clear. It was identified that progenitor cells that present with a luminal phenotype and pluripotent markers in mice models of prostate cancer (Wang et al 2010; Chua et al 2014). However, the key histologic differences between the mice and human prostate , such as the absence of a double epithelial layer in mice could mean that the prostate cancer is just different between the two species (reviewed by Archer et al 2017).

On the other hand, human basal stem cells isolated from human prostate cancer show capacity of self-renew and differentiate into AR^{+} luminal cells (Collins et al 2005). It was also reported that human basal cells and not luminal were able to induce tumorigenesis with luminal phenotype in NOD/SCID/IL2Rγ^{null} mice induced by the expression of AKT, ERG and AR (Goldstein et al 2010). In contrast, a luminal CSC was found in the BM18 xenograft model. This small subpopulation of the tumour was able to establish a tumour upon introduction of androgen (Germann et al 2012). However, Archer et al argued that the BM18 xenograft model was not serially transplanted into mice, and that the model have been passed many times since its

establishment in 2005, which likely inserted evolutionary modifications to the cells (reviewed by Archer et al 2017).

Several mutation drivers could be responsible for the appearance of prostate cancer. As an isolated microenvironment is observed in these tumours, the creation of an independent niche or the ability to create an independent niche is potentially a key cancer driver (reviewed by Archer et al 2017). The presence of niches is also favourable to the accumulation of driver mutations by fixing passenger mutations. When mutations happen they can maintained by symmetric division of the stem cells, in this process changes in the niche creates successions that select advantageous mutations. The niche successions is a cyclic process that takes approximately 8.2 years to occur in the stem cells of the colon epithelial crypts, in prostate epithelium this process presumable takes much longer (reviewed by Archer et al 2017). The prostate stem cell that will originate the cancer probably is the able to maintain its stemness by keeping pathways associated with stem phenotype activated or hyper activated, that way mutations that would be deleterious to differentiated cells could be tolerated, that way these cells accumulate mutations through an individual's life time until tumour initiating change comes along.

Epigenetic regulations of the gene expression represent a way for the cancer cells to beneficiate from the adaptability of the more de-differentiated states while not relying on more inflexible changes such as genetic mutations or deletions. In prostate cancer DNA hyper methylation was able to predict gene downregulation (Pellacani at al 2014).

An important epigenetic phenomenon observed in cancer is the random monoallelic expression (RME). This phenomenon can contribute to the accumulations of genetic alteration, as, for example, activation of an oncogene in early in normal stem cells could be initially silenced in that fashion and later on be reactivated (reviewed by Archer et al 2017). In REM an allele present in a daughter cell had a stochastic activation when that cell is originated from a stem cell. The expression of a gene regulated by REM could be bi-allelic, maternally mono-allelic, paternally mono-allelic or the gene could not be expressed at all. The expression pattern observed in the daughter cell is phenotypically stable in non-stem cells generated by asymmetric division (Gendrel et a 2014).The REM is controlled by an asymmetric chromatin

signature, where the histones of the activated gene bodies are tri-methylated at H3K36 while the ones in the silenced allele are tri-methylated at H3K27 (Nag et al 2013).

Inflammatory responses present itself as potential driver for prostate cancer generation. In the event of infections, for example, the invasion of lymphocytes provides an external supply of IL-6, the presence of this interleukin in the niche promotes an adaptive changes into the stem cell pool creating an inflammatory environment that will confer advantage to stem cells that produce IL-6 and enter the an autocrine positive feedback loop of inflammatory signal (reviewed by Archer et al 2017). It is noteworthy that upon AR downregulation, IL-6 expression is upregulated and its consequent activation of STAT3 pathway acts as a bypass to androgen dependency during androgen deprivation therapy in prostate cancer (Schroeder et al 2014). However, the world health organisation consider that there is no concrete correlation between prostate cancer and any infectious disease (WHO 2014).

Molecularly speaking the four most common alterations observed in prostate cancer are: amplification of the androgen receptor (AR), fusion of TMPRSS2 and ETS genes, disruption of the TP53 gene and dysregulation of PTEN. The carcinogenic implications of the gene TP53 were discussed previously in this thesis. Studies showed that dysregulation of PTEN gene happen in approximately 41% of prostate cancer patients and that this dysregulation can occur due to alterations on the gene copy number, structural rearrangements and/or mutations of the gene. The effects of PTEN in as a tumour suppressor gene is due to its effects on the inositol ring of the PI3K, inhibiting PI3K proliferative effects (reviewed by wise et al 2017). Genomic aberrations are another commonly detect event in prostate cancer. These aberrations include numerical chromosomal aberrations (aneuploidy) and structural chromosome changes, aneuploidy is a reflection of mitotic defects while structural changes requires strand breaks that are left unrepaired or are repaired in a wrong fashion (Pecqueux et al 2018). It was reported that genomic instability plays a crucial role in the progression of prostate cancer (reviewed by Tapia-Laliena et al 2014). Single catastrophic chromosomal events could result in extensive DNA damage, however evidence shows that theses catastrophic events actually happens in prostate cancer causing rapid DNA evolution (Zhang et al 2013), in contrast to the

findings that shows that the damage accumulates over a long period of time (reviewed by Archer et al 2017).

The common phenomenons observed in prostate cancer that lead to genomic aberrations are: chromothripsis and chromoplexy. Chromothripsis are alterations that happens in clusters in a single chromosome, the mechanisms on how it happens are unclear but it is suggested that mutations on TP53 or DNA repair machinery are involved. In this processes the shattering of chromosomes cause random re-attachment by the DNA repair system of the cell (reviewed by Tapia-Laliena et al 2014). The locus 10q23 where the gene PTEN is inserted, is frequently affected by this process in prostate cancer (Feilotter et al. 1998).

Chromoplexy is the formation of “chain” patterns in chromosomal rearrangements created by the repair of a break where the some length of DNA is lost (Berger et al 2011), the genes in the lost strand of DNA simply disappear, these lost genes are called “deletions bridges” (Baca et al 2013). In prostate cancer chromoplexy is observed on the rearrangements of the gene ERG, where DNA repair induced gene fusion (reviewed by Tapia-Laliena et al 2014). TMPRSS2:ERG fusions are the most common genomic alteration in prostate and it results in overexpression of the overexpression of ERG, oncogene that encodes a transcription factor which presents key roles on the regulation of cell proliferation, differentiation, angiogenesis, inflammation and apoptosis (reviewed by Wang et al 2017).

Molecular risk of prostate cancer is increased by androgen, androgen receptor and growth factor activity (WHO 2014). The androgen receptor (AR) is a transcription factor activated by several ligands. AR ligands are steroids and peptide hormones. This transcription factor is essential for normal prostate epithelium cellular proliferation, and it is also involved in apoptosis, cell migration and cell differentiation. AR is commonly expressed in prostate cancer cells and metastases, providing an uncontrolled cellular proliferation signal (reviewed by Lamb et al. 2014; Culig & Santer 2014). For that reason, androgen deprivation therapy (ADT) is a common therapeutic approach to treat prostate cancer at all stages (Lu-Yao et al. 2009; Picard et al. 2012). ADT is a type of therapy where drugs that inhibit the secretion of androgens are used and it is commonly known as chemical castration. However, this treatment presents side effects, because hormonal deprivation can

interfere with the body metabolism and with calcium homeostasis in the bone. ADT is associated with increased incidence of diabetes, clinical fractures, and cardiovascular disease (Saylor & Smith 2010). Furthermore, ADT causes long term selection of prostate tumours leading to evolution into ADT-resistant tumours (castration resistant prostate adenocarcinoma) (Liu et al. 2014). There are several mechanisms through which prostate cancers can evolve into castration resistance, one example involves expression of a constitutively activated AR lacking the ligand binding domain (Dehm et al. 2008). Recent reports explore the allosteric alterations on the AR. More than 20 variations of the protein were identified, lacking different portions of the ligand-binding domain. Allosteric variations of the receptor were associated with ADT therapy, and specifically the variation AR-V7, it was demonstrated that the presence of this variation in patients predicted resistance to treatments with antiandrogen drugs (reviewed by Takuma et al. 2017). This can limit the application of ADT, however, alternative therapeutic approaches suggest that patients could benefit from an intermittent androgen deprivation (IDA) (Brungs et al. 2014).

Another treatment option for localised prostate cancer is radical prostatectomy, which is reported to present an improved survival rate alongside external beam radiotherapy (Hoffman et al. 2013). For patients initially diagnosed with advance prostate adenocarcinomas, ADT still might be a treatment option, however, for patients that developed castration resistant tumours after ADT treatment, chemotherapy is the next line treatment available (Ahmed et al. 2016). As TGF-β is an important driver of prostate cancer progression, new therapeutic strategies have investigated the efficacy of TGF-β blockage using antibodies. However, further contextual knowledge is needed to identify patients that would benefit from this treatment (de Gramont et al. 2017). Disruptions of the expression of the *CDH1* gene (encoding E-cadherin) represent an increased risk of prostate cancer (WHO 2014). There is no concrete correlation between prostate cancer and any infectious disease (WHO 2014). However, inflammation in the prostate is an important event in prostate carcinogenesis (WHO 2014; McNeal 1988).

The clinical diagnosis of prostate neoplasia is commonly made by the measurement of the blood levels of prostate-specific antigen (PSA). PSA is a glycoprotein synthetized in the prostate gland and its primary function is to enzymatically degrade

the cervical mucus to aid in spermatic mobility. Despite being widely used to diagnose prostate cancer, PSA is not a method with high specificity, blood levels of PSA shows high sensitivity (70%) as the antigen is organ specific, however, the predictive positive values is not very high (37%) (Bunting 2012) as the serum elevation of this marker can be triggered by other prostatic problems like: benign prostatic hypertrophy (BPH), recent manipulations of the prostate due to massage or biopsy, prostatitis (inflammation in the prostate), or age (Pezaro et al. 2014). However, PSA screening is still an important predictive tool. A recent population-based cohort study evaluated the impact of PSA screening for prostate cancer surveillance in men. The evaluation showed that PSA screening at age 50–54 significantly reduces the prostate cancer-specific mortality, concluding that the screening of younger man increases the chances of diagnosis before the disease becomes incurable (Carlsson et al 2017). These authors recommend an initial assessment of PSA levels for men at the middle or late 40's, if they presented PSA concentration <1.0 µg/L they would be invited for reassessment in their 50s and 60s (Vickers et al 2013).

Benign prostate hyperplasia (BPH) is the non-cancerous enlargement of the prostate gland. BPH is usually occurs in the transitional zone of the prostate gland and it is characterised by an increase in the prostate volume that results in compression of the urethra and partial bladder obstruction (Aaron et al. 2016). A study that analysed the database of the Irish Tertiary Referral Centre showed that 35% of men with prostate cancer had normal PSA levels (Walsh et al. 2014). The same study highlighted that digital rectal examination (DRE) is an important method of diagnosis that can diagnose early stage prostate cancer independently of PSA. DRE showed a sensitivity of 81% and a positive predictive value of 42%, making it the current best form of early diagnose for prostate cancer (Walsh et al. 2014).

The severity stage of prostate adenocarcinomas are measured with histopathological examinations of needle biopsies or tissues from radical prostatectomy (surgical removal of the prostate gland) (WHO 2014). The severity and the features associated with malignancy are describes by a grading score proposed by Gleason. The Gleason score was created in 1966 by the pathologist Donald F. Gleason. This classifies prostate neoplasia into five distinct grades with specific characteristics. The description to each grade is based in a systematic study conducted with 270

samples, searched for patterns to group samples by severity (Gleason 1966). To grade the tumour the pathologist grades, based on Gleason's descriptions, the two more common patterns observed in the histological section (grading varying from 2 to 10). The final tumour score is a sum of the two grades given (Gleason 1966).

In 1977, Gleason updated some information on this grading system. He proposed that the analysis should be conducted under low microscope magnification such that the whole tissue is considered in the analyses, and so that small areas of fused glands or disorganised cells would not bias the pathologist analysis (Epstein et al. 2005). In 2005, aiming to standardise controversial areas of the Gleason's score by pathologist around the world, a Consensus Conference was hosted by the International Society of Urological Pathology (ISUP) (Epstein et al. 2005). The consensus was that the Gleason pattern of 1+1 =2 grade should only be diagnosed, regardless of the type of specimen, in extremely special situations (Epstein et al. 2005). Another modification was the decision not to assign the so called "low grade Gleason's" (3 and 4) on a needle biopsy (Epstein et al. 2005). The reasons for that decision were based on the fact that this presented poor reproducibility even among experts, a low correlation between two cuts from the same tumours, one coming of a needle biopsy and the other coming from a radical proctectomy, was observed, and the misdiagnosis of a low-grade tumour could mislead clinicians basing their practice on the pathological examinations. The grade 4 is also controversial on a needle biopsy because one cannot see the edge of the tumour and therefore cannot guarantee that the whole lesion is completely circumscribed (Epstein et al. 2005). The description of each Gleason's score band is described in detail in the methodology section.

In 2014 further modifications were made to the Gleason scoring system due to changes in prostate cancer practices, lack of consensus in some issues in 2005, new research information being published and the realization that some gland issues were not covered in 2005. Among the discussions made in 2014 the grading of cribriform glands was one of the focus. Is was postulated that cribriform glands should be assigned Gleason pattern 4. Regarding the grading of glomeruloid glands, these glands should also be assigned as a Gleason pattern 4, regardless of morphology. Regarding mucinous glands, the grading of these glands should be based on its underlying growth pattern rather than grading them all as a pattern.

Regarding the grading of intraductal carcinoma of the prostate (IDC-P), in the absence of an invasive carcinoma, IDC-P should not be assigned a Gleason grade. The consensus conference also proposed a new grouping system to guide prostate cancer prognosis prediction and treatment (Epstein et al. 2016). Figure 1.7 shows a diagram of the different Gleason grades.

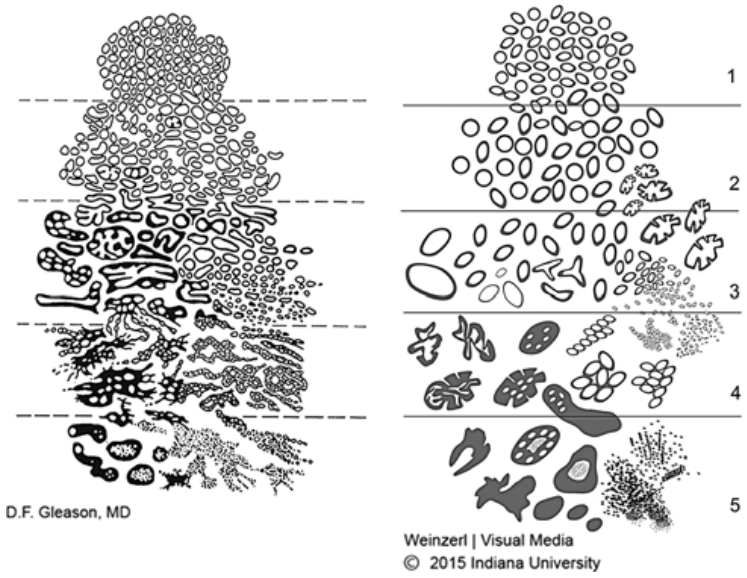

Figure 1.7 Prostatic adenocarcinoma (histologic patterns). Original (left) and 2015 Modified ISUP Gleason schematic diagrams (Epstein et al. 2016).

Age is highly associated with the risk of prostate cancer. The chance of diagnosis for men older than 65 years old is 40 times higher than for men younger than 65 (WHO 2014). Additionally, only approximately 1% of clinically diagnosed prostate cancers are found in men younger than 50 years (WHO 2014). The risk of prostate cancer is also increased with family history (Johns & Houlston 2003). About 25% of patients clinically diagnosed with prostate cancer have family history of this disease (Walsh & Partin 1997). The risk factor indicates that a man with a prostate cancer family history has a risk 3 times higher to have prostate cancer then a man with no family history (WHO 2014). This indicates that a genetic component could increase the risk for the population of men. In fact, when a close relative is diagnosed in ages younger than 40 years old, the prostate cancer risk increases up to 11 times greater than a man with no family risk (WHO 2014). In agreement, a study with twins indicated a 42% hereditary risk of prostate cancer (Lichtenstein et al. 2000).

The genetic component of prostate cancer risk is also observed in ethnicity correlations. In the United States, African Americans are 1.6 times more likely to have prostate cancer than Caucasians (WHO 2014), This increased risk is a reflexion of a higher incidence of polymorphism in the loci 8q24 and 17q21 (Henderson et al. 2012). However, increased risk rates were also observed in migrants who moved from low risk regions to high risk regions, suggesting an environmental risk (WHO 2014). The diets typical of high-risk countries seem to play a role in the increased environmental risk, mainly diets rich in processed red meat, dairy products and saturated fat presents an increase in the risk of prostate cancer, while tomatoes, marine food, soy and cruciferous vegetables possibly decrease the risk (WHO 2014).

Transforming growth factor β

Virtually all human cell types are responsive to Transforming Growth Factor beta (TGFβ) (Massagué 2008). There are 3 types of TGF-β protein, TGF-β1, TGF-β2 and TGF-β3, and they all signal through the same signal receptor system. The TGF-β proteins are growth factors that control cell migration, differentiation and proliferation (Reynisdóttir et al. 1995; Kingsley, 1994; reviewed by David and Massagué 2018), and in addition, they play an important role in several diseases. The TGF-β superfamily signal through the transmembrane serine-threonine kinase class of receptors (Wrana 2000; reviewed by David and Massagué 2018). Physiologically, TGF-β mainly acts through the Smad pathway, activating several regulatory genes, which normally up-regulate Cyclin-Dependent Kinase Inhibitors (CDKIs) preventing progression of the cell cycle. TGF-β can also induce apoptosis (Rotello et al. 1991; Oberhammer et al. 1992; reviewed by David and Massagué 2018), through mechanisms involving Smad7 (Landström et al. 2000). However, Caspase 8 (Shima et al. 1999) and Bcl-XL (Saltzman et al. 1998) are also reported to be involved in this.

TGF-β1 is commonly upregulated in cancer cells and from this point TGF-β1 will be referred to as TGF-β (Derynck et al. 2001). TGF-β is commonly secreted in an inactive form, which is formed by a TGF-β dimer. This dimer is normally activated by proteases cleavage (Robertson et al. 2015). Inactive TGF-β can be sequestered by the extra cellular matrix (ECM) and activated by degradation of the ECM by, for example, macrophage action (Munger et al. 1997; Robertson et al. 2015).

Smad activation is the best-known pathway for the TGF-β signalling. When TGF-β binds to the type II TGF-B receptor (TβRII), it forms a heterodimer with a Type I TGF-β receptor (TβRI). There are three type I receptors (ALK1/TSR-1, ALK2/Tsk7L, ALK5/TβRI). Most gene expression responses are thought to be mediated by the TβRI receptor (Derynck et al. 2001; reviewed by David and Massagué 2018). When the receptor heterodimer is former, TβRII phosphorylates TβRI at a glycine and serine rich motif (GS). Downstream to the GS in TβRI is a kinase domain, the kinase domain phosphorylates receptor regulated Smad transcription factors (R-Smads) at the MH1 and MH2 domains, and these phosphoproteins migrate to the nucleus to

implement TGF-β effects on gene expression (figure 1.8). (Santibañez et al, 2011). The R-Smads regulated by TβRI are Smad3 and Smad2. Normally, once phosphorylated Smad2 and Smad3 form a heterodimer before being translocated to the nucleus. The effects of R-Smads are also under the regulation of several cytoplasmic proteins, including other members of the Smad family such as common mediator Smads (co-Smad) and inhibitory Smads (I-Smad). Smad3 phosphorylation is commonly used to indicate TGF-β pathway activation (Santibañez et al. 2011).

TGF-β signalling can be regulated at different levels: the sequestration of the ligands by the ECM actively regulates the triggering of the pathway on the neighbouring cells. At the membrane levels interactions of the receptors with several coreceptors can modify the consequent signal to be transduced. The expression levels of intracellular mediators can also alter the event triggered by the activations of the TGF-β signal. The regulations of the signalling pathway were reviewed in detail by David and Massagué (David and Massagué 2018).

An important part of the TGF-β co-receptor complex is Endoglin (or CD109). Endoglin is a glycoprotein consisting of a homodimer of 180 kDa expressed in a broad spectrum of proliferating cells (Cheifetz et al, 1992). Endoglin plays a crucial role in angiogenesis, in cancer growth and in cancer cell migration, and also, regulates important cellular functions such as cell proliferation and cell adhesion (Valluru, et al. 2011). It has been reported that Endoglin deficient mice injected with Lewis lung carcinoma cells, presented reduced tumour vascularization and tumour growth (Düwel, el at. 2007). Endoglin can interact with both TβRI and TβRII, and through this interaction it can regulate the subcellular signalling of these receptors. In endothelial cells, Endoglin interacts with the TGF-β receptor complexes and changes the subsequent phosphorylation pathways (Guerrero-Esteo, et al. 2002; Bernabeu, et al. 2009).

As explained above, the cellular effects of TGF-β include different forms of cell proliferation inhibition, such as cellular arrest in G1 phase of the cell cycle (Mukherjee et al. 2010), promotion of terminal differentiation (Sánchez et al. 1998) and activation of cell death mechanisms (Rotello et al. 1991). Reports also link TGF-β activity (through Smad protein mediation) to epigenetic modifications, such as specific DNA de-methylation and relaxation of the chromatin structure through the

interactions with P300/CBP (reviewed by Bai and Xi 2017). However, in cancer cells, the effects of TGF-β on cell proliferation are altered, and pathway activation does not stop the cell cycle when it is needed. On the contrary, TGF-β stimulation leads cancer cells to proliferate. It also promotes immunosuppression of leukocytes, which would otherwise attack the cancer cells, and it promotes angiogenesis, contributing to the tumour progression (Hanahan & Weinberg 2011; Massagué 2008). Several cancer shows alterations in TGF-β signalling, including colon, gastric, biliary, pulmonary, ovarian, oesophageal, and head and neck carcinomas, (reviewed by Levy & Hill 2006).

The effects of TGF-β signalling are highly dependent on context. This comes from the observation that the regulation of different genes by TGF-β is achieved by the sharing of enhancer element configurations with other cofactors that interact with Smads, and thus the presence or absence of a cofactor in a cell line can make the TGF-β signalling display different patterns of regulation (reviewed by David and Massagué 2018). This characteristic creates a TGF-β signalling feature named “synexpression groups” of co-regulated genes (Silvestri et al. 2008; Gomis et al. 2006; Niehrs & Pollet 1999). The “synexpression groups” are thus genes co-regulated by TGF-β signalling and other elements that interact with TGF-β pathway.

TGF-β is a potent promoter of EMT. This effect has been described in several cancers, such as colorectal, pancreatic and prostate (Heldin et al. 2012). Our current understanding of the role of TGF-β in EMT and cancer still does not allow the use of TGF-β pathway inhibition in patients treatment (Biswas et al. 2007; Jones et al. 2009) mostly due to the highly context-dependent nature of TGF-β regulation (Massagué 2008; Massagué 2012; Gupta & Maitra 2016). Better understanding of the context in which TGF-β promotes its effects in each tumour could, in the future, help to direct treatments. This study will show that a novel EMT-TF regulates EMT in prostate cancer by regulating TGF-β signalling.

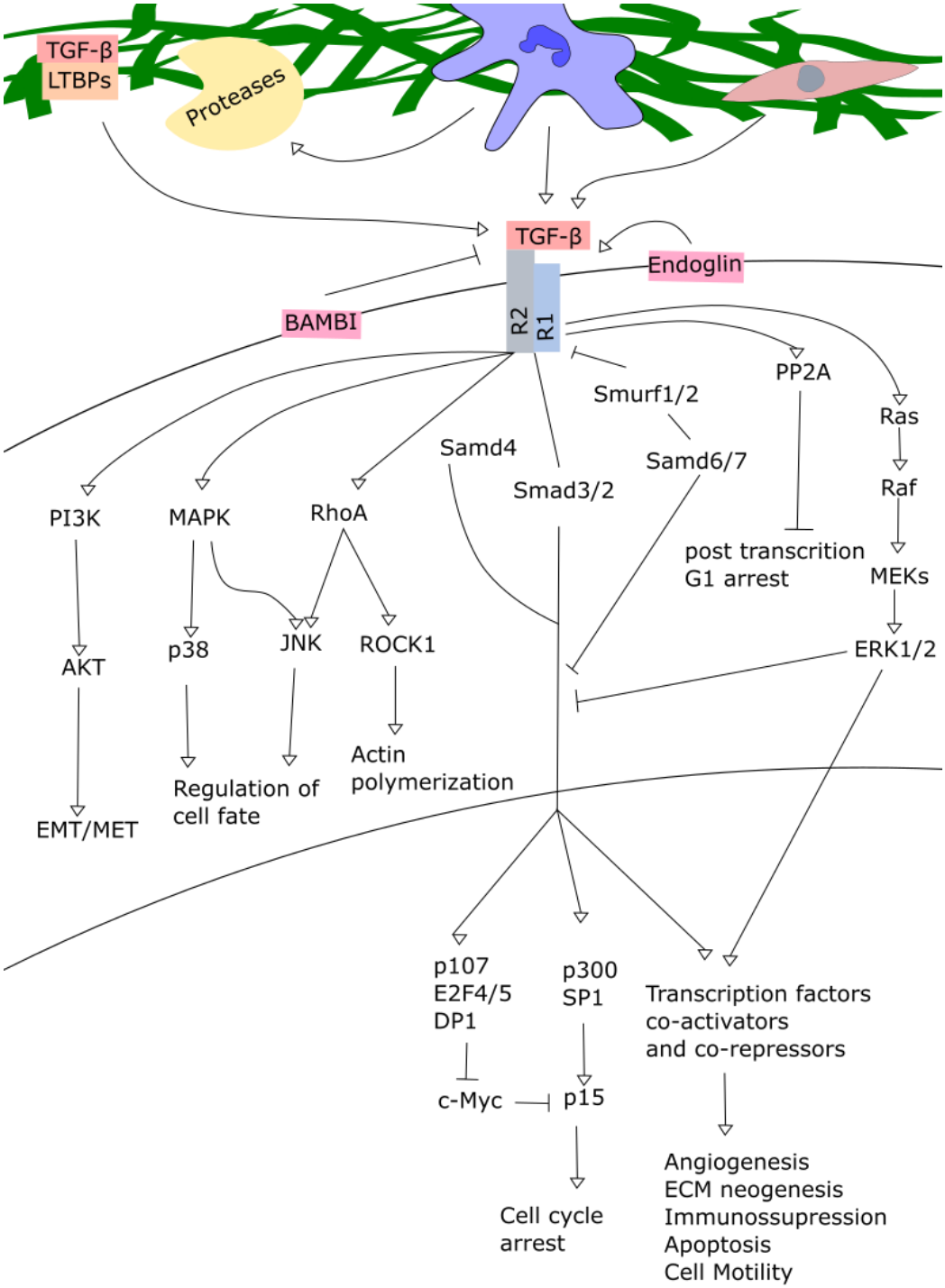

Figure 1.8. TGF-β Signalling pathway. TGF-β that is produced by stroma cells, immune cells and cancer cells is sequestrated by the ECM through latent TGF-β binding proteins (LTBPs). Rearrangements of the ECM and proteases can release and activate TGF-β. The TGF-β ligand binds to a hetero dimer of TGF-β receptor 1 (R1) and TGF-β receptor 2 (R2) creating an intracellular signalling cascade. Several cell membrane co-receptors can regulate intracellular response following TGF-β receptor activation. Among them are Endoglin and BAMBI TGF-β co-receptors. TGF-β intracellular signals through a broad range of mediators influencing different cellular functions. The classic TGF-β intracellular mediator is the Smad protein superfamily, however, several other pathways are reported to be activated by TGF-β receptors activation upon TGF-β ligand binding.

Platelets

Platelets are anuclear cells derived from megakaryocytes in the bone marrow. The process of blood cell formation in the bone marrow consists of a sequence of cell number expansion steps initiated by a stem progenitor cell and each step of this process leads to a higher cellular differentiation degree (Parise 2016). In the case of platelets, initially, the colony forming unit CFU-GEMM (colony forming unit that generates myeloid cells) is stimulated by cytokines such as IL-1, IL-3 andIL-6 to mature into a high proliferative potential–colony-forming unit–megakaryocyte (HPP-CFU-MK). In the next generation of cells, a burst-forming unit–megakaryocyte (BFU-MK) is generated, this is able to make a clonal expansion creating several megakaryocytic colony-forming units (CFU-Meg), The CFU-Meg undergo maturation steps generating megakaryoblasts, that are the precursors of the megakaryocytes which produce platelets (Naeim et al. 2013).

The major function of platelets is in homeostasis of the blood. Platelets play an important role in injury resolution. In these situations, platelets aggregate to clog the damage to the blood vessel preventing blood loss. In the bloodstream, platelets do not aggregate normally and this keeps the fluidity of the blood (Yip et al. 2005). The inhibition of platelets activation in the blood is through the production of nitric oxide (Riddell & Owen 1999), prostacyclin (Jones et al. 2012) and CD39 (Marcus et al. 2005) by the intact endothelium. However, in the event of an injury, components of the basal membrane of the endothelium (like collagen) bind to receptors present in the platelet's membrane triggering subcellular signals via a tyrosine kinase cascade, which activates the production of thromboxane A2 and decreases the production of prostacyclin (Yip et al. 2005). This initiates platelet aggregation to clog the blood leak (Yip et al. 2005). Platelets are also important in the immune response and inflammation. Platelets have roles in the innate immune response because they can adhere to pathogens within the vasculature, participating actively in their detection, sequestration and destruction (Jenne et al. 2013). Furthermore, cytokines are released when platelets adhere to pathogens recruiting inflammatory cells to the infection site (Jenne et al. 2013). Platelet released cytokines can directly regulate the activity of neutrophils, endothelium and lymphocytes, giving importance to the understanding of platelet functions, especially in pathological events (Jenne et al.

2013). A important immunomodulator molecule secreted by platelets is TGF-β; platelets can release and activate latent TGF-β when they are activated (Labelle et al. 2011; Blakytny et al. 2004a). An increased quantity of circulatory platelets is observed during inflammation, this effect is thought to be a reflection of increased production of IL-6 (Kaser et al. 2001). It was shown that the administration of IL-6 in primates increases the circulating platelet count and has effects on megakaryocyte morphology that result in cell death over long periods of administration (Stahl et al. 1991).

In the cancer context, platelets are reported to play a role in metastasis. Experiments with mice showed that a reduced blood platelets count (thrombocytopenia) was related to reduced metastatic activity of TA3 ascites tumour cells (Gasic et al. 1968). Furthermore, the use of a platelet aggregation inhibitor prevented the bone metastasis of B16 melanoma cells when injected in mice (Bakewell et al. 2003). One of the possible mechanisms through which platelets influence metastasis is surface shielding by platelet aggregation, an effect demonstrated in multiple cancer cell lines (fibrosarcoma, lymphoma and melanoma). Platelet aggregation protects cancer cells from natural killer cells destruction, by simple attaching to them (Toyoshima et al. 1995). Jae Hong Im and collaborators showed that melanoma and sarcoma cells adhere to lung microvasculature independently of platelets adhesion, however, the inhibition of platelets adhesion reduced the permanency of the tumour cells in contact with the lung endothelium (Im et al. 2004). More recently, it was demonstrated that platelets can also provide a stimulatory signal for cancer cells in the circulation. In an elegant experiment, Labelle and colleagues showed that mice lacking TGF-β specifically in their platelets formed less metastases when injected with cancer cells (colon carcinoma and breast carcinoma cells) (Labelle et al. 2011). They also demonstrated that the TGF-β released by platelets is able to activated an EMT program in those cells (Labelle et al. 2011).

Proline Rich Homeodomain

PRH/*HHEX* stands for Proline Rich Homeodomain/ haematopoietically Expressed homeobox. *HHEX* is an orphan homeobox gene, located on chromosome 10, that encodes the protein PRH (Hromas et al. 1993). PRH/*HHEX* is expressed in many tissues of vertebrate animals, both in the adult and embryonic phase (Hallaq et al. 2004; Martinez Barbera et al. 2000). The *HHEX* gene is highly conserved between species, especially in the homeodomain region. PRH is required for several developmental processes during embryogenesis especially in organogenesis of the brain, heart, liver, thyroid and thymus (Thomas et al. 1998; Hallaq et al. 2004; Martinez Barbera et al. 2000). It was shown that PRH knock out (KO) mice were not able to survive gestation. Foetal autopsy revealed malformation in the brain, liver, vascular system and haematopoietic system (Martinez Barbera et al. 2000). In adults, PRH/*HHEX* is required in hematopoietic cell differentiation, being essential to the commitment stages of lymphoid progenitor cells (Goodings et al. 2015). PRH is also implicated in pathological states, including cancer and diabetes (Puppin et al. 2006; Sladek et al. 2007; Gaston et al. 2016).

The PRH protein has 240 amino acids, with a theoretical molecular mass of 30 kDa. However, in SDS-page gels it presents an apparent molecular mass of 37 kDa (Soufi & Jayaraman 2008). The PRH proteins forms oligomers that are highly stable resisting chemically-induced denaturation or high temperatures treatments (Shukla et al. 2012). The protein possesses three domains: The proline-rich N-terminal domain is important for interactions with several proteins including eukaryotic translation initiation factor 4E, Groucho/transducing-like enhancer co-repressor proteins and the promyelocytic leukemic protein (Soufi & Jayaraman 2008). The N-terminal domain can repress transcription when it is attached to a heterologous DNA binding domain such as the GAL4 DBD protein (Guiral et al. 2001). The N-terminal domain is also involved in the inactivation of PRH transcriptional activity. Protein kinase CK2 β subunit interacts with PRH N-terminal domain and the CK2 a subunit phosphorylates the PRH homeodomain at S163 and S177 (Soufi et al. 2009). This phosphorylation abrogates PRH's ability to bind DNA inhibiting its transcriptional activities (Soufi et al. 2009). Furthermore, phosphorylated PRH becomes a target for proteasome processing. The proteasome then cleaves the C-terminal domain of

PRH (Noy et al. 2012). The cleavage product is a stable truncate PRH protein (PRHΔC) that can interact with PRH co-factors sequestering them, this creates a competitive inhibitory effect of PRHΔC on PRH activity at its target genes (Noy et al. 2012).

The second domain in PRH is the homeodomain (HD). The HD is the DNA recognition and binding region. The homeodomain is a 60 amino acids domain that contains a helix-loop-helix motif that can interact with DNA with sequence specificity (Billeter 1996). The specific DNA sequence bound by PRH was identified by gel retardation assays (Pellizzari et al. 2000). PRH can bind to the sequences 5'-CAAG-3' and 5'-ATTAA-3' when they repeat in multiple occasions in an oligonucleotide. Multiple PRH target genes contain repeats of these sequences, for example the *GSC* (gene that encodes the Goosecoid protein) promoter contains many of these sequences (Pellizzari et al. 2000; Williams et al. 2008).

The C-terminal domain is an acidic domain involved in transcriptional trans-activation, by interacting with other transcription factors and co-activators. For example, PRH facilitates the binding of serum response factor (SRF) (a transcription factor) to its binding site in the *SM22α* gene (Oyama et al. 2004). Furthermore, PRH can activate expression of the sodium-dependent bile acid co-transporter (NTCP) promoter only with the presence of the C-terminal domain (Kasamatsu et al. 2004) (figure 1.9).

The expression of PRH can be regulated by different factors in the context of different cell types. The Sp family of transcription factors can activate PRH expression in rat hepatoma and human leukaemia cells (Kikkawa et al. 2001). Meanwhile, GATA-1, GATA-2 and c-Myb activated PRH expression in leukaemia cells (Sato et al. 2004). During organogenesis, Wnt/β-catenin (Zorn et al. 1999), TGF-β (Zorn et al. 1999; Liu et al. 2004), fibroblast growth factor (FGF) (Zhang et al. 2004) and bone morphogenetic protein (BMP) (Shin et al. 2007; Zhang et al. 2004) can all regulate PRH expression. Similarly, TTF-1 (Puppin et al. 2003) and Pax8 (Puppin et al. 2004) can activate PRH transcription in thyroid cells (Puppin et al. 2004). HNF3β and GATA-4 were shown to regulate the PRH promoter in hepatic cancer cells (Denson et al. 2000). Finally, PRH can also regulate *HHEX* gene expression in a positive auto-regulatory feedback loop system (Puppin et al. 2003).

PRH can repress or activate the transcription of different genes, and many PRH targets genes are implicated in cancer progression. PRH represses the expression of *VEGFA* and it's the genes encoding VEGF receptors Vegfr-1 and Vegfr-2, these genes are involved in angiogenesis and are often found up-regulated in different cancers (Noy et al. 2010). Also, PRH represses the transcription of the gene encoding the homeodomain-containing repressor Goosecoid which is involved in EMT and over-expressed in highly metastatic cancers (Williams et al. 2008; Hartwell et al. 2006). *ESM-1* (endothelial cell-specific molecule) is also repressed by PRH (Cong et al. 2006). *ESM-1* is involved in cell migration and it is found over-expressed in some gastrointestinal tract cancers (Cong et al. 2006; Sarrazin et al. 2006). Meanwhile, PRH can up-regulate Endoglin expression, Endoglin is a TGF-β co-receptor that regulates TGF-β signalling (Kershaw et al. 2014). Reports suggests that Endoglin expression can counter the effects of TGF-β in human prostate cancer cells (Lakshman et al. 2011) and mouse skin cancer cells (Perez-Gomez et al. 2007). However, PRH effects can vary depending on the cell line context in which it is inserted, therefore, the extrapolation of its effects to other cells lines should be treated with caution.

PRH also presents post-translational regulation effects. PRH interacts with the translation initiation factor 4E (eIF4E), inhibiting the transport of some mRNAs from the nucleus to the cytoplasm. This mechanism is important for example in the PRH inhibition of Cyclin D1 in leukemic cells (Topisirovic et al. 2003).

Mis-expression or mis-localization of PRH is correlated with the progression of different cancers. For example, in hepatocellular carcinomas (HCC) PRH expression is lost during the progression from well-differentiated tumours (grade II) to poorly-differentiated tumours (grade III) (Su et al. 2012). Additionally, PRH over-expression in HCC cells injected into nude mice reduced tumour growth when compared to the control cells (Su et al. 2012). An example of PRH mis-localization is seen in breast ductal and lobular carcinomas (Puppin et al. 2006). While normal ductal and lobular epithelium show PRH immunostaining in the nucleus and cytoplasm, their cancerous equivalents lack significant nuclear staining for PRH (Puppin et al. 2006). A similar phenomenon is observed in thyroid carcinomas; in normal tissues and thyroid adenomas, the PRH protein is detected in the nucleus and cytoplasm of the epithelial cells, however, in their cancerous equivalents, nuclear expression is lost

(D'Elia et al. 2002). Recently, PRH mis-function was associated with prostate cancer. It was reported that Benign Prostatic Hyperplasia (BPH) samples presented higher staining for phosphorylated PRH than normal prostate tissues (Siddiqui et al. 2017).

Although some progress has been made, the mechanisms that lead to PRH mis-function, mis-expression and mis-localization in cancer progression are not well understood. Part of the reason for this is due to its cell type specific effects. The work presented here will investigate the relevance of PRH in prostate cancer progression and its interaction with the TGF-β signalling pathway, proposing a mechanism that explains how PRH function is disrupted during prostate cancer progression.

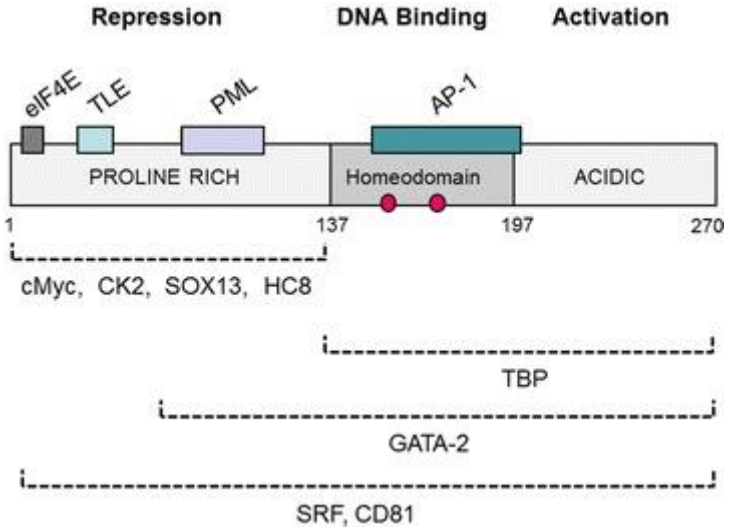

Figure 1.9. The PRH/HHEX protein and its interacting proteins. A diagrammatic representation of the human PRH protein. The PRH protein has three functional domains. The boxed and bracketed areas represent the regions of PRH that interact with the proteins indicated. The brackets indicate poorly mapped interactions. The filled circles represent residues that are phosphorylated by CK2 (Gaston et al. 2016).

Aims

The general objectives of this research project are to elucidate the molecular pathways involved in the EMT processes stimulated by TGF-β in prostate cells, observing the involvement of the transcriptional factor PRH.

To achieve this goal, the specific objectives are:

a) To investigate the influence of TGF-β treatment on EMT and the migratory ability of prostates cell lines.

b) To investigate the role of PRH in EMT processes in these cells by over-expressing its gene.

c) To investigate the co-regulation of EMT and MET by the crosstalk between TGF-β and PRH in prostate cancer cells.

d) To study the possible direct regulation of TGF-β by PRH in prostate cancer cells.

Chapter 2: Methodology

List of chemicals

Table 2.1 – Chemicals	
Reagents	**Manufacturer**
2-Mercaptoethanol	Sigma®
2x Rotor-Gene SYBR Green Polymerase chain reaction Master Mix	Qiagen
Ammonium persulfate (APS)	Sigma®
Bio-Rad protein assay	BioRad®
Bis-acrylamide	Severn biotech ltd®
bromophenol blue	Sigma®
Bovine serum albumin (BSA)	Sigma®
Calcein-acetoxymethyl (Calcein-AM)	Thermo Fisher Scientific
Calcium chloride	Sigma®
Cell Lysis Buffer (10X)	Cell Signalling Technology®
4′,6-diamidino-2-phenylindole (DAPI)	Sigma®
Dimethyl sulfoxide (DMSO)	Thermo Fisher Scientific
Doxycycline	Sigma®
Dynabeads-Protein G	Thermo Fisher Scientific
Ethylenediaminetetraacetic acid (EDTA)	Sigma®
ethylene glycol-bis(β-aminoethyl ether)-N,N,N′,N′-tetraacetic acid (EGTA)	Sigma®
Ethanol	Sigma®
Foetal Bovine Serum (FBS)	Sigma®
G418	Sigma®
Glycerol	Thermo Fisher Scientific
Glycine	Severn biotech ltd®
4-(2-hydroxyethyl)-1-piperazineethanesulfonic acid (HEPES)	Sigma®
Isopropanol	Thermo Fisher Scientific
Lysogeny broth (LB) agar	MP biomedicals™
Lysogeny broth (LB) powder	MP biomedicals™

Lenti-X™ concentrator	Clontech
L-glutamine	Gibco™
LiCl	Sigma®
Methanol	Sigma®
NaCl	Sigma®
Na-deoxycholate	Sigma®
Opti-MEM™	Gibco™
Phosphate buffered saline (PBS)	Sigma®
Polyethylenimine (PEI)	Sigma®
Penicillin/streptomycin	Gibco™
Phenylmethanesulfonyl fluoride (PMSF)	Sigma®
PhoStop™	Roche
Propidium iodide	Sigma®
Proteinase K	Sigma®
RNAse	Sigma®
RPMI-1640 medium	Sigma® and Gibco™
Sodium dodecyl sulphate (SDS)	Sigma®
Sodium bicarbonate	Sigma®
2-ethylhexyl 2,3,4,5-tetrabromobenzoate (TBB)	Sigma®
Tetramethyl ethylenediamine (TEMED)	Sigma®
tetracycline	Sigma®
Transforming growth factor beta 1 (TGF-β)	PeproTech®
Triton X-100	Sigma®
Trizma	Sigma®
trypsin	Gibco™
Tween 20	Sigma®
UltraPure™ distilled water	Invitrogen
Virkon™	Du Pont®

Table 2.2 – Commercial kits	
Kit list	**Manufacturer**
Maxi prep	Qiagen
TransIT®	Mirus®
RNeasy	Qiagen
BM Chemiluminescence (POD)™	Roche
AXYPREP™	Axygen®
QuantiNova™ reverse transcription	Qiagen

Buffers

Table 2.3 – Buffer recipes	
Buffers	
Western blotting	
4X Stacking buffer	0.5M Tris; 0.4% SDS; pH 6.8
4X Resolving buffer	1.5M Tris; 0.4% SDS; pH 8.8
12% SDS-PAGE gel	Distilled water 7 mL; 4X Resolving buffer 5 mL; Bis-acrylamide 8mL; APS200 μl; TEMED 20 μl.
10X Tris Glycine	0.25 M Trizma; 2 M Glycine.
Running Buffer	TRIS Glycine 100 ml; SDS 10 ml (10% stock); Distilled water, add dH2O up to 1000 mL.
5X loading dye	50% Glycerol; 300mM Tris-HCL pH: 6.8; 10% 2-Mercaptoethanol; 5mg/ml bromophenol blue; 10% SDS.
Transfer Buffer	TRIS-Glycine 10x 100 ml; Methanol 200 ml; Distilled water add up to 1000 mL.
Blocking buffer	5% BSA in TBS-T
10X TBS	15 mM NaCl; 2 mM Tris-HCl pH: 7.6.
TBS-T	1.4 mM NaCl; 0.2 mM Tris-HCl pH: 7.6; 0.001% Tween-20.
ChIP	
BUFFER A	10 mM HEPES, pH 8.0; 10 mM EDTA; 0.5 mM EGTA; 0.25 % Triton X-100; 1uM PMSF and 1x PhoStop™.
BUFFER B	10 mM HEPES, pH 8.0; 200 mM NaCl; 1mM EDTA; 0.5 mM EGTA; 0.01 % Triton X-100; 1uM PMSF and 1x PhoStop™.
CHIP BUFFER	25 mM Tris-HCl, pH 8.0; 150 mM NaCl; 2 mM EDTA; 1 % Triton X-100; 0.25 % SDS; 1uM PMSF and 1x PhoStop™.
3X CHIP DILUTION BUFFER	25 mM Tris-HCl, pH 8.0; 150 mM NaCl; 2 mM EDTA; 1 % Triton X-100; 7.5 % Glycerol; 1uM PMSF and 1x PhoStop™.
WASH BUFFER 1	20 mM Tris-HCl (pH 8.0); 150 mM NaCl; 2 mM EDTA; 1 % Triton X-100; 0.1 % SDS.

WASH BUFFER 2	20 mM Tris-HCl (pH 8.0); 500 mM NaCl; 2 mM EDTA; 1 % Triton X-100; 0.1 % SDS.
LiCl BUFFER	10 mM Tris-HCl (pH 8.0); 250 mM LiCl; 1 mM EDTA; 0.5 % NP-40; 0.5 % Na-deoxycholate.
TE/NaCl BUFFER	10 mM Tris-HCl (pH 8.0); 50 mM NaCl.
ELUTION BUFFER	100 mM NaHCO3; 1 % SDS.
Tissue culture	
Complete media	RPMI-1640 medium (Gibco® or Sigma®) supplemented with 10% FBS, 2 mM L-glutamine and 1% penicillin/streptomycin. Filtered sterile.
Starvation media	RPMI-1640 medium (Gibco® or Sigma®) supplemented with 2% FBS. Filtered sterile.
Freezing media (PC3 and DU145)	45% RPMI; 45% FBS; 10% DMSO.
Freezing media (PNT2-C2)	70% RPMI; 20% FBS; 10% DMSO

Plasmids, primers and antibodies

Table 2.4 – Plasmid list		
Plasmid list	**Description**	**Source**
pMDG2	Plasmid encoding the lentivirus coat.	Addgene.
psPAX2	Plasmid encoding the lentivirus packaging protein.	Addgene.
pCLVi(3G)-PRH-CopGFP-IRES-Neo_BamHI-EcoRI	Plasmid with Myc-tagged PRH cDNA downstream to a doxycycline regulated promoter. The plasmid also expresses GFP constitutively and confers resistance to neomycin in mammalian cells. (Plasmid map as Appendix).	Based on pCLVi(3G) by SIRON Biotech.
pMUG1 Myc-PRH	Plasmid expresses human PRH (amino acids 7-270) tagged with the Myc9E10 epitope; under the control of a CMV promoter (Swingler et al. 2004).	Dr. Jayaraman (University of Birmingham).
pMUG1	Plasmid is the empty version of pMUG1	Dr. Jayaraman (University of Birmingham).

	Myc-PRH (Swingler et al. 2004)	
peGFP-C1	pEGFP-C1 expresses enhanced green fluorescence protein.	Dr. Jayaraman (University of Birmingham).

Table 2.5 – Antibodies

Name	Host species	Brand	Dilution	Cat. N.
anti-Hex Monoclonal Antibody, clone 4B7	Mouse	OriGene Technologies®	1:1000	TA500025
pPRH (YKN5)	Rabbit	In house	1:2500	
Phospho-Smad3 (Ser423/425)	Rabbit	Cell Signalling technology®	1:1000	9520
E-Cadherin	Rabbit	Cell Signalling technology®	1:1000	3195
β-Actin	Rabbit	Cell Signalling technology®	1:1000	4970
Snail	Rabbit	Cell Signalling technology®	1:1000	3879
Endoglin	Rabbit	Cell Signalling technology®	1:1000	4335
Vimentin	Rabbit	Cell Signalling technology®	1:1000	5741
Slug	Rabbit	Cell Signalling technology®	1:1000	9585
ZO-1	Rabbit	Cell Signalling technology®	1:1000	8193

β-catenin	Rabbit	Cell Signalling technology®	1:1000	8480
Lamin A/C	Rabbit	Cell Signalling technology®	1:1000	2032
Myc-tag	Mouse	Cell Signalling technology®	1:1000	2276
HRP-Anti-Mouse	Rabbit	Sigma®	1:5000	AP127P
HRP-Anti-Rabbit	Goat	Sigma®	1:5000	AP156P

Table 2.6 – Primers

Name	**Sequence**
E-Cadherin F	GTA ACG ACG TTG CAC CAA CC
E-Cadherin R	AGC CAG CTT CTT GAA GCG AT
***GAPDH* F**	TCC TTG GAG GCC ATG TGG GCC AT
***GAPDH* R**	TGA TGA CAT CAA GAA GGT GGT GAA G
Snail F	GAG GCG GTG GCA GAC TAG
Snail R	GAC ACA TCG GTC AGA CCA
PRH F	AAA CCT CTA CTC TGG AGC CC
PRH R	GGT CTG GTC GTT GGA GAA TC
CH18 F	TTC AGT CTG GTG GTG GTG AAC TA
CH18 R	GCC TTG GGA AAT CCA TCT TTT
-3472 *HHEX* F	TAG AGC AGC ACA GGG TTT GA
-3472 *HHEX* R	GCC TTG ATG TGG ATG AGT GC
Smad7 F	GCA AAT CCT TTC CAT CTC CA
Smad7 R	TGC TTT GTG ATT TGG CAG TC
-4.5K *CDH1* F	AGA GCC AGA AGT GAA TCC AGG
-4.5K *CDH1* R	GTG AAA CCC CAT CTC CCC AA
+4.5K *CDH1*	AGC CTA GTA ACC ACA GCT GT
+4.5K *CDH1*	TCA AGC AGC CAA ACC TCA AC
+54K *TGFB2*	GGA ACC TGT GCT GCT TTG TA
+54K *TGFB2*	AGG TGT GGG TAT GAA CGG AA
-11K *TGFBR2*	TCA AAA CTG TGT TCC TGG CT

-11K *TGFBR2*	AGT TGC AGC CTC AGA TGA CT
+30K *TGFBR1*	ACA GTA TCA GTT GAC CAC ATT GT
+30K *TGFBR1*	AGA AGG GAA ACA GAT GGC ATT
TGFB2	AGG AAA GGC GGG TAA TGG AA
TGFB2	AAG GAC TGC TGG GAT GAC AA
TGFBR2	AAA TGC TGG CTC TAC ACC CT
TGFBR2	GGG GAT GTT GGA CAG GAA GA
TGFBR1	CCC CAC TCC CCA CTT TAC AT
TGFBR1	TGC TGG CTG TAC AAC TCT GA

Experimental protocols

Plasmid amplification

Bacterial strain

Escherichia coli (*E. coli*) XL1 blue: Genotype - recA1 endA1 gyrA96 thi-1 hsdR17 supE44 relA1 lac [F′ proAB laclq ZΔM15 Tn10 (Tetr)].

Preparation of media and agar plates

LB broth was prepared by adding 25g of LB powder to 1L of boiling double-distilled water (ddH2O) and mixing until homogenous, the bottle was labelled, autoclaved at 121^0C for 15 mins and stored at 20°C.

LB agar was prepared by adding 4 capsules of agar to 100mL of ddH_2O, sterilized by autoclaving at 121^0C for 15 mins and stored at 20°C. When needed, the LB agar was melted in a water bath over a Bunsen burner and left on the bench to cool. The relevant antibiotic was added when the temperature of the bottle was comfortable to touch, and 50mL was poured onto sterile disposable Petri dishes.

Preparing competent cells

First, the selection of *E. coli* XL1 blue was performed overnight at 37°C in a LB agar plate containing tetracycline (50 µg/µl). The following day a single colony was picked and inoculated into a starter culture (5 ml LB broth supplemented with 50 µg/µl tetracycline), it was then left to grow in a shaking incubator at 37°C, again overnight. The starter culture was diluted 200 times (100mL final volume) using the same type of broth and incubated in a shaking incubator at 37°C until A600 reach 0.6OD. It was chilled on ice for 10 minutes and aliquoted onto pre-chilled 50mL falcon tubes. The aliquots were centrifuged (Eppendorf centrifuge 5804 R - 5min at 1500 rpm and 4°C) and the pellets resuspended in 5ml ice cold 0.1M $CaCl_2$, then left to rest in ice for 10 minutes. Another centrifugation was performed, and the pellets were this time resuspended in 1ml ice cold 0.1M $CaCl_2$ and incubated for 1 hour. After, 100 µl of 100% glycerol were add to each aliquot, they were further aliquoted into smaller volumes (100uL), snap frozen in liquid nitrogen and stored at -80°C.

Transformations

A 100 μL aliquot of XL1 blue competent cells was thawed on ice and 1 μg of DNA (desired plasmid) was add to it, the mix was left to rest on ice for 30 minutes. Subsequently, a 2 minutes heat shock at 42°C followed by an ice incubation of 1 minute allowed the cells to incorporate the foreign DNA. 700 μL of LB broth was added to the cells, the Eppendorf tube was stuck on to the bottom of a 37°C shaker incubator and left there for 90 minutes, centrifuged (Eppendorf microcentrifuge 5415 - 5000 rpm for 2 minutes) and the pellet resuspended in 100 μl LB broth. LB agar plates were prior poured as aforementioned with the relevant antibiotic selector and left to dry in a 37°C incubator, once dried, the 100 μL bacterial solution was spread across the agar using a plastic sterile disposable inoculation loop. The plate was then inverted inside a 37°C incubator overnight.

A single colony picked from the plate was inoculated onto a starter culture (5mL LB broth) and put into a 37°C shaker for 8h; the starter culture was diluted 500 times into LB broth (this time containing relevant antibiotic selector) and left on the shaker incubator (37°C) overnight. The cells were then harvest by centrifugation (Eppendorf centrifuge 5804 R - 5000 rpm for 5 minutes at 4°C).

Plasmid purification

The plasmids were extracted from cell pellets and purified using Maxi prep kits (Qiagen®) according to the manufacturer's protocol. Purified DNA was quantified using a nanodrop UV spectroscopy (Perkin Elmer lambda 14 UV/Vis spectrometer). The DNA concentration provided by the equipment is calculated using the absorbance at 260 nm (A260) considering A260 of 1.0 = 50 μg/ml pure DNA plasmid; the A260 / A280 ratio is also calculated to determine the purity of the purified DNA plasmid, ratio between 1.9 and 2.1 were considered high-quality plasmid DNA.

Lentivirus production

HEK 293 cells were plated in aT75 flask at the confluence of $8x10^4$ cells/cm^2 and left to settle overnight (day 0). The next morning (day 1), the cells were transfected using the PEI protocol (section 2.5.1). In this protocol two falcon tubes with 20°C Opti-

MEM™ media are prepared (to every T75 flask with cells), one of the falcon tubes received a final concentration of 2 μM of PEI the other one received the DNA constructs to be transfected. For the creation of the PRH carrying lentivirus construct three plasmids were used: pMDG2 (viral coat), psPAX2 (packaging protein) and PRH overexpression plasmid (short for modified pcLVi(3G)-PRH-CopGFP-IRES-Neo_BamHI-EcoRI). The three plasmids were added to the Opti-MEM™ media in the following quantities: 6.75 μg of pMDG2, 18.75 μg of psPAX2 and 25 μg of PRH overexpression plasmid. The contents of each falcon tube were filtered (0.2 μm pore filter) into a common fresh sterile falcon tube and the DNA-PEI mix was incubated under a fume hood for 20 minutes. The HEK 293 cells in the T75 flasks were washed with warm Opti-MEM™, and the DNA-PEI mix was added to it. The flasks were incubated in tissue a culture incubator for 4 hours at 37°C. After, the PEI-DNA mixture was aspirated using a vacuum pump attached to a sterile disposable Pasteur pipette and fresh media (10 mL per flask) was added to the flasks. The transfected cells were incubated for 48 hours at 37°C. After (day 3), the first viral harvest was performed. The 10 mL media containing lentivirus was pipetted out and safely stored in a 50 mL falcon tube at 4°C. Another 10 mL of fresh media was added to the cells and the flasks put in the incubator for another 24 hours. Next (day 4) a second harvest was made, the media extracted was added to the media stored on the previous day. The left-over cells and virus were terminated with Virkon™ and properly disposed. The media collected on the two harvests was filtered through a 0.4 μm pore filter to remove any cells or debris that might be present. Lenti-X™ concentrator (final volume was 1/3 of the total volume of viral solution) was used to concentrate the lentiviruses. The solution was incubated for 30 minutes at 4°C, after, the tubes were centrifuged (1500 xg at 4°C for 45 minutes). The supernatant was carefully decanted and properly discarded, and the viral pellet was resuspended in 1mL of media to be frozen and stored at -80°C for use. All the materials used were properly disposed into a sweet jar and taken for autoclaving and incineration.

Human tissue culturing and cell storage

Media requirements

PNT2-C2 is an adherent cell line derived from a normal human prostatic epithelium immortalized by the transfection with SV40 DNA. These cells present a definite epithelioid shape and grow as colonies until full confluency. They express cytokeratin 8, 18 and 19, while PSA and PAP were not detected in these cells. This cell line is dependent in serum to grow on culture and its doubling time in 10% serum media is approximately 36h (Berthon et al. 1995).

PC3 is an adherent cell line isolated from a bone metastasis of a prostate adenocarcinoma. They are cells of epithelial origin that form clusters in soft agar. They present a reduced dependency to serum and do not respond to androgens, glucocorticoids or epidermal or fibroblast growth factors. Its karyotype is aneuploid in the hypotriploid range . There are nearly 20 marker chromosomes commonly found while several normal markers are not found (N2, N3, N4, N5, N12, N15 and normal Y chromosomes). It expresses the antigens HLA A1 and A9 (Kaighn et al. 1979).

DU145 is an adherent epithelial cell line isolated from a brain metastasis of a prostate adenocarcinoma. These cells grow in isolated islands on plastic and form colonies on soft agar. This cell line is hypotriploid with 64 chromosomes, the karyotypic analysis showed translocation Y chromosome, metacentric minute chromosomes and three large acrocentric chromosomes, while N13 is absent. This cell line expresses the antigens Blood Type O and Rh+ (Stone et al. 1978).

PC3 and DU145 were both cultured in RPMI-1640 medium (Sigma®) PNT2-C2 cells in RPMI-1640 medium (Gibco®). All the culture media was supplemented with 10% FBS, 2 mM L-glutamine and 1% penicillin/streptomycin. The PC3 PRH overexpression cell line was derived from the PC3 line and created by Lentivirus transduction and subsequent selection (explained in the sections ahead), they were cultured in RPMI-1640 medium (Sigma®) supplemented with 10% FBS, 2 mM L-glutamine and 1% penicillin/streptomycin 3mg/mL G418. All cells were maintained in a humidified atmosphere at 37°C and 5% CO_2 during the selection steps, after they were grown in the same media as PC3 cells. The HUVEC cells used by Dr. Siddiqui

in extravasations assays were obtained from Promocell, they were maintained and grown in Promocell Endothelial Cell Growth Medium.

Cell counting

The cell suspension was placed by capillarity inside a Neubauer chamber, the chamber was observed under a bright field inverted microscope (CETI – Belgium) and the cells inside four 1 mm squares were counted. The average number of cells in the fours squares was used to calculate the cell concentration as follows. Each mm inside the chamber holds $0.1mm^3$, 1mL is equivalent to $1cm^3$, so by multiplying the average by 10^4, we obtain the number of cells/mL.

Storage of cells

Two storage methods were used to guarantee a viable stock in case of adversity. The cells were permanently stored in liquid nitrogen or a -80°C freezer. Briefly, Cells were resuspended in freezing media (45% RPMI; 45% FBS; 10% DMSO (PC3 and DU145) 70% RPMI; 20% FBS; 10% DMSO (PNT2-C2)) at $5x10^5$cell/mL density and aliquoted into cryovials. The vials were placed into a Mr Frosty™ and it was placed into the -80°C freezer for 24h. Afterwards frozen the vials were transferred to permanent storage in liquid nitrogen until required.

Transient transfection methods in human cells

Poly(ethyleneimine) (PEI)

PEI was used to transfect cells with plasmids. PEI self-assembles with nucleic acids to form polyplexes, PEI also acts as buffer, which helps the nucleic acids escape the endosome. The DNA PEI complexes were built in Opti-MEM™. Two experiment tubes were filled with 3.125 mL of Opti-MEM in the first tube, 2 μM of PEI was added, to the second the DNA to be transfected. The content of the two tubes were filtered through a 0.2 μm filter inside a third sterile tube and left at 20°C for 20 minutes. Meanwhile the plated cells (80% confluency) were washed with warm Opti-MEM™. After incubation the media was removed from the cells and the Opti-MEM containing the PEI DNA complexes were add to them. The plates were placed back in the tissue culture incubator and left there for 4 hours at 37°C. Next, the Opti-MEM containing the PEI-DNA complexes was removed and normal complete media was

added to the cell monolayer. After a 24h recovery step, the experiments were conducted.

Trans-IT® prostate transfection kit

TransIT® prostate transfection kit (Mirus, Madison, WI) was used following the manufacturer's protocol to transfect prostate cells. The cells were plated overnight prior to transfection (3.4 x 10^4 cells/cm^2). The appropriate transfection ratios TransIT reagent: DNA: Boost reagent were determined in previous standardization experiments and were: PNT2-C2 - 2.5:12.5; PC3 – 2.5:1:1.

Stable cell lines

A vial of PRH overexpression lentivirus (to preparation details refer to section 2.4.2) solution was thawed on ice. Appropriate quantities (3x10^5 cells per well) of PC3 cell suspension were incubated with the content of the lentivirus vial for 10 minutes at 20°C in a sterile falcon tube. Afterwards, the mix of cells and virus were plated at a confluency of 3.4 x 10^4 cells/cm^2 and left to settle for 24 hours (day 0), a no-virus control was also plated. Next day, the media content of each well was removed, placed into a tube with Virkon™ and properly disposed of. Fresh media was then added to each well and the cells were incubated again for another 48 hours (day 1). On day 3, the cells were taken to an inverted epifluorescence microscope to verify GFP expression. Afterwards, antibiotic (G148 2 mg/mL) was added to start the selection the transduced cells. The cells were observed daily and media with G148 was changed ever two days. Selection was carried for two weeks in the plate where the cells were originally plated. During this time, all the cells in the no-virus control died from the selection, and a few cells survived the selection in the PRH overexpression virus infected wells. The surviving cells were expanded and occupied nearly all the surface available, at this point, cell pictures were taken, and the cells were passaged to a bigger flask (T25 flasks). The media removed from the infected cells was treated as virus containing media for 2 passages, and the cells were kept in selection media for 3 passages. At this point there were several flaks confluent with PC3 PRH LV cells. They were harvested and resuspended in freezing media the cells were frozen into a Mr. Frosty™ at -80°C for 24 hours to be subsequently stored in liquid nitrogen, ready to be thawed and used when necessary.

The stable cell line generated here is polyclonal. Arguably, monoclonal lines can offer better reproducibility over several passages, due to the higher possibility of epigenetic silencing of the cloned gene in polyclonal lines. However, the insertion of the lentiviral vector is random, and polyclonal lines can compensate for positional effects from the site of integration, because they possess different places of insertion in different cells. Additionally, the heterogeneity observed in polyclonal lines can be considered advantageous, as cancer tumour cells presents a vast heterogeneity, so the effects studied *in vitro* would also be subjected heterogenic conditions. Therefore, the choice to work with a polyclonal line was considered appropriate for this study.

Experimental design

TGF-β treatment.

Molecular analyses and migration

Prostate cells were plated at the confluency of 1.7 x 10^4 cells/cm^2 and left to settle overnight (day 0). Next morning, the cells received appropriate treatment (Vehicle, TGF-β, TGF-β + TBB, TBB or platelets 1:1 ratio) (day 1) and were incubated for 48 hours. On the third day, the cells were harvested using appropriate cell dissociation solution (trypsin was used to pPRC and western blotting experiments, and non-enzymatic cell dissociation solution was used if the cells were to be used in ChIP-qPCR assays), in cases where trypsin was used, complete media was used to neutralize it. The concentration of the solution with cell suspension was counted using a haemocytometer (as described in section 2.4.4.2). The solution was then centrifuged at 20°C to a speed of 1000 RPM (Centurion centrifuge) for five minutes. The pellets were either frozen and stored at -80°C or further processing was carried out, according to the experiment in which the cells would be used.

Immunofluorescence analyses

A sterile square cover slip (22x22 mm and ~0.25mm thick) was placed in the bottom of a 6-well plate. Prostate cells were plated onto these cover slip-containing plates at the confluency of 1.7 x 104 cells/cm2 and left to settle overnight (day 0). Next

morning, the cells received appropriate treatment (Vehicle or TGF-β) (day 1) and were incubated for 48 hours. On the third day, the media was aspirated using a vacuum pump attached to a sterile disposable Pasteur pipette and the wells were washed with sterile PBS twice. The cells were fixed using appropriate fixing agent (4% paraformaldehyde) for ten minutes. The paraformaldehyde was pipetted out and properly disposed. Meanwhile, the wells were twice washed again using PBS. The cover slips containing cells were used for immunofluorescence staining or kept in 4°C for a maximum of 4 days before staining.

PRH overexpression experiments

Molecular analyses and migration

Adenoviral overexpression

The adenovirus used were made and purified by Dr Graciela Sala-Newby. PC3 cell suspension was incubated with each adenovirus (ΔE1, PRH, PRHCC or PRHM1) or no virus control at 100 MOI for 10 minutes at 20°C in a sterile falcon tube. Afterwards, the mix of cells and virus were plated at a confluency of 3.4 x 10^4 cells/cm^2 and left to settle for 24 hours (day 0). Next day, the media containing virus was pipetted out into a 50 mL falcon tube containing Virkon™ and properly disposed of. Fresh media was added to the cells and they were left to recover for another 24 hours (day 1). On day 2, the cells received treatment (with TGF-β or vehicle) or left in the incubator for another 48h. On day 4, the cells were harvested using appropriate cell dissociation solution (trypsin was used for qPCR and western blotting experiments, and non-enzymatic cell dissociation solution was used if the cells were to be used in ChIP-qPCR assays), in cases where trypsin was used, complete media was used to neutralize it. The concentration of cells was determined using a haemocytometer (as described in section 2.4.4.2). The solution was then centrifuged at 20°C to a speed of 1000 RPM for five minutes (Centurion centrifuge). The pellets were either frozen and stored at -80°C or further processing was carried, according to the experiment.

Stable cell line

PC3 PRH LV (For preparation details refer to section 2.6) cells were plated at the confluency of 1.7 x 10^4 cells/cm^2 with addition of 2 ug/mL of doxycycline or vehicle to

the media (day 0). Doxycycline was reconstituted in water and filtered sterilized to a stock concentration of 2mg/μL, the stocks were kept up to 4 weeks at 4ºC. The cells were then incubated for 7 days, but fresh doxycycline and media was added daily. If the cells were close to reaching confluence they were passaged to a bigger surface. At the seventh day, the cells were either harvested or brought to an inverted phase contrast microscope for image acquisition. The harvesting was carried out using trypsin and complete media was used to neutralize the trypsin. The concentration of cells in the cell suspension was determined using a haemocytometer (as described in section 2.4.4.2), and the cells were then centrifuged at 20°C to a speed of 1000 RPM (Centurion centrifuge) for five minutes. The pellets were either frozen and stored at -80°C or further processing was carried out.

Trans IT transfection

PC3 cells were plated at the confluency of 3.4 x 10^4 cells/cm^2 in a 6-well plate and left to recover overnight (day 0). Next morning, the cells were transfected with the Trans-IT reagent as explained in the section 2.5.2 (day 1). After transfection the cells were incubated for 48 hours. At day 3 the cells were harvested using trypsin and complete media was used to neutralize trypsin after detaching. The concentration of cells was determined as above (as described in section 2.4.4.2). The solution was then centrifuged at 20°C to a speed of 1000 RPM for five minutes, and the cells were used for migration assays.

Cell migration

The cells used in this assay came from the treatments described in sections 2.7.1.1, 2.7.2.1.1 , 2.7.2.1.2 and 2.7.2.1.3. Cell migration assays were performed as described previously (Kershaw et al 2014). Briefly, chemotaxis assays were performed by seeding cells into 200 μl Boyden chambers (Greiner Bio-One) in RPMI medium with 2% FBS in 24-well plates containing 800 μl complete media. After, the media was removed from both chambers, serum free media with Calcein-AM was added to the bottom chamber and incubated for one hour. The media was then removed, and the wells were washed with PBS twice. Warm trypsin (500 μl 37°C) was added to the bottom chamber and incubated for 10 minutes with gentle shaking being applied every 2 minutes. 200 μL cell suspension in trypsin were placed into a

black flat-bottom 96-well plate and read in fluorescent reader flex station (wavelength: 495 nm excitation and 515 nm emission). The results were fitted to a standard curve by linear regression to obtain the total number of migrated cells. The total migrated cells were divided by the total seeded cells to obtain the percentage of migrated cells.

Protein detection

Western blotting

Protein extraction

The pellets used in this assay came from the treatments described in sections 2.7.1.1, 2.7.2.1.1 and 2.7.2.1.2. The pellets were defrosted on ice and resuspended in 50 μl of 1x cell lysis buffer (Cell signalling® added 1uM PMSF and 1x PhoStop™). The solution was then put in a water bath sonicator (Ultrawave™) with ice cold water for 10 minutes. The extracts were centrifuged (Eppendorf microcentrifuge 5415 - at 11000RPM; 5min; 4°C) and 42 μl of the supernatant (protein extract) were placed in a labelled fresh tube.

Sample preparation

2 μl of the protein extract were used to determine the total protein concentration using the Bio-Rad® protein assay, following manufacture instructions and comparing the reads to a standard curve made with different concentrations of BSA. Subsequently, 10 μl of 5x Loading dye were added to the remaining 40 μl of protein extract, and the solution was boiled at 95°C for 5 minutes, the concentration was adjusted and the samples stored at -20°C until needed.

Electrophoresis and western-blotting.

Before loading into a 12% acrylamide SDS-PAGE gel, the samples were thawed and heated again at 95°C for 5 min. 5 μg of total protein were added to the gel and the loading order was registered. The gel was run at 180 V until appropriate separation was observed by the coloured ladder control. The proteins were then transferred to a PVDF membrane using the BioRad® wet transfer system at 240 mA for 2 h. The

membrane with the proteins was blocked with 5% BSA in TBS-T overnight (ON) Next morning the primary antibody on appropriate concentration were diluted in 5% BSA in TBS-T and used to replace the blocking solution, the membrane was placed on a rocker at 20°C for 1 h and 30 min, followed by 3x10 min washes using TBS-T. The secondary antibody was properly diluted in 5% BSA in TBS-T, added to the membrane and placed on the rocker at 20°C for 1h, followed by 3 sets of washes as described previously.

The luminescent reaction was made using BM Chemiluminescence (POD)™. Membranes were dipped into the solution for one minute and placed on a radiography cassette. The membranes were exposed to a radiography film and developed using an automatic radiography developer.

Immunofluorescence

The cells used in this assay came from the treatment described in sections 2.7.1.2. Permeabilization solution was added to cover slips carrying the fixed cells (500µl 0.2% Triton X-100/PBS on ice for 15min. The cells were then washed 4 times with PBS to completely remove all detergent, followed by addition of 500µl of 3% BSA/PBS and incubated for 20min at 20°C to block non-specific binding. The cells were then washed 3 times with PBS and 200µl of the desired primary antibody at appropriate dilution (in PBS) was then carefully added to cover all cells and incubated for a further 1h at 20°C. The cells were again washed three times with PBS before adding 200µl of the desired secondary antibody and incubated for 50min, in the dark, at 20°C. Finally, the cells were washed twice with PBS, and incubated with DAPI for 10 minutes. The DAPI was washed with PBS another two times and the coverslips were mounted with Immuno-Mount™ onto microscope slides. The coverslips were then sealed with nail varnish. Mounted coverslips were kept in the dark for at least 30min before imaging. Fluorescence microscopy was carried out using a Leica Q550 epifluorescence microscope fitted with DAPI, GFP, and TRITC filter sets.

Acid nucleic detection

qRT-PCR

The pellets used in this assay came from the treatments described in sections 2.7.1.1, 2.7.2.1.1 and 2.7.2.1.2. Quantitative reverse transcriptase-mediated PCR (qRT-PCR) was performed as described previously (Kershaw et al., 2014) in quadruplicate for the gene of interest and Glyceraldehyde-3-phosphate dehydrogenase (*GAPDH*) was used as an internal control. Data were analysed using Rotorgene 6 software (Corbett Research; Rotorgene RG-3000) and the fold-change determined using the efficiency adjusted quantitative PCR method (Kershaw et al. 2017).

ChIP-qPCR

Cells were treated as explained in sections 2.7.1.1 and 2.7.2.1.1. Cells were pelleted and resuspended ($1x10^7$ cells per 5 ml of complete media). The cells were fixed by adding a final concentration of 1% methanol free paraformaldehyde for 10min at 20°C. Glycine was then added to stop the cross-linking reaction, to a final concentration of 0.4 M, and then the cells were pelleted by centrifugation for 5 min at 300 x g, 4°C, followed by two washes of the pellet in ice cold PBS. The pellet was resuspended in 5 ml of ChIP buffer A and incubated on rocker for 10 min at 4°C, next the solution was centrifuged for 5 min at 500 x g, 4°C. The pellet was then resuspended in ChIP buffer B and incubated at 4°C for another 10 min, to be subsequently pelleted down (5 min at 500 x g, 4°C), obtaining a nuclei pellet, which can be snap frozen or used immediately after centrifugation.

After thawing, the nuclei pellet was resuspended in 1 ml ChIP buffer and disrupted on a vibra cell™ with a micro tip sonicator. The solution was kept on ice for 20 minutes prior to disruption. The sonication cycles were set to 1 second pulse followed by 3 seconds rest at 60% power, where one cycle consisted of 4 pulses. Each sample received 3 cycles. Between cycles the samples were kept on ice for at least 3 minutes. The disruption was followed by a 10 min centrifugation at 16000 x g 4°C, the supernatant was transferred to a fresh Falcon tube and 500 μl of 3x ChIP dilution buffer was added.

The samples were divided in 3 different Eppendorf tubes, 675 μl for the target antibody (pSmad3 or Myc-tag), 675 μl for the normal rabbit IgG antibody and 150 μl for the input control. 5 μl of the relevant antibody and a final concentration of 0.5% BSA were added and the samples were incubated on a rotating wheel at 4°C overnight. Next morning, enough Dynabeads-Protein G (10 μl per IP) were placed in a fresh tube and washed twice in phosphate buffer (pH 8.0). The beads were then resuspended in 0.5% BSA in phosphate buffer (pH 8.0) (10 μl per IP). Subsequently, 10 μl of beads suspension was add to each sample and incubated at 4°C for 4 h.

The beads were separated using a magnetic rack and a series of washes followed by magnetic separations were performed: 1 x Wash buffer 1; 2 x Wash buffer 2; 1 x LiCl buffer and 2 x TE/NaCl buffer. The beads were then transferred to a fresh tube and elution proceeded with 50 μl of Elution buffer, on shaker for 15 min at 20°C. The beads were magnetically separated and the eluate transferred to a fresh tube and the elution step repeated, and the second eluate mixed with the first one.

To reverse the crosslink, 1 μl of RNAse A (10 mg/ml) were add and samples incubated for 30 min at 20°C. Next, 1 μl of NaCl (5M), 2 μl of EDTA (0.5 M) and 1 μl of Proteinase K (50 mg/ml) were add and the samples incubated overnight at 60°C. The DNA was purified using AXYPREP™ magnetic PCR clean-up kit, following the manufacturer's instructions.

Quantitative PCR for ChIP samples was performed using 2x Rotor-Gene SYBR Green PCR Master Mix. For each primer pair, a Master Mix was produced (1.06x SYBR Green PCR Master Mix; 2.5 uM Reverse primer; 2.5 uM Forward primer) and aliquoted (8.5 μl per tube) onto QIAGEN® strip tubes and 0.5 μl of the sample added to the master mix. Each qPCR was performed in 4 replicates, with DNA from 3 independent experiments. The analysis was performed as published by Miller and Palhan (2008) and the results expressed as percentage of input.

Propidium iodide staining

PC3 PRH LV cells were plated in 6-well plate plates at a confluency of 1.7 x 10^4 cells/cm^2 with addition of 2ug/mL of doxycycline or vehicle to the media (day 0). The cells were incubated for 7 days, but fresh doxycycline and media was added daily, if the cells were close to reaching confluence they were be passaged to a bigger flask.

One of the wells treated with vehicle were chosen to become the positive control, and on day 6, high concentrations of G418 (9 mg/mL) were added to the chosen well, and the plate was incubated for another day. Next day (day 7), the media was aspirated using a vacuum pump attached to a sterile disposable Pasteur pipette and the wells were washed with sterile warm PBS twice (37°C). Warm PBS (37°C) was left in the wells and the plates were taken to an inverter epifluorescence microscope to acquire images.

Image analyses

Cell counting

Images obtained from the propidium iodide staining were opened on ImageJ (Schindelin et al. 2015). Each image was obtained with the same microscope and camera settings; therefore, each image was considered a microscope view for the purpose of counting. The setting for brightness and contrast were adjusted with the automatic settings in ImageJ. In each image field all of the propidium iodide stained cells were counted for a total of 10 fields/sample.

Morphometry

The images from the β-actin staining were opened in FIJI/ImageJ software (Schindelin et al. 2015). The images were saved in a stack with each two channels in a separate layer. The function ‘stack to images’ was used to separate the images. The option ‘merge channels’ was used to create a merged coloured image of the cells. In the ‘set measurements’ folder, the ‘fit ellipse’ option was selected. Using the tool ‘free hand selection’ each cell was circled as close as possible to the edge delimited by β-actin. The function ‘measure’ was activated after each cell was circled. The results were fed into a spreadsheet with 4 columns labelled: Label, Major, Minor, Angle. The Major column values were divided by the Minor column values to obtain the L/S ratio. A total of 150 cells per slide were measured across 15 fields of view.

Gleason scoring

The immunohistochemistry images were obtaining by slide scan and kindly supplied by Dr. Sheela Jayaraman (University of Birmingham). The file had 96 prostate samples with different degrees of neoplasia, ranging from benign prostate hyperplasia (BPH) to advanced prostate adenocarcinoma. The images were opened in ZEN (Zeiss 2018). First, they were scored following Gleason's scoring system for prostate cancer with the description modifications made by the 2005 International Society of Urological Pathology (ISUP) Consensus Conference on Gleason Grading of Prostatic Carcinoma (table 7).

On another occasion, the samples were randomised and blindly re-accessed to obtain a scoring for PRH staining. The scoring system was carried as follows: Two factors were considered during the staining scoring. The first was the intensity of the staining, there were 3 degrees of intensity considered: weak, moderate and strong. The weak signals were given a score 1, the moderate a score 2 and the strong a score 3. The second factor was the frequency of the staining that was observed. The frequency was given in percentage ranging from 0% to 100%. The intensity score was multiplied by the frequency to obtain a PRH staining factor. This procedure was made for both nuclear and cytoplasmic staining. The results from the two spread sheets were cross analysed using the Pearson's correlation test.

Table 2.7. 2005 ISUP Modified Gleason System

Pattern 1:

Circumscribed nodule of closely packed but separate, uniform, rounded to oval, medium-sized acini (larger glands than pattern 3).

Pattern 2:

Like pattern 1, fairly circumscribed, yet at the edge of the tumour nodule there may be minimal infiltration;

Glands are more loosely arranged and not quite as uniform as Gleason pattern 1.

Pattern 3:

Discrete glandular units;

Typically, smaller glands than seen in Gleason pattern 1 or 2

Infiltrates in and amongst nonneoplastic prostate acini

Marked variation in size and shape

Smoothly circumscribed small cribriform nodules of tumour;

Pattern 4:

Fused micro acinar glands;

Ill-defined glands with poorly formed glandular lumina;

Large cribriform glands;

Cribriform glands with an irregular border;

Hypernephromatoid (resembles renal cell carcinoma).

Pattern 5:

Essentially no glandular differentiation, composed of solid sheets, cords, or single cells

Comedocarcinoma (central necrosis within involved ducts) with central necrosis surrounded by papillary, cribriform, or solid masses.

(Epstein et al. 2005)

Densitometry

Western blotting images were obtaining by scanning the radiography films (add the fume type). The images were opened using the '1D gel analysis' tool from ImageQuant (GE healthcare). The lanes for analyses were made manually and all had the same dimensions. The 'automatic background subtraction' tool was used with the radius set to 200. The bands were detected using the 'click and detect wand' tool. The volume subtracted from the background was used in normalization steps. To normalise the expression of interested proteins, the volume of their bands were divided by the volume of the loading control bands.

MTT

Cells were treated as described in section 2.7.2.1.2. After treatment, the cells were harvested and re-plated at the confluence of 3.1 x 10^4 cells/cm^2. They were then incubated in tissue culture at 37°C overnight to settle. Next morning, 10 μl of tetrazolium Bromide (4 μg/μl) was added and the plate incubated for 4 hours. Afterwards, the media was aspirated using vacuum pump and the plate was left to air dry for 15 minutes. Next, 150 μl of DMSO was added, the colour was measured using VersaMax™ microplate reader (at 540 nm and 630 nm), and the 540 nm absorbance was subtracted from the 630 nm absorbance.

EdU incorporation

Cells were treated as described in section 2.7.2.1.2. After treatment, the cells were harvested and re-plated at the confluence of 3.1 x 10^4 cells/cm^2. The EdU incorporation and detection was carried using the Click-iT® EdU Microplate Assay kit, following the manufacturer's instructions.

Dose response

PC3 cells were seeded at 3.4 x 10^4 cells/cm^2 in a 96-well plate and left to recover overnight (day 0). Next day increasing concentrations of Doxy or G418 were added. The plates were incubated for 48h then10 μl of tetrazolium bromide (4 μg/μl) was

added and the plate incubated for 4 hours. Afterwards, the media was aspirated using a vacuum pump and the plate was left to air dry for 15 minutes. Next, 150 μl of DMSO was added, the colour was measured using VersaMax™ microplate reader (at 540 nm and 630 nm), and the 540 nm absorbance was subtracted from the 630 nm absorbance.

Statistical analysis

All statistical analyses were made using GraphPad Prism® (GraphPad Software 2018). For the results expressed in fold-change, the statistical analysis used a was one-sample t-test to compare the column mean the 1. The error bars are standard error of the mean (SEM). The variables were considered statistically different when the p value was equal to or lower than 0.05.

For the numerical variables with normal distribution such as percentage of migration and optical density, a two-tailed unpaired t-test was performed. The error bars are SEM, and variables were considered statistically different when the p value was equal to or lower than 0.05.

For the numerical variables with multiple group comparison such as percentage of input. Standard two-way ANOVA followed by Bonferroni post-test to compare all the variables to the background (ΔE1 IgG ChIP) was used. Statistical relevance was accepted when the p value was equal to or lower than 0.05.

All correlation tests were made with the Pearson's correlation test assuming that the data presents a normal distribution with the p values analysed by a two-tail test. A p value lower than 0.05 meant that the correlation was statistically significant. The Pearson's r value was used to determine how strong the correlation was. Values approximately between 0 and +/- 0.5 were considered a weak correlation, values approximately between +/- 0.3 and +/- 0.7 were considered a moderate correlation and values approximately between +/- 0.7 and +/- 0.99 were considered a strong correlation. The r^2 values were used to express how much of the variability in the first variable were explained by the second variable in percentage.

Chapter 3: TGF-β induces partial EMT and increased cell migration in prostate cell lines.

Introduction

TGF-β is known to induce EMT in some cells (Massagué 2008). The aim of this chapter is to characterise the EMT effects of TGF-β treatment on two prostate cell lines (PNT2-C2 and PC3) and to examine the effects that this treatment has on the migratory behaviour of these cells. Setting the milestones that will be used in the next chapters. PNT2-C2 is a normal immortalised prostate epithelial cell line that displays epithelial morphology and expresses typical epithelial markers such as E-cadherin. PC3 is a prostate adenocarcinoma cell line isolated from a prostate adenocarcinoma bone marrow metastasis. PC3 displays a mesenchymal morphology in culture and express low levels of epithelial markers like E-cadherin. Actin immuno-staining will be used to analyse cell morphology and images will be analysed using Fiji (Schindelin et al. 2015) for cell measurements. Cell migration will be measured with a chemotaxis assays performed in Boyden Chambers. Western blotting and qPCR will also be used to find molecular markers that change with TGF-β treatment.

Results

Morphological characterization of TGF-β treated PNT2-C2.

Cells morphology was assessed by observation of cellular β-actin through immunofluorescence microscopy. β-Actin is a component of the cell cytoskeleton, that can be stained by immunofluorescence to study the cell morphology. As described in section 2.9.2, the cells were grown on coverslips, fixed, and incubated with rabbit monoclonal anti-Actin antibody. The coverslips were inverted and mounted onto a microscope slide, and the cells photographed using a Leica Q550 epifluorescence microscope using the same exposure time, shuttle opening and gain through all of the pictures (Figure 3.1). The images were then taken to FIJI/ImageJ to analyses and a total of 200 cells were measured. For each cell a long axis (L) and a short axis (S) were measured, and each L was divided by the respective S to obtain a ratio that correlates to cell elongation (Figure 3.2).

Figure 3.1 shows that TGF-β treatment induced morphological changes in ‘normal’ immortalised prostate epithelial cells (PNT2-C2). A statistically significant ($p<0.05$) higher number of spindle-shaped cells appeared in the TGF-β treated group, when compared to the vehicle treated group (figure 3.2). The TGF-β treated cells presented signs of stress fibre formation and disruption of cell clusters. These are typical features of mesenchymal cells (Nieto et al. 2016; Heldin et al. 2012; Brabletz et al. 2018) Thus the morphological analyses of the TGF-β treated PNT2-C2 cells suggests that TGF-β induces EMT-like changes in these cells.

Figure 3.3 show stress fibres (yellow arrows) in TGF-β treated PNT2-C2 cells. Stress fibres are formed while the cell pulls itself away from a cell cluster disrupting the adhesion to neighbour cells. The comparative images with similar numbers of cells to the vehicle treated cells shows a compact cluster with all of the cells in maximum contact with their neighbouring cells. In figure 3.4 we see a busier field, but both treatments have a similar number of cells in the fields shown. The vehicle treated cells are in clusters with all the cells making full contact with its neighbour cells. The TGF-β treated cells do not form clusters and appear more elongated (yellow arrows) and only touching their neighbours focally (blue arrows). In figure 3.4 we also see some stress fibres with actin fibres aligning to the same axis within each cell (green arrows).

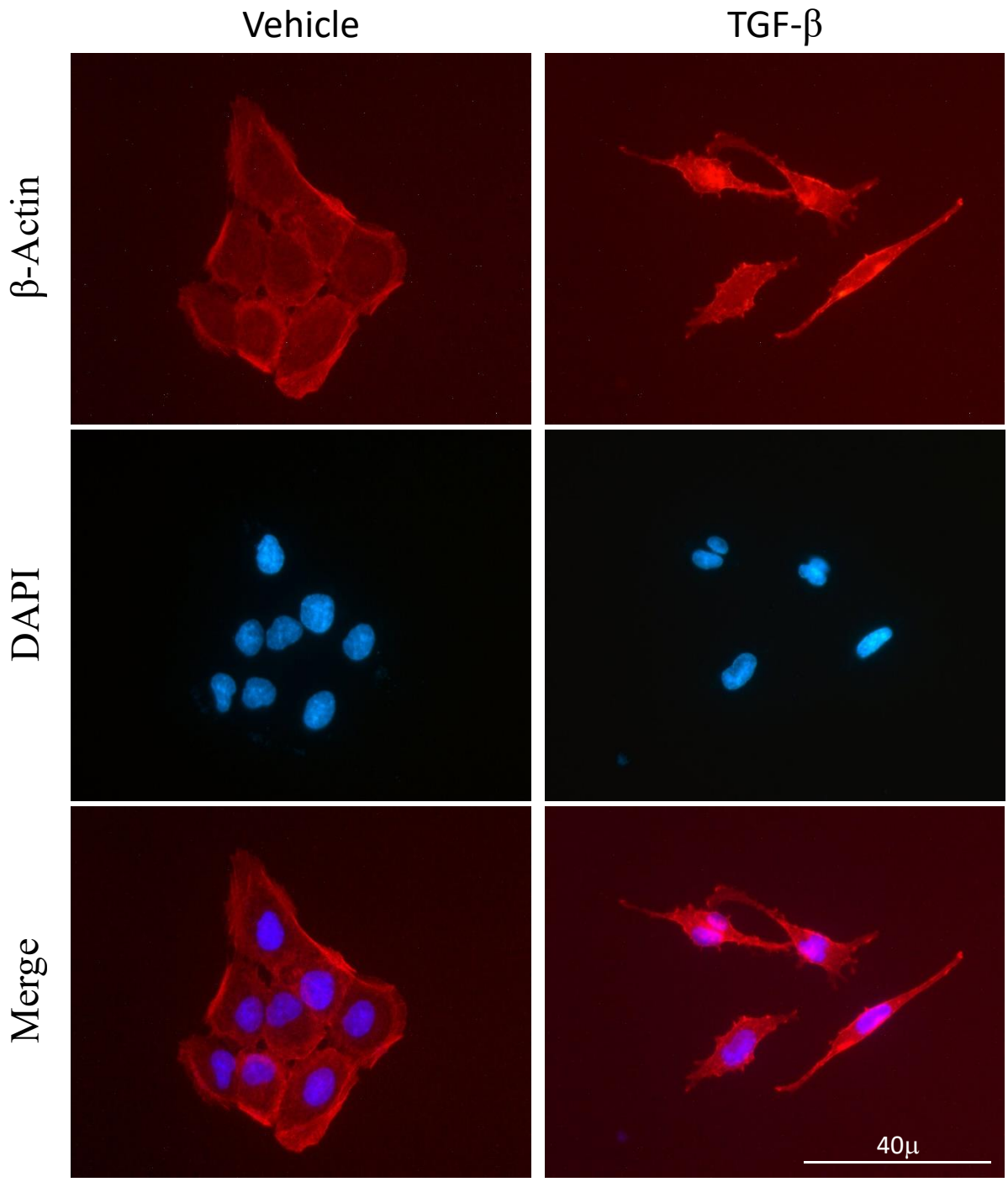

Figure 3.1. Photomicrography of β-actin stained PNT2-C2 cells (1). Immunofluorescence staining for β-actin. On the left, the cells treated with Vehicle for 48 hours. On the Right, the cells treated with TGF-β for 48h. The pictures were taken with a Leica Q550 epifluorescence microscope equipped with a LED monochromatic light source on 40x magnification. All the images were taken with the same exposure time and gain.

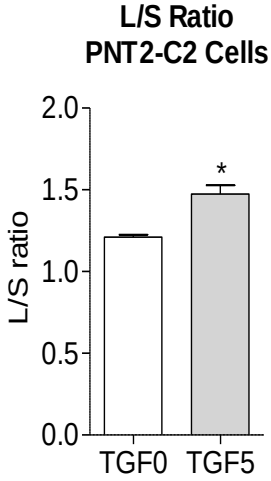

Figure 3.2. PNT2-C2 L/S ratio. Cell measurements obtained with FIJI-ImageJ from images of β-actin stained PNT2-C2 cells. The higher the ratio the more elongated is the cell. TGF-β treatment significantly augmented the average L/S ratio of PNT2-C2 cells. 200 cells/coverslip were measured using Fiji. Mean±Standard

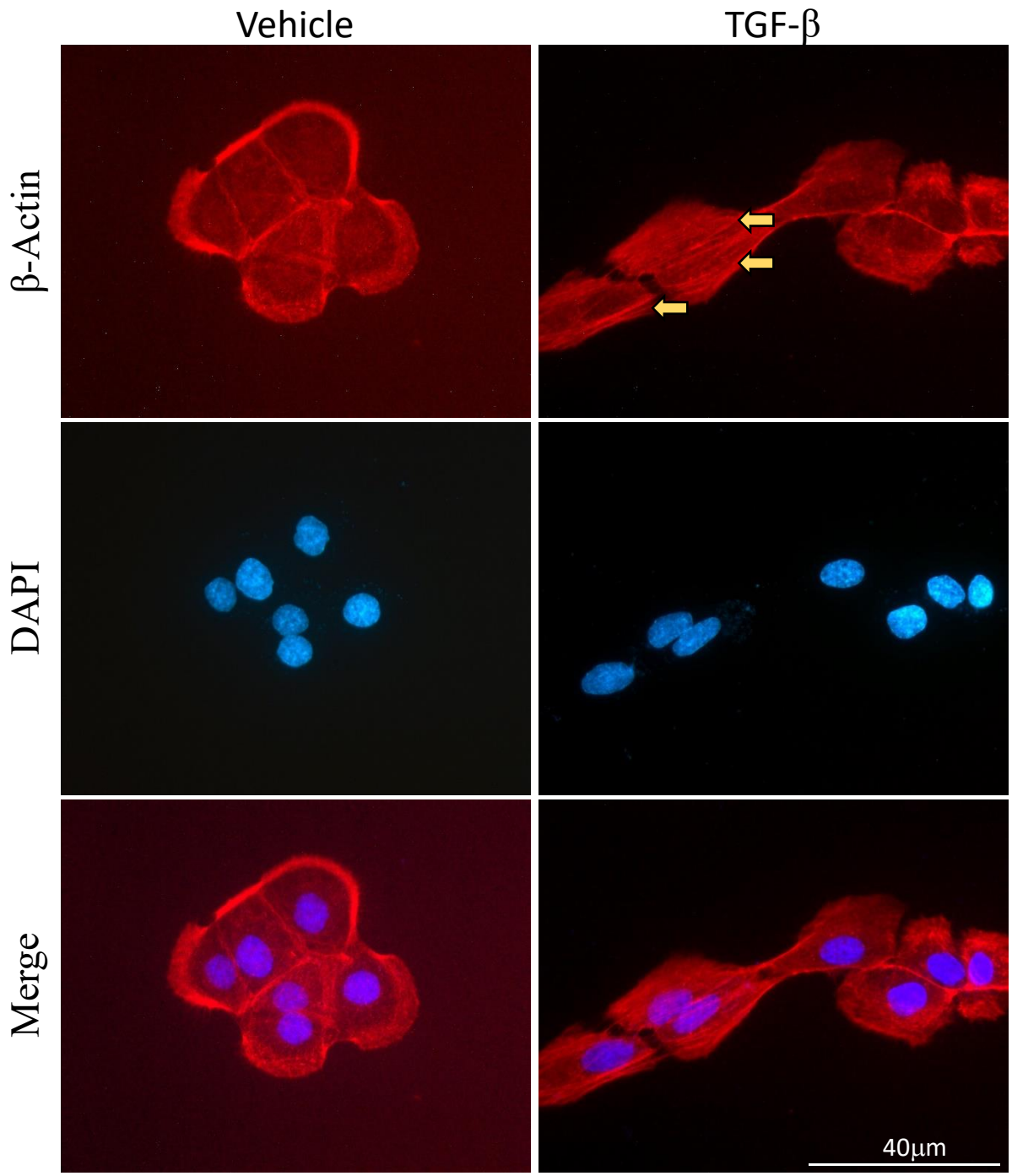

Figure 3.3. Photomicrography of β-Actin stained PNT2-C2 cells (2). Immunofluorescence stain for β-actin. A similar number of cells in each field was taken for comparison. On the left, the cells treated with vehicle for 48 hours. On the Right, the cells treated with TGF-β for 48 hours. Yellow arrows indicate stress fibres. The pictures were taken with a Leica Q550 epifluorescence microscope equipped with a LED monochromatic light source on 40x magnification. All the images were taken with the same exposure time and gain.

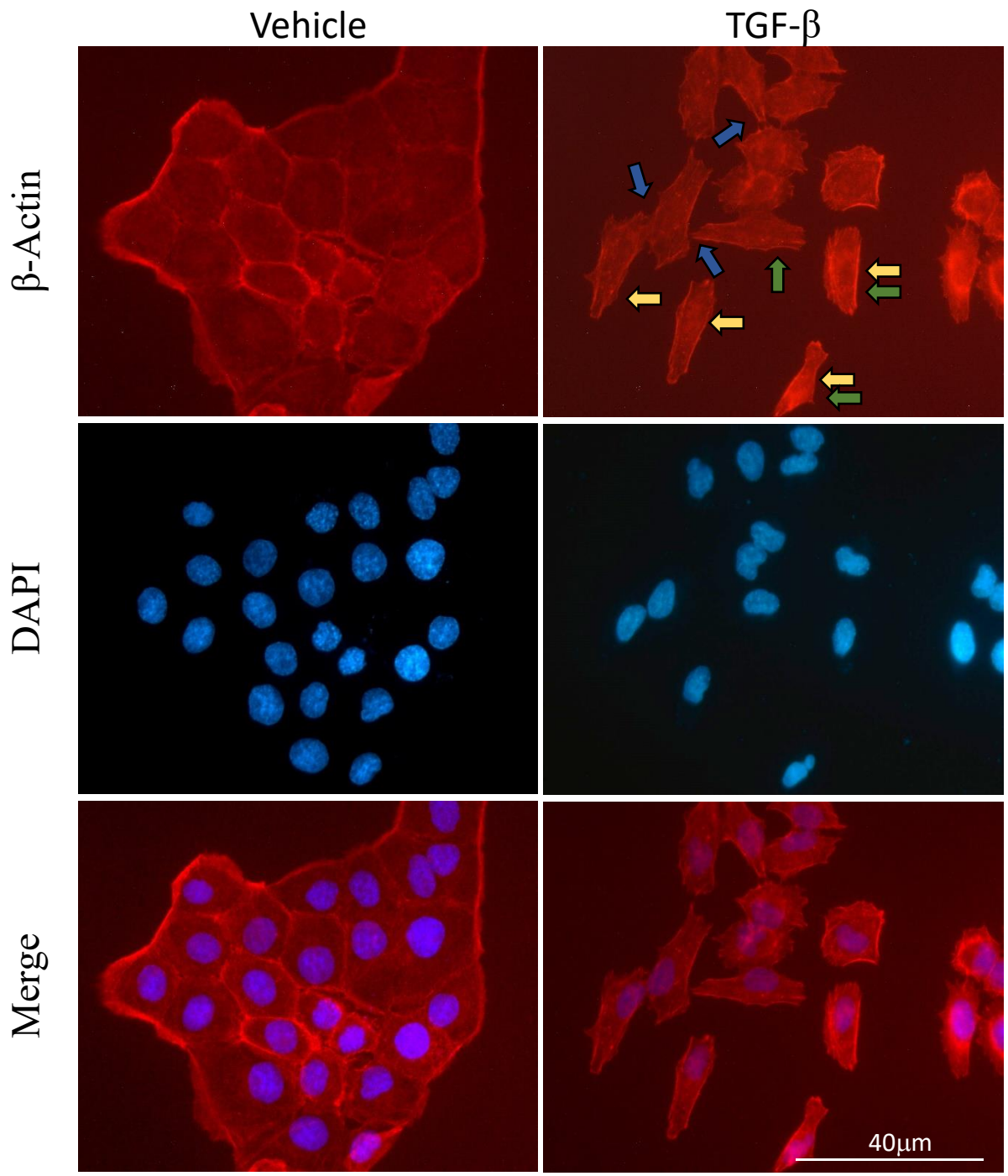

Figure 3.4. Photomicrography of β-Actin stained PNT2-C2 cells (3). Immunofluorescence stain for β-actin. Field with a similar number of cells in each treatment were imaged for comparison. On the left, the cells treated with vehicle for 48 hours presented the same growth pattern observed in figure 3.3, a tight cluster with maximum cell to cell contact. On the Right, the cells treated with TGF-β for 48 hours. Blue arrows indicate the cells connecting to neighbouring cells focally. Green arrows indicate cells with elongated morphology. Yellow arrows indicate actin stress fibres. The pictures were taken with a Leica Q550 epifluorescence microscope equipped with a LED monochromatic light source on 40x magnification. All the images were taken with the same exposure time and gain.

Molecular characterization of TGF-β treated PNT2-C2 and PC3 cells

The EMT is a well-characterised phenomenon, with markers that are accepted in the literature as defining points, although to diagnose EMT not all of the markers need to be present. To assess which EMT markers were relevant to the treatment with TGF-β in PNT2-C2, whole cell protein extracts from three independent 48h TGF-β treatments (as described in section 2.7.1), were tested to the presence of seven antibodies that recognise different EMT markers (as described in section 2.9.1) (figure 3.5). Equal amounts of protein were loaded into 12% acrylamide SDS-PAGE gels and separated by electrophoresis. The proteins were then transferred to an Immobilon-P membrane and probed with specific antibodies. β-Actin or Lamin A/C were used as loading controls.

After 48h TGF-β incubation E-cadherin protein expression was down-regulated in PNT2-C2 cells when compared to the loading control β-actin. On the other hand, Snail protein expression was up-regulated in PNT2-C2 cells treated with TGF-β. Endoglin and β-catenin showed some changes in expression, but the changes were not consistent through repetitions of these experiments. The marker proteins Vimentin, Slug and ZO-1 levels did not change with the treatment.

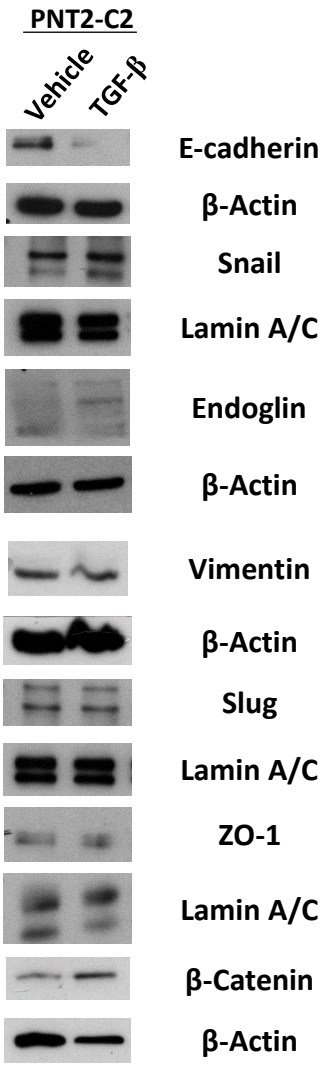

Figure 3.5. EMT marker screening in PNT2-C2 cells. Photoradiography of seven different EMT markers analysed by western blot using PNT2-C2 whole cell protein extracts. On the left, protein extracted from PNT2-C2 cells treated with vehicle. On the right, protein extracted from PNT2-C2 cells treated with TGF-β (5ng/mL) for 48h. The expression of each EMT marker was compared to the expression of a house keeping protein (β-Actin or Lamin A/C). E-cadherin expression was consistently down-regulated with the TGF-β treatment in 3 experiments. Snail expression was up-regulated with the TGF-β treatment. The end stage marker Vimentin did not show a difference between the treatments, the same was observed with Slug and ZO-1 antibodies. Endoglin and β-catenin showed inconsistent changes in expression pattern though multiple repetitions.

Detailed morphological and cell metric analysis was not carried with PC3 cells as this has transitioned through EMT, and the cells present a mesenchymal morphology with elongated cells and fewer EMT markers were assessed in these cells. After the markers were screened in PNT2-C2 cells, only the ones that showed changes in expression in TGF-β treated PNT2-C2 were tested with PC3 protein extracts, along with the end stage marker Vimentin. Endoglin showed conflicting expression changes through the repetitions in PNT2-C2 cells, so it was also assessed in PC3. Whole cell protein extracts from three independent 48h TGF-β treatments (as described in section 2.7.1), were tested using four different EMT marker antibodies (as described in section 2.9.1) (figure 3.6). Equal amounts of protein were loaded into 12% acrylamide SDS-PAGE gels and separated by electrophoresis. The proteins were transferred to an Immobilon-P membrane and probed as above. β-Actin or Lamin A/C were used as loading controls.

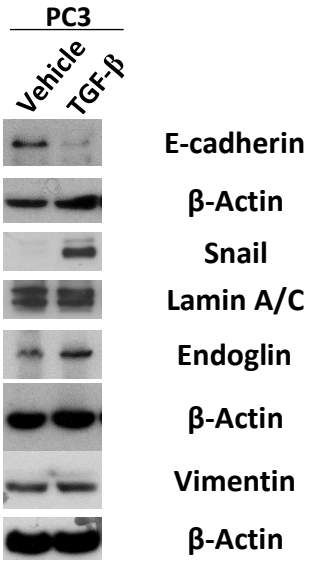

Figure 3.6. EMT marker screening in PC3. Photoradiography of four different EMT markers analysed by western blot using PC3 whole cell protein extracts. On the left, protein extracted from PC3 cells treated with vehicle. On the right, protein extracted from PC3 cells treated with TGF-β (5ng/mL) for 48h. The expression of each EMT marker was compared to the expression of a house keeping protein (β- Actin or Lamin A/C). TGF-β down-regulated E-cadherin expression consistently. Snail expression was up-regulated with the TGF-β treatment. The end stage marker Vimentin did not show difference between the treatments. Endoglin showed inconsistent changes in expression pattern though the repetitions.

The EMT marker changes observed in PNT2-C2 cells were confirmed in PC3 cells. E-cadherin presents a low expression in this cell line, but with a longer exposure it was still possible to detect it by western blot. TGF-β incubation down-regulated E-cadherin expression in PC3 cells when compared with the loading control β-actin. Snail expression was up-regulated in PC3 cells treated with TGF-β. Endoglin showed some changes in expression, but the changes were again not consistent through the repetitions. Expression of the end stage marker Vimentin did not change with the TGF-β treatment.

To compare the EMT markers changes in PNT2 (figure 3.7) and in PC3 (figure 3.8). The western blots for E-cadherin and Snail were scanned and their densitometry analysed with ImageQuant (A and C respectively). Immunofluorescence images for E-cadherin staining (as explained in section 2.9.2) were made to corroborate the western blot findings (E), all the images were obtained with the same exposure time and gain.

Densitometry of 3 independent E-cadherin western blots are in figure 3.7 A, E-cadherin was reduced in TGF-β treated cells when compared to vehicle treatment in a statistically significant manner. The densitometry analysis of Snail bands showed that, in PNT2-C2 cells, the TGF-β treatment significantly ($p<0.05$) up-regulated Snail expression (figure 3.7 C). Representative photomicrographs of the western blots analysed show downregulation of E-cadherin and up-regulation of Snail compared to β-acting and Lamin A/C (figure 3.7 F). Western blotting for pSmad3 shows that there is activation of TGF-β signalling. In figure 3.7 E, representative immunofluorescence photomicrographs confirm that the E-cadherin protein expression is downregulated in the TGF-β treated PNT2-C2 cells, when compared to vehicle control.

To assess if the regulation of E-cadherin (B) and Snail (D) happened at the transcriptional level, whole cell mRNA extract was use in a reverse transcription reaction to make cDNA that was analysed by qPCR (as explained in section 2.10.1). In PNT2-C2 cells (figure 3.7), TGF-β treatment significantly ($p<0.05$) reduced E-cadherin mRNA levels (figure 3.7 B), and significantly ($p<0.05$) up-regulated Snail mRNA (figure 3.7 D), when compared to vehicle treatment.

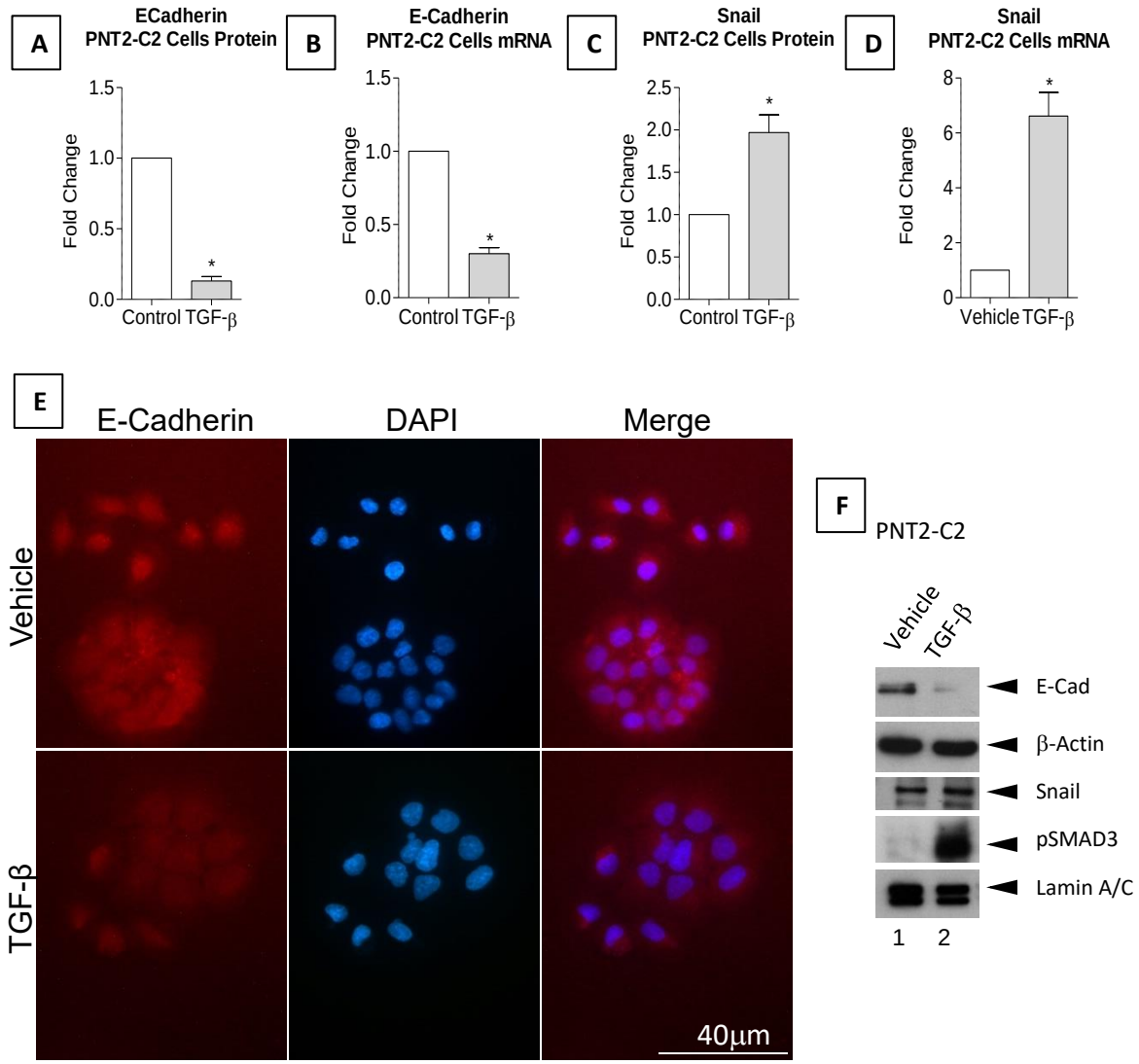

Figure 3.7. PNT2-C2 EMT phenotype. PNT2-C2 cells were treated with Vehicle or TGF-β for 48h prior to analysis. E-cadherin expression was downregulated by TGF- β treatment when compared to Vehicle treatment at both the protein (A) and mRNA level (B). Snail was up-regulated with TGF- β treatment at the protein (C) and mRNA (D) level. (E) Lower E-cadherin signal on immunofluorescence stain of PNT2-C2 cells treated with TGF- β when compared to Vehicle. Images were obtained using a Leica Q550 epifluorescence microscope equipped with a LED monochromatic light source on 40x magnification and were taken with the same exposure time and gain. (F) Representative radiomicrography of western blots for E-cadherin, Snail, pSmad3 and housekeeping proteins. In column 1 are the Vehicle treated cell extracts and in column 2 the TGF- β treated cell extracts. M+SD, n=3, *p>0.05.

Densitometry graphs of 3 independent western blots for E-cadherin (figure 10 A) and Snail (figure 3.8 C), shows statistically significant ($p<0.05$) changes in PC3 cells. E-cadherin expression was reduced and Snail expression up-regulated. Representative photomicrographs of the western blots analysed are in figure 3.8 F. E-cadherin expression is low to begin with in PC3 cells, but E-Cadherin can still be detected by western blot by using a longer exposure. With 30 minutes exposure E-cadherin bands are visible in vehicle treatment, but TGF-β treatment further reduced E-cadherin expression in PC3 cells. Snail expression is upregulated when compared to its loading control (Lamin A/C). The pSmad3 blot demonstrate activation of TGF-β signalling. Representative immunofluorescence photomicrographs of E-cadherin protein show downregulation of E-cadherin protein expression when PC3 cells were treated with TGF-β. In PC3 cells (figure 3.8), TGF-β treatment also significantly ($p<0.05$) reduced E-cadherin mRNA levels (figure 3.8 B), and up-regulated Snail mRNA levels ($p<0.05$) (figure 3.8 D).

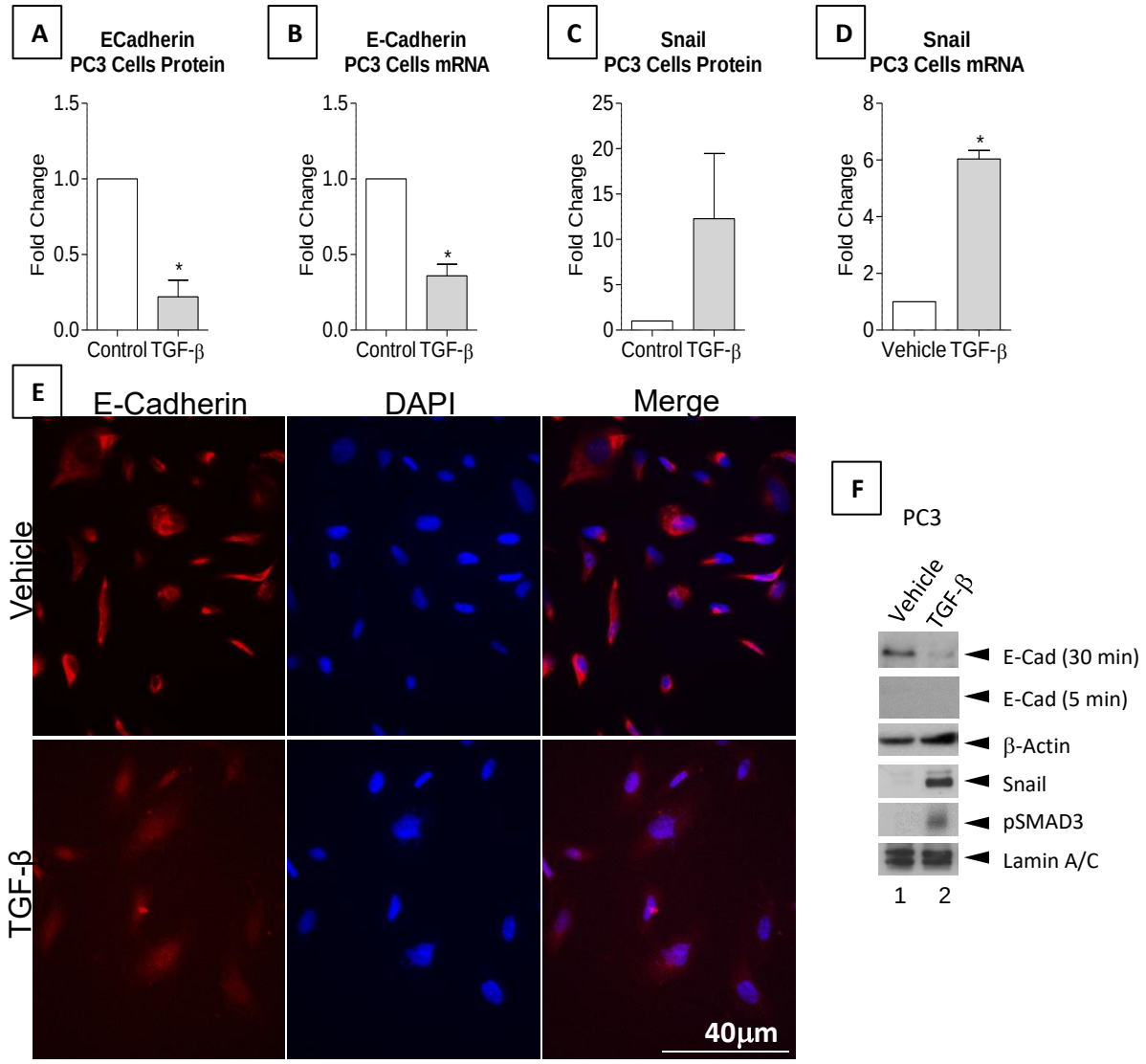

Figure 3.8. PC3 EMT phenotype. PC3 cells were treated with vehicle or TGF-β for 48h prior to analysis. E-cadherin expression was downregulated by TGF- β treatment when compared to Vehicle treatment in both protein (A) and mRNA level (B). Snail was up-regulated with TGF- β treatment at the protein (C) and mRNA (D) level. (E) Lower E-cadherin signal on immunofluorescence staining of PC3 cells treated with TGF- β when compared to vehicle. Images were obtained using a Leica Q550 epifluorescence microscope equipped with a LED monochromatic light source on 40x magnification and were taken with the same exposure time and gain. (F) Representative radiomicrography of western blots for E-cadherin, Snail, pSmad3 and housekeeping proteins. In column 1 are the Vehicle treated cell extracts and in column 2 the TGF- β treated cell extract. M+SD, n=3, *p>0.05.

TGF-β induced migration of prostate cells..

A characteristic of mesenchymal cells acquired by cells that undergo EMT is a higher migratory ability. To assess if TGF-β treated PNT2-C2 and PC3 cells acquire higher migratory competence, the cells were treated with TGF-β for 48h prior to performing chemotaxis assays in Boyden chambers. The chemotaxis assay was performed with addition of hydroxyurea to inhibit cell division. Hydroxyurea inhibits the enzyme ribonucleotide reductase decreasing the production of nucleic acids and inhibiting cell proliferation. This causes the cell cycle to stop and the cells cannot, for this experiment is important to add hydroxyurea to the media because when you discount the cell division factor, all the cell detected in the bottom chamber of the Boyden chamber arrived there by trespassing the membrane that divides the two chambers. The cells were counted and suspended in starvation media (as explained in section 2.8) before being put in the upper chamber of the Boyden chamber. The lower chamber was filled with complete media, and the cells were incubated for 12h, before being stained with Calcein-AM and trypsinised. The migrated cells were put in a black flat bottom 96-well plate and read using a flex station. The readings were fitted to a standard curve and the percentage of migrated cells obtained by dividing the number of migrated cells by the total amount of seeded cells. Figure 3.9 has graphs with the percentage of migrated cells in 3 independent experiments with PNT2-C2 (A) and PC3 (B) cells.

The results show that PNT2-C2 and PC3 cells treated with TGF-β migrate more than the equivalent cells treated with vehicle in both cases. TGF-β treatment increased the number of migrated PNT2-C2 and PC3 cells in the chemotaxis assay in a statistically significant manner.

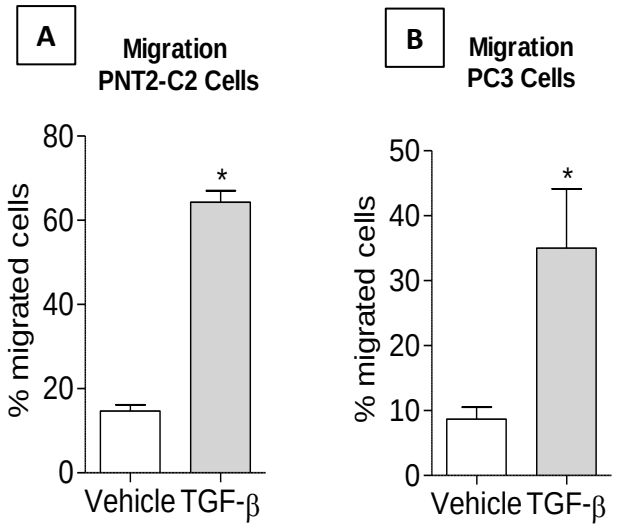

Figure 3.9. TGF-β treatment induced migration. PNT2-C2 (A) and PC3 (B) cells were treated with 5ng/mL TGF-β for 48 hours, they were then trypsin dissociated, counted and suspended in starvation media. 8x10^4 cells were placed in the upper chamber of a Boyden's chamber, the bottom was filled with complete media to create a FBS gradient. Hydroxyurea was added to all the media used in the chemotaxis assay to inhibit cell division. TGF-β treated cells show a higher migratory ability when compared with vehicle treated cells. M+SD, n=3, *p>0.05.

Discussion

The initial part of this project aimed to examine the effects of TGF-β on two prostate cell lines. This chapter describes the screening of the EMT markers and the final EMT phenotype pattern shown by PNT2-C2 and PC3 cell lines following TGF-β treatment.

β-actin is a component of the cytoskeleton often used in immunofluorescence staining to define the body shape of cells (Xiang & Rensing 1999; Ferret-Bernard et al. 2008; Goldman et al. 1996). Detailed manual search of the images of TGF-β or vehicle treated PNT2-C2 cells was performed to detect the presence of EMT associated morphological changes. During EMT β-actin fibres align paralleled to the long axis forming stress fibres (Taiyab et al. 2016), the cells loses polarity and the characteristic clusters formed by epithelial cells are dispersed with the loss of cell adhesion proteins (Moreno-Bueno et al. 2008). The β-actin immunofluorescence images of TGF-β treated PNT2-C2 cells showed changes in its morphology, the cells became more elongated and lost their polarity. In culture, epithelial cells keep contact with their neighbouring cells with the aid of adhesion proteins, the cells then form clusters that grow as extensive sheets of cells over time. The strong connection between adhesion proteins on the lateral surfaces of the cells keeps the epithelial cell polarity in place (Eurell et al. 2006). TGF-β treatment made most of the PNT2-C2 cells grow with little contact with neighbouring cells, this indicates a loss in cell polarity. Further evidence of cell polarity loss is seen in a rearrangement of the cytoskeleton with the formation of stress fibres (Kaunas et al. 2005; Hirata et al. 2007), here the presence of stress actin fibres was often observed in TGF-β treated PNT2-C2 cells.

The phosphorylation of Smad3 is used to show activation of TGF-β signalling (Massagué 2012). Here pSmad3 was detected with a 5ng/mL dose of TGF-β for 48h. With this condition, a screening of EMT markers was conducted by western blot where several end-point EMT markers and EMT-TFs were assayed. The loss of E-cadherin protein expression and up-regulation of Snail protein expression were seen in TGF-β treated PNT2-C2 and PC3 cells, which agrees with the EMT literature

available (Heldin et al. 2012; Takeyama et al. 2010; Krebs et al. 2017; Nieto et al. 2016; Brabletz et al. 2018; Heldin et al. 2012).

TGF-β is implicated in several human diseases including cancer (Gordon & Blobe 2008). It is also reported as an important inducer of EMT in cancer (as reviewed by Heldin et al. 2012). In early stages of carcinogenesis TGF-β1 has a growth-inhibitory effect, yet in advanced carcinomas this grow factor loses this inhibitory effect and promotes cancer growth and EMT (Levy & Hill 2006). TGF-β regulation of EMT is well-studied and a number of transcription factors (EMT-TFs) are reported to co-regulate each other in a complex and highly context-dependent orchestration. The most common reported TGF-β associated EMT-TFs are basic helix-loop-helix (Twist and E47), zinc finger proteins (Snail and Slug) and zinc finger and homeodomain proteins (*ZEB1* and *ZEB2*) (Heldin et al. 2012). The main effect of these EMT-TFs is on regulation of E-cadherin expression for example. TGF-β treatment of differentiated mammary epithelial cells or the ectopic up-regulation of Snail or Twist stimulated the expression of stem markers and down regulate E-cadherin expression (Mani et al. 2008).Here, only Snail was up regulated with the TGF-β treatment in PC3 and PNT2-C2, which agrees with published reports where Snails upregulation was shown to trigger EMT in colon carcinoma and melanoma cells (Medici et al. 2008). Interestingly, Snail expression is seen in untreated PNT2-C2 cells, with increase following TGF-β treatment. In contrast, Snail protein expression is not seen in untreated PC3 cell, but it is notably expressed following TGF-β treatment.

Snail is a transcriptional repressor responsible for regulating genes involved in cell adhesion and is reported to be an important mediator of TGF-β related EMT (reviewed by Thiery et al. 2009). Its up regulation here could explain the loss of E-Cadherin expression. As previously demonstrated, transcription factor Snail binds strongly to E-box of the E-Cadherin promoter, and it was demonstrated that Snail repression of E-Cadherin expression is enough to induce EMT (Villarejo et al. 2014). Finally, over-expression of Snail can induce EMT in prostate cancer cell lines ARCaP and LNCaP (Odero-Marah et al. 2008) and in pancreatic carcinoma (Yang et al. 2006).

At the end of EMT the cells can express several mesenchymal markers (Kalluri & Weinberg 2009) (such as α-SMA, FSP1, vimentin and desmin). Nevertheless, full

EMT completion is rarely observed in cancer (Brabletz et al. 2018), so the expression of all of these end-stage markers is often not observed. PNT2-C2 and PC3 cells treated with TGF-β did not show changed in end-stage marker vimentin, nonetheless, it presented a considerable loss of E-Cadherin expression and an increase in cell motility, which indicates a loss of epithelial phenotype. Cells which lose surface E-cadherin expression are more susceptible to various EMT inducers, additionally it is well established that E-cadherin expression is lost on cells that undergo EMT (Heldin et al. 2012b; Brabletz et al. 2018; Gupta & Maitra 2016; Krebs et al. 2017; Puisieux et al. 2014). The expression of E-cadherin *in vitro* is directly correlated to the epithelial phenotype, and the simple perturbation of the E-Cadherin mediated tight cell-cell bond using monoclonal antibodies is enough induce a mesenchymal phenotype in MDCK cells (Imhof et al. 1983). In general, a negative correlation is observed between E-Cadherin expression and cancer grade (Birchmeier & Behrens 1994), which agrees with the demonstration, in several cell lines models, that cells with low E-cadherin expression present higher tumour growth and metastasis when injected in nude-mice (Thiery 2002). Interestingly, nuclear expression β-catenin is correlated to loss of E-cadherin protein expression (Tian et al. 2011), therefore, an analysis of the subcellular localization of β-catenin could reveal an involvement of this protein on TGF-β induced EMT in prostate cells.

The TGF-β treatment also increased the migration of both PC3 and PNT2-C2 cells. Which is consistent with EMT, since cells that undergo EMT acquire higher migration ability (Heldin et al. 2012). It is interesting that PNT2-C2 presented a higher background migration when compared with PC3 cells. It was expected that PC3 might have a higher basal migration ability (Lang et al 1999). However, the chemotaxis assay only detects cells that stay attached to the bottom of the Boyden chamber membrane, and a possible explanation is that PC3 cells detach from the bottom of the membrane quicker than PNT2-C2 cells and some signal was lost, nonetheless, a significant difference was observed between the vehicle and the TGF-β treatments.

To add another layer on the complexity of EMT regulation, EMT is also promoted by several other stimuli that trigger the event via different pathways. However, these pathways often cross talk and compensate each other in a context-dependent manner. For example, in cultured rat lens epithelial explants the inhibition of β-

catenin/CBP interactions decreased TGF-β-induced EMT (Taiyab et al. 2016). In endothelial cells, Notch1, Notch4 and TGF-β synergistically up regulate Snail during the EMT to forms the cardiac cushion morphogenesis (Niessen et al. 2008). In sight of the complexity of the cellular signalling that regulates EMT, more contextual knowledge is needed before they can be helpful in the cancer treatment. The following chapters will evaluate PRH, a novel EMT-TF that communicates with the TGF-β pathway, analysing it importance in clinical prostate cancer, its effects on EMT and its molecular interactions with TGF-β pathway.

Chapter 4: PRH represses EMT and cell migration in prostate adenocarcinoma cells

Introduction

PRH/*HHEX* is a homeodomain protein which act as transcription factor and regulates the proliferation and differentiation of multiple cell types. Disruption of PRH activity is associated with a variety of cancers including breast cancer, thyroid cancer and liver cancer (reviewed by (Gaston et al. 2016)). PRH/*HHEX* knock-down can trigger downregulation of E-cadherin and mRNA protein in PNT2-C2 cells, and its overexpression reduced cell migration in prostate cancer cells (Siddiqui et al. 2017). PRH regulates the TGF-β pathway through the regulation of Endoglin (Kershaw et al. 2014b), a TGF-β co-receptor that reduces TGF-β subcellular signalling. Hence the need for a more detailed evaluation of the role of PRH in EMT during prostate cancer development.

The aims of this chapter are to investigate the expression of PRH in prostate cancer samples and to examine the relationship between PRH and EMT in prostate cancer cells. In this chapter I use online databases to assess the expression of PRH in prostate tumours from patients. I will examine the correlation between PRH expression and prostate adenocarcinoma differentiation through immunohistochemistry staining of a large number of prostate tumour samples. Furthermore, I will use microarrays to find possible PRH targets genes and further test some of those targets using western blotting, qRT-PCR and ChIP-qPCR.

Results

The PRH gene is altered in prostate adenocarcinoma

To examine the relevance of PRH to prostate adenocarcinoma in more detail, two online cancer sequencing databases were used to generate statistics on PRH. cBioportal was used to analyse PRH gene alterations in prostate adenocarcinomas. Data from four different studies were analysed giving a total of 1627 patients (figure 4.1). PRH was altered in 5% of the prostate samples sequenced (figure 4.1 A). The majority of alterations were deep deletions of the gene. The studies presented percentages of alterations, the highest percentage of alterations was observed in the study ‘Prostate (MICH)’, which detected alterations in 10% of their samples, 8% of

them being deep deletions of the gene (Figure 4.1 B). The difference in percentage observed in the different studies is probably due to different numbers of samples. Figure 4.1 C, D and E shows the samples for the 4 studies that presented PRH deep deletion. In C the samples were grouped based on whether patients received ADT treatment prior to the sample collection or not. 40% of the samples that presented PRH deep deletion came from patients that did not receiver ADT. In D samples that presented PRH deep deletion were grouped on co-alterations in the PTEN gene. 66% of the sample that presented PRH deletion also presented alterations in PTEN. Finally, E shows frequency of each Gleason's score observed in samples that presented PRH deep deletion. Most of the samples presented Gleason's score higher than 7. The two most common scores observed were 7 and 9 (30% and 22%).

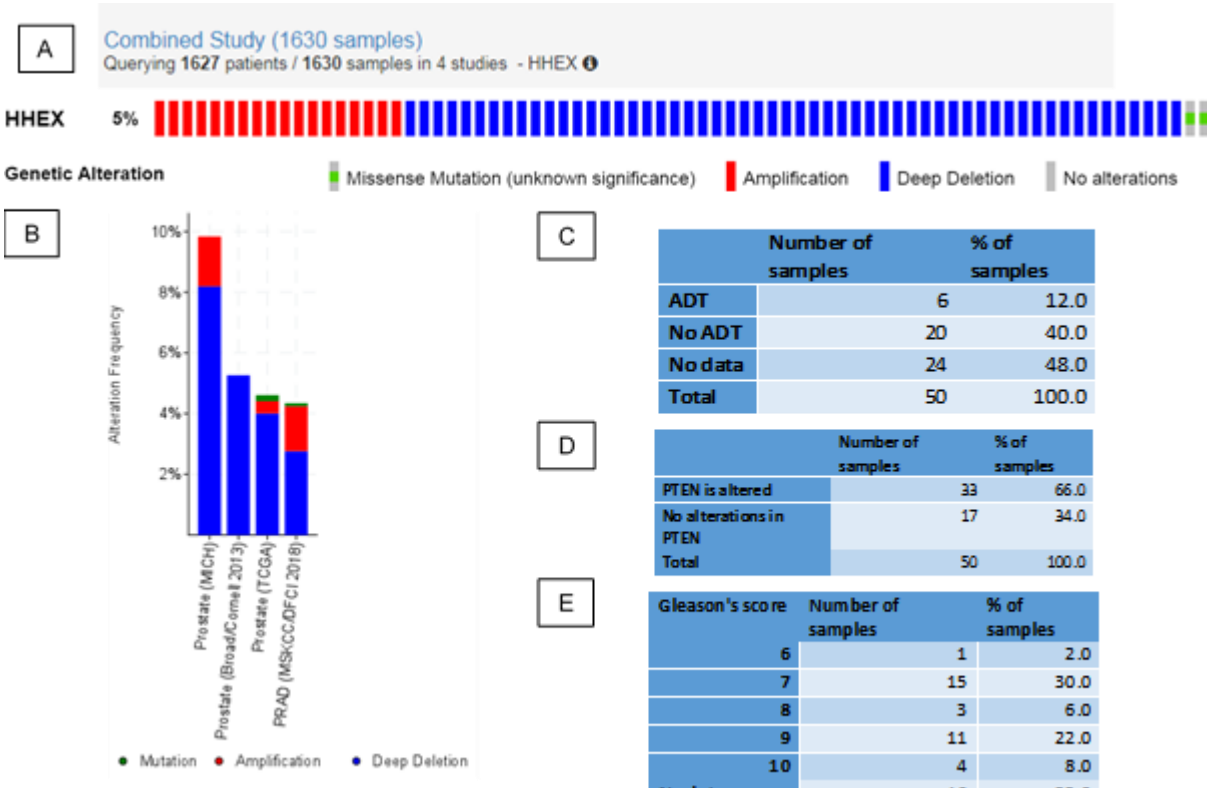

C

	Number of samples	% of samples
ADT	6	12.0
No ADT	20	40.0
No data	24	48.0
Total	50	100.0

D

	Number of samples	% of samples
PTEN is altered	33	66.0
No alterations in PTEN	17	34.0
Total	50	100.0

E

Gleason's score	Number of samples	% of samples
6	1	2.0
7	15	30.0
8	3	6.0
9	11	22.0
10	4	8.0
No data	16	32.0
total	50	100.0

Figure 4.1. PRH alterations in prostate adenocarcinoma. Data obtained from cBioportal. Compiling data from four different studies with a total of 1627 sequenced cases. (A) each bar represents a patient, 5% of the patients presented alterations in PRH, the majority of alterations were deep deletions. (B) shows a bar graph with the detailed results for each study. The highest incidence of PRH deep deletion was just over 8%, and the lowest was about 3%. (C) The table shows the stratification of prostate tumours that presented PRH deletion. Samples were grouped based on whether patients received ADT treatment prior to the sample collection or not. (D) The table shows the number of prostate tumours that presented PRH deletion and PTEN alterations in the same sample. (E) The table shows the frequency of each Gleason score on the samples that presented PRH deletion on cBioportal.

cBioportal was also used to analyse the disease-free survival rate of patients with prostate adenocarcinoma after their surgical treatment, comparing the rates for patients with HHEX alterations to patients that did not present them (Figure 4.2). The survival curves were not statistically significance, however, there is a trend for higher risk of incidence in patients with alterations in HHEX.

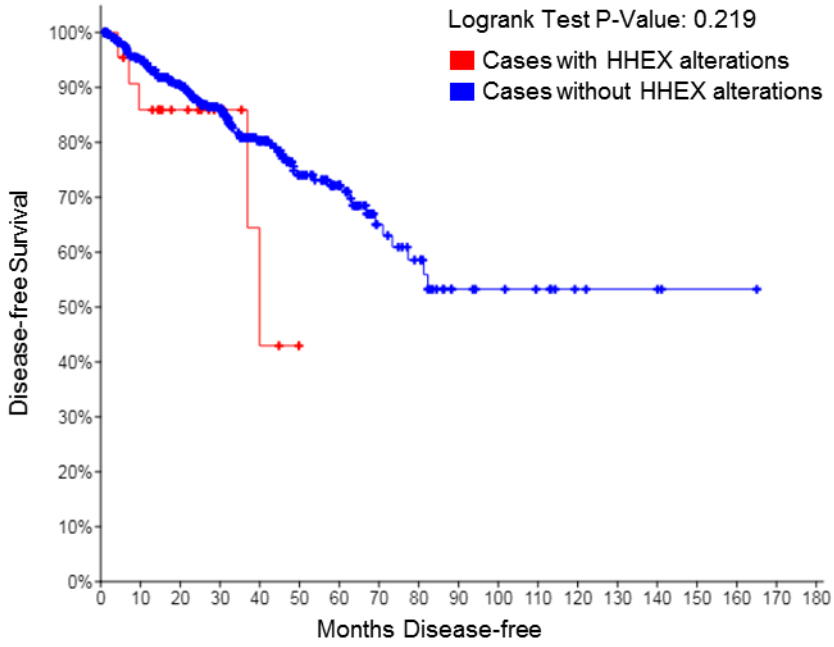

Figure 4.2. Disease-free survival of patients with prostate adenocarcinoma. Data obtained from cBioportal. Compiling data from four different studies with a total of 1627 sequenced cases. Kaplan-Meier plot was traced for the patients with and without HHEX alterations.

CpG methylation of the PRH gene

Gene expression can be silenced by CpG methylation and this process is known to be important in the down-regulation of tumour suppressor genes in multiple cancer types including the *RB* gene in Retinoblastoma (Greger et al. 1989) and *p16/CDKN2* gene in bladder (Gonzalez-Zulueta et al. 1995), breast, prostate, renal, and colon cancers (Herman et al. 1995). MethHC database was used to compare PRH gene methylation in prostate adenocarcinoma with normal prostate samples. The database also provides a correlation of methylation in the PRH gene body with PRH mRNA expression in prostate samples (figure 4.3). Methylation in the PRH gene body was correlated with low PRH mRNA expression levels. A moderate correlation (R= -0.389) between the two variables was observed (figure 4.3 A). Meanwhile the β-value, which is the average ratio of methylated: unmethylated amplification signal, in prostate tumour samples was higher than in normal samples (figure 4.3 B) ($p<0.005$). The majority of tumour samples presented β-values higher then 0.6, this indicates that at least 60% of the CpG sites in the sample were methylated. Thus there is increased CpG methylation of the PRH gene in the prostate cancer samples and this is correlated to downregulation of PRH mRNA expression.

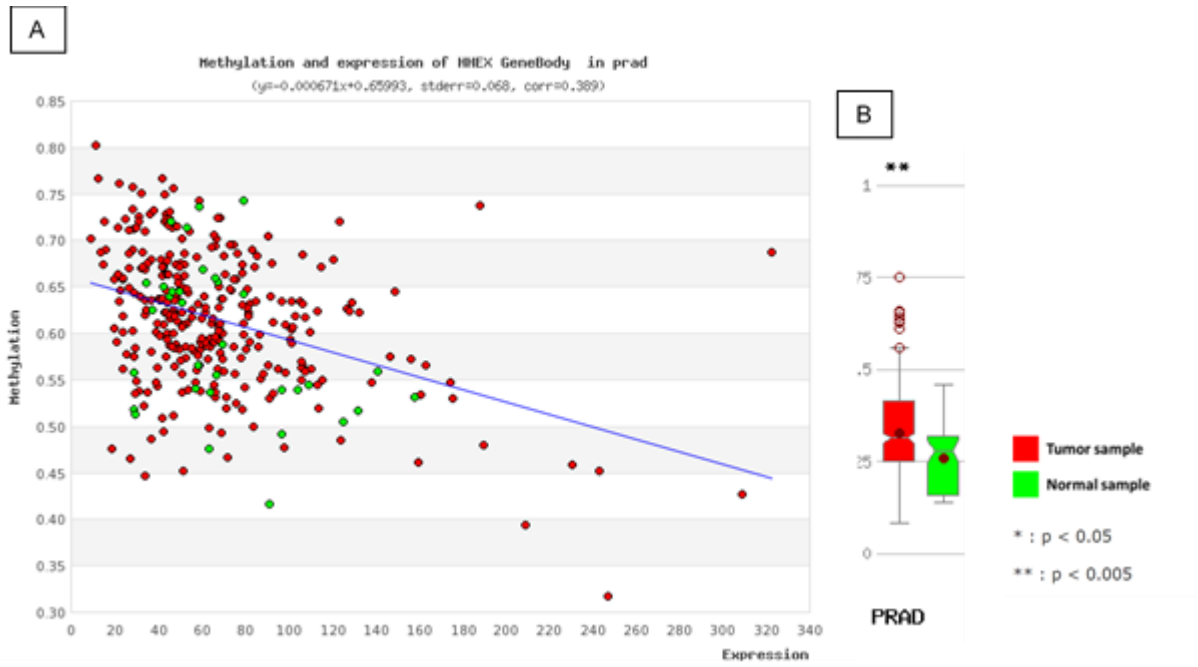

Figure 4.3. PRH gene is methylated in prostate adenocarcinoma. Data obtained from MethHC. (A) correlation between PRH gene body methylation and PRH expression detected by RNAseq. A moderate negative correlation was found between the two variables. (B) Graph showing a comparison of methylation β-values between tumour samples and normal samples. Prostate tumour samples presented statistically higher methylation in the PRH gene body when compared to normal prostate samples.

PRH expression in prostate cancer.

To assess PRH protein expression in prostate adenocarcinoma 96 prostate adenocarcinoma samples obtained from needle biopsies from Abcam were stained by immunohistochemistry for total PRH using M6 antibody. After a histology grading training session with the pathologist, each sample was initially scored using Gleason's scoring system (see section 2.11.3) to determine the differentiation degree of the glands in the histological view, and separately, they were blindly analysed to assess PRH immunostaining intensity and frequency of staining in the nucleus and cytoplasm. The numbers from the two analyses were compiled in a scatter plot and Pearson's correlation test was used to determine whether there is a correlation between the two variables (Figure 4.4 and Figure 4.5).

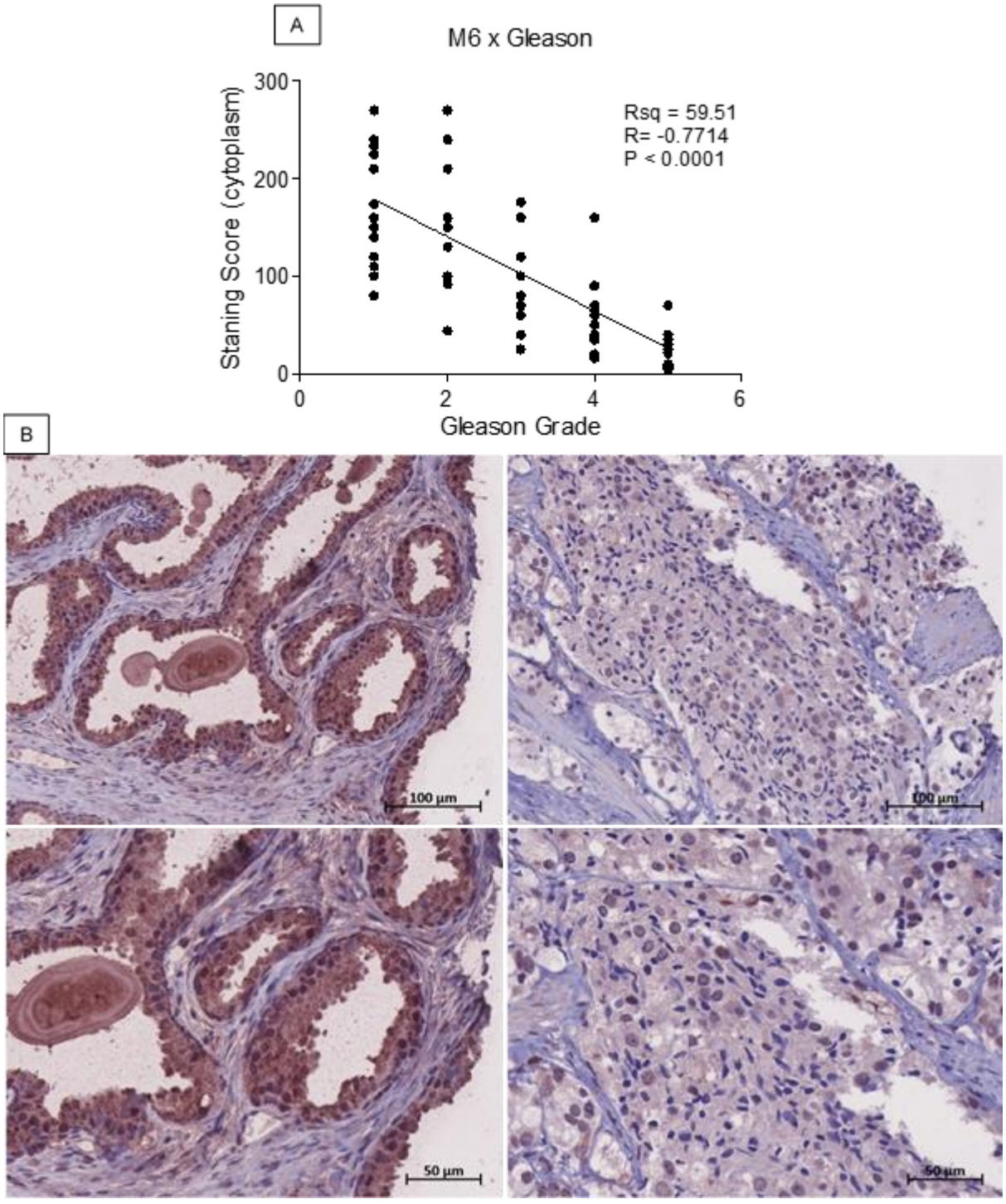

Figure 4.4. Gleason's grade is negatively correlated to cytoplasmic PRH expression in prostate adenocarcinomas. 96 specimens from patients with various degrees of prostate neoplasia, from benign prostatic hyperplasia to prostate adenocarcinoma were stained for PRH and scored for correlation analysis. (A) shows the correlation between cytoplasmic PRH immunostaining with Gleason's score. The correlation method used was Pearson's correlation with assumption that the data distributes as a Gaussian curve. The 'R' value found indicates a strong negative correlation, with the Gleason's score explaining 59.51% of the variability in PRH expression. (B) on the left is 'scene 50' the sample presented a good number of normal glands with some areas where there was more stroma space within the glands. The PRH staining is moderately strong and highly frequent in this specimen epithelium's cytoplasm. Nuclear staining, besides being strong, was not as frequent. On the right is 'scene 40', presented a large area of compact glans with marginal infiltration and an area with poor distinction between epithelium and stroma. Its cytoplasm PRH staining was, on average, weak and low frequency in the cytoplasm and nucleus.

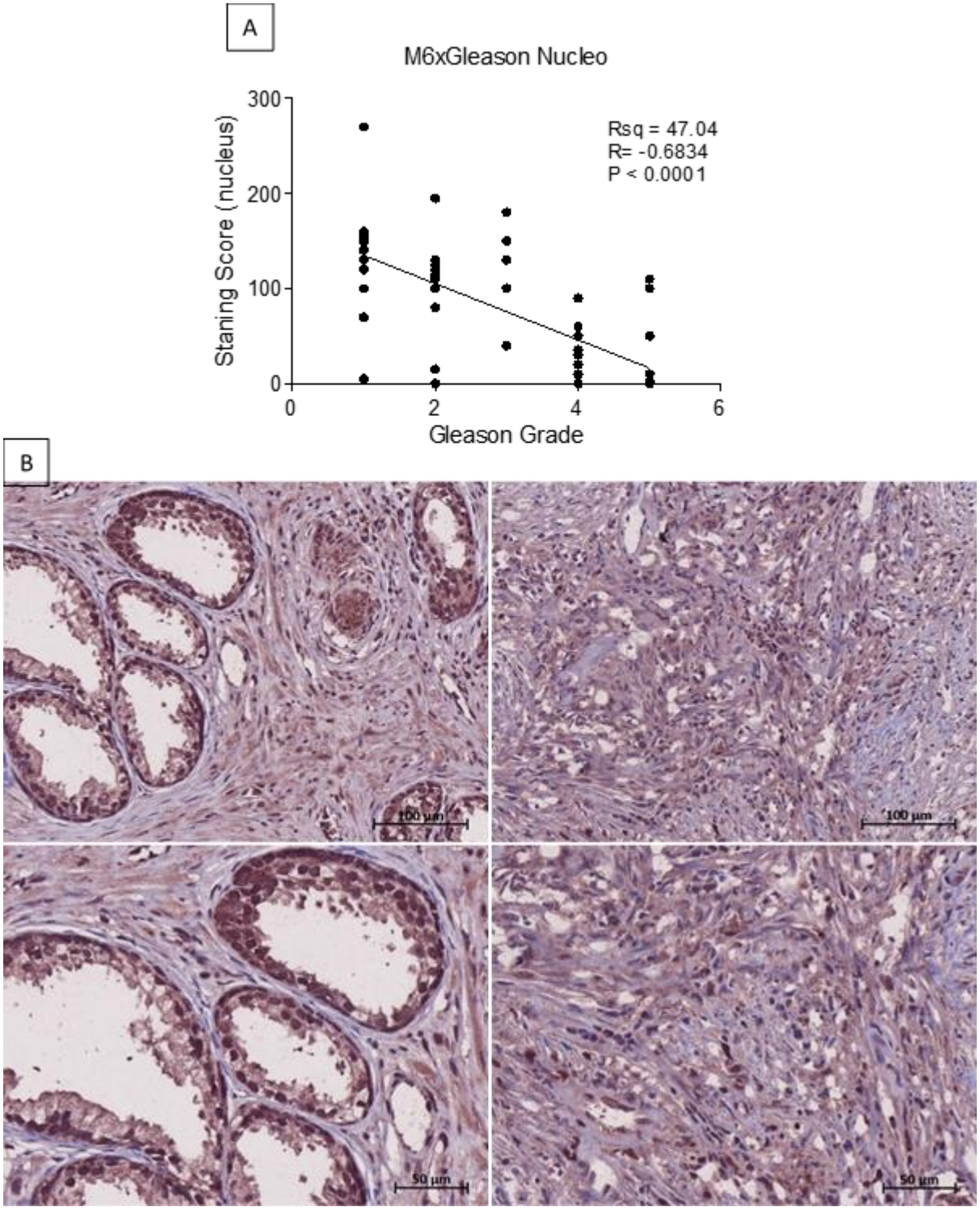

Figure 4.5. Gleason's grade is negatively correlated to nuclear PRH expression in prostate adenocarcinomas. 96 specimens from patients with various degrees of prostate neoplasia, from benign prostatic hyperplasia to prostate adenocarcinoma were stained for PRH and scored for correlation analysis. (A) shows the correlation between nuclear PRH immunostaining with Gleason's score. The correlation method used was Pearson's correlation with assumption that the data distributes as a Gaussian curve. The 'R' value found indicates a moderate negative correlation, with the Gleason's score explaining 47.04% of the variability in PRH expression. (B) on the left is 'scene 65', the sample presented large areas of glands with enlarged stroma and several normal glands. The PRH staining is assigned strong and highly frequent in the nuclei of epithelial cells. Cytoplasmic strain was similarly frequent with a moderate intensity. On the right is 'scene 70', this showed large areas of indistinguishable cell mass and no clear glandular formation. Its nuclear PRH staining was weak and in low frequency, while a considerable number of cells have a moderate PRH expression in the cytoplasm.

The fitted data comparing cytoplasmic PRH stain with Gleason's score shows a strong negative correlation between these two variables as the Pearson's R= -0.771. This means that 59.51% of the variance in cytoplasm PRH staining was explained by the Gleason's score. The representative photomicrography (Figure 4.4 B) of a benign prostate hyperplasia (on the left) stained for PRH, is a picture cropped from 'scene 50' of the microscope scan. The specimen had mainly hyperplastic glands with more stroma space and occasional normal glands, being graded 1 for both, main finds and secondary finds, giving the sample a total score of 2 on the Gleason's scoring system. The same sample was scored for PRH staining in the cytoplasm and nucleus. The PRH staining scoring took into account intensity and frequency of the prostate epithelium coloration. The specimen in scene 50 (Figure 4.4 B left) shows a moderate cytoplasmic colour (intensity 2) with 90% of the epithelium, being scored a stain factor of 180 (as in 2x90).

Figure 4.4 B right, shows a representative photomicrography of a prostate adenocarcinoma scored 4, cropped from 'scene 40' of the tissue array scan. The largest area of the tumour showed infiltration of gland cells (grade 3), while the second bigger distinctive area of the tumour showed poor distinction of gland with irregular masses of tumorigenic tissue (grade 4). The cytoplasmic stain for PRH was weak (intensity 1) and not frequent (observed in 5% of the epithelial cells), giving a total stain score of 5.

Figure 4.5 shows a similar result, the correlation between differentiation degree of the gland (i.e. Gleason's score) and the nuclear PRH staining was negative moderate. The scatterplot of Gleason's score versus PRH nuclear staining in patient's prostates samples showed R=-0.6834, therefore, Gleason's score explained 47.04% of the variance in PRH staining. Figure 4.5 B shows photomicrographs of two of those specimens used on the analysis. On the left, a cropped area from 'scene 65', the sample was score 2 in total regarding the Gleason's scoring system, due to a large area with hyperplasic stroma and the presence of normal looking glands (Grade 1). Nuclear PRH staining was considered strong (intensity 3) and highly frequent (90% of the epithelium nuclei) in this sample (total colour score 270). On the right, there is a cropped area from 'scene 70'. The sample in scene 70 shows a large area of poor differentiation with indistinguishable epithelium (grade 5), on a marginal area another in indistinguishable mass of cells

presented a glandular structure (grade 4), this sample was given a Gleason's score 9. Although there was some staining for PRH in this sample, it was not frequent. Some few cells (10%) retained a high intensity (intensity 3) PRH stain in the nucleus, giving a total colour score of 30. These results show that PRH is more frequently expressed in well-differentiated tumours.

Microarray analysis shows that PRH regulates TGF-β signalling genes.

Aiming to unveil PRH targets in prostate cell lines I took a genome-wide approach using microarrays. The microarray data was kindly provided by Dr Rachel Kershaw and Dr Sheela Jayaraman (University of Birmingham). The data were extracted from PNT2-C2 cells infected with either an adenovirus containing myc-PRH downstream of the CMV promoter (Soufi et al. 2006) or the control empty virus. mRNA from 3 different experiments were taken and used in a microarray assay. A total of 6094 genes were significantly up-regulated and 2373 genes down-regulated between PRH over-expressing cells and the control cells (fold change >1.5). Gene ontology was then performed using Gene Set Enrichment Analysis (for genes with FDR adjusted p>0.01) using the Hallmark gene sets. Figure 4.6 shows the significantly enriched gene sets. Figure 4.7 shows a heat map with data from the three PNT2-C2 Myc-PRH expressing and empty virus controls for the TGF-β gene cluster.

TGF-β was detected by the gene ontology as a gene group significantly ($p<0.01$) altered by the Myc-PRH expressing virus. In the TGF-β gene cluster *TGFB2* (x0.36) and *TGFBR2* (x0.34) were down regulated. On the other hand SMAD6 (x2.56), ENG (x1.61), TGFB3 (x3.8) and TGFBR3 (x1.54) were up-regulated.

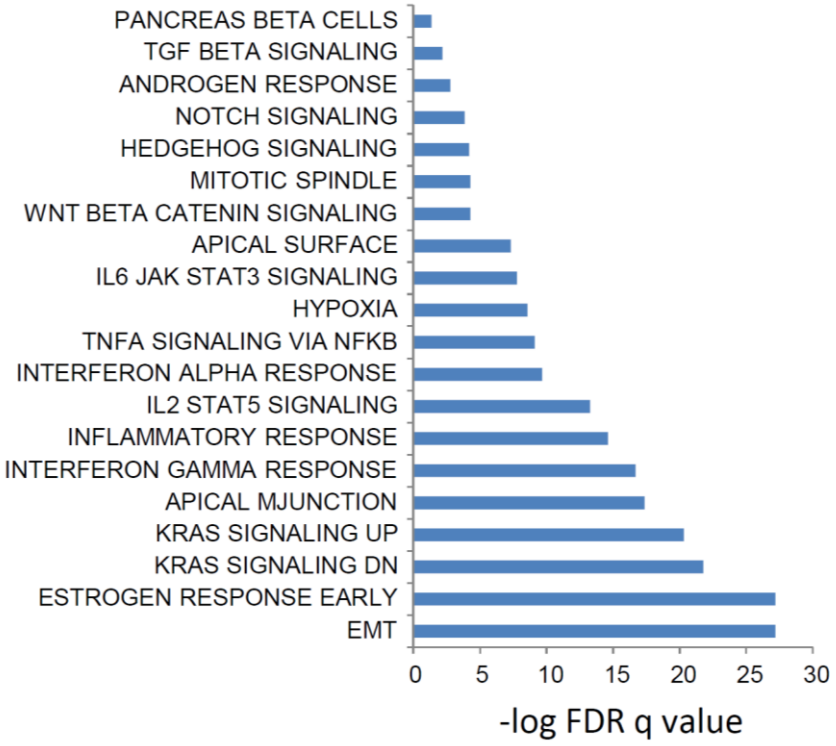

Figure 4.6. PNT2-C2 PRH overexpression gene ontology. The gene sets with the most significant alterations were genes involved in EMT and Estrogen response. Other significantly altered gene sets includes p53 pathway and TGF-β signalling.

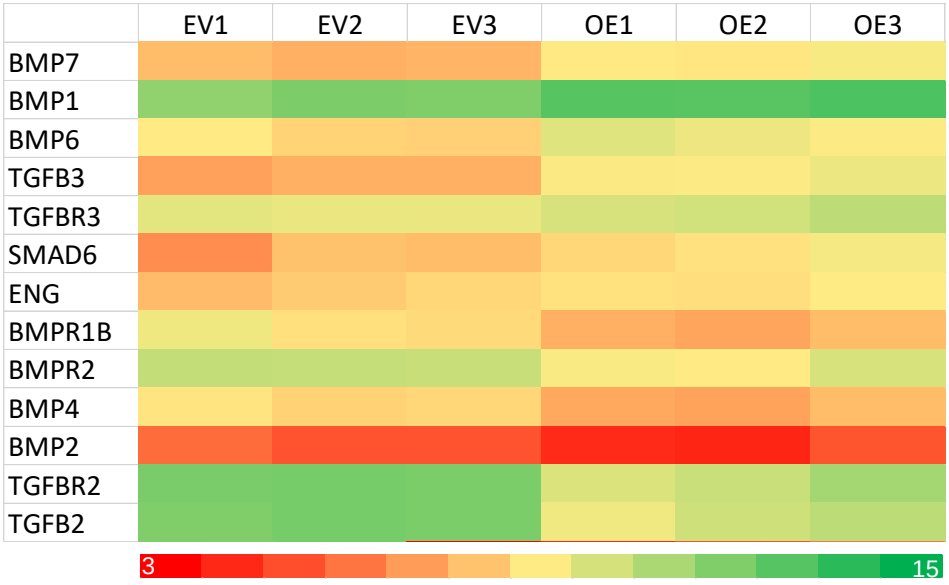

Figure 4.7. TGF-β signalling altered genes in PNT2-C2 PRH overexpression microarray. The numbers used in the heat map are the relative expression of each gene detected by micro array. The mRNA extracted from PNT2-C2 PRH overexpression (OE) or empty virus control (EV) were used in the microarray to detect gene expression alteration in an unbiased fashion. The heat map shows the main TGF-β signalling altered genes, *TGFB2* and *TGFBR2* were down-regulated and presented the highest difference among the displayed genes.

PRH ChIP sequencing

Using the same adenovirus (Soufi et al. 2006), a colleague performed a ChIPseq analysis and allowed me to analyse the myc-PRH trace sequence aligned to the whole human genome. I analysed peaks near the TGF-β genes detected by microarray. Figure 4.8 shows ChIP-seq traces aligned with a portion of the human genome (Human Feb. 2009 (GRCh37/hg19) Assembly) in the UCSC Genome Browser. The upper represents accumulation of H3K27Ac and was provided by UCSC Genome Browser. H3K27Ac is a marker is often found in active regulatory sites. The bottom trace shows IgG ChIP representing the background. The four genes observed in the images were chosen because they are important to the TGF-β signalling and they were among the biggest alterations in the TGF-β family altered genes in the microarray screening. The genome region aligned with the ChIP peaks (yellow arrows) had their sequence used to design primers latter used in the ChIP-qPCR assay.

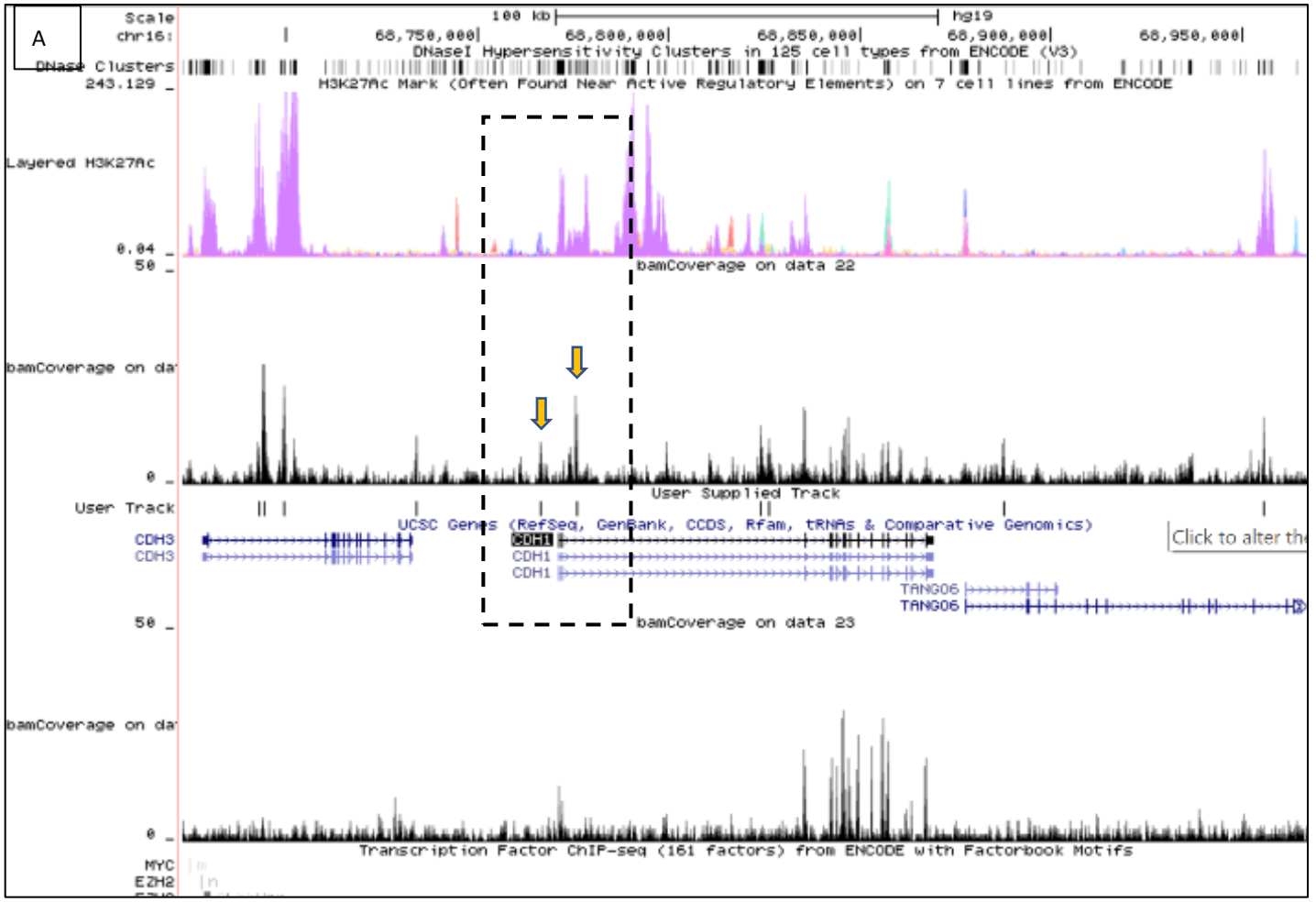
A
Scale
100 kb
hg19
chr16:
68,750,000
68,800,000
68,850,000
68,900,000
68,950,000
DNaseI Hypersensitivity Clusters in 125 cell types from ENCODE (V3)
DNase Clusters
243.129
H3K27Ac Mark (Often Found Near Active Regulatory Elements) on 7 cell lines from ENCODE
Layered H3K27Ac
0.04
50
bamCoverage on data 22
bamCoverage on da
0
User Supplied Track
User Track
UCSC Genes (RefSeq, GenBank, CCDS, Rfam, tRNAs & Comparative Genomics)
CDH3
CDH3
CDH1
CDH1
CDH1
TANGO6
TANGO6
Click to alter th
50
bamCoverage on data 23
bamCoverage on da
0
Transcription Factor ChIP-seq (161 factors) from ENCODE with Factorbook Motifs
MYC
EZH2

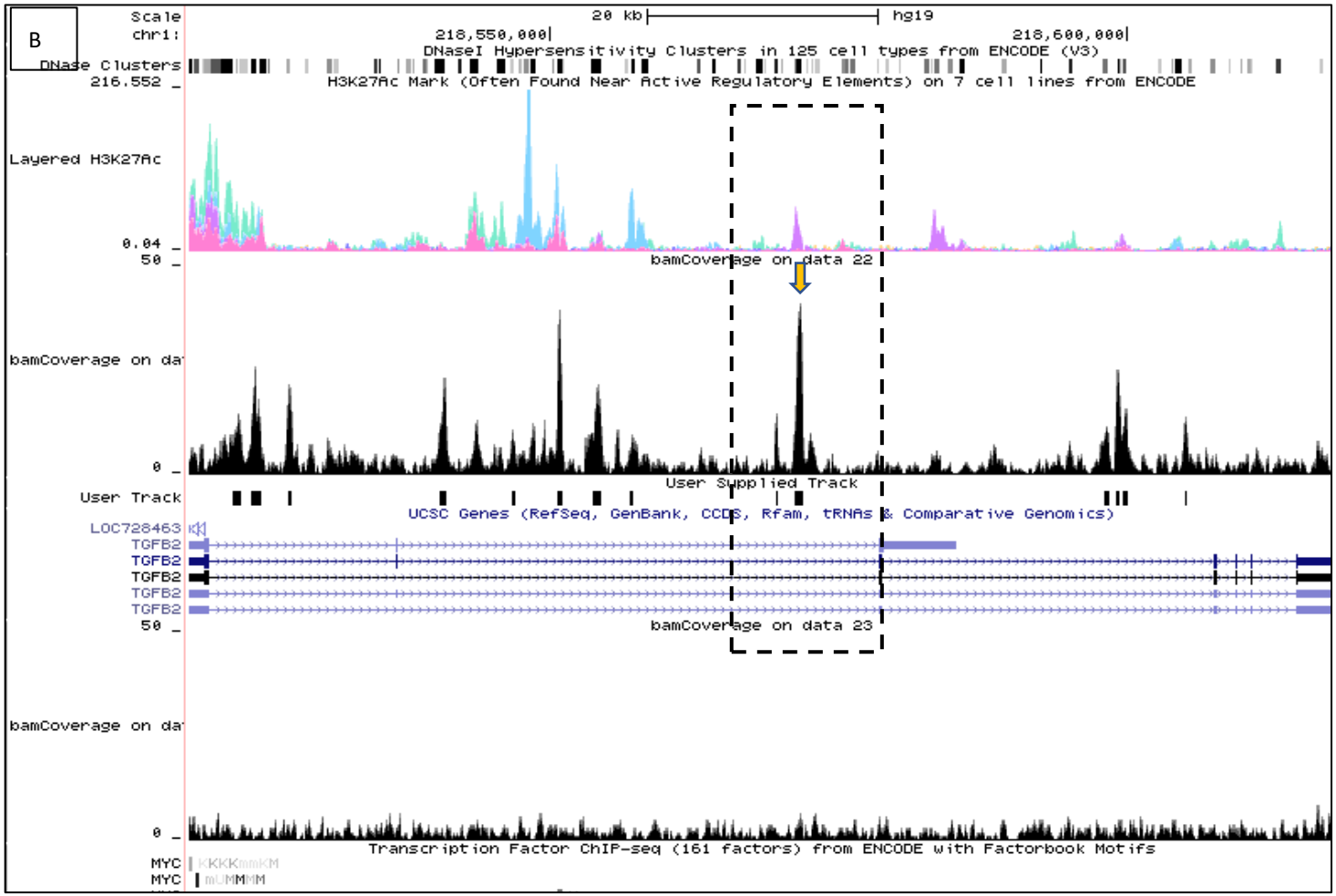
B
Scale
chr1:
20 kb
hg19
218,550,000
218,600,000
DNaseI Hypersensitivity Clusters in 125 cell types from ENCODE (V3)
DNase Clusters
216.552
H3K27Ac Mark (Often Found Near Active Regulatory Elements) on 7 cell lines from ENCODE
Layered H3K27Ac
0.04
50
bamCoverage on data 22
bamCoverage on da
0
User Supplied Track
User Track
UCSC Genes (RefSeq, GenBank, CCDS, Rfam, tRNAs & Comparative Genomics)
LOC728463
TGFB2
TGFB2
TGFB2
TGFB2
TGFB2
50
bamCoverage on data 23
bamCoverage on da
0
Transcription Factor ChIP-seq (161 factors) from ENCODE with Factorbook Motifs
MYC
MYC

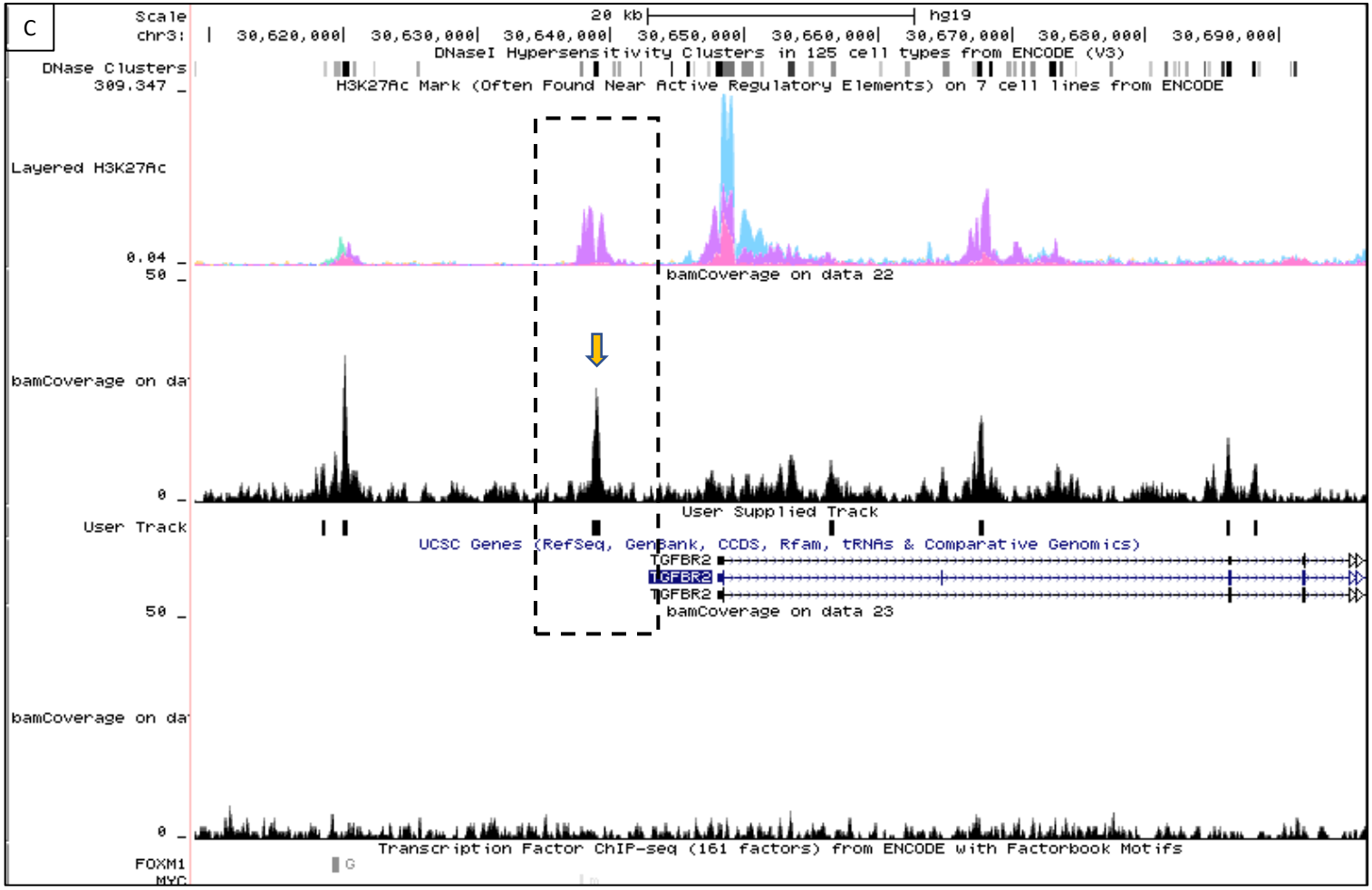
C
Scale
chr3:
20 kb
hg19
30,620,000
30,630,000
30,640,000
30,650,000
30,660,000
30,670,000
30,680,000
30,690,000
DNaseI Hypersensitivity Clusters in 125 cell types from ENCODE (V3)
DNase Clusters
309.347
H3K27Ac Mark (Often Found Near Active Regulatory Elements) on 7 cell lines from ENCODE
Layered H3K27Ac
0.04
50
bamCoverage on data 22
bamCoverage on da
0
User Supplied Track
User Track
UCSC Genes (RefSeq, GenBank, CCDS, Rfam, tRNAs & Comparative Genomics)
TGFBR2
TGFBR2
TGFBR2
50
bamCoverage on data 23
bamCoverage on da
0
Transcription Factor ChIP-seq (161 factors) from ENCODE with Factorbook Motifs
FOXM1
MYC

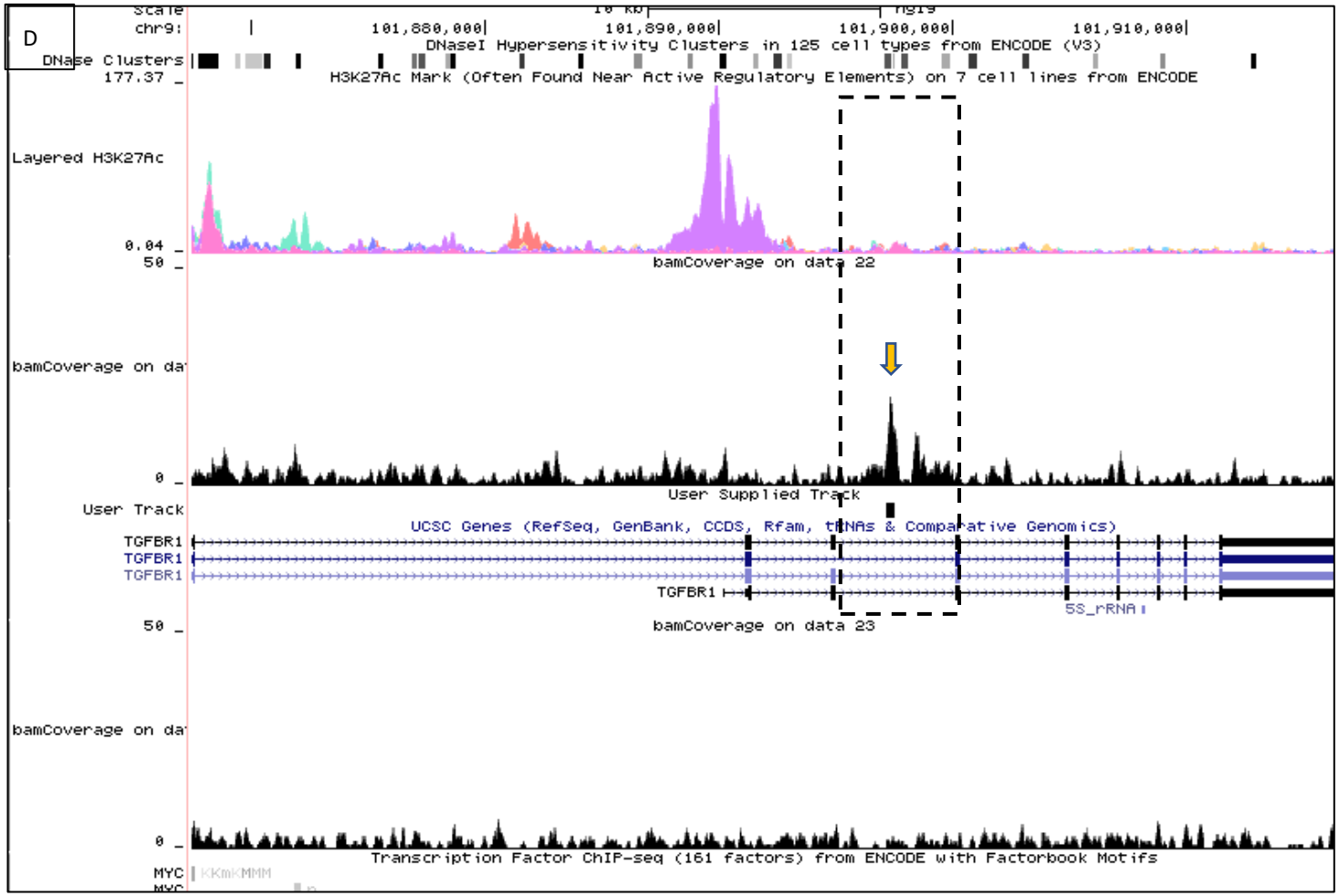

Figure 4.8. ChIP sequencing trace. The ChIP-seq trace was aligned with whole human genome version 'Human Feb. 2009 (GRCh37/hg19) Assembly' using UCSC Genome Browser. In each picture the H3K27Ac marker (upper trace) was provided by UCSC Genome Browser. The yellow arrows show the peaks from where the DNA sequence was used to design the PCR primers. (A) *CDH1* gene had two relatively small equidistant peaks, the sequences of the regions were used to design the PCR primers. The first peak is located on the promoter region of *CDH1*, and the second at an equidistant region in the first intron. Both peaks were in regions where H3K27Ac marker was present. (B) *TGFB2* gene showed several high peaks, the highest one was chosen as region of interest. The region had H3K27Ac marker and is located in the second intron. (C) *TGFBR2* gene showed a peak at the promoter region, the peak also aligned with the presence of H3K27Ac marker. (D) *TGFBR1* gene showed a peak in the third intron, the peak was not aligned with H3K27Ac markers. ChIP-seq was performend by Dr Philip Kitchen at University of Birmingham.

PRH seems to be an important regulator of TGF-β signalling since TGF-β signalling genes were alerted in microarray. One of the more dramatic alterations was observed in the genes *TGFB2* and *TGFBR2*. The myc-PRH ChIP-seq traces showed peaks in both these genes.

PRH overexpression downregulates TGF-β genes and upregulates E-cadherin gene expression

To confirm that multiple TGF-β signalling genes are regulated by PRH, I overexpressed PRH in PC3 cells. The choice of an adenovirus vector containing myc-PRH downstream of the CMV promoter (Soufi et al. 2006), was made based on the high efficiently of infection with this method. The cells were infected with the myc-PRH (PRH) or empty virus (ΔE1) and left to grow for 48h post infection (as explained in section 2.7.2.1.1). mRNA extracts were used in qPCR (Figure 4.9), for the genes flagged in the microarray analysis (*TGFB2* and *TGFBR2*). *HHEX* qPCR was used to show successful over-expression of PRH and *CDH1* (E-cadherin) was used as an epithelial marker. The same infection protocol was used to extract cross-linked cell nuclei and they were used in a ChIP-qPCR assay (figure 4.10), to confirm if PRH binds to the genes flagged (*CDH1*, *TGFB2*, *TGFBR1* and *TGFBR2*). PC3 cells were infected with ∆E1 or PRH virus, cross-linked and the nuclei were extracted. The DNA was shredded and ChIPed using either Myc-tag or normal rabbit IGG antibody. The purified DNA was used in qPCR detection. Primers were produced to amplify regions of the chosen peaks in the ChIP-seq.

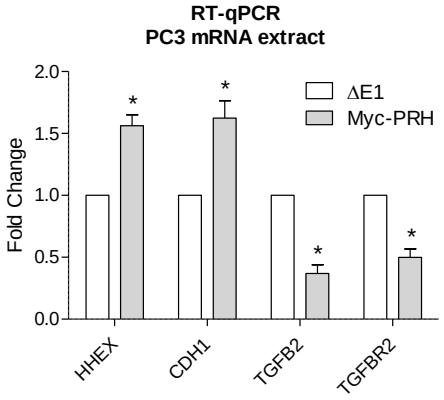

Figure 4.9. PRH regulates epithelial marker gene *CDH1* and TGF-β signalling genes. Two adenoviruses were used to infect PC3 cells. ΔE1= empty virus control, PRH= wild type myc-tagged PRH. qRT-PCR of the mRNA extracted from the infected cells. *HHEX* was used to show successful over-expression. *CDH1* was up-regulated in PRH when compared to ΔE1. *TGFB2* and *TGFBR2* were both downregulated. No detectable quantities of *TGFBR1* were found. Statistical analysis: one-sample t test with hypothetical value 1. *different from ΔE1 with p<0.05.

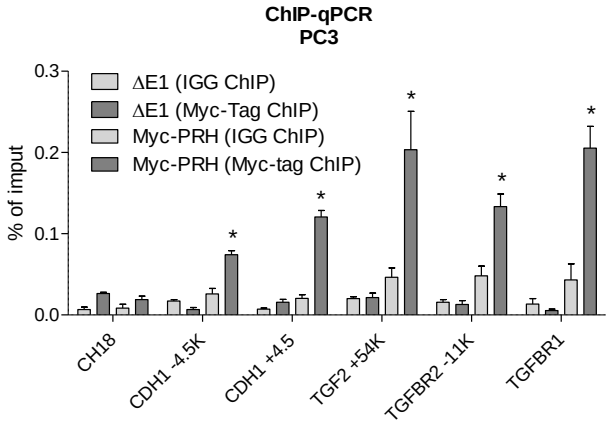

Figure 4.10. PRH regulates EMT/MET genes and TGF-β signalling genes. Two adviruses were used to infect PC3 cells. ΔE1= empty virus control, PRH= wild type myc-tagged PRH. Myc-tag ChIP-qPCR of PC3. Myc-PRH bind to E-cadherin gene (*CDH1*) in the regions -4500bp (3-fold increase) and +4500bp (6-fold increase). It also binds to +54000bp region of the gene *TGFB2* (5-fold increase), -11000bp region of the gene *TGFBR2* (3-fold increase) and +30000bp region of the gene *TGFBR1* (5-fold increase). Statistical analysis: one-way ANOVA with Bonferroni post-test to compare each column *different from controls (ΔE1 (IGG ChIP) with p<0.05.

qRT-PCR shows the mRNA levels of the TGF-β signalling genes tested, *TGFB2* and *TGFBR2* were downregulated (p<0.05) in the PRH group when compared to the ΔE1 group. *HHEX* upregulation (p<0.05) was used to show successful over-expression of PRH. *CDH1* (E-cadherin) was used as an epithelial marker and was found to be up-regulated with PRH expression when compared to ΔE1.

In the ChIP-qPCR, two primers were used to detect E-cadherin gene (*CDH1*) one probing the region - 4500bp and the other to the + 4500bp of the gene, a 3-fold

increased binding of myc-PRH above the background was found in the - 4500bp region and a 6-fold increase in the + 4500bp region. The + 54000bp region of *TGFB2* presented a 5-fold PRH binding increase above the background. In the *TGFBR2* gene the primers detected the region - 11000bp, and showed a 3-fold above the background PRH binding. The + 30000bp region of *TGFBR1* presented a 5-fold increase in the Myc-PRH (Myc-tag ChIP). These findings suggest that PRH overexpression can trigger partial MET in PC3 cells rescuing the epithelial status of these cells by directly regulating the expression of E-cadherin while downregulating the expression of TGF-β signalling genes.

To test whether PRH also interfered with the migration of PC3 cells I performed a chemotaxis assay using Boyden chambers. Initially, the adenovirus carrying PRH overexpression (PRH) plasmids or empty vectors (ΔE1) plasmids were used to infect the cells and analyse the effects of PRH on cell migration. Unfortunately, the virus infection itself interfered with the cell migration (figure 4.11 A): the ΔE1 virus reduced cell migration as much as the PRH overexpression virus. Nonetheless, we still observed an apparent morphological change in the PRH overexpression adenovirus infected cells, which was not observed in the empty virus treated cells. As seen in figure 4.11 B, the PRH adeno-virus infected cells showed smaller surface coverage, and the cells looked more rounded. To avoid this viral effect on migration, a plasmid transfection using lipofectamine was used to evaluate the effect of PRH expression on PC3 cell migration. The transfection efficiency was relatively low, so PRH plasmid was co-transfected with a plasmid expressing GFP, and GFP alone was used as a control. From the migrated cells only green ones, the cells expressing GFP, were considered. Figure 4.11 C shows that PRH overexpression significantly ($p<0.05$) reduced the cell migration of PC3 cells.

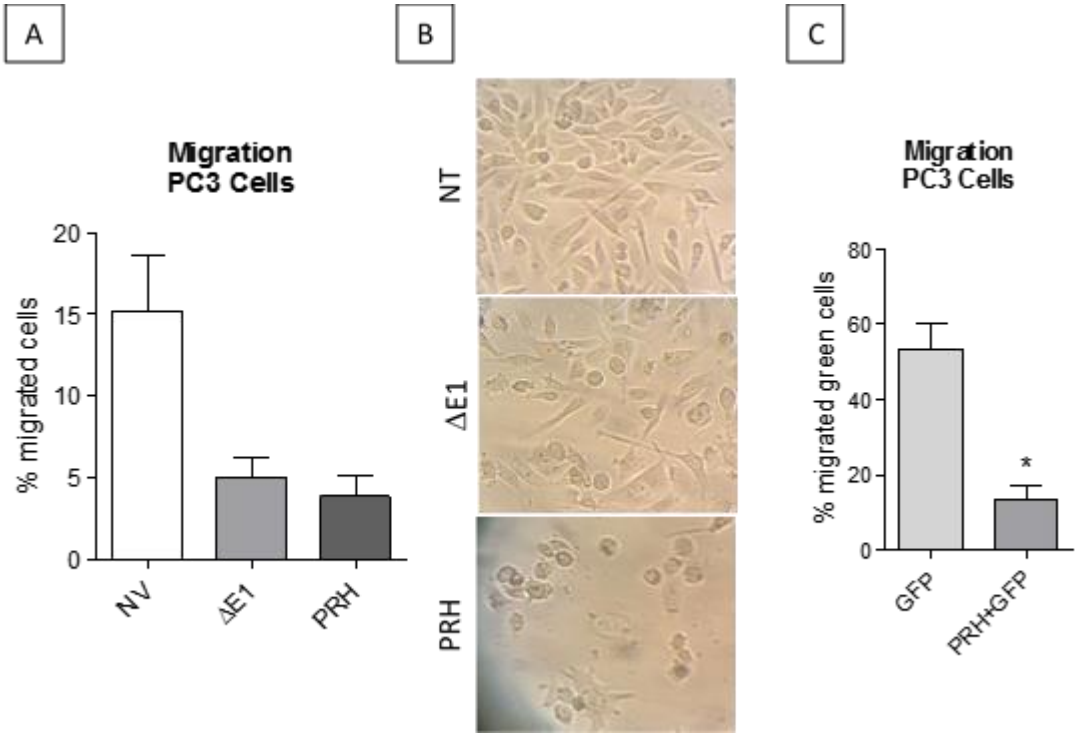

Figure 4.11. The effects of PRH overexpression on cell migration. (A) PRH over expression in PC3 cells using adenovirus, the viral infection showed interference with the cell migration and proved itself unsuitable for this analysis. (B) Photomicrography of PC3 cells infected with no virus (NV), empty virus (ΔE1) or PRH virus. PRH virus infected cells showed reduced surface coverage at this time point and altered morphology when compared to NV and ΔE1 controls. (C) Migration assay to analyse the effect of PRH overexpression on PC3 cell migration using lipofectamine transfection. PRH was co-transfected with GFP and GFP alone used as the control. PRH transfected group showed a reduced number GFP expressing migrated cells when compared to GFP only group.

The use of adenovirus provided a good PRH overexpression in a high percentage of the cells, therefore, although not being useful in migration assays, it produced an excellent model to study the molecular alterations caused by PRH overexpression. Four different adenoviruses were used to infect PC3 cells. The same ΔE1 was used as an empty virus control, and PRH virus to express myc-tagged wild type PRH. However, two other myc-tagged PRH viruses containing mutations were also used, PRHCC is a myc-PRH with mutations that prevent phosphorylation by CK2 and PRHM1 is a myc-PRH mutant that cannot bind to DNA (Soufi et al 2006). A no viral infection control was used as a comparison (figure 4.12). Following infection, the cells in each group were divided in two, half of the cells were treated with TGF-β and the other half treated with vehicle for 48h. As shown in figure 4.11 whole protein extracts from these treatments were used in western blot analysis (as explained in section 2.9.1). To assess successful overexpression of the PRH and its variants, a myc-tag western blot was performed. To assess epithelial status of the cells, the

epithelial marker E-cadherin was evaluated by western blot using a low exposure time (5 minutes).

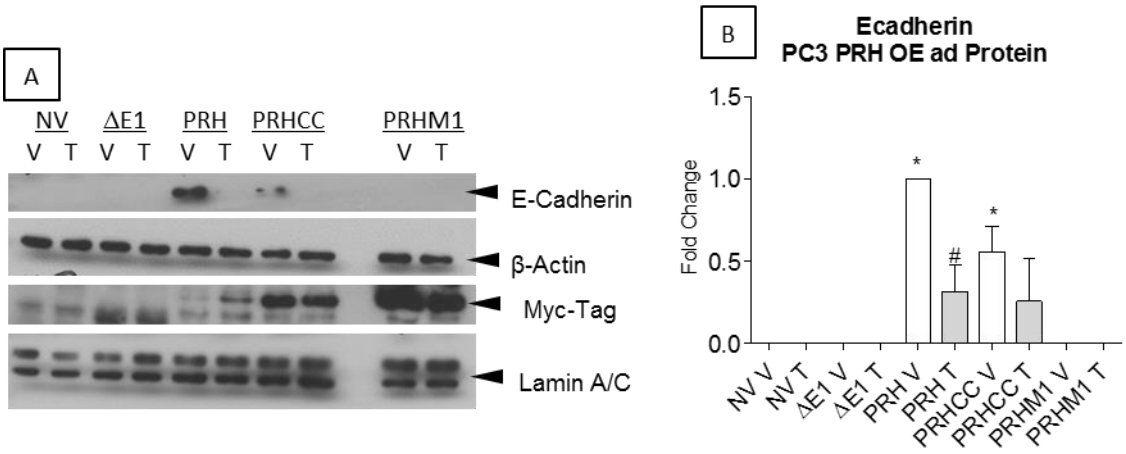

Figure 4.12. PRH induces MET in PC3 cells. Different adenoviruses were used to infect PC3 cells. NV= no virus control, ΔE1= empty virus control, PRH= wild type myc-tagged PRH, PRHCC= myc-tagged PRH mutant that cannot be phosphorylated and PRHM1= myc-tagged PRH mutant that cannot bind to DNA, T= TGF-β treated and V=vehicle treated (V). (A) Representative western blot images. E-cadherin, β-actin, Lamin A/C and Myc-tag with different virus infections and TGF-β or vehicle treatment. (B) PRH expression increased E-cadherin expression and the TGF-β treatment abolished the effect of PRH on E-cadherin. Densitometry of three independents short-exposure E-cadherin western blot, bands normalised to β-actin. E-cadherin up-regulation was observed in PRH and PRHCC groups, TGF-β treatment partially rescued PRH effect on E-cadherin in both treatments. No other treatment increased E-cadherin expression. Statistical analysis: one-sample t test with hypothetical value 1. *different from NV V with $p<0.05$ #different from PRH V with $p<0.05$.

The PRH wildtype group showed a significantly ($p<0.05$) stronger E-cadherin expression when treated with vehicle. TGF-β treatment significantly ($p<0.05$) reduced the expression of E-cadherin in the presence of PRH overexpression. PRHCC also showed a significant ($P<0.05$) upregulation in E-Cadherin expression, although the band was less intense than the PRH band. TGF-β treatment rescued the low expression status of E-Cadherin but the reduction was not statistically significantly. None of the other treatments showed E-cadherin expression in short exposure times. I conclude that PRH up-regulates E-Cadherin in PC3 cells inducing a partial MET. TGF treatment blocks the up-regulation of E-Cadherin by PRH, despite the fact that PRH expression is not driven by the PRH promoter in this experiment. This suggests that TGF treatment reduces PRH mRNA levels or otherwise blocks PRH action without regulating the activity of the PRH promoter.

Inducible PRH overexpression in PC3 cells

The results described thus far in this chapter suggest that PRH regulates the expression of multiple TGF-β signalling multiple genes and that PRH overexpression represses cell migration. However the adenovirus infection interfere with cell migration. Stable cell line models are important in the study of gene function in mammalian cells, as they are genetically homogeneous in culture, and because the DNA is integrated into the genome of the cells and, even subsequent generations will carry the transgene. Here I describe the creation of a doxycycline inducible PRH overexpression system based on the PC3 cell line. The model will offer the opportunity to study the effects of PRH on proliferation over a longer time in a system where all of the cells will carry the PRH gene. This system could enhance the reproducibility of PRH overexpression. Moreover, the use of a second overexpression system will confirm that the results obtained using the adenoviral expression system are robust and reliable.

Cell line production and doxycycline dose response

To create a doxycycline inducible PRH overexpression stable cell line, PC3 cells were transduced with lentivirus particles carrying a myc-tagged PRH cDNA downstream of a doxycycline inducible promoter (as described in section 2.4.2). The lentivirus also carries constitutively expressed genes to conferred gentamicin resistance and GFP expression to the transduced cells. The antibiotic resistance is important to select the transduced cells. The GFP tag will allow the observation of the cells using a fluorescence microscope. Figure 4.13 shows images of the transduced cells before and after selection.

The initial incubation with the lentiviral particles transduced approximately 50% of the PC3 cells. The selection with G148 killed all of the uninfected cells, while the other ones proliferated, resulting in approximately 100% of the cells in the well expressing GFP. The cells were named PC3 PRH LV and expanded still in selection media for another two passages. When the number of cells was sufficient in number to keep stocks and conduct experiments, the cell stocks were frozen in freezing media and kept in liquid nitrogen until needed.

Is important to mention that the PC3 PRH LV cell line is polyclonal. Alternatively, a stable cell line can be made by selecting clones that efficiently express the inserted gene and by growing the cell line from a single starter cell. Both methods have merit but the choice to use a polyclonal lineage was made to account for the heterogenicity observed in prostate tumours. Additionally, polyclonal cell lines compensate for effects brought by the random insertion of the vector gene into the genome.

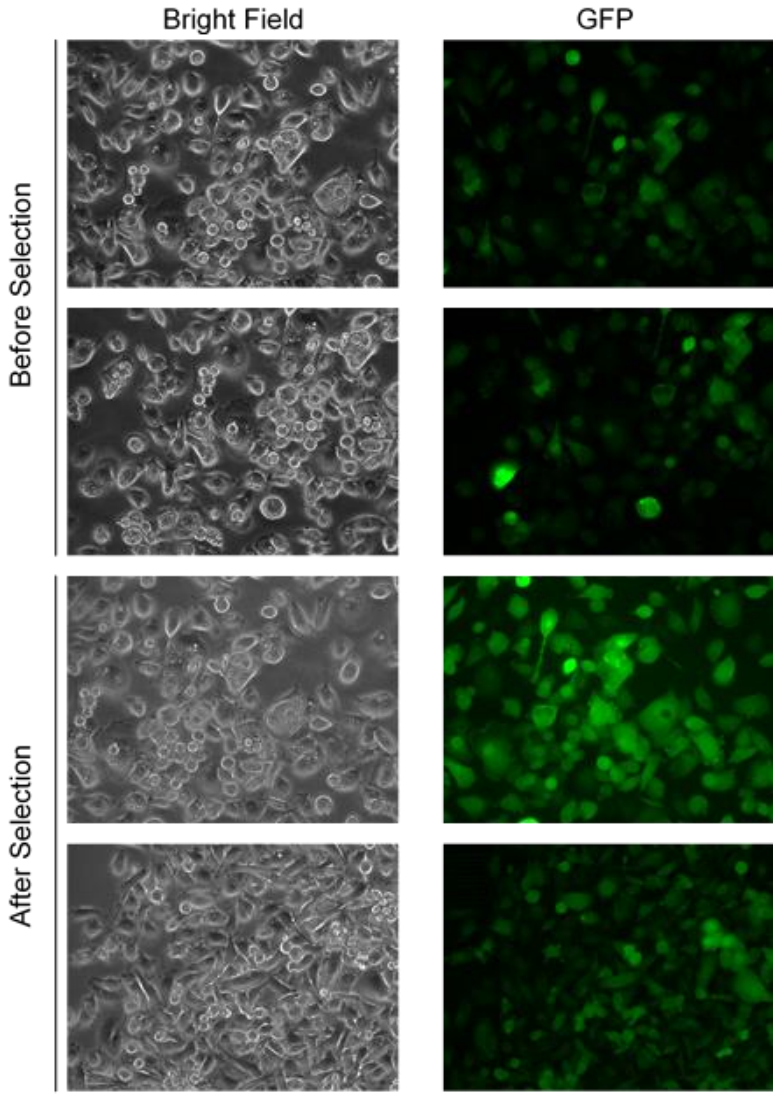

Figure 4.13. Establishment of a PC3 PRH overexpression cell line. Constitutively expressed GFP showed successful transduction of the vector carrying the inducible PRH overexpressing lentivirus. Photomicrography taken in a Leica DMI 6000 B microscope shows an approximate rate of 50% GFP expressing cells. The lentivirus particle used also carry a constitutively resistance to gentamicin, the section 'After selection' shows pictures of PC3 with PRH lentivirus after being selected with G418 for 15 days. Approximately 100% of the cells that survived the selection expressed GFP.

To assess the doxycycline dose to be used in the PRH overexpression analysis, a doxycycline dose-response experiment was performed. The PC3 PRH LV cells were seeded in 6 well plates and treated with vehicle or various doses of doxycycline (as explained in section 2.7.2.1.2). After seven days of treatment, whole cell protein extract was used in a myc-tag western blot to examine overexpression of myc-PRH (Figure 4.14). Although there was a variation in lower doses, PRH overexpression behaved in a dose-dependent fashion, in that, the highest doxycycline dose (1.5 ug/mL) showed the most intense myc-tag band. Photomicrographs were also taken to analyse the cell morphology and confluence changes caused by the treatment (Figure 4.15).

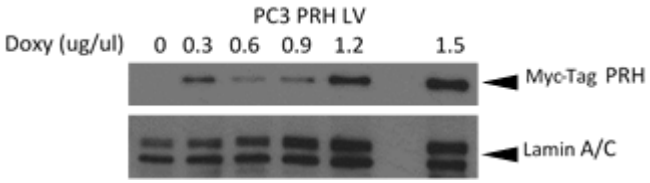

Figure 4.14. Doxycycline induced Myc-PRH expression in PC3 PRH LV. Western blot image of PC3 PRH LV cells treated with vehicle or increasing doses of doxycycline. Myc-tag western showed PRH overexpression and Lamin A./C was used as loading control (n=1).

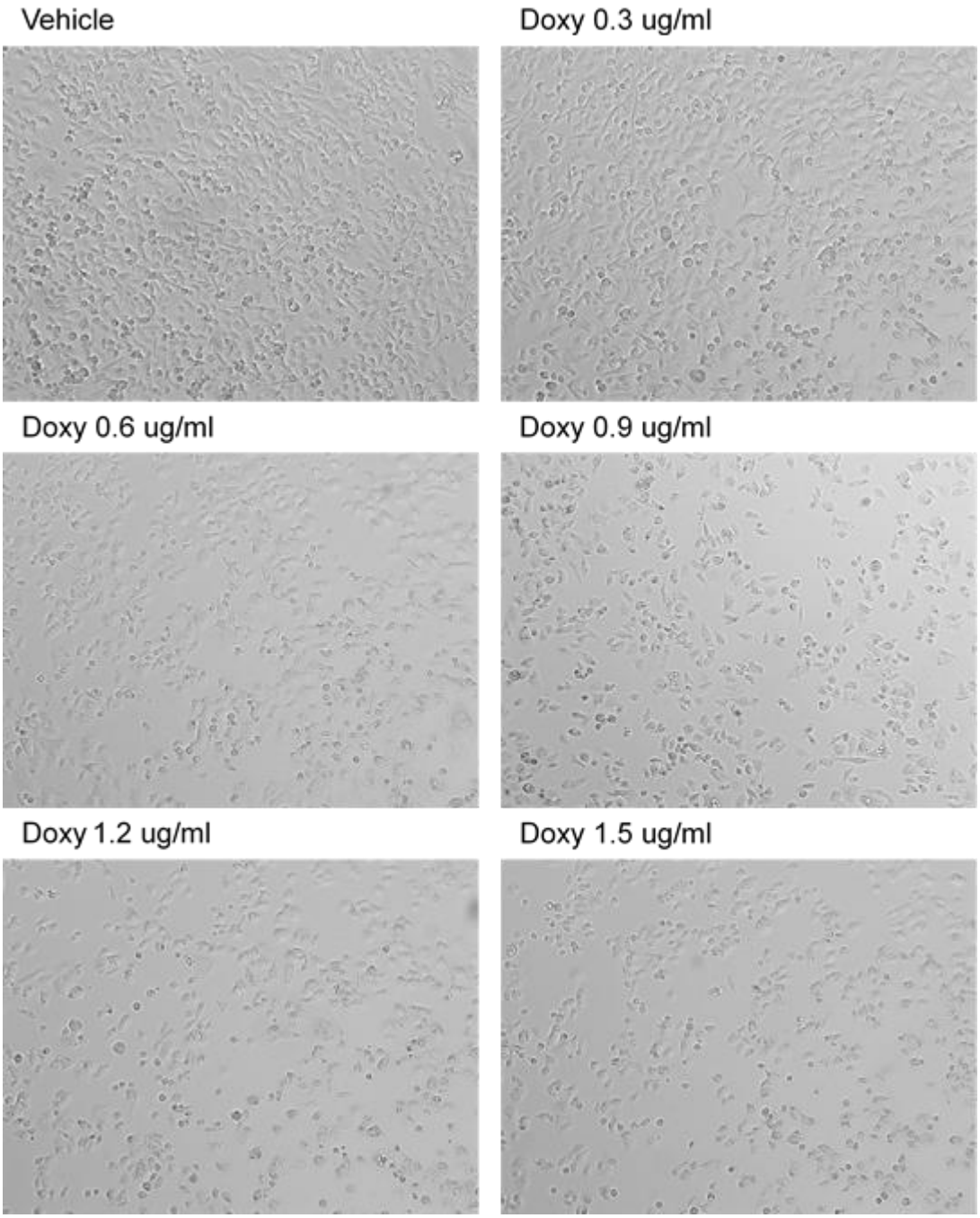

Figure 4.15. Doxycycline reduced PC3 PRH LV confluence. Photomicrography taken in a Leica DMI 6000 B microscope. Equal amounts of cells were seeded in 6-well plates and treated with different amounts of doxycycline or vehicle for seven days. An apparent increase in the frequency of rounded cells was also observed in all the doxycycline doses from 1.2 ug/mL and higher.

Doxycycline treatment reduced the PC3 PRH LV cell confluence in a dose-dependent fashion; the cell confluence went from approximately 100% in vehicle to approximately 90% in 0.3 ug/mL doxycycline, 50% in 1.2 and 1.5 ug/mL doxycycline confluence was between 50% and 40% (Figure 4.15). This finding suggests that the cell proliferation was reduced with the doxycycline treatment. Furthermore, the treatment seemed to reduce the presence of elongated cells in a dose-dependent manner. Although the appropriate cell measurements were not made, observations suggested that doxycycline treatment presented a higher frequency of rounded cells, clearly observed in figure 4.15 (0.6, 0.9, 1.2 and 1.5 ug/mL doxycycline).

Figure 4.16 A shows an MTT assay performed in PC3 cells to assess toxicity of Doxycycline to PC3 cells. To assess the effects of PRH overexpression on cell viability, the cells were treated with either vehicle or increasing doses of doxycycline for seven days. On the seventh day, MTT assays were performed as explained in section 2.12 (figure 4.16 B). Concomitantly, cells were seeded in a 6-well plate and treated with vehicle or doxycycline 1.5 ug/mL. Over eighteen days, cells were trypsinised, counted and reseeded in a known dilution every 2 days. The total number of cells on each day was determined and normalised to the dilution factor. The results were plotted in a growth curve graph (figure 4.16 C). To evaluate if the cells were dividing slower, cells were treated with doxycycline 1.5 ug/mL or vehicle, and on the seventh day, cells were trypsinised, seeded in equal numbers in a 96 well plate and left to recover overnight. An EdU incorporation assay was then performed to determine the number of cells transitioning through S-phase (as explained in section 2.13) (figure 4.16 D).

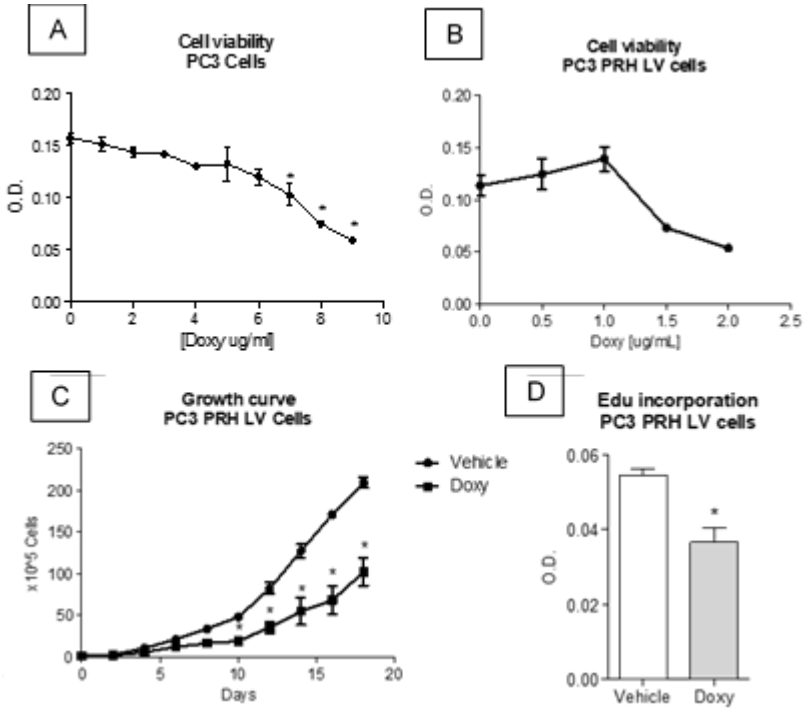

Figure 4.16. Doxycycline reduced PC3 PRH LV cell growth. (A) The graph shows the average formazan salt formation measured using a spectrophotometer (viability assay) in doxycycline and vehicle treated cells with 8 technical replicates. Statistical analysis: One-way ANOVA followed by Bonferroni post-test, $p<0.05$. (B) The graph shows viability assay in PC3 PRH LV cells treated with vehicle or increasing doses of doxycycline. (C) The graph shows total number of PC3 PRH LV cells in several time points over eighteen days, doxycycline (1.5 ug/mL) or vehicle. Statistical analyses: two-way ANOVA with Bonferroni post-test to compare the treatments in each time point, $p<0.05$. (D) The graph shows EdU incorporation in PC3 PRH LV cells treated with 1.5 ug/mL of doxycycline or vehicle for seven days. The incorporated EdU was measured by colorimetric assay using spectrophotometer. Statistical analysis: two tailed unpaired t-test, $p<0.05$

The MTT assay showed that doxycycline only induced statistically significant changes in the number of viable cells at doses higher than 7 ug/mL, however, dosed higher than 1 ug/mL, reduced the number of viable PC3 PRH LV cells after seven days of treatment. The growth curve showed that PC3 PRH LV cells treated with doxycycline (1.5 ug/mL) reduced the proliferation rate observed ($p<0.05$). Cell growth was observed for eighteen days, but the trend observed indicates a widening in the difference between the vehicle treated cell proliferation curve and the doxycycline treated PC3 PRH LV cell proliferation curve. EdU is incorporated into the DNA of dividing cells, making its measurement a reflection of the cell division rate. The data show a reduced EdU incorporation in doxycycline treated PC3 PRH LV cells when compared to vehicle treatment ($p<0.05$). Thus, the low number in the doxycycline treated PC3 PRH LV cells observed is likely due to a reduced cell division rate.

The reduction in cell number could also be a result of increased cell death caused by antibiotic toxicity. To assess if the doxycycline treatment is toxic and killing the PC3 PRH LV cells, I performed propidium iodide staining. Propidium iodide is a fluorescent DNA intercalating dye that cannot cross the cell membrane, and it is useful to stain dead cells. Three conditions were used: as a positive control, an excessive dose of the antibiotic G148 (9 mg/mL), as a negative control doxycycline vehicle, and 1.5 ug/mL of doxycycline (figure 4.17).

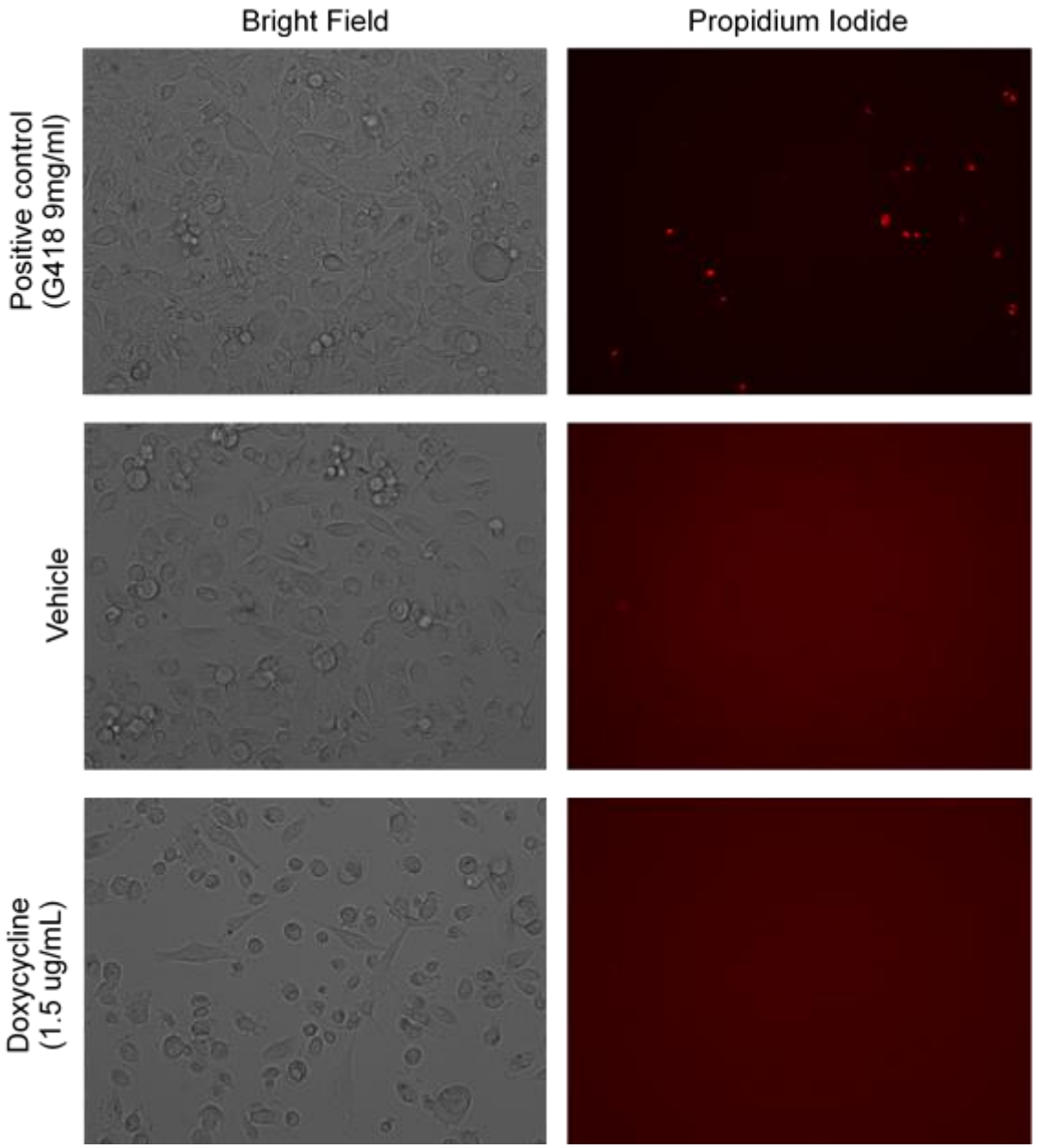

Figure 4.17. 1.5 ug/mL of Doxycycline does not kill PC3 PRH LV cells. Photomicrography taken in a Leica DMI 6000 B microscope shows PC3 PRH LV cells treated with 1.5 ug/mL of doxycycline for 7 days do not stain with propidium iodide. The positive control presented an average of 15 cells/field stained with propidium iodide.

Doxycycline treatment is not toxic to the PC3 PRH LV cells since no propidium iodide stained cells were present in doxycycline treated cells. The positive control presented an average of 15 propidium iodide stained cells per counted field from a total of 10 fields (n=1).

PC3 PRH LV characterisation

To assess whether doxycycline treatment would affect the migration of PC3 PRH LV cells, the cells were treated with vehicle or increasing doses doxycycline for 7 days before being used in a chemotaxis assay (as explained in section 2.8) (figure 4.18 A). Only one repetition of this migration dose-response was made, but migration in PC3 PRH LV cell is reduced in a dose-dependent fashion. Therefore, the most efficient migration inhibition, observed with 1.5 ug/mL of doxycycline was chosen to confirm the effects on migration. To confirm reproducibility, cells in three independent experiments were treated with 1.5 ug/mL of doxycycline or vehicle, these cells were used in chemotaxis assays (figure 4.18 B). Doxycycline 1.5 ug/mL significantly reduced PC3 PRH LV cell migration when compared to vehicle treatment ($p<0.05$), Hydroxyurea was used in all of the chemotaxis assays to inhibit cellular proliferation.

A reduced migration ability is a characteristic of epithelial cells in comparison to mesenchymal cells. Earlier I showed that transient PRH overexpression reduced cell migration and recovered an epithelial phenotype in PC3 cells. Therefore, the reduced in migration observed here could be a reflection of reactivation of epithelial phenotype in doxycycline treated PC3 PRH LV cells. To evaluate cell morphology changes, the cells were treated with doxycycline or vehicle for seven days. Microscope photographs were used to analyse cell morphology (figure 4.18 C). The cells treated with 1.5 ug/mL of doxycycline presented an apparent lower frequency of elongated cells. Detailed manual observation of the cell morphology revealed the existence of cell arrangements in clusters, characteristic of epithelial cells, in doxycycline treated PC3 PRH LV cells. An example of doxycycline treated PC3 PRH LV cells growing in a small cluster is observed on the right, in figure 4.18 C.

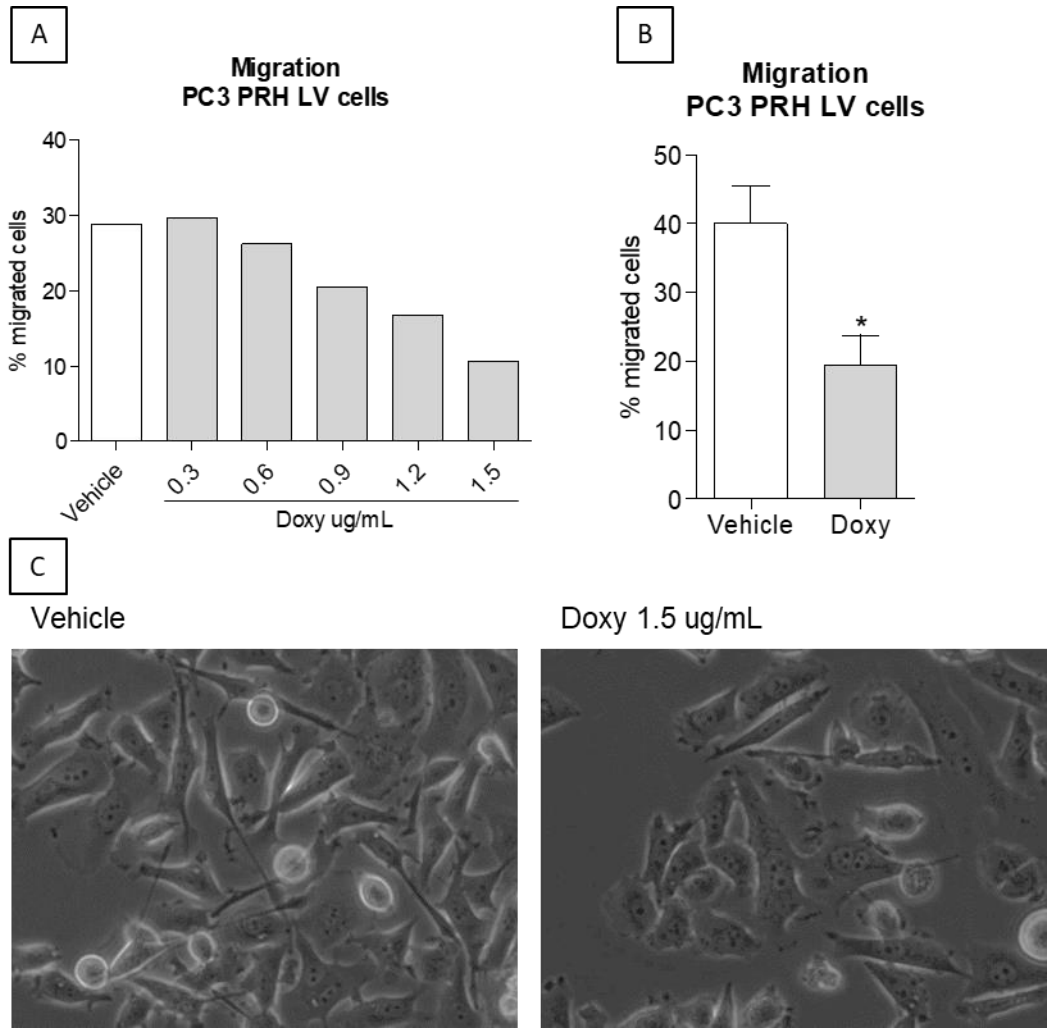

Figure 4.18. Doxycycline reduces PC3 PRH LV cell migration in chemotaxis assays. (A) The graph shows the percentage of migrated PC3 PRH LV cells (18h) after treatment with vehicle or increasing doses of doxycycline (n=1) for 7 days. (B) The graph shows the percentage of migrated cells in 3 independent experiments where PC3 PRH LV cells were treated with vehicle or 1.5 ug/mL of doxycycline for 7 days. Statistical analyses: two tailed unpaired t-test, $p<0.05$. (C) Photomicrographs of PC3 PRH LV in culture treated with vehicle or 1.5 ug/mL of doxycycline for 7 days. Doxycycline treated cells showed an apparent lower average of elongated cells and some cases where the cells grew in clusters (characteristic of epithelial cells) were observed, as seen in the picture of the doxycycline treated cells.

The reduction in migration plus the morphology changes showed by microscope observation indicates a possible reactivation of an epithelial phenotype in PC3 PRH LV cells. However, epithelial marker protein expression is the best way to demonstrate epithelial phenotype. To assess if the PRH overexpression induced by doxycycline in PC3 PRH LV cells can recover an epithelial phenotype, the cells were treated with doxycycline or vehicle for seven days. Whole cell mRNA extract was then used in qRT-PCR (as explained in section 2.10.1) to measure the expression levels of epithelial markers and TGF-β signalling genes, *HHEX* qRT-PCR was used to confirm PRH mRNA overexpression (figure 4.19 A). Doxycycline induced PRH

mRNA overexpression when compared to vehicle treated cells ($p<0.05$). PRH overexpression significantly upregulated E-cadherin mRNA (*CDH1*) expression ($p<0.05$), while significantly downregulated TGF-β pathway genes (*TGFB2* and *TGFBR2*) ($p<0.05$).

Whole cell protein extract was also used to assess epithelial protein phenotype. Myc-tag western blotting was used to confirm overexpression (figure 4.19 B). Myc-tag western blot showed myc-PRH being detected only in PC3 PRH LV treated with doxycycline. Lamin A/C shows equal protein loading. E-cadherin western blot confirms the qRT-PCR results seen in figure 4.19 A.

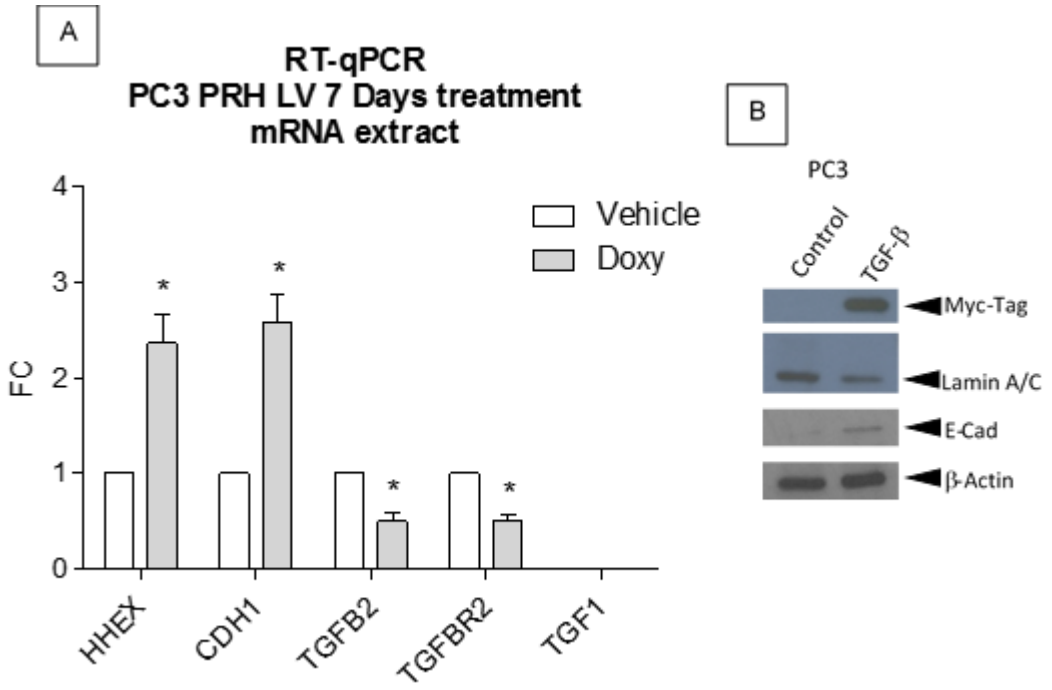

Figure 4.19. Doxycycline reactivates epithelial phenotype in PC3 PRH LV. (A) The graph shows the relative mRNA expression of various genes in PC3 PRH LV cells treated with vehicle or 1.5 ug/mL of doxycycline. *HHEX* mRNA upregulation shows successful PRH mRNA overexpression. All statistical comparisons made were between doxycycline 1.5 ug/mL and vehicle treatment. Statistical analyses: one-sample t-test with hypothetical value set to '1', $p<0.05$, $n=3$. (B) Western blot images of PC3 PRH LV protein extract probed with myc-tag antibody show PRH overexpression. E-cadherin western blot was used as an epithelial phenotype marker. Lamin A/C and β-actin were used to show equal loading ($n=1$).

Discussion

It was previously shown that PRH mis localisation is observed in breast cancer (Puppin et al. 2006). Also, the hyper-phosphorylation of PRH and its subsequent degradation by the proteasome is correlated to increased cell migration and proliferation in prostate cancer cells (Noy et al. 2012; Siddiqui et al. 2017). These reports suggest that PRH plays a role in cancer progression. Here I showed that *HHEX* is altered in 4% of the sequenced patients with prostate adenocarcinoma, and that the majority of the alterations were deep deletions. The loss PRH /*HHEX* gene in prostate cancer suggests that this gene is a potential tumour suppression gene. Interestingly, using the same database showed that *HHEX* gene deletion co-occurrence with *PTEN* gene deletion is statistically significant. *PTEN* is a tumour suppressor gene commonly deleted in many cancers, (as reviewed by Chu & Tarnawski 2004). *PTEN* and *HHEX* are both located at chromosome 10 in the region 10q23, this region presents loss of heterozygosity in approximately 50% of prostate cancers (Feilotter et al. 1998). Epigenetic regulation of PRH in prostate adenocarcinoma may also play a role in prostate cancer progression. The data obtained from the MethHC database compares the β-value of prostate adenocarcinoma samples to normal prostate samples. The methylation test is made by enquiring the CpG site with a methylated-specific probe and an un-methylated-specific probe, the β-value is the ratio of methylated probe intensity (Du et al. 2010). Here I showed that the average β-value of prostate adenocarcinoma in the *HHEX* gene body is higher than in normal prostate samples. CpG methylation is usually associated with gene silencing. My analysis shows that the increase in CpG methylation correlates with reduced PRH mRNA expression. This adds further weight to the suggestion that PRH is a tumour suppressor protein in prostate cancer.

The PRH immunostaining in a large number of prostate adenocarcinoma tissues also further illustrates the importance of PRH in prostate cancer progression. The Gleason's score (GS) description used here was described by the 2005 International Society of Urological Pathology (ISUP) Consensus Conference, with some modifications (Epstein et al. 2005). This newer system does not score tumours that would be originally scored GS 2–5 on a needle biopsy. The reason for this change is that the progression of the disease will depend on the most dedifferentiated part of

the tumour, with scoring being assigned to those areas. A needle biopsy can randomly pick a relatively well differentiated part of the tumour and mislead the prognosis prediction (Epstein et al. 2005). Because in this work we aimed to assess the correlation between PRH expression and differentiation degree of the gland, a scoring of each gland specifically would be more suitable, so the implementation of a narrower view of the prostate tissue could offer a more consistent population of glands on the histological section. Furthermore, I needed to score all the samples with the same criteria. Therefore, tumours that would be normally not be graded by needle biopsies due to low GS, here were still graded with the low scores of the original system, that way numeric variables could be used to compare the samples in the correlation test.

The PRH immunohistochemistry showed that PRH staining in the cytoplasm and nucleus of prostate cancer samples were negatively correlated to the differentiation degree of the tumours, expressed in the form of Gleason score. Interestingly, the results found in the correlation test were somewhat different from the ones published by Siddiqui and co-workers (Siddiqui et al 2017). This work showed that total cytoplasmic PRH appears to be elevated in these BPH and in a small number of prostate adenocarcinomas. However, the sample size in this work did not allowed a proper statistical evaluation, so a larger scale test, such as the one presented here, was still needed. The most consistent finding in the histopathology work in Siddiqui et al 2017 paper was the hyper-phosphorylation of nuclear PRH in BPH. The phosphorylation of PRH leads to PRH degradation, as shown by Noy et al 2012. This early stage phosphorylation, potentially, could lead to down-regulation of total PRH, via degradation of PRH by proteasome. Additionally, from the 9 adenocarcinoma (AC) samples presented, four samples were graded with GS >9 and presented moderate staining intensity. While from the 5 samples graded with GS =9, three presented low intensity staining, the sample size was too small to predict this correlation, but the trend agrees with my findings.

Another difference between the two reports is the sample type. Here the samples were obtained in needle biopsies, while the samples in Siddiqui et al 2017 paper were from a total prostate examination. The total prostate examination allows a whole tumour Gleason grading, which is important for the treatment and prognosis of the patient. However, the expression levels of neoplastic driving factors is known to

change in different parts of the tumour (Zieglschmid et al. 2007; Hu et al. 2013; Norton et al. 2016). The complex microenvironment can create different levels of differentiation within the same tumour and an equivalent difference in the expression levels of some proteins. Therefore, within the same tumour, it is possible to find areas expressing more or less PRH. This created a necessity to grade each gland separately in order to obtain a realistic comparison between PRH expression and gland differentiation, as discussed above. Finally, it is important to note that these samples should be re-scored by a pathologist before publication.

The results obtained *in vitro* also corroborate the correlation between PRH expression and tumour cell differentiation. The PC3 cell line was established in 1979 from a bone metastasis of a prostate adenocarcinoma. Morphological studies of PC3 showed that it is compatible with poorly differentiated adenocarcinoma. It presents a high metastatic and high tumour forming capability. The overexpression of PRH in PC3 cells reduced the migratory ability of PC3 cells and altered cell morphology. The expression of the epithelial marker E-cadherin was also affected. A clear E-cadherin up regulation was observed by western blot and by qPCR when PRH is over-expressed. As discussed on the previous chapter, E-cadherin expression is correlated with epithelial phenotype and better prognosis in cancer, including prostate cancer (Wade & Kyprianou 2018).

The ChIP data showed a possible direct regulation of the *CDH1* gene by PRH. ChIP-qPCR confirmed binding of Myc-PRH on both *CDH1* sites tested. Additionally, PRH seems to bind to multiple sites on the *CDH1* gene, as shown on the ChIP-seq trace. the PRH. The binding of PRH in different sites of the same gene could suggest the activation of expression via enhancer cooperation. A transcription factor can change the shape of the DNA in order to move from one binding site to another, forming a DNA loop in the process, reviewed by (Yesudhas et al. 2017). By forming a loop, a transcription factor can also serve as a protein bridge on the DNA, recruiting a distant enhancer to increase gene expression (Matthews 1992). For example, a DNA-loop activating an enhancer cooperation was demonstrated during the MET in non-tumorigenic mouse mammary gland cells. The DNA-loop was able to activated re-expression of E-cadherin by bringing two enhancers together (Alotaibi et al. 2015). The presence of enhancers on both regions identified by ChIP-qPCR (enhancer ID GH16J068731 and GH16J068736) opens the interesting possibility of

a future study to evaluate reactivation of E-cadherin expression by a similar mechanism in prostate adenocarcinoma cells. However, the possibility that PRH can activate E-cadherin expression simply by initiating the transcription is not discarded, Chromatin Conformation Capture (3C) studies could help elucidate this question, since 3C provided information on 3D chromatin structures that occur in living cells.

Another important alteration that PRH over-expression brought about was the regulation of TGF-β pathway proteins. The microarray data showed that the PRH over expression down-regulated the expression of *TGFB2* and *TGFBR2* mRNA. Additionally, the ChIP seq showed peaks at theTGF2, *TGFBR2* and *TGFBR1* genes, all confirmed by ChIP-qPCR. TGF-β signalling is important in prostate cancer progression. The blockage of TGF-β signalling by overexpressing a dominant-negative *TGFBR2* supressed tumour formation by PC3MM2 cells injected into nude mice (Zhang et al. 2005). Moreover, TGF-β has been shown to have a context-dependent effect on prostate cancer. Initially, TGF-β presents a tumour suppressor activity, but in advanced prostate tumours, it shows a pro-proliferative effect (Wade & Kyprianou 2018; Massagué 2008a). Mice expressing dominant negative *TGFBR2* showed higher metastatic activity than the controls (Tu et al. 2003). As shown here, PRH overexpression in PNT2-C2 cells caused down-regulation of TGF-β signalling genes (*TGFB2* and *TGFBR2*), while the over-expression of PRH in PC3 cells down-regulated the TGF-β signalling genes (TGF2 and *TGFBR2*) and repressed cell migration. *TGFBR1* expression was not detected here, data from the cancer cell line encyclopaedia (CCLE) shows that TGBR1 expression in PC3 cells is lower than TGF2 and *TGFBR2* but is detectable by RNAseq. The fact that *TGFBR1* was not detected here might be due to low mRNA concentration, or low primer quality. Therefore, the repetition of the qPCR should be done using a different primer pair to clarify this question. Nevertheless, the downregulation of *TGFB2* and *TGFBR2* is an important modification to the TGF-β pathway and it is likely to be effective in triggering MET in PC3 cells. Moreover PRH directly activates the expression of Endoglin, a TGF-β co-receptor that down-regulates TGF-β signalling (Siddiqui et al. 2017).

The establishment of a stable inducible PRH overexpressing cell line base on PC3 cells was successful. The dose-dependent response observed in PRH overexpression with doxycycline treatment showed that the overexpression could be

regulated by adjusting the dose of doxycycline. Moreover, even the highest dose of doxycycline tested does not seem to be cause direct toxicity. There was a reduction in the number of viable cells at the highest doxycycline dose tested, however, the reduction in the number of viable cells is a reflection of the reduction of cell proliferation rate, observed by the EdU incorporation assay.

MTT is a popular method to determine the number of viable cells due to its low cost and easy execution. It is based on the metabolisation of tetrazolium salt by the mitochondria of living cells (Sylvester 2011). The metabolite product (formazan blue) is coloured and can be measured using a spectrophotometer. In the assay executed here, the same number of cells were seeded in each well of a 96-well plate. However, the cells were incubated after seeding for 48 hours. That gives time for the cells to proliferate, therefore cells presenting a lower proliferation rate would display a lower quantity of formazan blue formed after the addition of MTT salt. The reduced incorporation of EdU and reduced growth rate support the theory that the lower number of viable cells is a reflection of the lower number of cells rather than a toxic effect of doxycycline. Furthermore, the propidium iodide staining shows no difference in the number of dead cells between the vehicle treatment and the highest dose of doxycycline tested.

Published data shows that PRH overexpression reduced the cell migration in prostate and breast cells (Kershaw et al. 2014b). Lower migratory ability is a characteristic of cells displaying an epithelial phenotype (Thompson et al. 2005). Epithelial cells are closely attached to their neighbouring cells by adhesion proteins such as E-cadherin. In some cases, they are also attached to a basal membrane where they remain indefinitely (Gartner et al. 2011). Actually, the detaching of epithelial cells from their basal membrane is one of the last stages of EMT (Kalluri & Weinberg 2009). In culture, epithelial cells are normally strongly attached to their neighbouring cells, growing in clusters and presenting low migratory ability (Lang et al. 2001). In PC3 PRH LV cells treated with doxycycline, I observed a reduction of migration and in culture, a cluster growth pattern was occasionally seen. Additionally, the expression of the main epithelial phenotype marker, E-cadherin, was found upregulated in PC3 PRH LV cells when they were treated with doxycycline.

The demonstration of similar effects of PRH overexpression in PC3 cells in a second model shows the robustness of the data. Stable cell line models have the advantage of a more homogenous overexpression, which can increase reproducibility (Savage et al. 2013; Büssow 2015). The qRT-PCR from the stable overexpression showed less variability than the adenoviral overexpression. However, they show the same results regarding the expression of epithelial markers and TGF-β signalling genes.

With this, it possible to speculate that the expression of PRH can influence TGF-β signalling in prostate cancer. I showed that PRH protein expression is often down-regulated in advanced prostate adenocarcinoma, that PRH directly regulates TGF-β signalling genes *TGFB2* and *TGFBR2*, and that the overexpression of PRH can re-activate epithelial markers expression in PC3 cells. So, it is secure to say that PRH could regulate EMT in prostate adenocarcinoma cells by downregulating some of the proteins in the TGF-β signalling pathway.

The use of a TGF-β inhibitor to treat prostate cancer treatment had been discussed previously (Jones et al. 2009). In general, most of the data available comes from pre-clinical research. The inhibition of TGF-β pathway using antibodies prevented the appearance of lung metastasis caused by breast cancer (Biswas et al. 2007). However, as there are a number of contradictory publications and a much greater contextual understanding of TGF-β signalling is necessary. As TGF-β and PRH both regulate EMT in prostate cancer cells, and PRH seems to regulate the TGF-β pathway, PRH expression is likely to be important to TGF-β signalling during prostate cancer progression. With a better understanding of this process, we may be able to make more educated decisions regarding the treatment of earlier stages of prostate cancer in the future.

Chapter 5: TGF-β regulates PRH expression in prostate cell lines.

Introduction

An association between TGF-β signalling and PRH expression has been shown before. Published data showed that Smad3 and Smad2 regulates PRH expression in mice embryos, since animals that were heterozygous for a deletion of both genes presented PRH down-regulation accompanied by craniofacial axis, liver and thyroid malformations (Liu et al. 2004). However, in vitro experiments with *HHEX* promoter fragments cloned upstream from a luciferase gene suggested that Smad3 and Smad2 did not bind to the region studied (Zhang et al. 2002). Therefore, it remains to be clarified how TGF-β signalling regulates PRH expression and whether it does so in prostate cells. Here I use qRT-PCR and western blotting to examine the effects of TGF-β treatment on PRH expression and PRH phosphorylation in prostate cell lines. To examine the mechanism by which TGF-β regulates PRH activity, I also use phosphorylation inhibitors to examine whether the PRH phosphorylation is responsible for the effects of TGF-β on PRH expression in prostate cells. In parallel, I assess whether the *HHEX* promoter region is enriched following TGF treatment, meaning that pSmad3 binds to *HHEX* gene.

Results

TGF-β treatment down-regulates PRH expression

PC3 cells were treated with TGF-β or vehicle for 48 hours. After harvesting, whole cell protein extracts were used in PRH western blotting (as described in section 2.9.1) (Figure 5.1 A), and Lamin A/C was used as a loading control. The western blot images were analysed in ImageQuant to obtain densitometry of each band. PRH densitometry was normalised by Lamin A/C densitometry in three independent experiments for statistical analysis (Figure 5.1 B). As can be seen in the Figure, TGF-β treatment brings about a 50% reduction in PRH protein levels in PC3 cells. TGF-β treatment also down-regulates PRH protein expression in PNT2-C2 cells (Figure 5.2 A). The 50% decrease in protein expression found in PNT2-C2 cells was also statistically significant.

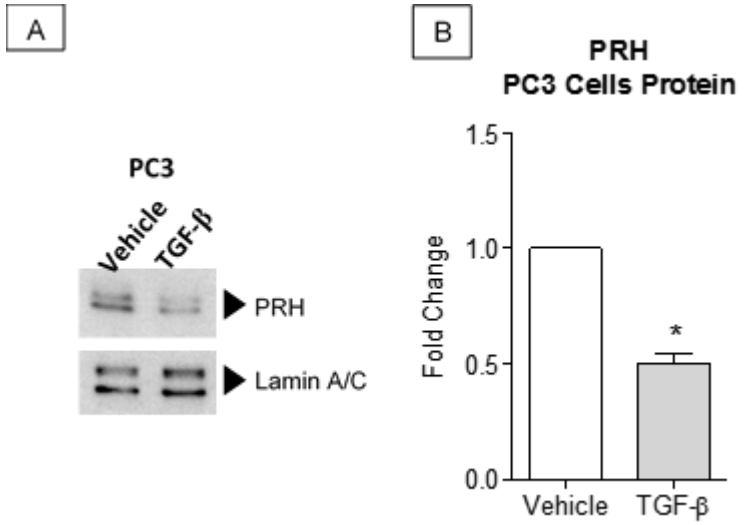

Figure 5.1. TGF-β down regulates PRH protein levels in PC3 cells. PC3 cells were treated with TGF-β or vehicle for 48h, whole cells lysates were used to protein to be used in western blotting. (A) Representative western blot images of PC3 protein extract probed with PRH and Lamin A/C antibodies. (B) The graph shows the results of densitometry of three independent PRH western blots normalised to the loading control Lamin A/C. Statistical comparisons made were between TGF-β and vehicle groups. Statistical analyses: one-sample t-test with hypothetical value set to '1', n=3, $p<0.05$.

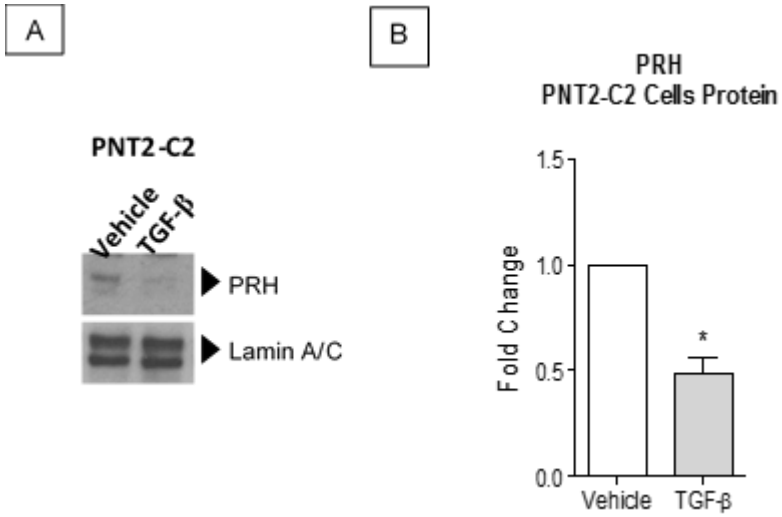

Figure 5.2. TGF-β down regulates PRH protein levels in PNT2-C2 cells. PNT2-C2 cells were treated with TGF-β or vehicle for 48h, whole cells lysates used in western blotting. (C) Representative western blot images of PNT2-C2 protein extract probed with PRH and Lamin A/C antibodies. (B) The graph shows the results of densitometry of three independent PRH western blots normalised to the loading control Lamin A/C. Statistical comparisons made were between TGF-β and vehicle groups. Statistical analyses: one-sample t-test with hypothetical value set to '1', n=3, $p<0.05$.

TGF-β treatment increases PRH phosphorylation through protein kinase CK2

Published data shows that protein kinase CK2 phosphorylates PRH (Noy et al. 2012). Phosphorylated PRH (pPRH) is unable to bind DNA and is a substrate for proteasomal processing. It is also known that TGF-β stimulation activates CK2 during EMT (Kim et al. 2018). To assess whether TGF-β treatment alters PRH phosphorylation in PNT2-C2 and PC3 cells, these cells were treated with 5 ng/mL of TGF-β for 48h. Whole cell extracts were used for pPRH western blotting, and Lamin A/C was used as a loading control (figure 5.3). Western blotting images showed a small increase in the pPRH signal. Repetitions of the experiment showed the consistency of the increase. To quantify and compare the signal in each condition, the images were used in densitometry analyses using ImageQuant and the densitometry values for pPRH were normalised to Lamin A/C densitometry values. Statistical analysis showed significance, confirming that the expression of pPRH in TGF-β treated cells is higher than in vehicle treated controls.

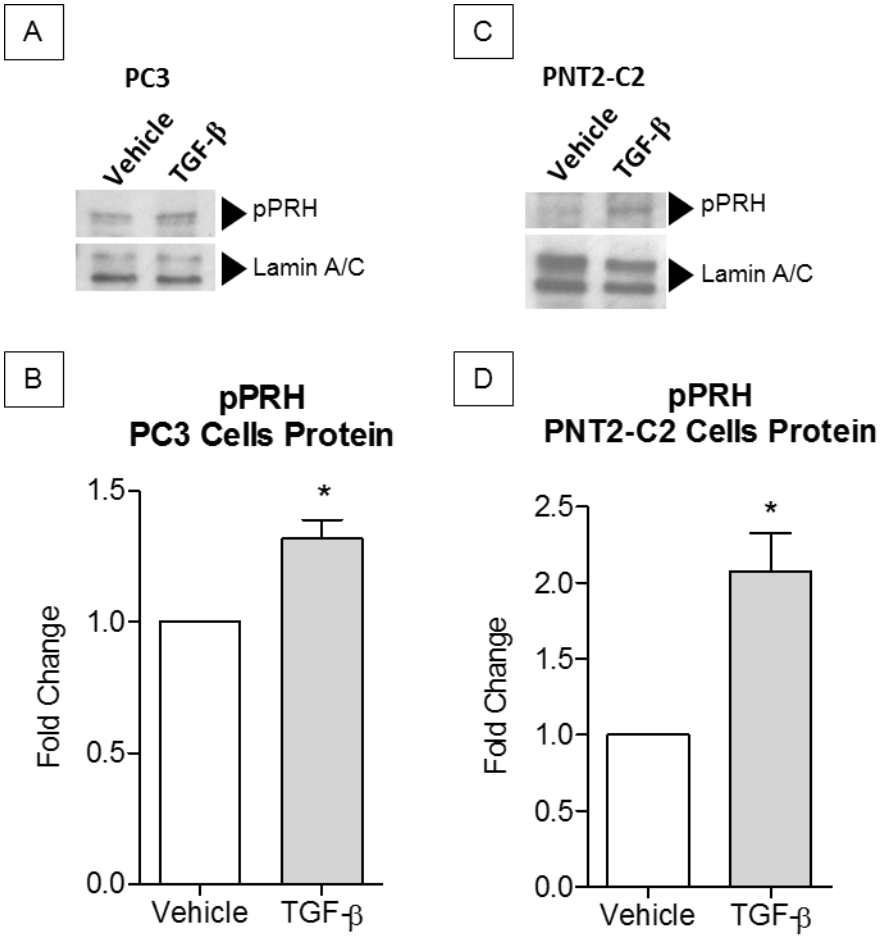

Figure 5.3. TGF-β induces PRH phosphorylation in prostate cell lines. PNT2-C2 and PC3 cells were treated with TGF-β or vehicle for 48h, whole cells lysates were used in western blot experiments. (A) Representative western blot images of PC3 protein extract probed with pPRH and Lamin A/C antibodies. (B) The graph shows the results of densitometry of three independent pPRH western blots normalised to the loading control Lamin A/C. All statistical comparisons made were between TGF-β and vehicle groups. Statistical analyses: one-sample t-test with hypothetical value set to '1', n=3, $p<0.05$. (C) Representative western blot images of PNT2-C2 protein extracts probed with pPRH and Lamin A/C antibodies. (D) The graph shows the results of densitometry of three independent pPRH western blots normalised to the loading control Lamin A/C in PNT2-C2 cells. Statistical comparisons made were between TGF-β and vehicle groups. Statistical analyses: one-sample t-test with hypothetical value set to '1', n=3, $p<0.05$.

To determine whether CK2 is responsible for the TGF-β induced phosphorylation of PRH, PC3 and PNT2-C2 cells were treated with either vehicle, 5 ng/mL of TGF-β, 5 ng/mL of TGF-β plus 10 uM of the well characterised CK2 inhibitor TBB or 10uM TBB alone. Whole cell protein extract was used in pPRH western blot, and Lamin A/C was used as a loading control (Figure 5.4). TGF-β significantly augmented the pPRH signal while co-treatment with TGF-β plus TBB abolished the increase in pPRH in both PNT2-C2 and PC3 cells.

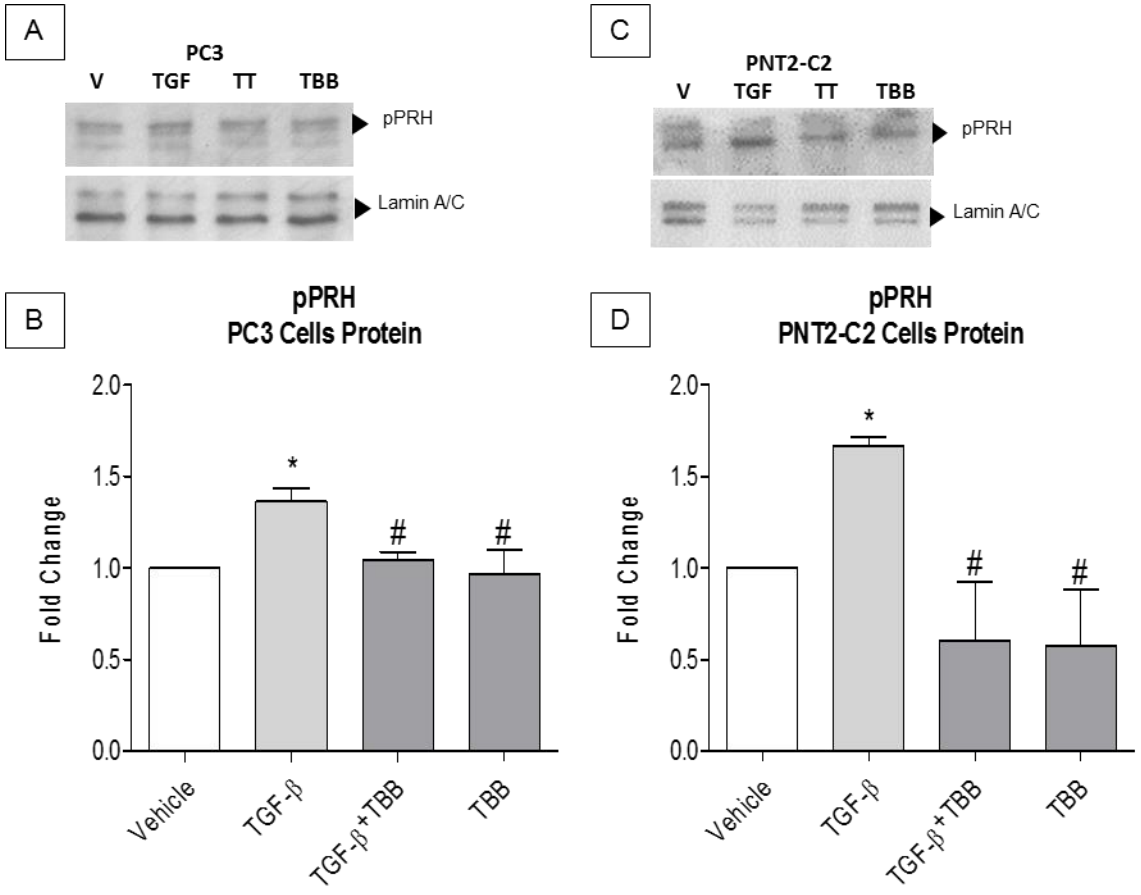

Figure 5.4. TBB prevents TGF-β induced PRH phosphorylation in prostate cell lines. PNT2-C2 and PC3 cells were treated with vehicle, TGF-β, TGF-β+TBB or TBB alone for 48h, whole cells lysates used in western blotting. (A) Representative western blot images of PC3 protein extract probed with pPRH and Lamin A/C antibodies. (B) The graph shows the densitometry of three independent pPRH western blots normalised to the loading control Lamin A/C in PC3 cells. Statistical analyses: one-way ANOVA followed by Bonferroni test for multiple column comparison, n=3, $p<0.05$. (C) Representative western blot images of PNT2-C2 protein extract probed with pPRH and Lamin A/C antibodies. (D) The graph shows the densitometry of three independent pPRH western blots normalised to the loading control Lamin A/C in PNT2-C2 cells. Statistical analyses: one-way ANOVA followed by Bonferroni test for multiple column comparison, n=3, $p<0.05$.

CK2 inhibition does not block the effects of TGF-β on cell migration

To determine if TGF-β induced phosphorylation of PRH by CK2 was required for TGF-β induced cell migration, PC3 and PNT2-C2 cells were treated with either vehicle, 5 ng/mL of TGF-β, 5 ng/mL of TGF-β plus 10 uM of TBB or 10uM of TBB alone. After 48h, the cells were harvested and counted. Equal amounts of cells were then used in a chemotaxis assay (as explained in section 2.8) (figure 5.5). TGF-β treatment significantly increased the percentage of migrated cells in both PC3 and PNT2-C2 in three independent experiments. TBB treatment did not reduce cell migration back to basal levels in either of the cell lines tested. TBB treated cells did not show any difference in migration when compared to vehicle group in both cell lines. I conclude that phosphorylation of PRH is not required for the effect of TGF-β on cell migration.

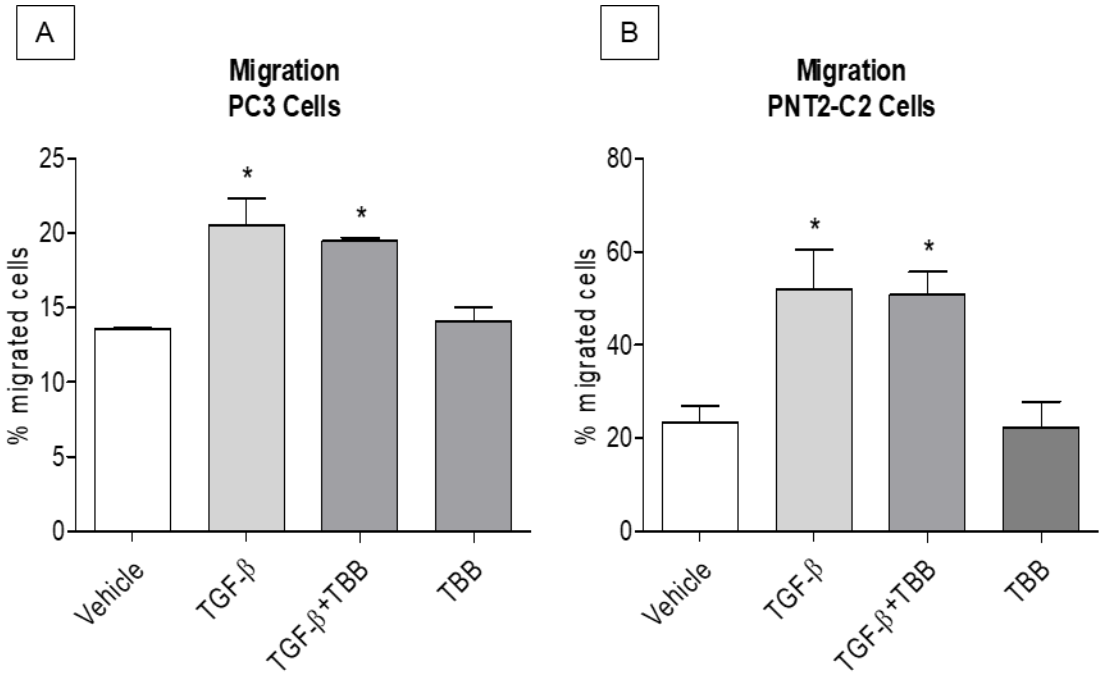

Figure 5.5. TBB does not prevent TGF-β induced prostate cell migration in chemotaxis assays. PNT2-C2 and PC3 cells were treated with vehicle, TGF-β, TGF-β+TBB or TBB alone for 48h, cells were then harvested, and their concentration adjusted to be used in migration chemotaxis assays. The assays were performed after cell concentration adjustment were performed in the presence of hydroxyurea to compensate for effects on cell proliferation the cell growth component on the number of migrated cells to be detected. (A) The graph shows the average percentage of migrated PC3 cells in three independent experiment submitted to chemotaxis assay. Statistical analyses: one-way ANOVA followed by Bonferroni test for multiple column comparison, n=3, $p<0.05$. (B) The graph shows the average percentage of migrated PNT2-C2 cells in three independent experiment submitted to chemotaxis assay. Statistical analyses: one-way ANOVA followed by Bonferroni test for multiple column comparison, n=3, $p<0.05$.

TGF-β regulates PRH mRNA expression possibly by a direct effect of pSmad3

To evaluate the effects of TGF-β treatment on PRH mRNA expression, PNT2-C2 and PC3 cells were treated with TGF-β or vehicle for 48h. Whole cell mRNA extract was then purified and used in qRT-PCR. *HHEX* (PRH) mRNA expression was measured relative to *GAPDH* and β-Actin expression (PNT2-C2- Figure 5.6 A PC3 – Figure 5.6 B). TGF-β treatment significantly down-regulated the relative expression of PRH mRNA when compared to the vehicle treatment ($p<0.05$) in both PNT2-C2 and PC3 cells.

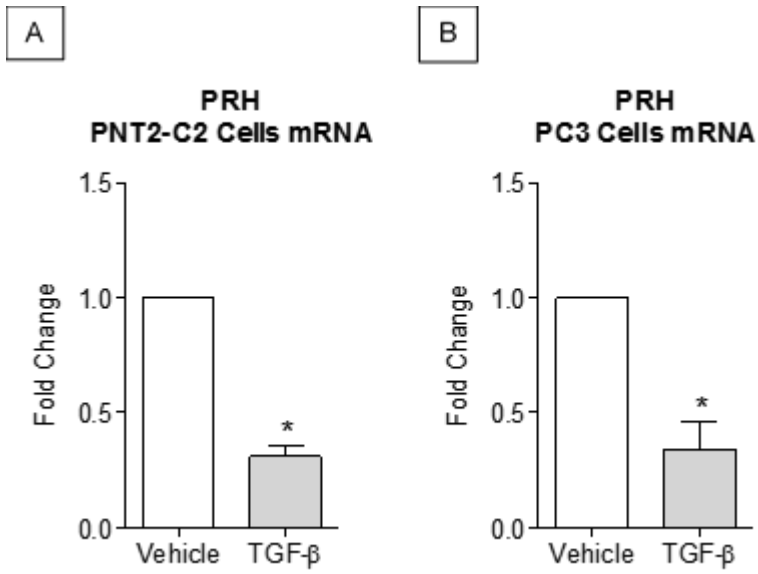

Figure 5.6. TGF-β down- regulates PRH mRNA expression in prostate cells. PNT2-C2 and PC3 cells were treated with TGF-β or vehicle for 48h. Whole cell mRNA extract was then used in qRT-PCR experiments. (A) The graph shows the relative expression of *HHEX* mRNA in PNT2-C2 cells treated with vehicle or 5 ng/mL of TGF-β. Statistical comparisons made were between TGF-β and vehicle groups. Statistical analyses: one-sample t-test with hypothetical value set to '1', n=3, $p<0.05$. (B) The graph shows the relative expression of *HHEX* mRNA in PC3 cells treated with vehicle or TGF-β. Statistical comparisons made were between TGF-β and vehicle groups. Statistical analyses: one-sample t-test with hypothetical value set to '1', n=3, $p<0.05$.

To determine whether TGF-β signalling could directly regulate PRH expression through activation of the transcription factor pSmad3, PC3 cells were treated with TGF-β or vehicle and used for pSmad3 ChIP experiments. After 48 hours, protein-DNA complexes in the cells were cross-linked using methanol free formaldehyde. Chromatin was then extracted and used in pSmad3 ChIP-qPCR. ChIP-qPCR with rabbit IgG was used as a control for background. Primers specific for Chromosome 18 sequences were used as a negative control and the Smad7 gene was used as a positive control (as explained in section 2.10.2) (figure 5.7). ChIP-qPCR shows that pSmad3 presented a 3.5-fold enrichment of *HHEX* promoter chromatin immunoprecipitation above the background with TGF-β treated PC3 cells. The vehicle treatment did not enrich *HHEX* promoter gene ChIP above the background. The positive control Smad7 was significantly enriched on both vehicle and TGF-β treatment. However the negative control CH18 did not present any enrichment above background levels.

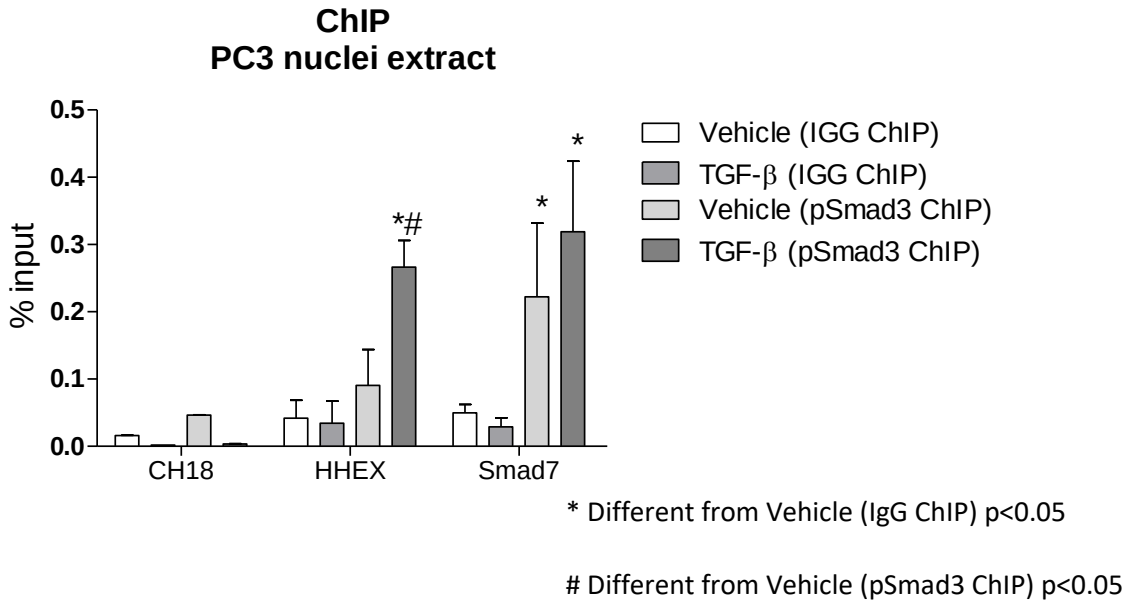

Figure 5.7. *HHEX* promoter enrichment in pSmad3 ChIP-qPCR in TGF-β treated PC3 cells. PC3 cells were treated with vehicle or TGF-β for 48hand used in a ChIP assay using pSma3 or normal rabbit IgG antibodies.10% of the extracts were separated to be used to quantify the input. After the ChIP, DNA was purified and used in qPCR to detect regions of the *HHEX* gene and *HHEX* promoter. CH18 primers were used as a negative control and Smad7 primers used as a positive control. The levels of amplicon were normalised by the input expression and calculated as percentage of input. The graph shows the average percentage of input detected by ChIP-qPCR using PC3 cells in three independent experiment. Statistical comparisons were made between the results for each primer on the IgG ChIP (background) versus the pSmad3 ChIP. Statistical analyses: two-way ANOVA followed by Bonferroni test for multiple column comparison, * different from IgG vehicle. # different from pSmad3 vehicle, n=3, p<0.05.

TGF-β effects in DU145 cells: Context is important in PRH-TGF-β crosstalk in prostate cancer cells

It is known that TGF-β effects are dependent on the context in which it is activated (Massagué 2012). For example, TGF-β can induce cell death or cancer progression depending on whether Smad4 is expressed or not in pancreatic ductal adenocarcinoma (PDA) cells (David et al. 2016). To investigate and compare the effects of TGF-β in EMT and PRH regulation in another prostate cancer cell line, I used prostate cancer cell line DU145 and repeated the TGF-β treatment previously performed in PC3 and PNT2-C2 cells.

TGF-β induced EMT markers in DU145 cells

To screen for TGF-β markers, DU145 cells were treated with 5 ng/mL of TGF-β for 48 hours (as described in section 2.7.1). Whole cell protein extract was then used in western blot assays with EMT marker antibodies (Figure 5.8 A). mRNA cell extract was also used in qRT-PCR to assess the mRNA expression of EMT markers that were altered in PC3 cells (Snail and E-cadherin) (Figure 5.8 B and C).

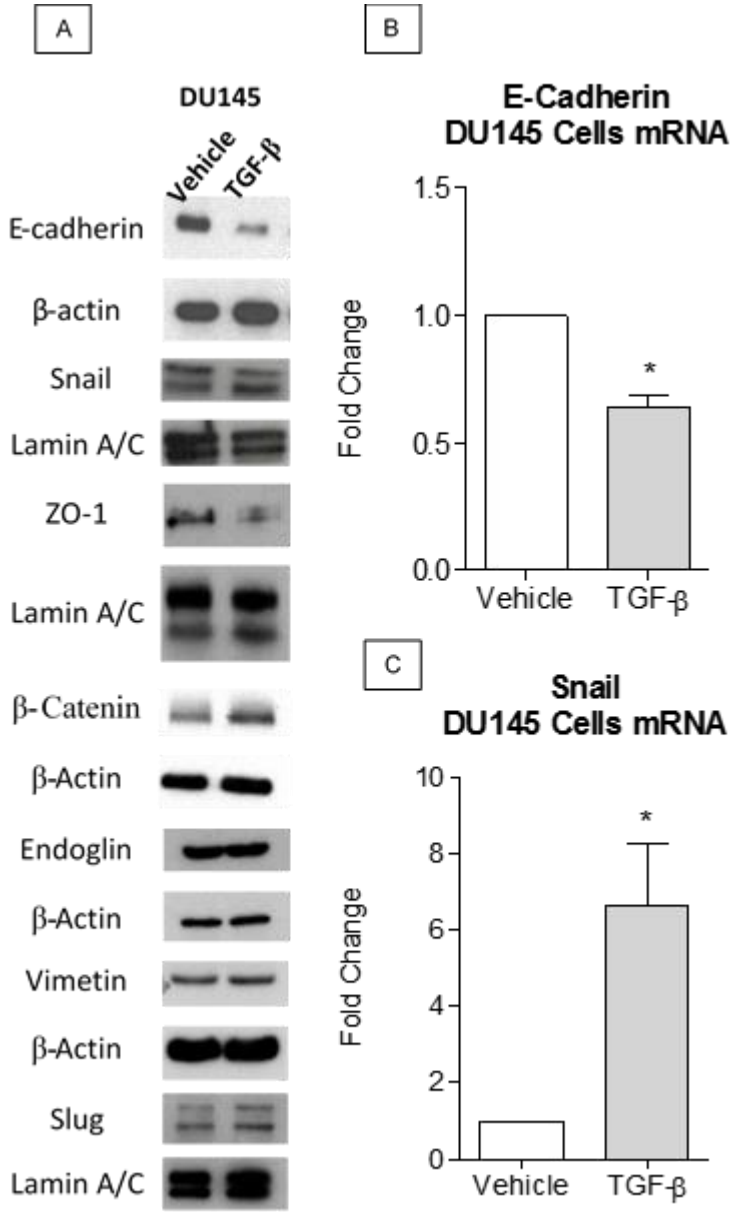

Figure 5.8. EMT markers screening in DU145 cells. (A) Photoradiography of seven EMT markers analysed by western blotting in DU145 whole cell protein extracts. In the left column, protein extracted from DU145 cells treated with vehicle. In the right column, protein extracted from DU145 cells treated with TGF-β (5ng/mL) for 48h. The expression of each EMT marker was compared to the expression of a housekeeping protein (β-Actin or Lamin A/C). (B) The graph shows the relative expression of *CDH1* mRNA in DU145 cells treated with vehicle or 5 ng/mL of TGF-β. Statistical comparisons made were between TGF-β and vehicle groups. Statistical analyses: one-sample t-test with hypothetical value set to '1', n=3, $p<0.05$. (C) The graph shows the relative expression of Snail mRNA in DU145 cells treated with vehicle or TGF-β. Statistical comparisons made were between TGF-β and vehicle groups. Statistical analyses: one-sample t-test with hypothetical value set to '1', n=3, $p<0.05$.

The EMT markers western blot screening showed that TGF-β caused changes in the expression of four proteins. E-cadherin was found to be down-regulated when DU145 cells were treated with TGF-β, in comparison to vehicle treated cells. β-actin western blot in the same membrane was used to show equal protein loading. Snail was found up-regulated in TGF-β treated DU145 cells when compared to vehicle treated DU145 cells. Lamin A/C western blot in the same membrane shows equal loading. ZO-1 was found down-regulated in DU145 cells treated with TGF-β in comparison to vehicle with Lamin A/C as a control. β-catenin was found up-regulated in TGF-β treated DU145 cells in comparison with vehicle treated DU145 with β-Actin as a control.

qRT-PCR for E-cadherin and Snail expression agreed with the western blot results. E-cadherin mRNA levels normalised to *GAPDH* mRNA levels, were found significantly down-regulated after TGF-β treated DU145 when compared to vehicle. Conversely, Snail mRNA, also normalised to *GAPDH* mRNA expression, was up-regulated in TGF-β treated cells in comparison to vehicle treated cells.

Increased stability of PRH protein in DU145 cells

To evaluate TGF-β regulation of PRH expression in DU145 cells, the cells were treated with TGF-β for 48 hours (as described in section 2.7.1). To evaluate PRH protein expression and its phosphorylation, whole cell protein extract was used in PRH and pPRH western blots (figure 5.9 A) in four independent experiments. The western blot analysis showed that TGF-β treatment did not reduce PRH protein expression over this time scale in DU145 cells when compared with the vehicle treatment. Another interesting finding was that TGF-β treatment did not augmented PRH phosphorylation in DU145 cell when compared to vehicle treatment. Lamin A/C western blots were used to show equal loading.

TGF-β or vehicle treated DU145 whole cell mRNA extract was then used in qRT-PCR to evaluate *HHEX* mRNA expression (Figure 5.9 B) in three independent experiments. The PRH mRNA levels were normalised to *GAPDH* mRNA levels. PRH mRNA relative expression was down-regulated in TGF-β treated DU145 cells when compared to vehicle treated cells. Thus TGF-β treatment reduces PRH mRNA levels within 48 hours but this does not result in a reduction in PRH protein levels.

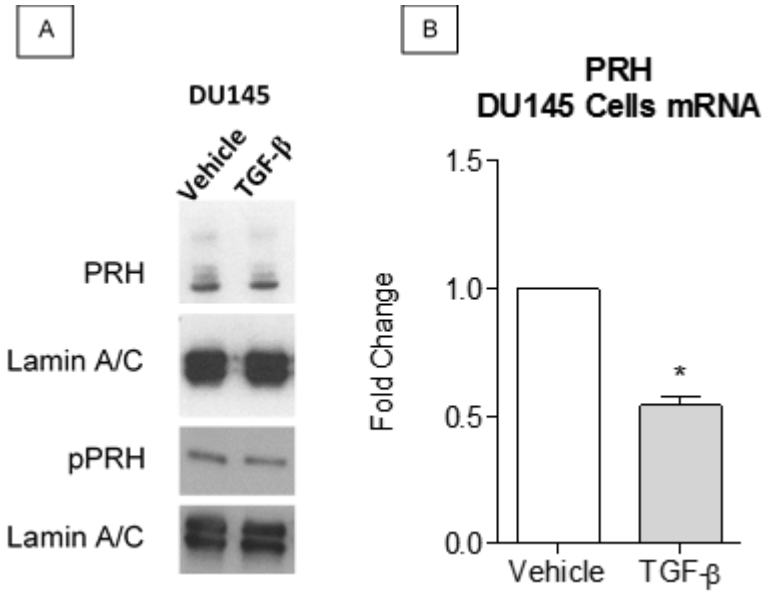

Figure 5.9. TGF-β effects on PRH expression in DU145 cells. (A) Western blotting images of TGF-β or vehicle treated DU145 cells. Whole cell protein extract was used in western blot analysis, the membranes were probed with PRH or pPRH antibodies. Lamin A/C was used to show equal loading. (B) The graph shows the relative expression of *HHEX* mRNA in DU145 cells treated with vehicle or 5 ng/mL of TGF-β. All statistical comparisons made were between TGF-β and vehicle groups. Statistical analyses: one-sample t-test with hypothetical value set to '1', n=3, $p<0.05$.

Blood platelets stimulate prostate cell migration and extravasation through TGFβ-mediated down-regulation of PRH/*HHEX*.

Extravasated blood platelets can influence the tumour microenvironment through the release of cytokines including PDGF, VEGF and TGF-β (Blakytny et al. 2004; Haemmerle et al. 2016). Blood platelets release TGF-β and induce EMT-like changes in cancer cells and the simple inhibition of TGF-β signalling in platelets of mice protected then against lung metastasis (Labelle et al. 2011). This shows the important role that platelets can play in providing TGF-β at the tumour site and to circulating tumour cells, facilitating the emergence of a malignant phenotype. As TGF-β is known to be important to the progression of prostate cancer I examined the effect of blood platelets on prostate cells and PRH expression.

Platelets induce cell migration and extravasation by activating the TGF-β pathway

Dr Yusra Siddiqui kindly ceded some preliminary data from experiments conducted in our laboratory. To assess if blood platelets could increase extravasation by PNT2-C2 cells, plasmid expressing PRH shRNA or empty vector (SVC) shRNA were transfected into PNT2-C2, the cells were then selected and treated with platelets or vehicle and used in *in vitro* extravasation assays (figure 5.10 A). To test if the extravasation induced was related to activation of TGF-β, the pathway, PRH knockdown (KD) and control PNT2-C2 cells were treated with blood platelets plus or minus SB431542 (a TGFβR1 inhibitor) (figure 5.10 B). A diagram of the extravasation assay is showed in the Annex.

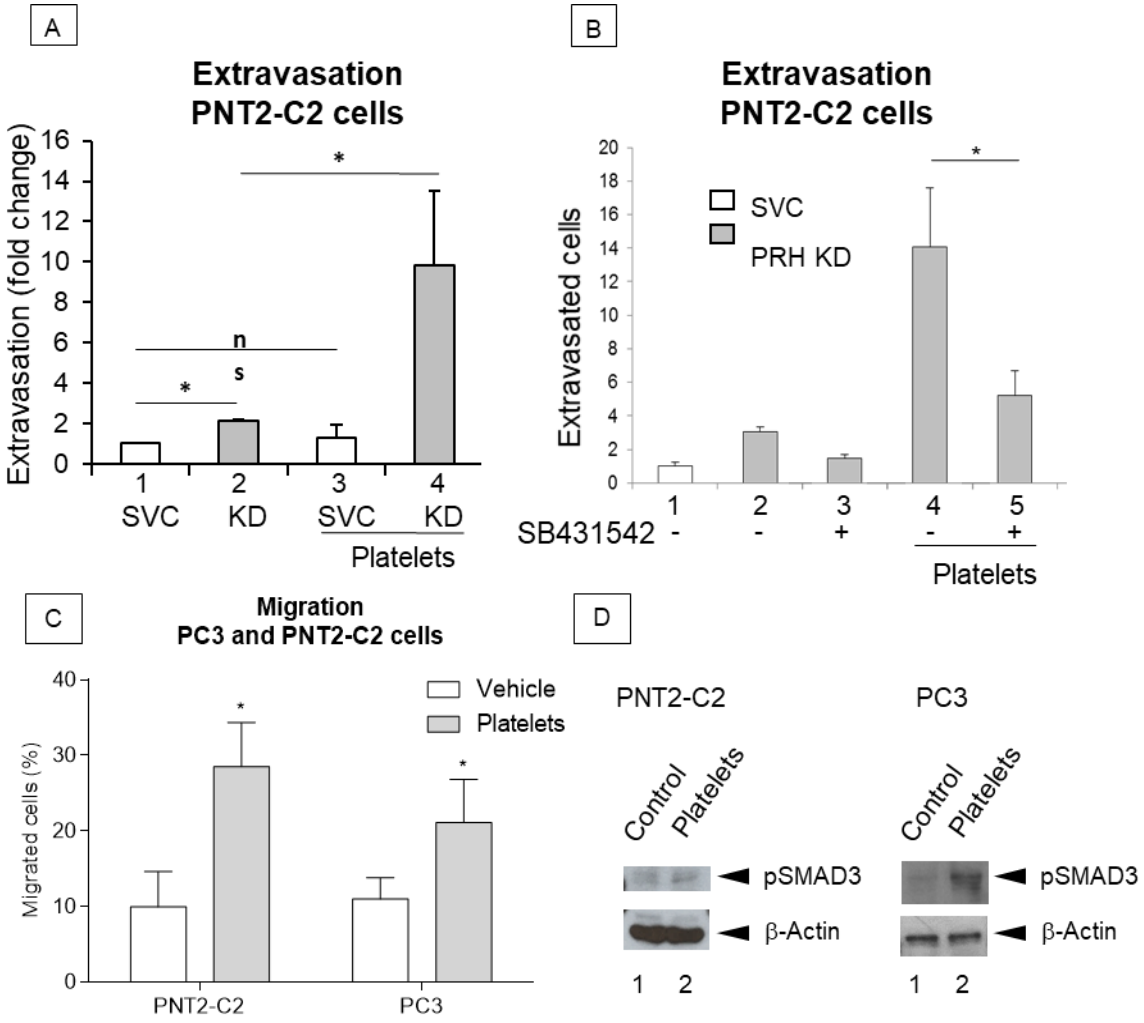

Figure 5.10. Blood platelets released TGF-β induces prostate cell migration and extravasation. (A) PRH shRNA KD (KD) or vector control (SVC) were transfected into PNT2-C2 cells. After 10 days in selection transfected cells were treated with platelets or vehicle before being used in extravasation assays. The graph shows the average number of extravasated cells in three independent experiments performed in the presence of hydroxyurea. Statistical analyses: one-way ANOVA followed by Bonferroni test for multiple column comparison, n=3, $p<0.05$. (B) SB431542 is an established inhibitor of TGF-β signalling. KD and SVC PNT2-C2 cells were treated with vehicle, vehicle + platelets or SB431542 + platelets and used in extravasation assays as above. Statistical analyses: one-way ANOVA followed by Bonferroni test for multiple column comparison, n=3, $p<0.05$. all the extravasation assays showed here were performed by Dr Yusra Hasan Siddiqui and used here with authorisation. (C) PNT2-C2 and PC3 cells were treated with platelets or vehicle before being used in chemotaxis assays. Statistical analyses: two-tailed unpaired t-test, n=3, $p<0.05$. (D) The cells used in the migration assays showed in 'C' were used to make whole cell protein extracts. The protein extracts were used in pSmad3 western blotting analysis to show activation of TGF-β signalling pathway.

The data in Figure 6.1 A shows that PRH knockdown significantly increased PNT2-C2 extravasation when compared to SVC transfected PNT2-C2 cells. Platelets alone were not able to increase PNT2-C2 extravasation, but platelet treatment significantly increased the migration of PHR KD cells when compared to vehicle treated PRH KD PNT2-C2 cells. Furthermore, when PRH KD PNT2-C2 cells were treated with platelets and SB431542, there was statistically significant reduction in extravasation (Figure 5.10 B). Treatment with SB431542 did not affect cell migration induced by PRH KD alone. To assay the effect of platelets on cell migration, I treated PC3 and PNT2-C2 cells with blood platelets for 48 hours and performed cell migration assays (Figure 5.10 C). To confirm the activation of TGF-β pathway, the leftover cells from the migration assay were used in pSmad3 western blotting experiments (figure 5.10 D). The migration assay showed that platelet treatment augmented the migration of both PNT2-C2 and PC3 cells when compared to vehicle treatment. The pSmad3 western blot showed TGF-β activation in both PNT2-C2 and PC3 cells treated with platelets when compared to vehicle treated cells.

Platelets treatment presents the same alterations as TGF-β treatment

To assess if platelet treatment would produce the same changes in PRH levels as TGF-β, PNT2-C2 and PC3 cells were treated with either TGF-β, platelets or vehicle controls (as described in section 2.7.1). Whole cell protein extracts were used in PRH and pPRH western blots (figure 5.11) with Lamin A/C to show equal loading. Platelet treatment down-regulated PRH protein levels and augmented pPRH levels in both prostate cell lines. As previously shown, TGF-β treatment down-regulated PRH expression and augmented pPRH levels in both PC3 and PNT2-C2 cells.

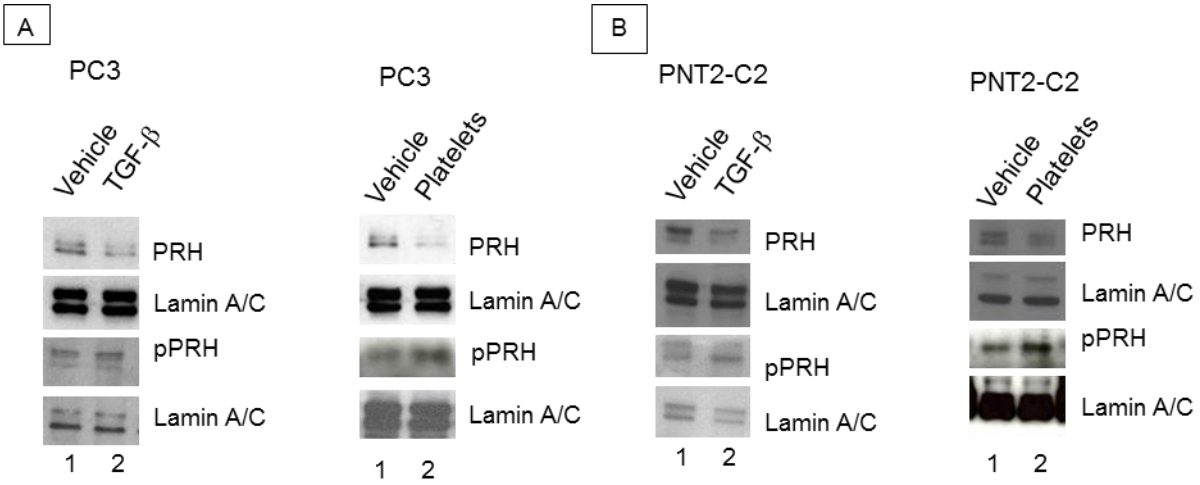

Figure 5.11. Platelets regulation of PRH expression. The western blot images compare the effects of platelets and TGF-β treatments on PRH expression in PC3 and PNT2-C2 cells. Lamin A/C was used to show equal loading. (A) Photoradiography of PRH and pPRH expression analysed by western blot from PC3 whole cell protein extract. On the left, cells treated with vehicle or TGF-β. On the right, cells treated with platelets or vehicle. (B) Photoradiography of PRH and pPRH expression analysed by western blot from PNT2-C2 whole cell protein extract. On the left, cells treated with vehicle or TGF-β. On the right, cells treated with platelets or vehicle.

To assess if platelet treatment could induce an epithelial phenotype, PC3 cells were treated with platelets or vehicle for 48 hours on two independent occasions. Whole cell mRNA extract was then used in *CHD1* (E-cadherin) qPCR. *CDH1* expression levels were normalised to *GAPDH* levels (figure 5.12 A). Treated cells were also used to produce whole cell extracts used in E-cadherin and β-actin western blots. Platelet treatment reduced *CDH1* mRNA levels in two independent experiments, when compared to vehicle treatment. Platelet treatment also reduced E-cadherin protein levels when compared to vehicle treatment.

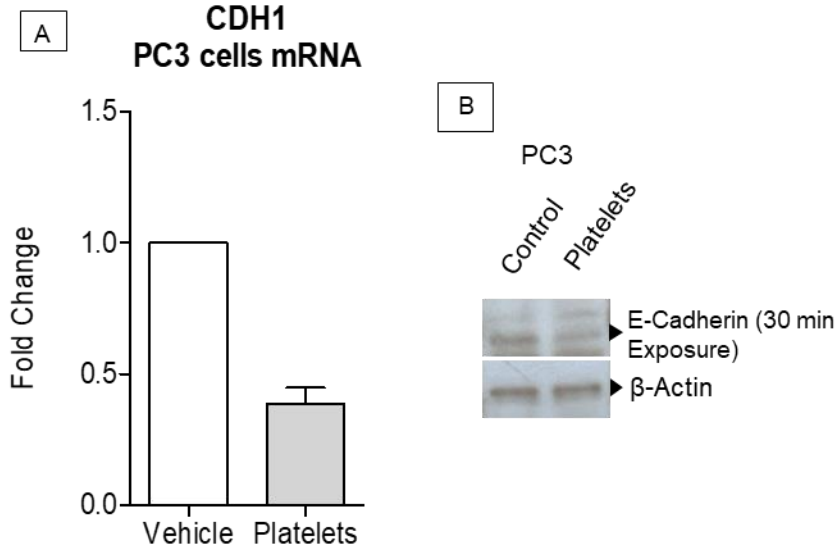

Figure 5.12. The effects of platelet treatment on the epithelial marker E-cadherin. PC3 cells were treated with platelets or vehicle for 48 hours before being harvested and lysed to be used in qRT-PCR and western blotting assays. (A) The graph shows the relative *CDH1* mRNA expression in two independent experiments (n=2). Error bars show SEM (B) Photoradiography of E-cadherin expression. B-actin was used to show equal protein loading.

PRH binds to the IL-6 promoter

Platelets are reported to aid cancer cells through direct interaction, triggering EMT, extravasation and immune system evasion (Haemmerle et al. 2016; Carr et al. 2014; Labelle et al. 2011). IL-6 is a cytokine known to induce platelet production (Stahl et al. 1991) and to be up-regulated in prostate cancer (Nguyen et al. 2014). Evaluation of ChIP-seq data showed that myc-PRH binding is enriched in the IL-6 gene region (Figure 5.13). Several locations within the gene were detected in the sequencing and one of the most frequently detected regions was at the promoter, close to the transcription initiation site. The promoter regions detected in the sequencing also shows accumulation of the marker H3K27Ac, which is associated with highly regulated regions.

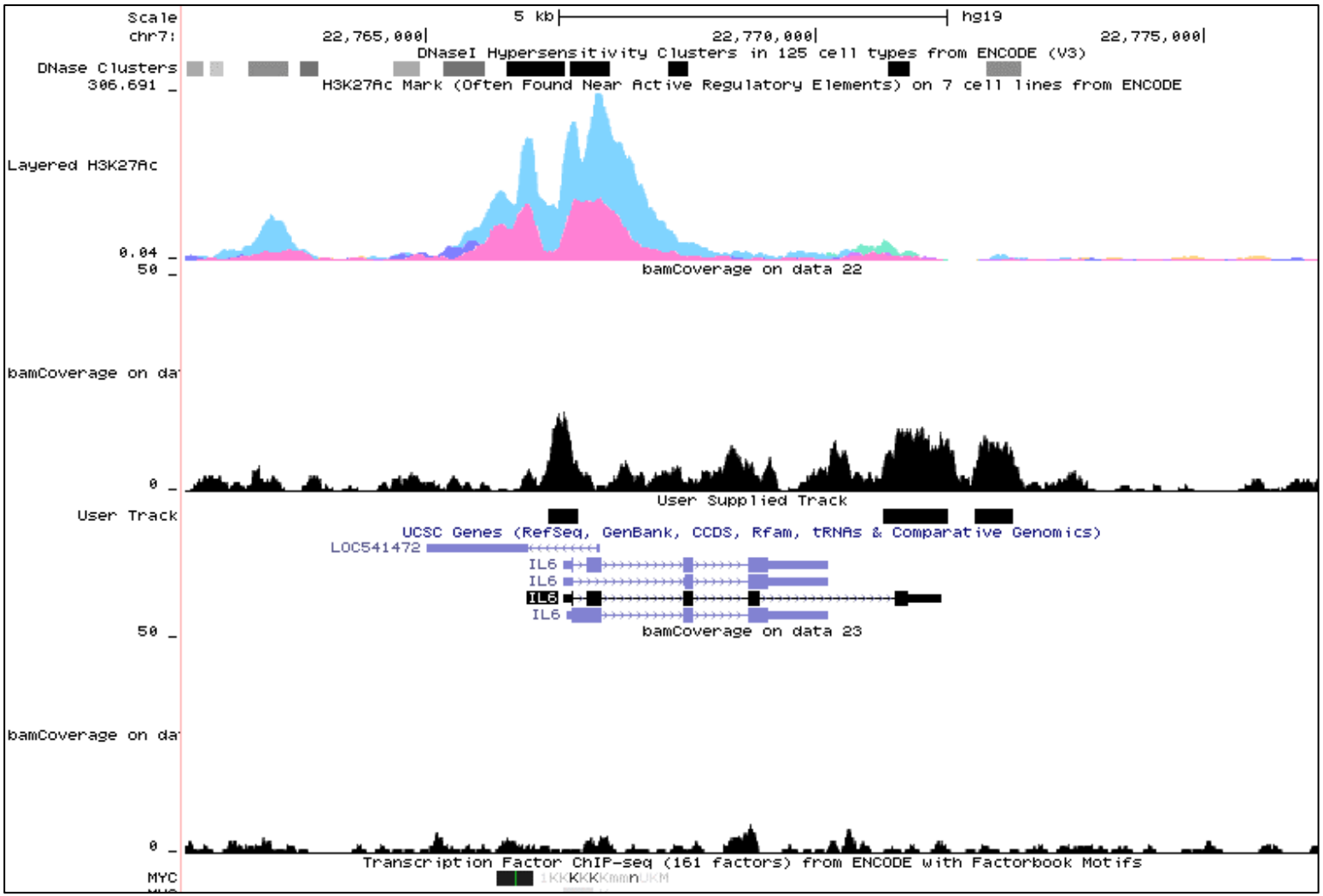

Figure 5.13. PRH occupation on IL-6 gene. ChIP-seq trace aligned with whole genome version 'Human Feb. 2009 (GRCh37/hg19) Assembly'. The image is a screen shot of IL-6 and surrounding regions showing occupation by PRH in several different locations. Background trace in the bottom of the image shows ChIP for cells infected with empty virus.

Discussion

TGF-β signalling is an important factor in prostate adenocarcinoma progression, (reviewed by (Derynck et al. 2001; Levy & Hill 2006). Promising new anti-TGF-β drugs were found to be effective in clinical trials. However, identifying predictive biomarkers to flag patients who would most likely benefit from these inhibitors is also an important issue to be overcome (reviewed by (de Gramont et al. 2017).

PRH is a novel EMT-TF shown to regulate cell proliferation and migration in prostate cancer cell lines (Kershaw et al. 2014; Siddiqui et al. 2017). The previous chapters showed that PRH protein expression is correlated to gland differentiation in patients with prostate cancer. This chapter presents evidence that PRH directly regulates TGF-β signalling genes. As aforementioned, published data shows that the inhibition of TGF-β signalling by expression of a heterozygote dominate negative of Smad3 and Smad2 down-regulated *HHEX* expression in embryos (Liu et al. 2004). However, this paper did not show the mechanism of how *HHEX* expression came to be down-regulated. This chapter studied the effects of TGF-β on PRH protein and mRNA expression in prostate cancer for the first time, and, proposed a mechanism that could explain how TGF-β regulates PRH expression.

Interestingly, inhibition of TGF-β signalling activation by down-regulating the functions of Smad3 and Smad2 was shown to reduce PRH expression in mice embryos (Liu et al. 2004). Here, the activation of Smad3 by treatment with TGF-β in prostate cell lines down-regulated PRH expression at both the protein and mRNA levels. These conflicting results may be explained by the different models used in these experiments. While embryo models will most likely show primary functions of the TFs, in adenocarcinomas TFs are known to be dysregulated. Dysregulation and disrupted cooperation between transcription factors are reported to be a driving factor in cancer progression, (reviewed by (Ell & Kang 2013; Wang et al. 2016). Specifically, TGF-β in prostate cancer is known to be dysregulated, as the primary effect of TGF-β in prostate epithelium is anti-proliferative, but as the cancer progresses, TGF-β becomes an inducer of cell proliferation and migration, (reviewed by (Zhang et al. 2005; Massagué 2008; Stepanenko et al. 2013; Brabletz et al. 2018).

Thus, the differences observed in the data here and from Liu's et al could be a reflection of the contextual interactions that the TFs face in different cells. For example, the context in which TGF-β pathway is activated in pancreatic ductal adenocarcinoma was shown to regulate cell fate (David et al. 2016). The complex of r-Smads formed by Smad2/Samd3 activate transcription of the gene *SOX4*, together with *SOX4*, Klf5 (normally expressed in this cell line) promotes tumorigenesis. In the presence of the co-Smad Smad4, the r-Smads form a Smad2/Smad3/Smad4 complex. The triple Smad complex can now activate the transcription of the gene encoding the EMT-TF Snail. Snail can associate with the Smad2/Smad3/Smad4 complex forming a unit that inhibits the transcription of Klf5. However, Smad2/Smad3/Smad4 can still activate transcription of the gene *SOX4*. *SOX4* alone without the presence of Klf5 drives a totally different cell fate; an apoptotic system is activated leading the majority of cells to death (David et al. 2016).

The data here also show that treatment with TGF-β increases PRH phosphorylation by CK2. This corroborates published data which showed that CK2 causes hyper phosphorylation of the PRH protein and that PRH phosphorylated by CK2 can no longer bind to DNA and becomes a substrate for proteasome processing/cleavage (Noy et al. 2012). Conversely, TGF-β is reported to activate CK2 and this is essential for TGF-β induced EMT in a human non-small cell lung cancer cell line (A549) (Kim et al. 2018). Interestingly, inhibition of CK2 activity reduced the migration induced by TGF-β in A549 cells, but this effect was not observed here in prostate cells. However, there were some key differences in the migration experiments conducted here and the ones conducted by Kim and co-workers (Kim et al 2018). Here the CK2 inhibition was achieved using TBB, an established CK2 inhibitor. Kim and co-workers inhibited CK2 activity by generating a stable *CSNK2A1* knockdown in A549 cells. The *CSNK2A1* gene encodes the subunit α of the protein CK2 (CK2α1), and its knockdown is reported to decrease cellular activity of CK2 (Ko et al. 2012). However, they did not knockdown *CSNK2A2* which encodes CK2 α' an alternative CK2 catalytic subunit. Knockdown of both α and α' is required to inhibit CK2 in some cells types (Wadey et al. 2017). Kim and co-workers made use of CK2 inhibitors in other experiments, but a migration assay using drug inhibition was not performed (Kim et al 2018). Perhaps the CK2 inhibition achieved with genetic modification was different from that achieved with the utilization of drugs. Here the CK2 inhibition using TBB in

the TGF-β treated cells was enough to reduce the pPRH western blot signal to the same levels seen in cells treated with only vehicle, but the TGF-β induced cell migration remained unaffected by the TBB treatment. The conflict observed between the two studies could also be a result of the cell line model in which they were performed. Here the studies were performed in two prostate cell lines, one immortalised and the other cancerous, while Kim and co-workers made use of a lung cancer cell line. Several proteins are reported to have different effects in different tissues. For example, the effect of Histone-lysine N-methyltransferase SETD7 (SET7/9) in apoptosis (Gu et al. 2017). SET7/9 is protein that methylate histones and non-histones proteins and is important in epigenetic regulation of the genome. SET7/9 is reported to induce apoptosis in human acute myeloid leukaemia cells (AML) but in non-small-cell lung cancer (NSCLC) cells it inhibits apoptosis (Gu et al. 2017).

The possibility that TGF-β directly regulates PRH expression should also be considered. Here I have shown that pSmad3 can bind to the *HHEX* promoter region at the distance of around -1Kbp upstream of the transcription initiation site. Approximately 3.5-fold enrichment above the background was detected in a pSmad3 Chip-qPCR assay. A paper published in 2002 reported the *HHEX* gene is regulated by a Smad-dependent pathway (Zhang et al. 2002). This paper showed an elegant experiment where several pieces of the PRH promoter were cloned upstream of a luciferase gene in plasmids. The plasmids were then transfected to stem cell line (C3H10T1/2) and embryo adenocarcinoma (P19) cells and the cells were treated with different TGF-β pathway activators including TGF-β2 and BMP2. The cells were also co-transfected with different Smad-expressing plasmids. Only the co-expression of Smad1 and Smad4 was able to increase luciferase activity with some of the constructs tested. Smad2 and Smad3 were not able to increase the luciferase activity in this model. These findings conflict with the data presented here. However, TGF-β is known to signal through Smad3 and Smad2 only (Ikushima & Miyazono 2010), and a regulatory effect was observed on PRH gene expression when the cells were treated with TGF-β. The reason for the differences may relate to the promoter regions that were studied. Here a region approximately 1Kbp upstream from the transcription initiation site of the PRH gene showed enrichment for pSmad3 ChIP-qPCR. In contrast in the study reported by Zhang et al the furthest region analysed

was 454bp upstream to the transcription initiation site (Zhang et al. 2002). Therefore, the reason for Smad3 not being able to regulate luciferase activity might be because a Smad3 regulatory main site in *HHEX* promoter was not cloned into any of the luciferase constructs (Zhang et al. 2002). Alternatively, TGF may regulate PRH through other pathways. The results shown in Chapter 4 showed that TGF-β blocks the effects of PRH on E-cadherin expression even when PRH is expressed from a heterologous promoter.

Apart from the changes in E-cadherin and Snail, also observed in PC3 cells, TGF-β treated DU145 cells presented down-regulation of ZO-1. ZO-1 is a protein present in tight junctions, it is an epithelial marker and its down-regulation signals loss of epithelial phenotype (Zeisberg & Neilson 2009). Loss of ZO-1 expression is associated with cancer progression (Salvador et al. 2016). ZO-1 expression is down-regulated in breast cancer (Hoover et al. 1998), and its expression in non-small cell lung cancer is associated with a good prognosis (Ni et al. 2013). Interestingly, ZO-1 was reported to interact with β-catenin in migrating colorectal cancer cells (Hirakawa et al. 2009). During the migratory phase, ZO-1 interacts with β-catenin at tight junctions, but once cells are confluent and polarised, Cortactin replaces β-catenin for ZO-1 interactions at the tight junctions (Hirakawa et al. 2009). β-catenin is an adhesion protein that presents a second effect as a transcription factor and its role in prostate cancer is a controversial topic. Studies show conflicting results, but in general, the most likely influence of the β-catenin/Wnt signal pathway is during the emergence of castration-resistant tumours (Kypta & Waxman 2012). β-catenin also interacts with the TGF-β pathway. It was demonstrated that β-catenin knockdown in alveolar epithelial cells abrogates the EMT effects of TGF-β indicating a dependency on β-catenin for TGF-β effects in this cell model (Zhou et al. 2012). Here both β-catenin and ZO-1 showed altered expression in DU145 cells treated with TGF-β, changes that were not observed in PC3 cells. This suggests that the differences in TGF-β effects observed here could be partially explained by the absence or presence of these proteins.

Another interesting observation was the lack of down-regulation of PRH protein in DU145 cells with TGF-β treatment. In previous chapters it was shown that TGF-β treatment in PC3 cells down-regulated PRH at the protein and mRNA levels. Furthermore, it was found that pSmad3 binds to PRH promoter in TGF-β treated

PC3 cells. However, in DU145 cells TGF-β treatment did not down-regulate PRH protein levels. Perhaps, as discussed above, the different context in which TGF-β acts in each cell type modifies its effects on PRH expression. However, TGF-β did down-regulate PRH mRNA levels in DU145 cells. Down-regulation of mRNA levels that is not followed by a decrease in protein signal indicates a higher level of protein stability. TGF-β treatment did not increase pPRH signal in DU145 cells. As shown and discussed in previous chapters, TGF-β activates CK2 to phosphorylate PRH which becomes subject to proteasomal processing (Noy et al. 2012; Kim et al. 2018). Additionally, PRH turnover studies in K562 cells showed that the PRH protein has a very long half-life in these cells (Bess et al. 2003). Longer time course experiments may therefore be required to see down-regulation of PRH protein levels in DU145 cells by TGF-β treatment.

Experiments with a protein synthesis inhibitor such as cycloheximide to examine the PRH turnover in DU145 would also help to clarify these results. Future experiments comparing PRH stability in PC3 and DU145 cell lines facing TGF-β treatment would enhance our understanding of PRH/TGF-β interactions in prostate cancer.

Platelets are known to be important in cancer metastasis through activation of TGF-β and other mechanisms of signalling (Haemmerle et al. 2016). Colon carcinoma cells treated with platelets formed more lung metastasis in a tail vein injection assay, while the same experiment done in mice with platelets that lack TGF-β showed reduced lung metastasis (Labelle et al. 2011). Platelets were also shown to aid cancer cell extravasation. TGF-β released by platelets can disrupt adhesion proteins at cell junctions opening spaces in the endothelium (Labelle et al. 2011). These reports are aligned with the findings reported here. Blood platelets induced cell migration and extravasation in PRH knockdown prostate cells. pSmad3 western blot showed activation of TGF-β signalling. Conversely, inhibition of TGF-β signal reduced platelet-induced extravasation. It is important to acknowledge that platelets are not the only possible source of TGF-β in the tumour context, for example infiltrating T cells could account for part of the production of TGF-β in the tumour (Donkor et al 2011).

Additionally, cells treated with platelets presented signs of EMT in published reports, for example, increased migration of hepatocellular cancer cells treated with platelets

(Carr et al. 2014) and EMT in murine colon adenocarcinoma cells treated with platelets (Labelle et al. 2011). This corroborates my findings in prostate cancer cells, since here I showed that platelets induce a loss of epithelial phenotype, indicated by the down-regulation of E-cadherin and increased migratory ability. Additionally, TGF-β released by platelets induced extravasation only in PNT2-C2 PRH knockdown cells. Together with the demonstration that platelets can down-regulate PRH expression as seen with TGF-β treatment, these results indicate that the TGF-β released by platelets could compromise PRH activity in relatively well-differentiated prostate cells in the early stages of the cancer triggering or potentiating the EMT which develops subsequently.

Altogether these data indicate that platelets can be an important factor in prostate cancer, especially in early stages. Several reports show that late stage prostate cancer can be associated with a low platelet count (thrombocytopenia) (Betsch et al. 2010). However, the thrombocytopenia associated with metastatic prostate cancer is thought to be a consequence of bone marrow dysfunction caused by bone marrow metastases. On the other hand, Interleukine-6 (IL-6) is reported to induce the production of platelets (thrombopoiesis) (Stahl et al. 1991) and is reported to correlate with poor prognosis when detected in early prostate cancer (Nguyen et al. 2014). Patients with untreated metastatic prostate adenocarcinoma presented high serum levels of IL-6 (Nguyen et al., 2014). IL-6 overproduction mediates thrombopoiesis through the production of thrombopoietin in several cancers (Kaser et al., 2001). This information could help trace a hypothetical time line in the effects of platelets and PRH over prostate cancer progression (figure 5.14). Early stage cancer causes inflammation, augmenting the production of IL-6 (Culig, 2014). IL-6 over-production triggers thrombopoiesis and later excessive quantities of platelets (thrombocytosis) (Kaser et al., 2001). Platelets can extravasate and interact with cancer cells activating TGF-β signalling (Haemmerle et al., 2016). TGF-β down-regulates PRH facilitating EMT and metastasis. Cancer cells in the blood stream also interact with platelets and thereby evade the immune system, this interaction is also thought to facilitate extravasation. Prostate metastasis formed in the bone marrow would disrupt haematopoiesis and thrombopoiesis, causing thrombocytopenia. Interestingly, our ChIP-seq data showed a possible occupation of the IL-6 promoter by PRH, suggesting that PRH could have an effect on thrombopoiesis. This opens

perspectives to experiments to further study the interplay between blood platelets and PRH.

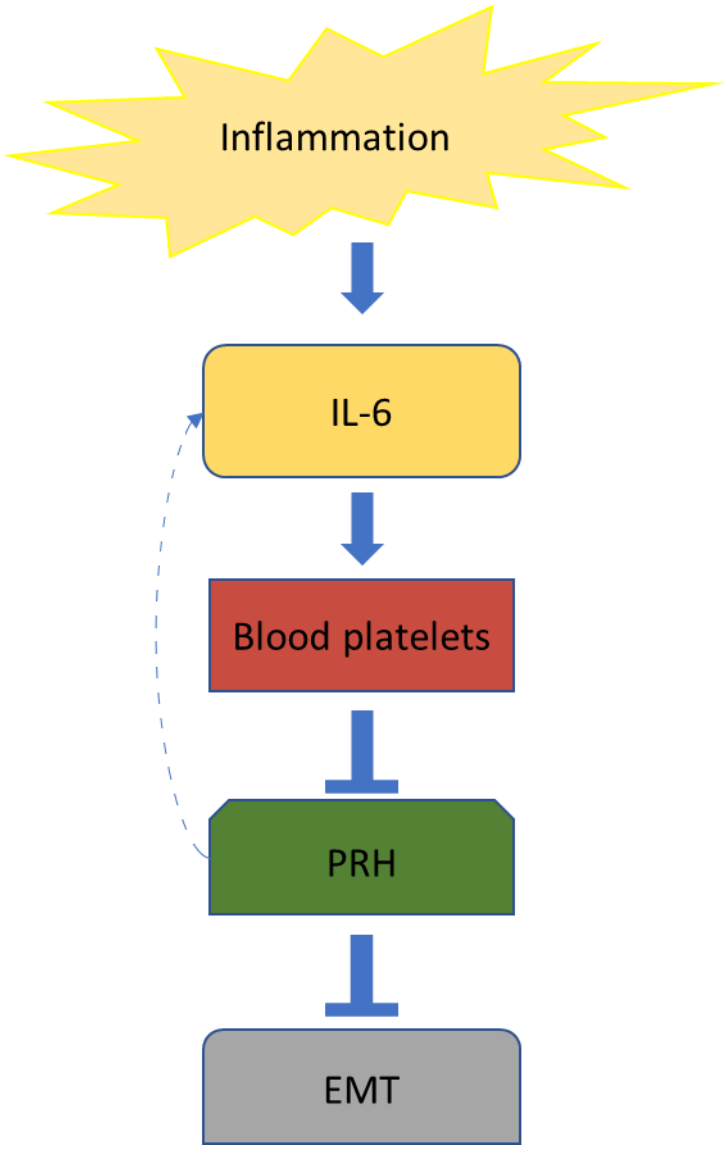

Figure 5.14. Hypothetical timeline of the effects of platelets and PRH over prostate cancer.

Chapter 6: Final conclusions

This work explores the regulation of a novel EMT-TF, PRH, in prostate cancer cells. However, there is a general discussion on the roles and actual relevance of EMT-TFs to cancer. This is mainly due the complexity of EMT regulation and use of sub-optimal models (Brabletz et al. 2018) that can show conflicting results. EMT is not a uniform process limited by a unique pathway as different cell signalling programmes can initiate EMT-like changes in prostate cancer. Among them androgen receptor (AR) signalling, oestrogen signalling, TGF-β, IGF and EGF are commonly flagged as activators (as reviewed by Montanari et al 2017). Furthermore, there are several EMT-TFs, including Snail, Slug *TWIST1* and ZEB (Jolly et al. 2015, Gasior et al 2017) and inflammatory mediators such as NF-κB that can be involved (Tong et al 2018). Additionally, cancer cells need to adapt to different and severe environments, which creates a selection for constant change and adaptability (Brabletz et al. 2018). This is noticeable in tumours, where intermediate states of cell differentiation are observed. The microenvironment creates a dynamic system where cells can differentiate and de-differentiate according to environmental inputs (Jolly et al. 2015). Therefore, the arbitrary silencing of a marker and the use of end-stage classification systems in a plurally regulated process that is in constant modification can often mask its real relevance in cancer progression. Nonetheless, the use of simplistic models can still provide data on the plasticity of the EMT and give conclusions that are often valuable (as reviewed by Brabletz et al. 2018).

EMT might not play a role in tumourigenesis but ins0074ead influence later stages of cancer. For example, the specific knockout (KO) of the EMT-TF *TWIST1* in oncogene-induced breast cancer in mice, showed that tumorigenesis was the same between control and *TWIST1* KO animals. However, tumours in *TWIST1* KO mice presented reduced EMT markers and notably reduced frequency of lung metastases (Xu et al. 2017). Here, I demonstrated that TGF-β can induce EMT in a normal immortalised epithelial prostate cell line. TGF-β treatment also showed an aggravation of EMT markers in prostate adenocarcinoma cells, mimicking the effects of EMT in late stage cancers. I also highlighted the relevance of PRH studies in prostate cancer. Mutations and epigenetic regulations often cause PRH down-regulation in patients' samples as shown by the analysis of the cancer databases cBioportal and Meth HC. Furthermore, I showed that PRH expression is negatively correlated to the differentiation degree of prostate tumours.

Unlike *TWIST1*, Snail and Slug, which actively repress E-Cadherin expression and thereby induce EMT (Medici et al. 2008; Y. Wang et al. 2016), PRH appears to activate transcription of E-Cadherin in prostate cells. Microarray analysis of PRH knockdown in breast cell line MCF-7 showed down-regulation of E-cadherin (Kershaw et al. 2017). My research shows that PRH overexpression caused an up-regulation of E-cadherin protein and its mRNA encoded by *CDH1*. In addition, PRH overexpression counteracts EMT by overexpressing E-cadherin. Therefore, PRH dysregulation would be expected to induce or facilitate EMT.

One of the major contributors to the balance of EMT/MET (or EMP) observed in this study was TGF-β. As explained before, TGF-β can reach the tumour site through several routes. It can be produced by infiltrating inflammatory cells, platelets, stromal cells, additionally, it can be produced endogenously by cells from the carcinoma lineage (reviewed by David and Massagué 2018). TGF-β protein availability to the receptor can also be regulated by several factors, among which is the sequestering of TGF-β by components of the ECM, for example the Latent TGF-beta Binding Protein (LTBPs). These regulators can also transport the protein activating signals to a distant site from the cell that originally produced it. The regulation of TGF-β signalling is discussed in more detail in the review by David and Massagué 2018.

Additionally, I have demonstrated that TGF-β regulates the expression of PRH in prostate adenocarcinoma cells. This effect in late stages of prostate cancer aligns well with the observation of decreased PRH expression in patients' prostate cancer samples. Interestingly, treatment of PRH over-expressing PC3 cells with TGF-β caused the abrogation of the re-epithelization effect of PRH. Together, this indicates that, in prostate adenocarcinoma, the balance shifts between these signalling pathways, augmenting TGF-β signalling during cancer progression. This generates several changes in cellular gene expression, including up-regulation of Snail and down-regulation of PRH, which drive EMT. Furthermore, by down-regulating PRH, which inhibits the expression of *TGFBR2* and *TGFB1*, TGF-β creates a positive feed-back loop, which would be expected to sensitise the cells to TGF-β. This makes it important to study the temporal expression of PRH during tumorigenesis and tumour development, potentially making PRH a good marker of cancer progression stage in patients.

Studies of *TGFBR2* function in prostate cancer have shown conflicting data. The expression of a *TGFBR2* dominant negative in PC-3MM2 reduced the tumour growth rate and metastatic incidence when these cells were injected into the prostate of nude mice (Zhang et al. 2005). Interestingly, over-expression of *TGFBR2* in LNCaP cells restores the sensitivity of this cell line to TGF-β inhibitory effects on cell proliferation (Guo & Kyprianou 1998) and inhibits tumorigenicity by apoptosis induction (Guo & Kyprianou 1999). However, as these studies were conducted in different cell lines, important expression context is lost in the analysis. The TGF-β signal effect is known to vary with context, for example the abundance of receptors and regulators can alter TGF-β signal outcome (as reviewed by Massagué 2012, David and Massagué 2018). Therefore, the different effects of *TGFBR2* observed could be a reflection of the contextual environment each cell line tested provided. Among other differences, according to the cancer cell line encyclopaedia, *HHEX* mRNA was detected less in LNCaP cells than in PC3 cells by mRNA seq. Based on the results presented here, it is not farfetched to speculate that differences in PRH expression between the two cell lines could be important in the contextual activation of the TGF-β pathway. This information is interesting and raises the question: in what contexts does TGF-β signalling repress PRH expression? Further experiments in additional cell lines and cancer models could help elucidate the answer to this in the future.

I also propose that a TME component could be involved in the TGF-β induced downregulation of PRH. TGF-β pathway activation by platelets in prostate adenocarcinoma cells, triggered changes like the ones triggered by TGF-β treatment, including the down-regulation of PRH mRNA and protein levels. I also raise the possibility of PRH having an indirect effect on the recruitment of platelets. ChIP-seq showed that PRH binds to IL-6 promoter, and IL-6 can regulate the quantity of circulating platelets. Additionally, PRH is known to regulate genes from the VEGF signalling pathway in leukaemia cells (Noy et al. 2012) and PRH over-expression has been shown to regulate VEGF signalling genes in endothelial cells (Nakagawa et al. 2003). This demonstrates the potential role of PRH in regulating the creation of new blood vessels, an important event in cancer progression. The repression of PRH could stimulate neovascularisation, and with it, platelets and other blood-borne factors might have increased access to the tumours.

In summary, TGF-β and PRH seem to co-regulate each other's effects in prostate cancer EMT. TGF-β signalling (potentially activated by platelets) may down-regulate PRH expression directly by binding of pSmad3 protein to the *HHEX* promoter and indirectly by activation of CK2 and consequent PRH phosphorylation. PRH regulates the expression of multiple genes involved in the TGF-β signalling pathway, including *TGFB2*, *TGFBR2* and Endoglin. PRH effects in prostate adenocarcinoma cells also included reduced migratory ability, reduced cell proliferation and reactivation of an epithelial phenotype. However, TGF-β signalling abrogates the reactivation of the epithelial marker E-cadherin by PRH over-expression, indicating that PRH is by no means the dominant mediator of TGF-β signalling.

The existing information available about PRH in cancer plus the new information generated here shows that PRH interfaces with the establishment of at least three of the hallmarks of cancer. As mentioned above, PRH regulates the expression of VEGF signalling genes, possibly impacting angiogenesis. PRH also regulates cellular proliferation, showed here using EdU incorporation, and PRH expression is lower in advanced prostate adenocarcinomas samples and cell lines, so its down-regulation can be interpreted as a mechanism that enables prostate cancer cells to evade growth suppressor signals. And finally, PRH regulates the EMT program in prostate cancer cell lines, therefore, its down-regulation could also facilitate the activation of invasion and metastasis in prostate cancer (figure 6.1). Additional experiments in animal models are required in order to investigate these points. For example, it would be interesting to study tumour formation by PC3 cells and PC3 cells expressing PRH in nude mice as well as looking at the formation of metastases following tail vein injection.

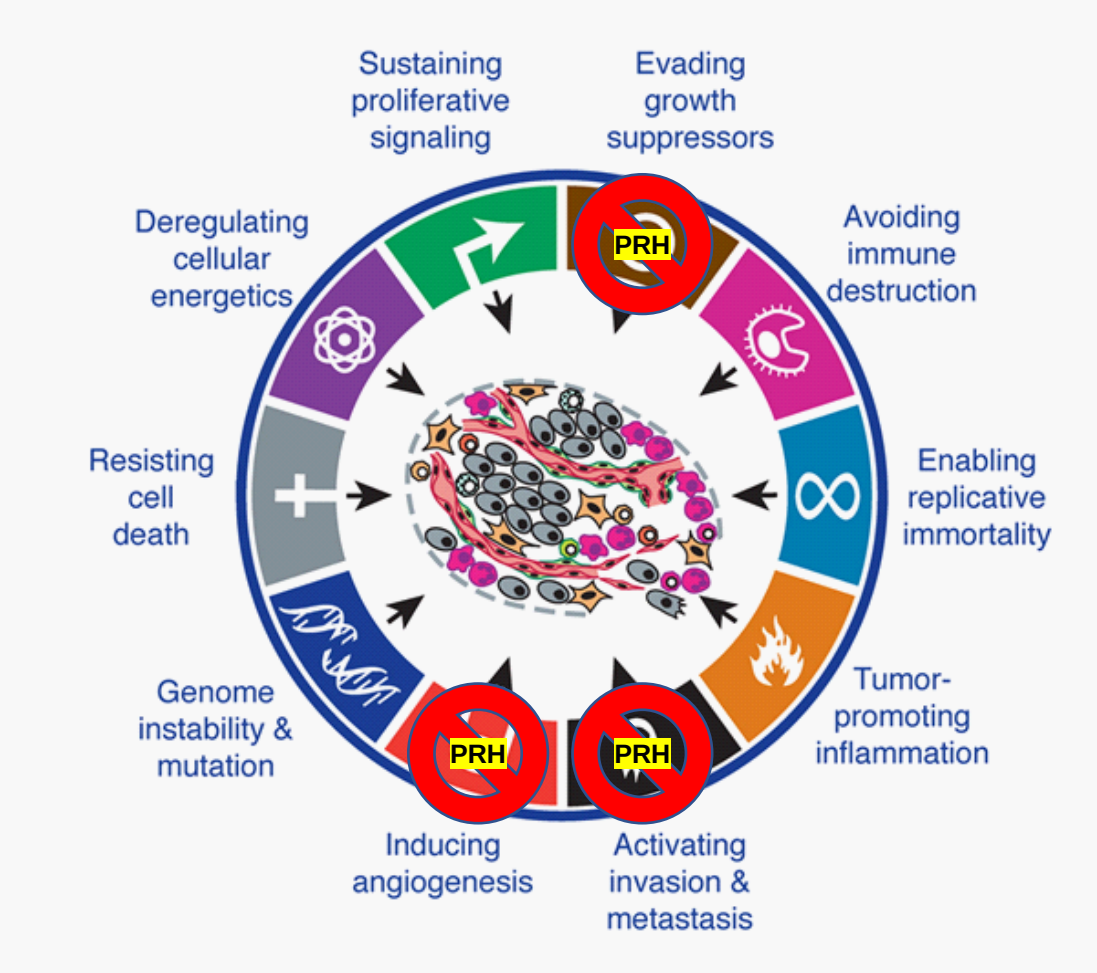

Figure 6.1. PRH interferes with three aspects of hallmarks of cancer. PRH suppresses growth signals, potentially blocks neovascularization and counter acts EMT in prostate cancer.

EMT targeting is a novel strategy to overcome drug resistance in cancer treatment (reviewed by Du et al. 2016), as EMT is reported to be involved in drug resistance. PRH down-regulation was shown to induce EMT-like changes in immortalised prostate cells (Siddiqui et al. 2017). Here I have shown that PRH over-expression can re-activate the epithelial phenotype in prostate adenocarcinoma cells. PRH is therefore in a strategic position for studies of drug resistance mechanisms. The inducible PRH over-expression model I created in the PC3 cell line may be useful in drug screening. An established model that shows co-culture of stromal cells and cancer cells in 3D has relevant predictive value to the drug resistance profile of patients' tumours (Saunders et al. 2017). This model is useful since it recreates a TME-like environment for the cancer cells *in vitro*. With the ability to regulate PRH expression in PC3 cells, this methodology could be applied to study the effects of PRH expression on drug resistance of prostate adenocarcinoma.

In the case of prostate cancer, castration therapy is widely implemented. This therapy can reduce tumour volume initially, however it may induce genetic evolution of the tumour and resistance to therapy. PRH deletion was observed in some prostate tumours, and in many cases in tumours that did not receive such therapies. This suggests that the lost of PRH happens in pre-treatment stages of prostate cancer, therefore PRH could be important in the process of tumourigenesis and carcinogenesis. With further experiments PRH could become an important marker that would, potentially, help to guide prostate cancer treatment in the future. Perhaps aiding the decision not to use ADT therapy to avoid tumour evolution and tackling the tumour with effective therapy from the beginning, instead of using palliative solutions that ultimately cause the tumour to become aggressive and difficult to treat.

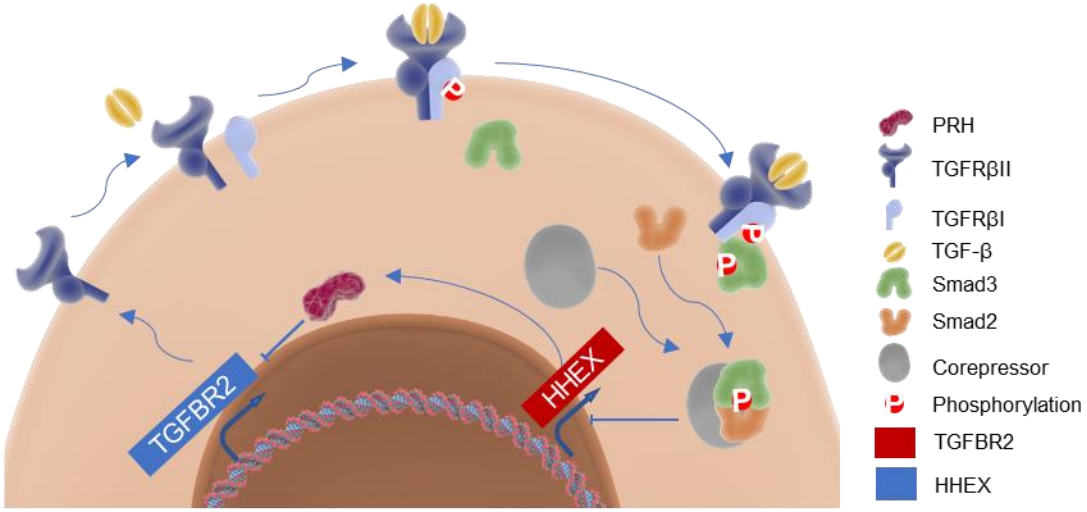

Figure 6.2. Crosstalk between PRH and TGF-β. When TGF-β binds to the TGFβRII it forms a heterodimer with TGFβRI, TGFβRI then phosphorylates Smad3. pSmad3 can forms a heterodimer with Smad2 or a repressor complex with different corepressors. pSmad3 activity in PRH promoter may down-regulate *HHEX* gene expression. Alternatively, TGF-β signalling may down-regulate PRH activity by mechanisms that do not involve the regulation of *HHEX* gene transcription such as regulation of mRNA stability. PRH is a repressor of TGFβRII gene and a regulator of many other TGF-β signalling genes.

References

Aaron, LaTayia, Omar E Franco, and Simon W Hayward. 2016. “Review of Prostate Anatomy and Embryology and the Etiology of Benign Prostatic Hyperplasia.” The Urologic Clinics of North America 43 (3). NIH Public Access: 279–88. doi:10.1016/j.ucl.2016.04.012.

ACS, American Cancer Society. 2014. “Sources of Statistics 66 Screening Guidelines for the Early Detection of Cancer in Average-Risk Asymptomatic People* 68.” https://www.cancer.org/content/dam/cancer-org/research/cancer-facts-and-statistics/annual-cancer-facts-and-figures/2014/cancer-facts-and-figures-2014.pdf.

Adams M, Smith UM, Logan CV, Johnson CA. Recent advances in the molecular pathology, cell biology and genetics of ciliopathies. J Med Genet. 2008 May;45(5):257-67. doi: 10.1136/jmg.2007.054999.

Ahmed, Hashim, Vanessa Basketter, Kate Bullen, Wayne De Leeuw, Nikola Hawkins, and Chris Parker. 2016. “Advanced Prostate Cancer.” European Urology 39 (6): 1–10. doi:10.1016/j.beem.2008.01.009.A.

Alotaibi, Hani, M. Felicia Basilicata, Huma Shehwana, Tyler Kosowan, Ilona Schreck, Christien Braeutigam, Ozlen Konu, Thomas Brabletz, and Marc P. Stemmler. 2015. “Enhancer Cooperativity as a Novel Mechanism Underlying the Transcriptional Regulation of E-Cadherin during Mesenchymal to Epithelial Transition.” Biochimica et Biophysica Acta (BBA) - Gene Regulatory Mechanisms 1849 (6): 731–42. doi:10.1016/j.bbagrm.2015.01.005.

Amit, Ido, Ami Citri, Tal Shay, Yiling Lu, Menachem Katz, Fan Zhang, Gabi Tarcic, et al. 2007. “A Module of Negative Feedback Regulators Defines Growth Factor Signaling.” Nature Genetics 39 (4). Nature Publishing Group: 503–12. doi:10.1038/ng1987.

Ammirante, Massimo, Jun-Li Luo, Sergei Grivennikov, Sergei Nedospasov, and Michael Karin. 2010. “B-Cell-Derived Lymphotoxin Promotes Castration-Resistant Prostate Cancer.” Nature 464 (7286): 302–5. doi:10.1038/nature08782.

Anderson K, Lutz C, van Delft FW, Bateman CM, Guo Y, Colman SM, Kempski H, Moorman AV, Titley I, Swansbury J, Kearney L, Enver T, Greaves M. Genetic variegation of clonal architecture and propagating cells in leukaemia. Nature. 2011 Jan 20;469(7330):356-61. doi: 10.1038/nature09650.

Archer LK, Frame FM, Maitland NJ. Stem cells and the role of ETS transcription factors in the differentiation hierarchy of normal and malignant prostate epithelium. J Steroid Biochem Mol Biol. 2017 Feb;166:68-83. doi: 10.1016/j.jsbmb.2016.05.006.

Baca SC, Prandi D, Lawrence MS, Mosquera JM, Romanel A, Drier Y, Park K, Kitabayashi N, MacDonald TY, Ghandi M, Van Allen E, Kryukov GV, Sboner A, Theurillat JP, Soong TD, Nickerson E, Auclair D, Tewari A, Beltran H, Onofrio RC, Boysen G, Guiducci C, Barbieri CE, Cibulskis K, Sivachenko A, Carter SL, Saksena G, Voet D, Ramos AH, Winckler W, Cipicchio M, Ardlie K, Kantoff PW, Berger MF,

Gabriel SB, Golub TR, Meyerson M, Lander ES, Elemento O, Getz G, Demichelis F, Rubin MA, Garraway LA. Punctuated evolution of prostate cancer genomes. Cell. 2013 Apr 25;153(3):666-77. doi: 10.1016/j.cell.2013.03.021.

Bai J, Xi Q. Crosstalk between TGF-β signaling and epigenome. Acta Biochim Biophys Sin (Shanghai). 2018 Jan 1;50(1):60-67. doi: 10.1093/abbs/gmx122.

Bakewell, S. J., P. Nestor, S. Prasad, M. H. Tomasson, N. Dowland, M. Mehrotra, R. Scarborough, et al. 2003. “Platelet and Osteoclast 3 Integrins Are Critical for Bone Metastasis.” Proceedings of the National Academy of Sciences 100 (24): 14205–10. doi:10.1073/pnas.2234372100.

Bell RJ1, Rube HT, Xavier-Magalhães A, Costa BM, Mancini A, Song JS, Costello JF. Understanding TERT Promoter Mutations: A Common Path to Immortality. Mol Cancer Res. 2016 Apr;14(4):315-23. doi: 10.1158/1541-7786.MCR-16-0003.

Berger MF, Lawrence MS, Demichelis F, Drier Y, Cibulskis K, Sivachenko AY, Sboner A, Esgueva R, Pflueger D, Sougnez C, Onofrio R, Carter SL, Park K, Habegger L, Ambrogio L, Fennell T, Parkin M, Saksena G, Voet D, Ramos AH, Pugh TJ, Wilkinson J, Fisher S, Winckler W, Mahan S, Ardlie K, Baldwin J, Simons JW, Kitabayashi N, MacDonald TY, Kantoff PW, Chin L, Gabriel SB, Gerstein MB, Golub TR, Meyerson M, Tewari A, Lander ES, Getz G, Rubin MA, Garraway LA. The genomic complexity of primary human prostate cancer. Nature. 2011 Feb 10;470(7333):214-20. doi: 10.1038/nature09744.

Bergstralh, Daniel T., and Daniel St Johnston. 2012. “Epithelial Cell Polarity: What Flies Can Teach Us about Cancer.” Essays In Biochemistry 53 (August): 129–40. doi:10.1042/bse0530129.

Bernabeu, Carmelo, Jose M Lopez-Novoa, and Miguel Quintanilla. 2009. “The Emerging Role of TGF-Beta Superfamily Coreceptors in Cancer.” Biochimica et Biophysica Acta 1792 (10): 954–73. doi:10.1016/j.bbadis.2009.07.003.

Berthon P, Cussenot O, Hopwood L, Leduc A, Maitland N. Functional expression of sv40 in normal human prostatic epithelial and fibroblastic cells - differentiation pattern of nontumorigenic cell-lines. Int J Oncol. 1995 Feb;6(2):333-43.

Bess, Kirstin L, Tracey E Swingler, A Jennifer Rivett, Kevin Gaston, and Padma-Sheela Jayaraman. 2003. “The Transcriptional Repressor Protein PRH Interacts with the Proteasome.” Biochem. J. Vol. 374. https://www.ncbi.nlm.nih.gov/pmc/articles/PMC1223646/pdf/12826010.pdf.

Betsch, D M, S Gray, and S E Zed. 2017. “A Case of Metastatic Prostate Cancer and Immune Thrombocytopenia.” Current Oncology (Toronto, Ont.) 24 (5). Multimed Inc.: e434–36. doi:10.3747/co.24.3592.

Bhowmick, Neil A., Eric G. Neilson, and Harold L. Moses. 2004. “Stromal Fibroblasts in Cancer Initiation and Progression.” Nature 432 (7015): 332–37. doi:10.1038/nature03096.

Billeter, M. 1996. “Homeodomain-Type DNA Recognition.” Progress in Biophysics and Molecular Biology 66 (3): 211–25. http://www.ncbi.nlm.nih.gov/pubmed/9284451.

Birchmeier, W, and J Behrens. 1994. “Cadherin Expression in Carcinomas: Role in the Formation of Cell Junctions and the Prevention of Invasiveness.” Biochimica et Biophysica Acta 1198 (1): 11–26. http://www.ncbi.nlm.nih.gov/pubmed/8199193.

Biswas, Swati, Marta Guix, Cammie Rinehart, Teresa C Dugger, Anna Chytil, Harold L Moses, Michael L Freeman, and Carlos L Arteaga. 2007. “Inhibition of TGF-Beta with Neutralizing Antibodies Prevents Radiation-Induced Acceleration of Metastatic Cancer Progression.” The Journal of Clinical Investigation 117 (5). American Society for Clinical Investigation: 1305–13. doi:10.1172/JCI30740.

Blakytny, Robert, Anna Ludlow, Gail E.M. Martin, Grenham Ireland, Leif R. Lund, Mark W.J. Ferguson, and Georg Brunner. 2004. “Latent TGF-?1 Activation by Platelets.” Journal of Cellular Physiology 199 (1): 67–76. doi:10.1002/jcp.10454.

Blasco, Maria A. 2005. “Telomeres and Human Disease: Ageing, Cancer and beyond.” Nature Reviews Genetics 6 (8): 611–22. doi:10.1038/nrg1656.

Borah S, Xi L, Zaug AJ, Powell NM, Dancik GM, Cohen SB, Costello JC, Theodorescu D, Cech TR. TERT promoter mutations and telomerase reactivation in urothelial cancer. Science. 2015 Feb 27;347(6225):1006-10. doi: 10.1126/science.1260200.

Brabletz, T., A. Jung, S. Reu, M. Porzner, F. Hlubek, L. A. Kunz-Schughart, R. Knuechel, and T. Kirchner. 2001. “Variable -Catenin Expression in Colorectal Cancers Indicates Tumor Progression Driven by the Tumor Environment.” Proceedings of the National Academy of Sciences 98 (18): 10356–61. doi:10.1073/pnas.171610498.

Brabletz, Thomas, Raghu Kalluri, M. Angela Nieto, and Robert A. Weinberg. 2018. “EMT in Cancer.” Nature Reviews Cancer 18 (2). Nature Publishing Group: 128–34. doi:10.1038/nrc.2017.118.

Brown, R M, and C A Middleton. 1985. “MORPHOLOGY AND LOCOMOTION OF INDIVIDUAL EPITHELIAL CELLS IN CULTURE.” J. Cell Sci. Vol. 78. http://jcs.biologists.org/content/joces/78/1/105.full.pdf.

Brungs, D, J Chen, P Masson, and R J Epstein. 2014. “Intermittent Androgen Deprivation Is a Rational Standard-of-Care Treatment for All Stages of Progressive Prostate Cancer: Results from a Systematic Review and Meta-Analysis.” Prostate Cancer and Prostatic Diseases 17 (2): 105–11. doi:10.1038/pcan.2014.10.

Bukholm, I. K., J. M. Nesland, and A.-L. Borresen-Dale. 2000. “Re-Expression of E-Cadherin, ?-Catenin and ?-Catenin, but Not of ?-Catenin, in Metastatic Tissue from Breast Cancer Patients.” The Journal of Pathology 190 (1): 15–19. doi:10.1002/(SICI)1096-9896(200001)190:1<15::AID-PATH489>3.0.CO;2-L.

Bunting PS. Screening for prostate cancer with prostate-specific antigen: beware the biases. Clin Chim Acta. 2002 Jan;315(1-2):71-97.

Burkhart, Deborah L., and Julien Sage. 2008. “Cellular Mechanisms of Tumour Suppression by the Retinoblastoma Gene.” Nature Reviews Cancer 8 (9). Nature Publishing Group: 671–82. doi:10.1038/nrc2399.

Carlsson S, Assel M, Ulmert D, Gerdtsson A, Hugosson J, Vickers A, Lilja H. Screening for Prostate Cancer Starting at Age 50-54 Years. A Population-based Cohort Study. Eur Urol. 2017 Jan;71(1):46-52. doi: 10.1016/j.eururo.2016.03.026.

Carr, Brian I, Aldo Cavallini, Rosalba D’Alessandro, Maria Grazia Refolo, Catia Lippolis, Antonio Mazzocca, and Caterina Messa. 2014. “Platelet Extracts Induce Growth, Migration and Invasion in Human Hepatocellular Carcinoma in Vitro.” BMC Cancer 14 (1). BioMed Central: 43. doi:10.1186/1471-2407-14-43.

Cheifetz, S, T Bellón, C Calés, S Vera, C Bernabeu, J Massagué, and M Letarte. 1992. “Endoglin Is a Component of the Transforming Growth Factor-Beta Receptor System in Human Endothelial Cells.” The Journal of Biological Chemistry 267 (27): 19027–30. http://www.ncbi.nlm.nih.gov/pubmed/1326540.

Chin, Koei, Carlos Ortiz de Solorzano, David Knowles, Arthur Jones, William Chou, Enrique Garcia Rodriguez, Wen-Lin Kuo, et al. 2004. “In Situ Analyses of Genome Instability in Breast Cancer.” Nature Genetics 36 (9): 984–88. doi:10.1038/ng1409.

Chin, L, S E Artandi, Q Shen, A Tam, S L Lee, G J Gottlieb, C W Greider, and R A DePinho. 1999. “p53 Deficiency Rescues the Adverse Effects of Telomere Loss and Cooperates with Telomere Dysfunction to Accelerate Carcinogenesis.” Cell 97 (4): 527–38. http://www.ncbi.nlm.nih.gov/pubmed/10338216.

Chu, Eric C, and Andrzej S Tarnawski. 2004. “PTEN Regulatory Functions in Tumor Suppression and Cell Biology.” Medical Science Monitor : International Medical Journal of Experimental and Clinical Research 10 (10): RA235-41. http://www.ncbi.nlm.nih.gov/pubmed/15448614.

Chua CW, Shibata M1, Lei M, Toivanen R, Barlow LJ, Bergren SK, Badani KK, McKiernan JM, Benson MC, Hibshoosh H, Shen MM1. Single luminal epithelial progenitors can generate prostate organoids in culture. Nat Cell Biol. 2014 Oct;16(10):951-61, 1-4. doi: 10.1038/ncb3047.

Collins AT, Berry PA, Hyde C, Stower MJ, Maitland NJ. Prospective identification of tumorigenic prostate cancer stem cells. Cancer Res. 2005 Dec 1;65(23):10946-51.

Cong, Rong, Xiaobing Jiang, Christine M. Wilson, Michael P. Hunter, Hemaxi Vasavada, and Clifford W. Bogue. 2006. “*HHEX* Is a Direct Repressor of Endothelial Cell-Specific Molecule 1 (ESM-1).” Biochemical and Biophysical Research Communications 346 (2): 535–45. doi:10.1016/j.bbrc.2006.05.153.

Culig, Zoran, and Frédéric R. Santer. 2014. “Androgen Receptor Signaling in Prostate Cancer.” Cancer and Metastasis Reviews 33 (2-3): 413–27. doi:10.1007/s10555-013-9474-0.

Curi, Rui, Philip Newsholme, and Eric A Newsholme. 1988. “Metabolism of Pyruvate by Isolated Rat Mesenteric Lymphocytes, Lymphocyte Mitochondria and Isolated Mouse Macrophages.” Biochem. J. Vol. 250. https://www.ncbi.nlm.nih.gov/pmc/articles/PMC1148867/pdf/biochemj00236-0074.pdf.

D’Elia, Angela V., Gianluca Tell, Diego Russo, Franco Arturi, Fabio Puglisi, Guidalberto Manfioletti, Valter Gattei, et al. 2002. “Expression and Localization of the Homeodomain-Containing Protein HEX in Human Thyroid Tumors.” The Journal of Clinical Endocrinology & Metabolism 87 (3): 1376–83. doi:10.1210/jcem.87.3.8344.

David CJ, Huang YH, Chen M, Su J, Zou Y, Bardeesy N, Iacobuzio-Donahue CA, Massagué J. TGF-β Tumor Suppression through a Lethal EMT. Cell. 2016 Feb 25;164(5):1015-30. doi: 10.1016/j.cell.2016.01.009.

David CJ, Massagué J. Contextual determinants of TGFβ action in development, immunity and cancer. Nat Rev Mol Cell Biol. 2018 Jul;19(7):419-435. doi: 10.1038/s41580-018-0007-0.

David, Charles J., Yun-Han Huang, Mo Chen, Jie Su, Yilong Zou, Nabeel Bardeesy, Christine A. Iacobuzio-Donahue, and Joan Massagué. 2016. “TGF-β Tumor Suppression through a Lethal EMT.” Cell 164 (5): 1015–30. doi:10.1016/j.cell.2016.01.009.

Davies M, Robinson M, Smith E, Huntley S, Prime S, Paterson I. Induction of an epithelial to mesenchymal transition in human immortal and malignant keratinocytes by TGF-beta1 involves MAPK, Smad and AP-1 signalling pathways. J Cell Biochem. 2005 Aug 1;95(5):918-31.

de Gramont, Armand, Sandrine Faivre, and Eric Raymond. 2017. “Novel TGF-β Inhibitors Ready for Prime Time in Onco-Immunology.” Oncoimmunology 6 (1). Taylor & Francis: e1257453. doi:10.1080/2162402X.2016.1257453.

De Marzo AM, Haffner MC, Lotan TL, Yegnasubramanian S, Nelson WG. Premalignancy in Prostate Cancer: Rethinking What we Know. Cancer Prev Res (Phila). 2016 Aug;9(8):648-56. doi: 10.1158/1940-6207.CAPR-15-0431.

De Marzo, Angelo M., Elizabeth A. Platz, Siobhan Sutcliffe, Jianfeng Xu, Henrik Grönberg, Charles G. Drake, Yasutomo Nakai, William B. Isaacs, and William G. Nelson. 2007. “Inflammation in Prostate Carcinogenesis.” Nature Reviews Cancer 7 (4). Nature Publishing Group: 256–69. doi:10.1038/nrc2090.

DeBerardinis, Ralph J., Julian J. Lum, Georgia Hatzivassiliou, and Craig B. Thompson. 2008. “The Biology of Cancer: Metabolic Reprogramming Fuels Cell

Growth and Proliferation.” Cell Metabolism 7 (1). Cell Press: 11–20. doi:10.1016/J.CMET.2007.10.002.

Degenhardt, Kurt, Robin Mathew, Brian Beaudoin, Kevin Bray, Diana Anderson, Guanghua Chen, Chandreyee Mukherjee, et al. 2006. “Autophagy Promotes Tumor Cell Survival and Restricts Necrosis, Inflammation, and Tumorigenesis.” Cancer Cell 10 (1). NIH Public Access: 51–64. doi:10.1016/j.ccr.2006.06.001.

Dehm, S. M., L. J. Schmidt, H. V. Heemers, R. L. Vessella, and D. J. Tindall. 2008. “Splicing of a Novel Androgen Receptor Exon Generates a Constitutively Active Androgen Receptor That Mediates Prostate Cancer Therapy Resistance.” Cancer Research 68 (13): 5469–77. doi:10.1158/0008-5472.CAN-08-0594.

DeNardo, David G., Pauline Andreu, and Lisa M. Coussens. 2010. “Interactions between Lymphocytes and Myeloid Cells Regulate pro- versus Anti-Tumor Immunity.” Cancer and Metastasis Reviews 29 (2): 309–16. doi:10.1007/s10555-010-9223-6.

Denson, L A, M H McClure, C W Bogue, S J Karpen, and H C Jacobs. 2000. “HNF3beta and GATA-4 Transactivate the Liver-Enriched Homeobox Gene, Hex.” Gene 246 (1-2): 311–20. http://www.ncbi.nlm.nih.gov/pubmed/10767553.

Dermer, G B. 1978. “Basal Cell Proliferation in Benign Prostatic Hyperplasia.” Cancer 41 (5): 1857–62. http://www.ncbi.nlm.nih.gov/pubmed/77182.

Derynck, Rik, Rosemary J. Akhurst, and Allan Balmain. 2001. “TGF-|[beta]| Signaling in Tumor Suppression and Cancer Progression.” Nature Genetics 29 (2). Nature Publishing Group: 117–29. doi:10.1038/ng1001-117.

Dighe, Anand S., Elizabeth Richards, Lloyd J. Old, and Robert D. Schreiber. 1994. “Enhanced in Vivo Growth and Resistance to Rejection of Tumor Cells Expressing Dominant Negative IFNγ Receptors.” Immunity 1 (6). Cell Press: 447–56. doi:10.1016/1074-7613(94)90087-6.

Du, Bowen, Joong Shim, Bowen Du, and Joong Sup Shim. 2016. “Targeting Epithelial–Mesenchymal Transition (EMT) to Overcome Drug Resistance in Cancer.” Molecules 21 (7). Multidisciplinary Digital Publishing Institute: 965. doi:10.3390/molecules21070965.

Du, Pan, Xiao Zhang, Chiang-Ching Huang, Nadereh Jafari, Warren A Kibbe, Lifang Hou, and Simon M Lin. 2010. “Comparison of Beta-Value and M-Value Methods for Quantifying Methylation Levels by Microarray Analysis.” doi:10.1186/1471-2105-11-587.

Dunn, Gavin P., Lloyd J. Old, and Robert D. Schreiber. 2004. “The Three Es of Cancer Immunoediting.” Annual Review of Immunology 22 (1): 329–60. doi:10.1146/annurev.immunol.22.012703.104803.

Düwel, Annette, Nélida Eleno, Mirjana Jerkic, Miguel Arevalo, Juan P Bolaños, Carmelo Bernabeu, and Jose M López-Novoa. 2007. “Reduced Tumor Growth and Angiogenesis in Endoglin-Haploinsufficient Mice.” Tumour Biology : The Journal of the International Society for Oncodevelopmental Biology and Medicine 28 (1): 1–8. doi:10.1159/000097040.

Ell, Brian, and Yibin Kang. 2013. “Transcriptional Control of Cancer Metastasis.” Trends in Cell Biology 23 (12). NIH Public Access: 603–11. doi:10.1016/j.tcb.2013.06.001.

Engel, A M, I M Svane, J Rygaard, and O Werdelin. 1997. “MCA Sarcomas Induced in Scid Mice Are More Immunogenic than MCA Sarcomas Induced in Congenic, Immunocompetent Mice.” Scandinavian Journal of Immunology 45 (5): 463–70. http://www.ncbi.nlm.nih.gov/pubmed/9160088.

Epstein JI, Egevad L, Amin MB, Delahunt B, Srigley JR, Humphrey PA; Grading Committee. The 2014 International Society of Urological Pathology (ISUP) Consensus Conference on Gleason Grading of Prostatic Carcinoma: Definition of Grading Patterns and Proposal for a New Grading System. Am J Surg Pathol. 2016 Feb;40(2):244-52. doi: 10.1097/PAS.0000000000000530.

Epstein, Jonathan I, William C Allsbrook, Mahul B Amin, Lars L Egevad, and ISUP Grading Committee. 2005. “The 2005 International Society of Urological Pathology (ISUP) Consensus Conference on Gleason Grading of Prostatic Carcinoma.” The American Journal of Surgical Pathology 29 (9): 1228–42. http://www.ncbi.nlm.nih.gov/pubmed/16096414.

Eurell, Jo Ann Coers., Brian L. Frappier, and Horst-Dieter. Dellmann. 2006. Dellmann’s Textbook of Veterinary Histology. Blackwell Pub. https://books.google.co.uk/books?id=FnS4uiOlRT0C&redir_esc=y.

Feilotter, Harriet E, Maria A Nagai, Alexander H Boag, Charis Eng, and Lois M Mulligan. 1998. “Analysis of PTEN and the 10q23 Region in Primary Prostate Carcinomas.” Oncogene 16 (13): 1743–48. doi:10.1038/sj.onc.1200205.

Feron, Olivier. 2009. “Pyruvate into Lactate and Back: From the Warburg Effect to Symbiotic Energy Fuel Exchange in Cancer Cells.” Radiotherapy and Oncology 92 (3): 329–33. doi:10.1016/j.radonc.2009.06.025.

Ferret-Bernard, Stéphanie, Rachel Sally Curwen, and Adrian Paul Mountford. 2008. “Proteomic Profiling Reveals That Th2-Inducing Dendritic Cells Stimulated with Helminth Antigens Have a ‘Limited Maturation’ Phenotype.” Proteomics 8 (5): 980–93. doi:10.1002/pmic.200700538.

Fidler, Isaiah J, and George Poste. 2008. “The ‘seed and Soil’ Hypothesis Revisited.” The Lancet Oncology 9 (8): 808. doi:10.1016/S1470-2045(08)70201-8.

Franco OE, Jiang M, Strand DW, Peacock J, Fernandez S, Jackson RS, Revelo MP, Bhowmick NA, Hayward SW. Altered TGF-β signaling in a subpopulation of human

stromal cells promotes prostatic carcinogenesis. Cancer Res. 2011 Feb 15;71(4):1272-81. doi: 10.1158/0008-5472.CAN-10-3142.

Gartner, Leslie P., James L. Hiatt, and Judy M. (Judy May) Strum. 2011. Cell Biology and Histology. Wolters Kluwer Health/Lippincott Williams & Wilkins. https://books.google.co.uk/books/about/Cell_Biology_and_Histology.html?id=CdBmQgAACAAJ&source=kp_book_description&redir_esc=y.

Gasic, G. J., Tatiana B Gasic, and Carleton C Stewart. 1968. “Antimetastatic Effects Associated with Platelet Reduction.” Proceedings of the National Academy of Sciences 61 (1): 46–52. doi:10.1073/pnas.61.1.46.

Gasior K, Hauck M, Wilson A, Bhattacharya S. A Theoretical Model of the Wnt Signaling Pathway in the Epithelial Mesenchymal Transition. Theor Biol Med Model. 2017 Oct 10;14(1):19. doi: 10.1186/s12976-017-0064-7.

Gaston, Kevin, Maria-Angela Tsitsilianos, Kerry Wadey, and Padma-Sheela Jayaraman. 2016. “Misregulation of the Proline Rich Homeodomain (PRH/*HHEX*) Protein in Cancer Cells and Its Consequences for Tumour Growth and Invasion.” Cell & Bioscience 6 (1): 12. doi:10.1186/s13578-016-0077-7.

Geiger, B, and O Ayalon. 1992. “Cadherins.” Annual Review of Cell Biology 8 (1). Annual Reviews 4139 El Camino Way, P.O. Box 10139, Palo Alto, CA 94303-0139, USA : 307–32. doi:10.1146/annurev.cb.08.110192.001515.

Gendrel AV, Attia M, Chen CJ, Diabangouaya P, Servant N, Barillot E, Heard E. Developmental dynamics and disease potential of random monoallelic gene expression. Dev Cell. 2014 Feb 24;28(4):366-80. doi: 10.1016/j.devcel.2014.01.016.

Germann M, Wetterwald A, Guzmán-Ramirez N, van der Pluijm G, Culig Z, Cecchini MG, Williams ED, Thalmann GN. Stem-like cells with luminal progenitor phenotype survive castration in human prostate cancer. Stem Cells. 2012 Jun;30(6):1076-86. doi: 10.1002/stem.1087.

Gleason, D F. 1966. “Classification of Prostatic Carcinomas.” Cancer Chemotherapy Reports 50 (3): 125–28. http://www.ncbi.nlm.nih.gov/pubmed/5948714.

Globocan. 2018. “Age Standardized (World) Incidence Rates, Prostate, All Ages.” doi:10.6.

Goldman, R D, S Khuon, Y H Chou, P Opal, and P M Steinert. 1996. “The Function of Intermediate Filaments in Cell Shape and Cytoskeletal Integrity.” The Journal of Cell Biology 134 (4): 971–83. http://www.ncbi.nlm.nih.gov/pubmed/8769421.

Goldstein AS, Huang J, Guo C, Garraway IP, Witte ON. Identification of a cell of origin for human prostate cancer. Science. 2010 Jul 30;329(5991):568-71. doi: 10.1126/science.1189992.

Gomis, R. R., C. Alarcon, W. He, Q. Wang, J. Seoane, A. Lash, and J. Massague. 2006. “A FoxO-Smad Synexpression Group in Human Keratinocytes.” Proceedings

of the National Academy of Sciences 103 (34): 12747–52. doi:10.1073/pnas.0605333103.

Gonzalez-Zulueta, M, C M Bender, A S Yang, T Nguyen, R W Beart, J M Van Tornout, and P A Jones. 1995. “Methylation of the 5’ CpG Island of the p16/CDKN2 Tumor Suppressor Gene in Normal and Transformed Human Tissues Correlates with Gene Silencing.” Cancer Research 55 (20): 4531–35. http://www.ncbi.nlm.nih.gov/pubmed/7553622.

Goodings, Charnise, Elizabeth Smith, Elizabeth Mathias, Natalina Elliott, Susan M. Cleveland, Rati M. Tripathi, Justin H. Layer, et al. 2015. “*HHEX* Is Required at Multiple Stages of Adult Hematopoietic Stem and Progenitor Cell Differentiation.” STEM CELLS 33 (8): 2628–41. doi:10.1002/stem.2049.

Gordon, Kelly J., and Gerard C. Blobe. 2008. “Role of Transforming Growth Factor-β Superfamily Signaling Pathways in Human Disease.” Biochimica et Biophysica Acta (BBA) - Molecular Basis of Disease 1782 (4). Elsevier: 197–228. doi:10.1016/J.BBADIS.2008.01.006.

Graham, T. R., H. E. Zhau, V. A. Odero-Marah, A. O. Osunkoya, K. S. Kimbro, M. Tighiouart, T. Liu, J. W. Simons, and R. M. O’Regan. 2008. “Insulin-like Growth Factor-I-Dependent Up-Regulation of *ZEB1* Drives Epithelial-to-Mesenchymal Transition in Human Prostate Cancer Cells.” Cancer Research 68 (7): 2479–88. doi:10.1158/0008-5472.CAN-07-2559.

Greger, V, E Passarge, W Höpping, E Messmer, and B Horsthemke. 1989. “Epigenetic Changes May Contribute to the Formation and Spontaneous Regression of Retinoblastoma.” Human Genetics 83 (2): 155–58. http://www.ncbi.nlm.nih.gov/pubmed/2550354.

Griffin, Patrick T, and Michael Jaglal. 2015. “Metastatic Prostate Cancer Mimicking Thrombotic Thrombocytopenic Purpura.” Blood 125 (8). American Society of Hematology: 1349. doi:10.1182/BLOOD-2014-11-608828.

Grivennikov, Sergei I., Florian R. Greten, and Michael Karin. 2010. “Immunity, Inflammation, and Cancer.” Cell 140 (6): 883–99. doi:10.1016/j.cell.2010.01.025.

Gu, Ye, Yuan Wang, Xinling Wang, Lili Gao, Weiping Yu, and Wei-Feng Dong. 2017. “Opposite Effects of SET7/9 on Apoptosis of Human Acute Myeloid Leukemia Cells and Lung Cancer Cells.” Journal of Cancer 8 (11): 2069–78. doi:10.7150/jca.19143.

Guerrero-Esteo, Mercedes, Tilman Sánchez-Elsner, Ainhoa Letamendia, and Carmelo Bernabéu. 2002. “Extracellular and Cytoplasmic Domains of Endoglin Interact with the Transforming Growth Factor-β Receptors I and II.” Journal of Biological Chemistry 277 (32): 29197–209. doi:10.1074/jbc.M111991200.

Guiral M, Bess K, Goodwin G, Jayaraman PS. PRH represses transcription in hematopoietic cells by at least two independent mechanisms. J Biol Chem. 2001 Jan 26;276(4):2961-70.

Guo, Y, and N Kyprianou. 1998. “Overexpression of Transforming Growth Factor (TGF) beta1 Type II Receptor Restores TGF-beta1 Sensitivity and Signaling in Human Prostate Cancer Cells.” Cell Growth & Differentiation : The Molecular Biology Journal of the American Association for Cancer Research 9 (2): 185–93. http://www.ncbi.nlm.nih.gov/pubmed/9486855.

Guo, Y, and N Kyprianou. 1999. “Restoration of Transforming Growth Factor Beta Signaling Pathway in Human Prostate Cancer Cells Suppresses Tumorigenicity via Induction of Caspase-1-Mediated Apoptosis.” Cancer Research 59 (6): 1366–71. http://www.ncbi.nlm.nih.gov/pubmed/10096572.

Gupta, Sonal, and Anirban Maitra. 2016. “EMT: Matter of Life or Death?” Cell 164 (5). Elsevier Inc.: 840–42. doi:10.1016/j.cell.2016.02.024.

Haemmerle, Monika, Justin Bottsford-Miller, Sunila Pradeep, Morgan L Taylor, Hyun-Jin Choi, Jean M Hansen, Heather J Dalton, et al. 2016. “FAK Regulates Platelet Extravasation and Tumor Growth after Antiangiogenic Therapy Withdrawal.” The Journal of Clinical Investigation 126 (5). American Society for Clinical Investigation: 1885–96. doi:10.1172/JCI85086.

Hajra, Karen M, David Y-S Chen, and Eric R Fearon. 2002. “The SLUG Zinc-Finger Protein Represses E-Cadherin in Breast Cancer.” Cancer Research 62 (6): 1613–18. http://www.ncbi.nlm.nih.gov/pubmed/11912130.

Hallaq, H., Emese Pinter, Josephine Enciso, James McGrath, Caroline Zeiss, Martina Brueckner, Joseph Madri, et al. 2004. “A Null Mutation of *HHEX* Results in Abnormal Cardiac Development, Defective Vasculogenesis and Elevated Vegfa Levels.” Development 131 (20): 5197–5209. doi:10.1242/dev.01393.

Hanahan, Douglas, and Judah Folkman. 1996. “Patterns and Emerging Mechanisms of the Angiogenic Switch during Tumorigenesis.” Cell 86 (3). Cell Press: 353–64. doi:10.1016/S0092-8674(00)80108-7.

Hanahan, Douglas, and Robert A. Weinberg. 2011. “Hallmarks of Cancer: The Next Generation.” Cell 144 (5): 646–74. doi:10.1016/j.cell.2011.02.013.

Hartwell, K. A., B. Muir, F. Reinhardt, A. E. Carpenter, D. C. Sgroi, and R. A. Weinberg. 2006. “The Spemann Organizer Gene, Goosecoid, Promotes Tumor Metastasis.” Proceedings of the National Academy of Sciences 103 (50): 18969–74. doi:10.1073/pnas.0608636103.

Hayward SW, Wang Y, Cao M, Hom YK, Zhang B, Grossfeld GD, Sudilovsky D, Cunha GR. Malignant transformation in a nontumorigenic human prostatic epithelial cell line. Cancer Res. 2001 Nov 15;61(22):8135-42.

He, Guangan, Zahid H Siddik, Zaifeng Huang, Ruoning Wang, John Koomen, Ryuji Kobayashi, Abdul R Khokhar, and Jian Kuang. 2005. “Induction of p21 by p53 Following DNA Damage Inhibits Both Cdk4 and Cdk2 Activities.” Oncogene 24 (18): 2929–43. doi:10.1038/sj.onc.1208474.

Heldin, Carl-Henrik, Michael Vanlandewijck, and Aristidis Moustakas. 2012. “Regulation of EMT by TGFβ in Cancer.” FEBS Letters 586 (14): 1959–70. doi:10.1016/j.febslet.2012.02.037.

Henderson, Brian E., Norman H. Lee, Victoria Seewaldt, and Hongbing Shen. 2012. “The Influence of Race and Ethnicity on the Biology of Cancer.” Nature Reviews Cancer 12 (9): 648–53. doi:10.1038/nrc3341.

Herman, J G, A Merlo, L Mao, R G Lapidus, J P Issa, N E Davidson, D Sidransky, and S B Baylin. 1995. “Inactivation of the CDKN2/p16/MTS1 Gene Is Frequently Associated with Aberrant DNA Methylation in All Common Human Cancers.” Cancer Research 55 (20): 4525–30. http://www.ncbi.nlm.nih.gov/pubmed/7553621.

Hervé, Marie-Astrid, Hélène Buteau-Lozano, Roger Vassy, Ivan Bieche, Guillaume Velasco, Marika Pla, Gérard Perret, Samia Mourah, and Martine Perrot-Applanat. 2008. “Overexpression of Vascular Endothelial Growth Factor 189 in Breast Cancer Cells Leads to Delayed Tumor Uptake with Dilated Intratumoral Vessels.” The American Journal of Pathology 172 (1). American Society for Investigative Pathology: 167–78. doi:10.2353/ajpath.2008.070181.

Hirakawa, Hiroshi, Kenichiro Shibata, and Toshiyuki Nakayama. 2009. “Localization of Cortactin Is Associated with Colorectal Cancer Development.” International Journal of Oncology 35 (6): 1271–76. http://www.ncbi.nlm.nih.gov/pubmed/19885549.

Hirata, Hiroaki, Hitoshi Tatsumi, and Masahiro Sokabe. 2007. “Dynamics of Actin Filaments during Tension-Dependent Formation of Actin Bundles.” Biochimica et Biophysica Acta (BBA) - General Subjects 1770 (8): 1115–27. doi:10.1016/j.bbagen.2007.03.010.

Hobson, B, and J Denekamp. 1984. “Endothelial Proliferation in Tumours and Normal Tissues: Continuous Labelling Studies.” Br. J. Cancer. Vol. 49. https://www.ncbi.nlm.nih.gov/pmc/articles/PMC1976759/pdf/brjcancer00114-0002.pdf.

Hoffman, R. M., T. Koyama, K.-H. Fan, P. C. Albertsen, M. J. Barry, M. Goodman, A. S. Hamilton, et al. 2013. “Mortality After Radical Prostatectomy or External Beam Radiotherapy for Localized Prostate Cancer.” JNCI Journal of the National Cancer Institute 105 (10): 711–18. doi:10.1093/jnci/djt059.

Hoover, K B, S Y Liao, and P J Bryant. 1998. “Loss of the Tight Junction MAGUK ZO-1 in Breast Cancer: Relationship to Glandular Differentiation and Loss of Heterozygosity.” The American Journal of Pathology 153 (6). American Society for Investigative Pathology: 1767–73. doi:10.1016/S0002-9440(10)65691-X.

Horn S, Figl A, Rachakonda PS, Fischer C, Sucker A, Gast A, Kadel S, Moll I, Nagore E, Hemminki K, Schadendorf D, Kumar R. TERT promoter mutations in

familial and sporadic melanoma. Science. 2013 Feb 22;339(6122):959-61. doi: 10.1126/science.1230062

Hromas, R., J. Radich, and S. Collins. 1993. “PCR Cloning of an Orphan Homeobox Gene (PRH) Preferentially Expressed in Myeloid and Liver Cells.” Biochemical and Biophysical Research Communications 195 (2): 976–83. doi:10.1006/bbrc.1993.2140.

Hu S, Yu W, Lv TJ, Chang CS, Li X, Jin J. Evidence of TGF-β1 mediated epithelial-mesenchymal transition in immortalized benign prostatic hyperplasia cells. Mol Membr Biol. 2014 Mar-May;31(2-3):103-10. doi: 10.3109/09687688.2014.894211.

Hu, Jie, Jason W Locasale, Jason H Bielas, Jacintha O’Sullivan, Kieran Sheahan, Lewis C Cantley, Matthew G Vander Heiden, and Dennis Vitkup. 2013. “Heterogeneity of Tumor-Induced Gene Expression Changes in the Human Metabolic Network.” Nature Biotechnology 31 (6). NIH Public Access: 522–29. doi:10.1038/nbt.2530.

Huang FW, Hodis E, Xu MJ, Kryukov GV, Chin L, Garraway LA. Highly recurrent TERT promoter mutations in human melanoma. Science. 2013 Feb 22;339(6122):957-9. doi: 10.1126/science.1229259.

Huang, Paul H, Alexander M Xu, and Forest M White. 2009. “Oncogenic EGFR Signaling Networks in Glioma.” Science Signaling 2 (87). American Association for the Advancement of Science: re6. doi:10.1126/scisignal.287re6.

Ikushima, Hiroaki, and Kohei Miyazono. 2010. “TGFβ Signalling: A Complex Web in Cancer Progression.” Nature Publishing Group 10. doi:10.1038/nrc2853.

Im, Jae Hong, Weili Fu, Hui Wang, Sujata K. Bhatia, Daniel A. Hammer, M. Anna Kowalska, and Ruth J. Muschel. 2004. “Coagulation Facilitates Tumor Cell Spreading in the Pulmonary Vasculature during Early Metastatic Colony Formation.” Cancer Research 64 (23): 8613–19. doi:10.1158/0008-5472.CAN-04-2078.

Imhof, Beat A., H. Peter Vollmers, Simon L. Goodman, and Walter Birchmeier. 1983. “Cell-Cell Interaction and Polarity of Epithelial Cells: Specific Perturbation Using a Monoclonal Antibody.” Cell 35 (3 PART 2): 667–75. doi:10.1016/0092-8674(83)90099-5.

INCA. 2018. “INCA - CÂNCER - Tipo - Próstata.” http://www2.inca.gov.br/wps/wcm/connect/tiposdecancer/site/home/prostata.

Jasuja R, Costello JC, Singh R, Gupta V, Spina CS, Toraldo G, Jang H, Li H, Serra C, Guo W, Chauhan P, Narula NS, Guarneri T, Ergun A, Travison TG, Collins JJ, Bhasin S. Combined administration of testosterone plus an ornithine decarboxylase inhibitor as a selective prostate-sparing anabolic therapy. Aging Cell. 2014 Apr;13(2):303-10. doi: 10.1111/acel.12174.

Jenne, C. N., R. Urrutia, and P. Kubes. 2013. “Platelets: Bridging Hemostasis, Inflammation, and Immunity.” International Journal of Laboratory Hematology 35 (3). Wiley/Blackwell (10.1111): 254–61. doi:10.1111/ijlh.12084.

Jerrold R. Turner. 2009. Intestinal mucosal barrier function in health and disease. Nat Rev Immunol. 2009 Nov;9(11):799-809. doi: 10.1038/nri2653.

Jiang, Bing-Hua, and Ling-Zhi Liu. 2009. “Chapter 2 PI3K/PTEN Signaling in Angiogenesis and Tumorigenesis.” In Advances in Cancer Research, 102:19–65. doi:10.1016/S0065-230X(09)02002-8.

Johns, L E, and R S Houlston. 2003. “A Systematic Review and Meta-Analysis of Familial Prostate Cancer Risk.” BJU International 91 (9): 789–94. http://www.ncbi.nlm.nih.gov/pubmed/12780833.

Jolly, Mohit Kumar, Marcelo Boareto, Bin Huang, Dongya Jia, Mingyang Lu, Eshel Ben-Jacob, José N Onuchic, and Herbert Levine. 2015. “Implications of the Hybrid Epithelial/Mesenchymal Phenotype in Metastasis.” Frontiers in Oncology 5: 155. doi:10.3389/fonc.2015.00155.

Jones, Chris I., Natasha E. Barrett, Leonardo A. Moraes, Jonathan M. Gibbins, and Denise E. Jackson. 2012. “Endogenous Inhibitory Mechanisms and the Regulation of Platelet Function.” In , 341–66. Springer, New York, NY. doi:10.1007/978-1-61779-307-3_23.

Jones, Elisabeth, Hong Pu, and Natasha Kyprianou. 2009. “Targeting TGF-? In Prostate Cancer: Therapeutic Possibilities during Tumor Progression.” Expert Opinion on Therapeutic Targets 13 (2). Taylor & Francis: 227–34. doi:10.1517/14728220802705696.

Jones, Elisabeth, Hong Pu, and Natasha Kyprianou. 2009. “Targeting TGF-? In Prostate Cancer: Therapeutic Possibilities during Tumor Progression.” Expert Opinion on Therapeutic Targets 13 (2). Taylor & Francis: 227–34. doi:10.1517/14728220802705696.

Kaighn ME, Narayan KS, Ohnuki Y, Lechner JF, Jones LW. Establishment and characterization of a human prostatic carcinoma cell line (PC-3). Invest Urol. 1979 Jul;17(1):16-23.

Kalluri, Raghu, and Eric G. Neilson. 2003. “Epithelial-Mesenchymal Transition and Its Implications for Fibrosis.” Journal of Clinical Investigation 112 (12): 1776–84. doi:10.1172/JCI20530.

Kalluri, Raghu, and Michael Zeisberg. 2006. “Fibroblasts in Cancer.” Nature Reviews Cancer 6 (5). Nature Publishing Group: 392–401. doi:10.1038/nrc1877.

Kalluri, Raghu, and Robert A. Weinberg. 2009. “The Basics of Epithelial-Mesenchymal Transition.” Journal of Clinical Investigation 119 (6): 1420–28. doi:10.1172/JCI39104.

Karlseder, J, D Broccoli, Y Dai, S Hardy, and T de Lange. 1999. “p53- and ATM-Dependent Apoptosis Induced by Telomeres Lacking TRF2.” Science (New York, N.Y.) 283 (5406): 1321–25. http://www.ncbi.nlm.nih.gov/pubmed/10037601.

Karnoub, Antoine E, and Robert A Weinberg. 2007. “Chemokine Networks and Breast Cancer Metastasis.” Breast Disease 26 (1): 75–85. doi:10.3233/BD-2007-26107.

Kaser, A, G Brandacher, W Steurer, S Kaser, F A Offner, H Zoller, I Theurl, et al. 2001. “Interleukin-6 Stimulates Thrombopoiesis through Thrombopoietin: Role in Inflammatory Thrombocytosis.” Blood 98 (9). American Society of Hematology: 2720–25. doi:10.1182/BLOOD.V98.9.2720.

Katsuno Y, Lamouille S, Derynck R. TGF-β signaling and epithelial-mesenchymal transition in cancer progression. Curr Opin Oncol. 2013 Jan;25(1):76-84. doi: 10.1097/CCO.0b013e32835b6371.

Kaunas, R., P. Nguyen, S. Usami, and S. Chien. 2005. “From The Cover: Cooperative Effects of Rho and Mechanical Stretch on Stress Fiber Organization.” Proceedings of the National Academy of Sciences 102 (44): 15895–900. doi:10.1073/pnas.0506041102.

Kennedy, Kelly M, and Mark W Dewhirst. 2010. “Tumor Metabolism of Lactate: The Influence and Therapeutic Potential for MCT and CD147 Regulation.” Future Oncology 6 (1): 127–48. doi:10.2217/fon.09.145.

Kershaw, R M, D Roberts, J Wragg, A M Shaaban, E Humphreys, J Halsall, L Price, R Bicknell, K Gaston, and P-S Jayaraman. 2017. “Proline-Rich Homeodomain Protein (PRH/*HHEX*) Is a Suppressor of Breast Tumour Growth.” Oncogenesis 6 (6). Nature Publishing Group: e346. doi:10.1038/oncsis.2017.42.

Kershaw, R M, Y H Siddiqui, D Roberts, P-S Jayaraman, and K Gaston. 2014. “PRH/*HHEX* Inhibits the Migration of Breast and Prostate Epithelial Cells through Direct Transcriptional Regulation of Endoglin.” Oncogene 33 (49). Nature Publishing Group: 5592–5600. doi:10.1038/onc.2013.496.

Kikkawa, E, M Hinata, V W Keng, Z Myint, A Sato, K Yamada, T Tanaka, and T Noguchi. 2001. “Sp Family Members Stimulate Transcription of the Hex Gene via Interactions with GC Boxes.” Journal of Biochemistry 130 (6): 885–91. http://www.ncbi.nlm.nih.gov/pubmed/11726291.

Kim, Seongrak, Sunyoung Ham, Kyungmi Yang, and Kunhong Kim. 2018. “Protein Kinase CK2 Activation Is Required for Transforming Growth Factor-β-Induced Epithelial-Mesenchymal Transition.” Molecular Oncology, September. doi:10.1002/1878-0261.12378.

Kingsley, David M. 1994. “The TGF-P Superfamily: New Members, New Receptors, and New Genetic Tests of Function in Different Organisms.” http://genesdev.cshlp.org/content/8/2/133.full.pdf.

Ko, H., S. Kim, C.-H. Jin, E. Lee, S. Ham, J. I. Yook, and K. Kim. 2012. “Protein Kinase Casein Kinase 2-Mediated Upregulation of N-Cadherin Confers Anoikis Resistance on Esophageal Carcinoma Cells.” Molecular Cancer Research 10 (8): 1032–38. doi:10.1158/1541-7786.MCR-12-0261.

Koch S, Tugues S, Li X, Gualandi L, Claesson-Welsh L. Signal transduction by vascular endothelial growth factor receptors. Biochem J. 2011 Jul 15;437(2):169-83. doi: 10.1042/BJ20110301.

Korc, M, B Chandrasekar, Y Yamanaka, H Friess, M Buchier, and H G Beger. 1992. “Overexpression of the Epidermal Growth Factor Receptor in Human Pancreatic Cancer Is Associated with Concomitant Increases in the Levels of Epidermal Growth Factor and Transforming Growth Factor Alpha.” Journal of Clinical Investigation 90 (4): 1352–60. doi:10.1172/JCI116001.

Krebs, Angela M., Julia Mitschke, María Lasierra Losada, Otto Schmalhofer, Melanie Boerries, Hauke Busch, Martin Boettcher, et al. 2017. “The EMT-Activator *ZEB1* Is a Key Factor for Cell Plasticity and Promotes Metastasis in Pancreatic Cancer.” Nature Cell Biology 19 (5): 518–29. doi:10.1038/ncb3513.

Krebs, Angela M., Julia Mitschke, María Lasierra Losada, Otto Schmalhofer, Melanie Boerries, Hauke Busch, Martin Boettcher, et al. 2017. “The EMT-Activator *ZEB1* Is a Key Factor for Cell Plasticity and Promotes Metastasis in Pancreatic Cancer.” Nature Cell Biology 19 (5): 518–29. doi:10.1038/ncb3513.

Kypta, Robert M., and Jonathan Waxman. 2012. “Wnt/β 2-Catenin Signalling in Prostate Cancer.” Nature Reviews Urology 9 (8). Nature Publishing Group: 418–28. doi:10.1038/nrurol.2012.116.

Labelle, Myriam, Shahinoor Begum, and Richard O Hynes. 2011. “Direct Signaling between Platelets and Cancer Cells Induces an Epithelial-Mesenchymal-like Transition and Promotes Metastasis.” Cancer Cell 20 (5). Howard Hughes Medical Institute: 576–90. doi:10.1016/j.ccr.2011.09.009.

Lakshman, Minalini, Xiaoke Huang, Vijayalakshmi Ananthanarayanan, Borko Jovanovic, Yueqin Liu, Clarissa S Craft, Diana Romero, Calvin P H Vary, and Raymond C Bergan. 2011. “Endoglin Suppresses Human Prostate Cancer Metastasis.” Clinical & Experimental Metastasis 28 (1). NIH Public Access: 39–53. doi:10.1007/s10585-010-9356-6.

Lamb, Alastair D., Charlie E. Massie, and David E. Neal. 2014. “The Transcriptional Programme of the Androgen Receptor (AR) in Prostate Cancer.” BJU International 113 (3): 358–66. doi:10.1111/bju.12415.

Lamouille S, Xu J, Derynck R. Molecular mechanisms of epithelial-mesenchymal transition. Nat Rev Mol Cell Biol. 2014 Mar;15(3):178-96. doi: 10.1038/nrm3758.

Landström, M, N E Heldin, S Bu, A Hermansson, S Itoh, P ten Dijke, and C H Heldin. 2000. “Smad7 Mediates Apoptosis Induced by Transforming Growth Factor Beta in

Prostatic Carcinoma Cells.” Current Biology : CB 10 (9): 535–38. http://www.ncbi.nlm.nih.gov/pubmed/10801443.

Lang, S H, R M Sharrard, M Stark, J M Villette, and N J Maitland. 2001. “Prostate Epithelial Cell Lines Form Spheroids with Evidence of Glandular Differentiation in Three-Dimensional Matrigel Cultures.” British Journal of Cancer 85 (4): 590–99. doi:10.1054/bjoc.2001.1967.

Lee JY, Wasinger VC, Yau YY, Chuang E, Yajnik V, Leong RW. Molecular Pathophysiology of Epithelial Barrier Dysfunction in Inflammatory Bowel Diseases. Proteomes. 2018 Mar 31;6(2). pii: E17. doi: 10.3390/proteomes6020017.

Levy, L, and C Hill. 2006. “Alterations in Components of the TGF-β Superfamily Signaling Pathways in Human Cancer.” Cytokine & Growth Factor Reviews 17 (1–2): 41–58. doi:10.1016/j.cytogfr.2005.09.009.

Li, G, K Satyamoorthy, and M Herlyn. 2001. “N-Cadherin-Mediated Intercellular Interactions Promote Survival and Migration of Melanoma Cells.” Cancer Research 61 (9): 3819–25. http://www.ncbi.nlm.nih.gov/pubmed/11325858.

Li, Ping, Ru Yang, and Wei-Qiang Gao. 2014. “Contributions of Epithelial-Mesenchymal Transition and Cancer Stem Cells to the Development of Castration Resistance of Prostate Cancer.” Molecular Cancer 13 (March). BioMed Central: 55. doi:10.1186/1476-4598-13-55.

Li, Yu-Zhen, Dao-Yuan Lu, Wei-Qi Tan, Jian-Xun Wang, and Pei-Feng Li. 2008. “p53 Initiates Apoptosis by Transcriptionally Targeting the Antiapoptotic Protein ARC.” Molecular and Cellular Biology 28 (2). American Society for Microbiology (ASM): 564–74. doi:10.1128/MCB.00738-07.

Lichtenstein, P, N V Holm, P K Verkasalo, A Iliadou, J Kaprio, M Koskenvuo, E Pukkala, A Skytthe, and K Hemminki. 2000. “Environmental and Heritable Factors in the Causation of Cancer--Analyses of Cohorts of Twins from Sweden, Denmark, and Finland.” The New England Journal of Medicine 343 (2): 78–85. doi:10.1056/NEJM200007133430201.

Liu, L L, N Xie, S Sun, S Plymate, E Mostaghel, and X Dong. 2014. “Mechanisms of the Androgen Receptor Splicing in Prostate Cancer Cells.” Oncogene 33 (24). NIH Public Access: 3140–50. doi:10.1038/onc.2013.284.

Liu, Ye, Maria Festing, John C. Thompson, Mark Hester, Scott Rankin, Heithem M. El-Hodiri, Aaron M. Zorn, and Michael Weinstein. 2004. “Smad2 and Smad3 Coordinately Regulate Craniofacial and Endodermal Development.” Developmental Biology 270 (2): 411–26. doi:10.1016/j.ydbio.2004.03.017.

Lopez A, Harada K, Vasilakopoulou M, Shanbhag N, Ajani JA. Targeting Angiogenesis in Colorectal Carcinoma. Drugs. 2019 Jan;79(1):63-74. doi: 10.1007/s40265-018-1037-9.

Lotz-Jenne C, Lüthi U, Ackerknecht S, Lehembre F, Fink T, Stritt M, Wirth M, Pavan S, Bill R, Regenass U, Christofori G, Meyer-Schaller N. A high-content EMT screen identifies multiple receptor tyrosine kinase inhibitors with activity on TGFβ receptor. Oncotarget. 2016 May 3;7(18):25983-6002. doi: 10.18632/oncotarget.8418.

Lu-Yao, Grace L., Peter C Albertsen, Dirk F Moore, Weichung Shih, Yong Lin, Robert S DiPaola, Michael J Barry, et al. 2009. “Outcomes of Localized Prostate Cancer Following Conservative Management.” JAMA 302 (11): 1202. doi:10.1001/jama.2009.1348.

Mani SA, Guo W, Liao MJ, Eaton EN, Ayyanan A, Zhou AY, Brooks M, Reinhard F, Zhang CC, Shipitsin M, Campbell LL, Polyak K, Brisken C, Yang J, Weinberg RA. The epithelial-mesenchymal transition generates cells with properties of stem cells. Cell. 2008 May 16;133(4):704-15. doi: 10.1016/j.cell.2008.03.027.

Mani, Sendurai A., Wenjun Guo, Mai-Jing Liao, Elinor Ng. Eaton, Ayyakkannu Ayyanan, Alicia Y. Zhou, Mary Brooks, et al. 2008. “The Epithelial-Mesenchymal Transition Generates Cells with Properties of Stem Cells.” Cell 133 (4): 704–15. doi:10.1016/j.cell.2008.03.027.

Marcus, Aaron J, M. Johan Broekman, Joan H. F Drosopoulos, Kim E Olson, Naziba Islam, David J Pinsky, and Roberto Levi. 2005. “Role of CD39 (NTPDase-1) in Thromboregulation, Cerebroprotection, and Cardioprotection.” Seminars in Thrombosis and Hemostasis 31 (02). Copyright © 2005 by Thieme Medical Publishers, Inc., 333 Seventh Avenue, New York, NY 10001, USA. Tel: +1(212) 584-4662.: 234–46. doi:10.1055/s-2005-869528.

Marrs, J A, and W J Nelson. 1996. “Cadherin Cell Adhesion Molecules in Differentiation and Embryogenesis.” International Review of Cytology 165: 159–205. http://www.ncbi.nlm.nih.gov/pubmed/8900959.

Martinez Barbera, J P, M Clements, P Thomas, T Rodriguez, D Meloy, D Kioussis, and R S Beddington. 2000. “The Homeobox Gene Hex Is Required in Definitive Endodermal Tissues for Normal Forebrain, Liver and Thyroid Formation.” Development (Cambridge, England) 127 (11): 2433–45. http://www.ncbi.nlm.nih.gov/pubmed/10804184.

Martinez-Lostao, L., A. Anel, and J. Pardo. 2015. “How Do Cytotoxic Lymphocytes Kill Cancer Cells?” Clinical Cancer Research 21 (22): 5047–56. doi:10.1158/1078-0432.CCR-15-0685.

Massagué, J, and K Polyak. 1995. “Mammalian Antiproliferative Signals and Their Targets.” Current Opinion in Genetics & Development 5 (1): 91–96. http://www.ncbi.nlm.nih.gov/pubmed/7749332.

Massagué, Joan. 2008. “TGFbeta in Cancer.” Cell 134 (2): 215–30. doi:10.1016/j.cell.2008.07.001.

Massagué, Joan. 2012. “TGFβ Signalling in Context.” Nature Reviews Molecular Cell Biology 13 (10). Nature Publishing Group: 616–30. doi:10.1038/nrm3434.

Matthews, K S. 1992. “DNA Looping.” Microbiological Reviews 56 (1). American Society for Microbiology (ASM): 123–36. http://www.ncbi.nlm.nih.gov/pubmed/1579106.

McNeal, J E. 1988. “Normal Histology of the Prostate.” Am J Surg Pathol. doi:10.1097/00000478-198911000-00008.

Medici, Damian, Elizabeth D Hay, and Bjorn R Olsen. 2008. “Snail and Slug Promote Epithelial-Mesenchymal Transition through Beta-Catenin-T-Cell Factor-4-Dependent Expression of Transforming Growth Factor-beta3.” Molecular Biology of the Cell 19 (11): 4875–87. doi:10.1091/mbc.E08-05-0506.

Mendez, Melissa G, Shin-Ichiro Kojima, and Robert D Goldman. 2010. “Vimentin Induces Changes in Cell Shape, Motility, and Adhesion during the Epithelial to Mesenchymal Transition.” FASEB Journal : Official Publication of the Federation of American Societies for Experimental Biology 24 (6). The Federation of American Societies for Experimental Biology: 1838–51. doi:10.1096/fj.09-151639.

Milyavsky, M, A Mimran, S Senderovich, I Zurer, N Erez, I Shats, N Goldfinger, I Cohen, and V Rotter. 2001. “Activation of p53 Protein by Telomeric (TTAGGG)n Repeats.” Nucleic Acids Research 29 (24). Oxford University Press: 5207–15. http://www.ncbi.nlm.nih.gov/pubmed/11812854.

Mitchell L. Schubert. Chapter 47 - Regulation of Gastric Acid Secretion in Physiology of the Gastrointestinal Tract (Fifth Edition), 2012 Vol 2:1281-1309. https://doi.org/10.1016/B978-0-12-382026-6.00047-6.

Montanari M, Rossetti S, Cavaliere C, D'Aniello C, Malzone MG, Vanacore D, Di Franco R, La Mantia E, Iovane G, Piscitelli R, Muscariello R, Berretta M, Perdonà S, Muto P, Botti G, Bianchi AAM, Veneziani BM, Facchini G. Epithelial-mesenchymal transition in prostate cancer: an overview. Oncotarget. 2017 May 23;8(21):35376-35389. doi: 10.18632/oncotarget.15686.

Moreno-Bueno, G, F Portillo, and A Cano. 2008. “Transcriptional Regulation of Cell Polarity in EMT and Cancer.” Oncogene 27 (55). Nature Publishing Group: 6958–69. doi:10.1038/onc.2008.346.

Mukherjee, P., S. L. Winter, and M. G. Alexandrow. 2010. “Cell Cycle Arrest by Transforming Growth Factor 1 near G1/S Is Mediated by Acute Abrogation of Prereplication Complex Activation Involving an Rb-MCM Interaction.” Molecular and Cellular Biology 30 (3): 845–56. doi:10.1128/MCB.01152-09.

Munger, John S., John G. Harpel, Pierre-Emmanuel Gleizes, Roberta Mazzieri, Irene Nunes, and Daniel B. Rifkin. 1997. “Latent Transforming Growth Factor-β: Structural Features and Mechanisms of Activation.” Kidney International 51 (5). Elsevier: 1376–82. doi:10.1038/ki.1997.188.

Murakami, Masaaki, Akemi Sakamoto, Jeremy Bender, John Kappler, Philippa Marrack, Harald von Boehmer, and Khashayarsha Khazaie. 2002. “CD25+CD4+ T Cells Contribute to the Control of Memory CD8+ T Cells.” Proceedings of the National Academy of Sciences of the United States of America 99 (13). National Academy of Sciences: 8832–37. doi:10.1073/pnas.132254399.

Naeim, Faramarz, P. Nagesh Rao, Sophie X. Song, Wayne W. Grody, Faramarz Naeim, P. Nagesh Rao, Sophie X. Song, and Wayne W. Grody. 2013. “Structure and Function of Hematopoietic Tissues.” Atlas of Hematopathology, January. Academic Press, 1–24. doi:10.1016/B978-0-12-385183-3.00001-2.

Nag A, Savova V, Fung HL, Miron A, Yuan GC, Zhang K, Gimelbrant AA. Chromatin signature of widespread monoallelic expression. Elife. 2013 Dec 31;2:e01256. doi: 10.7554/eLife.01256.

Nakagawa, Tomowaki, Mayumi Abe, Tohru Yamazaki, Hiroki Miyashita, Hitoshi Niwa, Shoichi Kokubun, and Yasufumi Sato. 2003. “HEX Acts as a Negative Regulator of Angiogenesis by Modulating the Expression of Angiogenesis-Related Gene in Endothelial Cells in Vitro.” Arteriosclerosis, Thrombosis, and Vascular Biology 23 (2): 231–37. http://www.ncbi.nlm.nih.gov/pubmed/12588764.

Nguyen, Daniel P., Jinyi Li, and Ashutosh K. Tewari. 2014. “Inflammation and Prostate Cancer: The Role of Interleukin 6 (IL-6).” BJU International 113 (6): 986–92. doi:10.1111/bju.12452.

Ni, Songshi, Liqin Xu, Jianfei Huang, Jian Feng, Huijun Zhu, Gui Wang, and Xudong Wang. 2013. “Increased ZO-1 Expression Predicts Valuable Prognosis in Non-Small Cell Lung Cancer.” International Journal of Clinical and Experimental Pathology 6 (12). e-Century Publishing Corporation: 2887–95. http://www.ncbi.nlm.nih.gov/pubmed/24294375.

Nieder, Carsten, Ellinor Haukland, Adam Pawinski, and Astrid Dalhaug. 2010. “Anaemia and Thrombocytopenia in Patients with Prostate Cancer and Bone Metastases.” BMC Cancer 10 (June). BioMed Central: 284. doi:10.1186/1471-2407-10-284.

Niehrs, Christof, and Nicolas Pollet. 1999. “Synexpression Groups in Eukaryotes.” Nature 402 (6761): 483–87. doi:10.1038/990025.

Niessen, Kyle, YangXin Fu, Linda Chang, Pamela A Hoodless, Deborah McFadden, and Aly Karsan. 2008. “Slug Is a Direct Notch Target Required for Initiation of Cardiac Cushion Cellularization.” The Journal of Cell Biology 182 (2). The Rockefeller University Press: 315–25. doi:10.1083/jcb.200710067.

Nieto MA, Huang RY, Jackson RA, Thiery JP. EMT: 2016. Cell. 2016 Jun 30;166(1):21-45. doi: 10.1016/j.cell.2016.06.028.

Nieto, M A. 2001. “The Early Steps of Neural Crest Development.” Mechanisms of Development 105 (1-2): 27–35. http://www.ncbi.nlm.nih.gov/pubmed/11429279.

Nieto, M. Angela, Ruby Yun-Ju Huang, Rebecca A. Jackson, and Jean Paul Thiery. 2016. “EMT: 2016.” Cell 166 (1): 21–45. doi:10.1016/j.cell.2016.06.028.

Norton, Nadine, Pooja P Advani, Daniel J Serie, Xochiquetzal J Geiger, Brian M Necela, Bianca C Axenfeld, Jennifer M Kachergus, et al. 2016. “Assessment of Tumor Heterogeneity, as Evidenced by Gene Expression Profiles, Pathway Activation, and Gene Copy Number, in Patients with Multifocal Invasive Lobular Breast Tumors.” PloS One 11 (4). Public Library of Science: e0153411. doi:10.1371/journal.pone.0153411.

Noy, P., H. Williams, A. Sawasdichai, K. Gaston, and P. S. Jayaraman. 2010. “PRH/*HHEX* Controls Cell Survival through Coordinate Transcriptional Regulation of Vascular Endothelial Growth Factor Signaling.” Molecular and Cellular Biology 30 (9): 2120–34. doi:10.1128/MCB.01511-09.

Noy, Peter, Anyaporn Sawasdichai, Padma-Sheela Jayaraman, and Kevin Gaston. 2012. “Protein Kinase CK2 Inactivates PRH/*HHEX* Using Multiple Mechanisms to de-Repress VEGF-Signalling Genes and Promote Cell Survival.” Nucleic Acids Research 40 (18): 9008–20. doi:10.1093/nar/gks687.

O’Byrne, K J, and A G Dalgleish. 2001. “Chronic Immune Activation and Inflammation as the Cause of Malignancy.” British Journal of Cancer 85 (4): 473–83. doi:10.1054/bjoc.2001.1943.

Oberhammer, F A, M Pavelka, S Sharma, R Tiefenbacher, A F Purchio, W Bursch, and R Schulte-Hermann. 1992. “Induction of Apoptosis in Cultured Hepatocytes and in Regressing Liver by Transforming Growth Factor Beta 1.” Proceedings of the National Academy of Sciences of the United States of America 89 (12): 5408–12. http://www.ncbi.nlm.nih.gov/pubmed/1608949.

Odero-Marah V, Hawsawi O, Henderson V, Sweeney J. Epithelial-Mesenchymal Transition (EMT) and Prostate Cancer. Adv Exp Med Biol. 2018;1095:101-110. doi: 10.1007/978-3-319-95693-0_6.

Odero-Marah, Valerie A, Ruoxiang Wang, Gina Chu, Majd Zayzafoon, Jianchun Xu, Chunmeng Shi, Fray F Marshall, Haiyen E Zhau, and Leland WK Chung. 2008. “Receptor Activator of NF-κB Ligand (RANKL) Expression Is Associated with Epithelial to Mesenchymal Transition in Human Prostate Cancer Cells.” Cell Research 18 (8): 858–70. doi:10.1038/cr.2008.84.

Olive, Kenneth P, Michael A Jacobetz, Christian J Davidson, Aarthi Gopinathan, Dominick McIntyre, Davina Honess, Basetti Madhu, et al. 2009. “Inhibition of Hedgehog Signaling Enhances Delivery of Chemotherapy in a Mouse Model of Pancreatic Cancer.” Science (New York, N.Y.) 324 (5933). NIH Public Access: 1457–61. doi:10.1126/science.1171362.

Olmeda, David, Gema Moreno-Bueno, Juana M Flores, Angels Fabra, Francisco Portillo, and Amparo Cano. 2007. “SNAI1 Is Required for Tumor Growth and Lymph

Node Metastasis of Human Breast Carcinoma MDA-MB-231 Cells.” Cancer Research 67 (24). American Association for Cancer Research: 11721–31. doi:10.1158/0008-5472.CAN-07-2318.

Onder TT, Gupta PB, Mani SA, Yang J, Lander ES, Weinberg RA. Loss of E-cadherin promotes metastasis via multiple downstream transcriptional pathways. Cancer Res. 2008 May 15;68(10):3645-54. doi: 10.1158/0008-5472.CAN-07-2938.

Oyama, Yuko, Keiko Kawai-Kowase, Kenichi Sekiguchi, Mahito Sato, Hiroko Sato, Miki Yamazaki, Yoshio Ohyama, et al. 2004. “Homeobox Protein Hex Facilitates Serum Responsive Factor–Mediated Activation of the SM22α Gene Transcription in Embryonic Fibroblasts.” Arteriosclerosis, Thrombosis, and Vascular Biology 24 (9): 1602–7. doi:10.1161/01.ATV.0000138404.17519.45.

Packer JR, Maitland NJ. The molecular and cellular origin of human prostate cancer. Biochim Biophys Acta. 2016 Jun;1863(6 Pt A):1238-60. doi: 10.1016/j.bbamcr.2016.02.016.

Parise, Leslie V. 2016. “Introduction to a Review Series: Megakaryocytes to Platelets in Health and Disease.” Blood 127 (10). American Society of Hematology: 1215. doi:10.1182/blood-2015-11-664029.

Pecqueux C, Arslan A, Heller M, Falkenstein M, Kaczorowski A, Tolstov Y, Sültmann H, Grüllich C, Herpel E, Duensing A, Kristiansen G, Hohenfellner M, Navone NM, Duensing S. FGF-2 is a driving force for chromosomal instability and a stromal factor associated with adverse clinico-pathological features in prostate cancer. Urol Oncol. 2018 Aug;36(8):365.e15-365.e26. doi: 10.1016/j.urolonc.2018.05.020.

Pellacani D, Kestoras D, Droop AP, Frame FM, Berry PA, Lawrence MG, Stower MJ, Simms MS, Mann VM, Collins AT, Risbridger GP, Maitland NJ. DNA hypermethylation in prostate cancer is a consequence of aberrant epithelial differentiation and hyperproliferation. Cell Death Differ. 2014 May;21(5):761-73. doi: 10.1038/cdd.2013.202.

Pellizzari, L., A. D’Elia, A. Rustighi, G. Manfioletti, G. Tell, and G. Damante. 2000. “Expression and Function of the Homeodomain-Containing Protein Hex in Thyroid Cells.” Nucleic Acids Research 28 (13): 2503–11. doi:10.1093/nar/28.13.2503.

Perez-Gomez, E., M. Villa-Morales, J. Santos, J. Fernandez-Piqueras, C. Gamallo, J. Dotor, C. Bernabeu, and M. Quintanilla. 2007. “A Role for Endoglin as a Suppressor of Malignancy during Mouse Skin Carcinogenesis.” Cancer Research 67 (21): 10268–77. doi:10.1158/0008-5472.CAN-07-1348.

Pezaro, C., H. H. Woo, and I. D. Davis. 2014. “Prostate Cancer: Measuring PSA.” Internal Medicine Journal 44 (5). Wiley/Blackwell (10.1111): 433–40. doi:10.1111/imj.12407.

Picard, Jonathan C., Ali-Reza Golshayan, David T. Marshall, Krisha J. Opfermann, and Thomas E. Keane. 2012. “The Multi-Disciplinary Management of High-Risk

Prostate Cancer.” Urologic Oncology: Seminars and Original Investigations 30 (1): 3–15. doi:10.1016/j.urolonc.2009.09.002.

Puisieux, Alain, Thomas Brabletz, and Julie Caramel. 2014. “Oncogenic Roles of EMT-Inducing Transcription Factors.” Nature Cell Biology 16 (6). Nature Publishing Group: 488–94. doi:10.1038/ncb2976.

Puppin, Cinzia, Angela V D’Elia, Lucia Pellizzari, Diego Russo, Franco Arturi, Ivan Presta, Sebastiano Filetti, Clifford W Bogue, Lee A Denson, and Giuseppe Damante. 2003. “Thyroid-Specific Transcription Factors Control Hex Promoter Activity.” Nucleic Acids Research 31 (7). Oxford University Press: 1845–52. http://www.ncbi.nlm.nih.gov/pubmed/12655000.

Puppin, Cinzia, Fabio Puglisi, Lucia Pellizzari, Guidalberto Manfioletti, Marta Pestrin, Maura Pandolfi, Andrea Piga, Carla Di Loreto, and Giuseppe Damante. 2006. “HEX Expression and Localization in Normal Mammary Gland and Breast Carcinoma.” BMC Cancer 6 (July). BioMed Central: 192. doi:10.1186/1471-2407-6-192.

Puppin, Cinzia, Ivan Presta, Angela V. D’Elia, Gianluca Tell, Franco Arturi, Diego Russo, Sebastiano Filetti, and Giuseppe Damante. 2004. “Functional Interaction among Thyroid-Specific Transcription Factors: Pax8 Regulates the Activity of Hex Promoter.” Molecular and Cellular Endocrinology 214 (1-2): 117–25. doi:10.1016/j.mce.2003.10.061.

Pursglove, Sharon E., and Joel P. Mackay. 2005. “CSL: A Notch above the Rest.” The International Journal of Biochemistry & Cell Biology 37 (12): 2472–77. doi:10.1016/j.biocel.2005.06.013.

Qian, Bin-Zhi, and Jeffrey W. Pollard. 2010. “Macrophage Diversity Enhances Tumor Progression and Metastasis.” Cell 141 (1): 39–51. doi:10.1016/j.cell.2010.03.014.

Qu, Xueping, Jie Yu, Govind Bhagat, Norihiko Furuya, Hanina Hibshoosh, Andrea Troxel, Jeffrey Rosen, et al. 2003. “Promotion of Tumorigenesis by Heterozygous Disruption of the Beclin 1 Autophagy Gene.” Journal of Clinical Investigation 112 (12): 1809–20. doi:10.1172/JCI20039.

Reymond, Nicolas, Bárbara Borda d’Água, and Anne J. Ridley. 2013. “Crossing the Endothelial Barrier during Metastasis.” Nature Reviews Cancer 13 (12). Nature Publishing Group: 858–70. doi:10.1038/nrc3628.

Reynisdóttir, I, K Polyak, A Iavarone, and J Massagué. 1995. “Kip/Cip and Ink4 Cdk Inhibitors Cooperate to Induce Cell Cycle Arrest in Response to TGF-Beta.” Genes & Development 9 (15): 1831–45. http://www.ncbi.nlm.nih.gov/pubmed/7649471.

Roberts, A B, M B Sporn, R K Assoian, J M Smith, N S Roche, L M Wakefield, U I Heine, L A Liotta, V Falanga, and J H Kehrl. 1986. “Transforming Growth Factor Type Beta: Rapid Induction of Fibrosis and Angiogenesis in Vivo and Stimulation of Collagen Formation in Vitro.” Proceedings of the National Academy of Sciences of

the United States of America 83 (12): 4167–71. http://www.ncbi.nlm.nih.gov/pubmed/2424019.

Robertson, Ian B, Masahito Horiguchi, Lior Zilberberg, Branka Dabovic, Krassimira Hadjiolova, and Daniel B Rifkin. 2015. “Latent TGF-β-Binding Proteins.” Matrix Biology : Journal of the International Society for Matrix Biology 47 (September). NIH Public Access: 44–53. doi:10.1016/j.matbio.2015.05.005.

Robson EJ, Khaled WT, Abell K, Watson CJ. Epithelial-to-mesenchymal transition confers resistance to apoptosis in three murine mammary epithelial cell lines. Differentiation. 2006 Jun;74(5):254-64.

Roerink, Sophie F., Nobuo Sasaki, Henry Lee-Six, Matthew D. Young, Ludmil B. Alexandrov, Sam Behjati, Thomas J. Mitchell, et al. 2018. “Intra-Tumour Diversification in Colorectal Cancer at the Single-Cell Level.” Nature 556 (7702). Nature Publishing Group: 457–62. doi:10.1038/s41586-018-0024-3.

Romijn JC. Polyamines and transglutaminase actions. Andrologia. 1990;22 Suppl 1:83-91.

Rotello, R J, R C Lieberman, A F Purchio, and L E Gerschenson. 1991. “Coordinated Regulation of Apoptosis and Cell Proliferation by Transforming Growth Factor Beta 1 in Cultured Uterine Epithelial Cells.” Proceedings of the National Academy of Sciences of the United States of America 88 (8): 3412–15. http://www.ncbi.nlm.nih.gov/pubmed/2014262.

Rusch, V, D Klimstra, E Venkatraman, P W Pisters, J Langenfeld, and E Dmitrovsky. 1997. “Overexpression of the Epidermal Growth Factor Receptor and Its Ligand Transforming Growth Factor Alpha Is Frequent in Resectable Non-Small Cell Lung Cancer but Does Not Predict Tumor Progression.” Clinical Cancer Research : An Official Journal of the American Association for Cancer Research 3 (4): 515–22. http://www.ncbi.nlm.nih.gov/pubmed/9815714.

Sahlgren, Cecilia, Maria V Gustafsson, Shaobo Jin, Lorenz Poellinger, and Urban Lendahl. 2008. “Notch Signaling Mediates Hypoxia-Induced Tumor Cell Migration and Invasion.” Proceedings of the National Academy of Sciences of the United States of America 105 (17). National Academy of Sciences: 6392–97. doi:10.1073/pnas.0802047105.

Saltzman, Alan, Robin Munro, George Searfoss, Carol Franks, Michael Jaye, and Yuri Ivashchenko. 1998. “Transforming Growth Factor-β-Mediated Apoptosis in the Ramos B-Lymphoma Cell Line Is Accompanied by Caspase Activation and Bcl-XLDownregulation.” Experimental Cell Research 242 (1): 244–54. doi:10.1006/excr.1998.4096.

Salvador, Ellaine, Malgorzata Burek, and Carola Y Förster. 2016. “Tight Junctions and the Tumor Microenvironment.” Current Pathobiology Reports 4. Springer: 135–45. doi:10.1007/s40139-016-0106-6.

Sánchez, Aránzazu, Roser Pagan, Alberto M. Álvarez, César Roncero, Senén Vilaró, Manuel Benito, and Isabel Fabregat. 1998. “Transforming Growth Factor-β (TGF-β) and EGF Promote Cord-like Structures That Indicate Terminal Differentiation of Fetal Hepatocytes in Primary Culture.” Experimental Cell Research 242 (1): 27–37. doi:10.1006/excr.1998.4088.

Santibañez, Juan F., Miguel Quintanilla, and Carmelo Bernabeu. 2011. “TGF-β/TGF-β Receptor System and Its Role in Physiological and Pathological Conditions.” Clinical Science 121 (6): 233–51. doi:10.1042/CS20110086.

Sarrazin, S., E. Adam, M. Lyon, F. Depontieu, V. Motte, C. Landolfi, H. Lortat-Jacob, D. Bechard, P. Lassalle, and M. Delehedde. 2006. “Endocan or Endothelial Cell Specific Molecule-1 (ESM-1): A Potential Novel Endothelial Cell Marker and a New Target for Cancer Therapy.” Biochimica et Biophysica Acta (BBA) - Reviews on Cancer 1765 (1): 25–37. doi:10.1016/j.bbcan.2005.08.004.

Sato, Ayuko, Vincent W Keng, Taichi Yamamoto, Shinya Kasamatsu, Tomoko Ban, Hironori Tanaka, Shin-ichi Satoh, Kazuya Yamada, and Tamio Noguchi. 2004. “Identification and Characterization of the Hematopoietic Cell-Specific Enhancer-like Element of the Mouse Hex Gene.” Journal of Biochemistry 135 (2): 259–68. http://www.ncbi.nlm.nih.gov/pubmed/15047729.

Saunders, John H, David Onion, Pamela Collier, Matthew S Dorrington, Richard H Argent, Philip A Clarke, Alex M Reece-Smith, Simon L Parsons, and Anna M Grabowska. 2017. “Individual Patient Oesophageal Cancer 3D Models for Tailored Treatment.” Oncotarget 8 (15). Impact Journals, LLC: 24224–36. doi:10.18632/oncotarget.12500.

Savage, Emilia Elizabeth, Denise Wootten, Arthur Christopoulos, Patrick Michael Sexton, and Sebastian George Barton Furness. 2013. “A Simple Method to Generate Stable Cell Lines for the Analysis of Transient Protein-Protein Interactions.” BioTechniques 54 (4): 217–21. doi:10.2144/000114013.

Saylor, Philip J, and Matthew R Smith. 2010. “Adverse Effects of Androgen Deprivation Therapy: Defining the Problem and Promoting Health among Men with Prostate Cancer.” Journal of the National Comprehensive Cancer Network : JNCCN 8 (2): 211–23. http://www.ncbi.nlm.nih.gov/pubmed/20141678.

Schindelin, Johannes, Curtis T. Rueden, Mark C. Hiner, and Kevin W. Eliceiri. 2015. “The ImageJ Ecosystem: An Open Platform for Biomedical Image Analysis.” Molecular Reproduction and Development 82 (7–8): 518–29. doi:10.1002/mrd.22489.

Schipper RG, Romijn JC, Cuijpers VM, Verhofstad AA. Polyamines and prostatic cancer. Biochem Soc Trans. 2003 Apr;31(2):375-80.

Schroeder A, Herrmann A, Cherryholmes G, Kowolik C, Buettner R, Pal S, Yu H, Müller-Newen G, Jove R. Loss of androgen receptor expression promotes a stem-

like cell phenotype in prostate cancer through STAT3 signaling. Cancer Res. 2014 Feb 15;74(4):1227-37. doi: 10.1158/0008-5472.CAN-13-0594.

Sedlmeier G, Sleeman JP. Extracellular regulation of BMP signaling: welcome to the matrix. Biochem Soc Trans. 2017 Feb 8;45(1):173-181. doi: 10.1042/BST20160263.

Seo JY, Pandey RP, Lee J, Sohng JK, Namkung W, Park YI. Quercetin 3-O-xyloside ameliorates acute pancreatitis in vitro via the reduction of ER stress and enhancement of apoptosis. Phytomedicine. 2018 Jul 20;55:40-49. doi: 10.1016/j.phymed.2018.07.011.

Shay, Jerry W., and Woodring E. Wright. 2000. “Hayflick, His Limit and Cellular Ageing.” Nature Reviews Molecular Cell Biology 1 (1). Nature Publishing Group: 72–76. doi:10.1038/35036093.

Shibue, Tsukasa, and Robert A. Weinberg. 2017. “EMT, CSCs, and Drug Resistance: The Mechanistic Link and Clinical Implications.” Nature Reviews Clinical Oncology. doi:10.1038/nrclinonc.2017.44.

Shields, J. D., I. C. Kourtis, A. A. Tomei, J. M. Roberts, and M. A. Swartz. 2010. “Induction of Lymphoidlike Stroma and Immune Escape by Tumors That Express the Chemokine CCL21.” Science 328 (5979): 749–52. doi:10.1126/science.1185837.

Shima, Yuka, Kazuhiko Nakao, Tomoki Nakashima, Atsushi Kawakami, Keisuke Nakata, Keisuke Hamasaki, Yuji Kato, Katsumi Eguchi, and Nobuko Ishii. 1999. “Activation of Caspase-8 in Transforming Growth Factor-?-Induced Apoptosis of Human Hepatoma Cells.” Hepatology 30 (5): 1215–22. doi:10.1002/hep.510300503.

Shin, D., C. H. Shin, J. Tucker, E. A. Ober, F. Rentzsch, K. D. Poss, M. Hammerschmidt, M. C. Mullins, and D. Y. R. Stainier. 2007. “Bmp and Fgf Signaling Are Essential for Liver Specification in Zebrafish.” Development 134 (11): 2041–50. doi:10.1242/dev.000281.

Shook, David, and Ray Keller. 2003. “Mechanisms, Mechanics and Function of Epithelial-Mesenchymal Transitions in Early Development.” Mechanisms of Development 120 (11): 1351–83. http://www.ncbi.nlm.nih.gov/pubmed/14623443.

Shukla, Anshuman, Nicholas M. Burton, Padma-Sheela Jayaraman, and Kevin Gaston. 2012. “The Proline Rich Homeodomain Protein PRH/*HHEX* Forms Stable Oligomers That Are Highly Resistant to Denaturation.” Edited by Pierre-Antoine Defossez. PLoS ONE 7 (4). Public Library of Science: e35984. doi:10.1371/journal.pone.0035984.

Shweiki, Dorit, Ahuva Itin, Dov Soffer, and Eli Keshet. 1992. “Vascular Endothelial Growth Factor Induced by Hypoxia May Mediate Hypoxia-Initiated Angiogenesis.” Nature 359 (6398): 843–45. doi:10.1038/359843a0.

Siddiqui, Y H, R M Kershaw, E H Humphreys, E M Assis Junior, S Chaudhri, P-S Jayaraman, and K Gaston. 2017. “CK2 Abrogates the Inhibitory Effects of

PRH/*HHEX* on Prostate Cancer Cell Migration and Invasion and Acts through PRH to Control Cell Proliferation." Oncogenesis 6 (1). Nature Publishing Group: e293. doi:10.1038/oncsis.2016.82.

Silvestri, Cristoforo, Masahiro Narimatsu, Ingo von Both, Yongmei Liu, Nicholas B.J. Tan, Luisa Izzi, Peter McCaffery, Jeffrey L. Wrana, and Liliana Attisano. 2008. "Genome-Wide Identification of Smad/Foxh1 Targets Reveals a Role for Foxh1 in Retinoic Acid Regulation and Forebrain Development." Developmental Cell 14 (3): 411–23. doi:10.1016/j.devcel.2008.01.004.

Sladek, Robert, Ghislain Rocheleau, Johan Rung, Christian Dina, Lishuang Shen, David Serre, Philippe Boutin, et al. 2007. "A Genome-Wide Association Study Identifies Novel Risk Loci for Type 2 Diabetes." Nature 445 (7130): 881–85. doi:10.1038/nature05616.

Smyth, M J, K Y Thia, S E Street, E Cretney, J A Trapani, M Taniguchi, T Kawano, S B Pelikan, N Y Crowe, and D I Godfrey. 2000. "Differential Tumor Surveillance by Natural Killer (NK) and NKT Cells." The Journal of Experimental Medicine 191 (4): 661–68. http://www.ncbi.nlm.nih.gov/pubmed/10684858.

Soufi, Abdenour, and Padma-Sheela Jayaraman. 2008. "PRH/Hex: An Oligomeric Transcription Factor and Multifunctional Regulator of Cell Fate." The Biochemical Journal 412 (3): 399–413. doi:10.1042/BJ20080035.

Soufi, Abdenour, Corinne Smith, Anthony R. Clarke, Kevin Gaston, and Padma Sheela Jayaraman. 2006. "Oligomerisation of the Developmental Regulator Proline Rich Homeodomain (PRH/Hex) Is Mediated by a Novel Proline-Rich Dimerisation Domain." Journal of Molecular Biology 358 (4): 943–62. doi:10.1016/j.jmb.2006.02.020.

Soufi, Abdenour, Peter Noy, Malcolm Buckle, Anyaporn Sawasdichai, Kevin Gaston, and Padma-Sheela Jayaraman. 2009. "CK2 Phosphorylation of the PRH/Hex Homeodomain Functions as a Reversible Switch for DNA Binding." Nucleic Acids Research 37 (10): 3288–3300. doi:10.1093/nar/gkp197.

Stahl, C P, D Zucker-Franklin, B L Evatt, and E F Winton. 1991. "Effects of Human Interleukin-6 on Megakaryocyte Development and Thrombocytopoiesis in Primates." Blood 78 (6): 1467–75. http://www.ncbi.nlm.nih.gov/pubmed/1884016.

Stepanenko, A.A., Y.S. Vassetzky, and V.M. Kavsan. 2013. "Antagonistic Functional Duality of Cancer Genes." Gene 529 (2): 199–207. doi:10.1016/j.gene.2013.07.047.

Stockinger, A, A Eger, J Wolf, H Beug, and R Foisner. 2001. "E-Cadherin Regulates Cell Growth by Modulating Proliferation-Dependent Beta-Catenin Transcriptional Activity." The Journal of Cell Biology 154 (6). The Rockefeller University Press: 1185–96. doi:10.1083/jcb.200104036.

Stone KR, Mickey DD, Wunderli H, Mickey GH, Paulson DF. Isolation of a human prostate carcinoma cell line (DU 145). Int J Cancer. 1978 Mar 15;21(3):274-81.

Su, Juan, Pu You, Jun-Peng Zhao, Shou-Long Zhang, Shao-Hua Song, Zhi-Ren Fu, Li-Wei Ye, et al. 2012. “A Potential Role for the Homeoprotein *HHEX* in Hepatocellular Carcinoma Progression.” Medical Oncology 29 (2): 1059–67. doi:10.1007/s12032-011-9989-6.

Sun Y, Wang BE, Leong KG, Yue P, Li L, Jhunjhunwala S, Chen D, Seo K, Modrusan Z, Gao WQ, Settleman J, Johnson L. Androgen deprivation causes epithelial-mesenchymal transition in the prostate: implications for androgen-deprivation therapy. Cancer Res. 2012 Jan 15;72(2):527-36. doi: 10.1158/0008-5472.CAN-11-3004.

Svane, Inge Marie, Anne-Marie Engel, Mai-Britt Nielsen, Hans-Gustaf Ljunggren, Jørgen Rygaard, and Ole Werdelin. 1996. “Chemically Induced Sarcomas from Nude Mice Are More Immunogenic than Similar Sarcomas from Congenic Normal Mice.” European Journal of Immunology 26 (8): 1844–50. doi:10.1002/eji.1830260827.

Swingler, Tracey E, Kirstin L Bess, Jing Yao, Stefano Stifani, and Padma-Sheela Jayaraman. 2004. “The Proline-Rich Homeodomain Protein Recruits Members of the Groucho/Transducin-like Enhancer of Split Protein Family to Co-Repress Transcription in Hematopoietic Cells.” The Journal of Biological Chemistry 279 (33). American Society for Biochemistry and Molecular Biology: 34938–47. doi:10.1074/jbc.M404488200.

Sylvester, Paul W. 2011. “Optimization of the Tetrazolium Dye (MTT) Colorimetric Assay for Cellular Growth and Viability.” In Methods in Molecular Biology (Clifton, N.J.), 716:157–68. doi:10.1007/978-1-61779-012-6_9.

Syverton, J T, E B Wells, H E Dascomb, and P Berry. 1950. “The Virus-Induced Rabbit Papilloma-to-Carcinoma Sequence III. Immunological Tests for Papilloma Virus in Cottontail Carcinomas*.” http://cancerres.aacrjournals.org/content/10/8/474.full-text.pdf.

Taiyab, Aftab, Anna Korol, Paula A. Deschamps, and Judith A. West-Mays. 2016. “β-Catenin/CBP–Dependent Signaling Regulates TGF-β–Induced Epithelial to Mesenchymal Transition of Lens Epithelial Cells.” Investigative Opthalmology & Visual Science 57 (13). The Association for Research in Vision and Ophthalmology: 5736. doi:10.1167/iovs.16-20162.

Takeuchi, Yoshiko, and Hiroyoshi Nishikawa. 2016. “Roles of Regulatory T Cells in Cancer Immunity.” International Immunology 28 (8). Oxford University Press: 401–9. doi:10.1093/intimm/dxw025.

Takeyama, Yoshihiro, Mitsuo Sato, Mihoko Horio, Tetsunari Hase, Kenya Yoshida, Toshihiko Yokoyama, Harunori Nakashima, et al. 2010. “Knockdown of *ZEB1*, a Master Epithelial-to-Mesenchymal Transition (EMT) Gene, Suppresses Anchorage-Independent Cell Growth of Lung Cancer Cells.” Cancer Letters 296 (2). Elsevier Ireland Ltd: 216–24. doi:10.1016/j.canlet.2010.04.008.

Tam WL, Weinberg RA. The epigenetics of epithelial-mesenchymal plasticity in cancer. Nat Med. 2013 Nov;19(11):1438-49. doi: 10.1038/nm.3336.

Tapia-Laliena MA, Korzeniewski N, Hohenfellner M, Duensing S. High-risk prostate cancer: a disease of genomic instability. Urol Oncol. 2014 Nov;32(8):1101-7. doi: 10.1016/j.urolonc.2014.02.005.

Terry S, Savagner P, Ortiz-Cuaran S, Mahjoubi L, Saintigny P, Thiery JP, Chouaib S. New insights into the role of EMT in tumor immune escape. Mol Oncol. 2017 Jul;11(7):824-846. doi: 10.1002/1878-0261.12093.

Thiery, Jean Paul, Hervé Acloque, Ruby Y.J. Huang, M. Angela Nieto, N. Ahmed, S. Maines-Bandiera, M.A. Quinn, et al. 2009. “Epithelial-Mesenchymal Transitions in Development and Disease.” Cell 139 (5). Elsevier: 871–90. doi:10.1016/j.cell.2009.11.007.

Thiery, Jean Paul. 2002. “Epithelial–mesenchymal Transitions in Tumour Progression.” Nature Reviews Cancer 2 (6): 442–54. doi:10.1038/nrc822.

Thomas, P Q, A Brown, and R S Beddington. 1998. “Hex: A Homeobox Gene Revealing Peri-Implantation Asymmetry in the Mouse Embryo and an Early Transient Marker of Endothelial Cell Precursors.” Development (Cambridge, England) 125 (1): 85–94. http://www.ncbi.nlm.nih.gov/pubmed/9389666.

Thompson, Erik W., Donald F. Newgreen, and David Tarin. 2005. “Carcinoma Invasion and Metastasis: A Role for Epithelial-Mesenchymal Transition?” Cancer Research 65 (14): 5991.1-5995. doi:10.1158/0008-5472.CAN-05-0616.

Tian, Xinrui, Zhuola Liu, Bo Niu, Jianlin Zhang, Thian Kui Tan, So Ra Lee, Ye Zhao, David C H Harris, and Guoping Zheng. 2011. “E-Cadherin/β-Catenin Complex and the Epithelial Barrier.” Journal of Biomedicine & Biotechnology 2011 (October). Hindawi: 567305. doi:10.1155/2011/567305.

Tong HB, Zou CL, Qin SY, Meng J, Keller ET, Zhang J, Lu Y. Prostate cancer tends to metastasize in the bone-mimicking microenvironment via activating NF-κB signaling. J Biomed Res. 2018 Sep 29;32(5):343-353. doi: 10.7555/JBR.32.20180035.

Topisirovic, Ivan, Biljana Culjkovic, Natalie Cohen, Jacqueline M Perez, Lucy Skrabanek, and Katherine L B Borden. 2003. “The Proline-Rich Homeodomain Protein, PRH, Is a Tissue-Specific Inhibitor of eIF4E-Dependent Cyclin D1 mRNA Transport and Growth.” The EMBO Journal 22 (3). European Molecular Biology Organization: 689–703. doi:10.1093/emboj/cdg069.

Toyoshima, M, M Nakajima, T Yamori, and T Tsuruo. 1995. “Purification and Characterization of the Platelet-Aggregating Sialoglycoprotein gp44 Expressed by Highly Metastatic Variant Cells of Mouse Colon Adenocarcinoma 26.” Cancer Research 55 (4). American Association for Cancer Research: 767–73. http://www.ncbi.nlm.nih.gov/pubmed/7850787.

Uo T, Plymate SR, Sprenger CC. Allosteric alterations in the androgen receptor and activity in prostate cancer. Endocr Relat Cancer. 2017 Sep;24(9):R335-R348. doi: 10.1530/ERC-17-0108.

Vakkila, Jukka, and Michael T. Lotze. 2004. “Inflammation and Necrosis Promote Tumour Growth.” Nature Reviews Immunology 4 (8): 641–48. doi:10.1038/nri1415.

Valluru, Manoj, Carolyn A Staton, Malcolm W R Reed, and Nicola J Brown. 2011. “Transforming Growth Factor-β and Endoglin Signaling Orchestrate Wound Healing.” Frontiers in Physiology 2: 89. doi:10.3389/fphys.2011.00089.

Valsesia-Wittmann, Sandrine, Maud Magdeleine, Sébastien Dupasquier, Elisabeth Garin, Anne-Catherine Jallas, Valérie Combaret, Alexander Krause, Philippe Leissner, and Alain Puisieux. 2004. “Oncogenic Cooperation between H-Twist and N-Myc Overrides Failsafe Programs in Cancer Cells.” Cancer Cell 6 (6): 625–30. doi:10.1016/j.ccr.2004.09.033.

van Roy, Frans. 2014. “Beyond E-Cadherin: Roles of Other Cadherin Superfamily Members in Cancer.” Nature Reviews. Cancer 14 (2). Nature Publishing Group: 121–34. doi:10.1038/nrc3647.

Vankelecom H1, Gremeaux L. Stem cells in the pituitary gland: A burgeoning field. Gen Comp Endocrinol. 2010 May 1;166(3):478-88. doi: 10.1016/j.ygcen.2009.11.007.

Venkateswaran, Niranjan, and Maralice Conacci-Sorrell. 2017. “MYC Leads the Way.” Small GTPases, November, 1–9. doi:10.1080/21541248.2017.1364821.

Vickers AJ, Ulmert D, Sjoberg DD, Bennette CJ, Björk T, Gerdtsson A, Manjer J, Nilsson PM, Dahlin A, Bjartell A, Scardino PT, Lilja H. Strategy for detection of prostate cancer based on relation between prostate specific antigen at age 40-55 and long term risk of metastasis: case-control study. BMJ. 2013 Apr 15;346:f2023. doi: 10.1136/bmj.f2023.

Villarejo, Ana, Álvaro Cortés-Cabrera, Patricia Molina-Ortíz, Francisco Portillo, and Amparo Cano. 2014. “Differential Role of *SNAIL1* and Snail2 Zinc Fingers in E-Cadherin Repression and Epithelial to Mesenchymal Transition.” Journal of Biological Chemistry 289 (2): 930–41. doi:10.1074/jbc.M113.528026.

Villarejo, Ana, Álvaro Cortés-Cabrera, Patricia Molina-Ortíz, Francisco Portillo, and Amparo Cano. 2014. “Differential Role of *SNAIL1* and Snail2 Zinc Fingers in E-Cadherin Repression and Epithelial to Mesenchymal Transition.” Journal of Biological Chemistry 289 (2): 930–41. doi:10.1074/jbc.M113.528026.

Vinagre, João, Ana Almeida, Helena Pópulo, Rui Batista, Joana Lyra, Vasco Pinto, Ricardo Coelho, et al. 2013. “Frequency of TERT Promoter Mutations in Human Cancers.” Nature Communications 4 (1): 2185. doi:10.1038/ncomms3185.

Wade, Cameron A, and Natasha Kyprianou. 2018. “Profiling Prostate Cancer Therapeutic Resistance.” International Journal of Molecular Sciences 19 (3). Multidisciplinary Digital Publishing Institute (MDPI). doi:10.3390/ijms19030904.

Wadey, K. S., B. A. Brown, G. B. Sala-Newby, P. S. Jayaraman, K. Gaston, and S. J. George. 2017. “Protein Kinase CK2 Inhibition Suppresses Neointima Formation via a Proline-Rich Homeodomain-Dependent Mechanism.” Vascular Pharmacology 99 (September 2017). Elsevier: 34–44. doi:10.1016/j.vph.2017.09.004.

Walsh, Anna Lucy, Shane W Considine, Arun Z Thomas, Thomas H Lynch, and Rustom P Manecksha. 2014. “Digital Rectal Examination in Primary Care Is Important for Early Detection of Prostate Cancer: A Retrospective Cohort Analysis Study.” The British Journal of General Practice : The Journal of the Royal College of General Practitioners 64 (629). Royal College of General Practitioners: e783–87. doi:10.3399/bjgp14X682861.

Walsh, P C, and A W Partin. 1997. “Family History Facilitates the Early Diagnosis of Prostate Carcinoma.” Cancer 80 (9): 1871–74. http://www.ncbi.nlm.nih.gov/pubmed/9351562.

Wang X, Kruithof-de Julio M, Economides KD, Walker D, Yu H, Halili MV, Hu YP, Price SM, Abate-Shen C, Shen MM. A luminal epithelial stem cell that is a cell of origin for prostate cancer. Nature. 2009 Sep 24;461(7263):495-500. doi: 10.1038/nature08361.

Wang Z, Wang Y, Zhang J, Hu Q, Zhi F, Zhang S, Mao D, Zhang Y, Liang H. Significance of the TMPRSS2:ERG gene fusion in prostate cancer. Mol Med Rep. 2017 Oct;16(4):5450-5458. doi: 10.3892/mmr.2017.7281.

Wang, Jing, Qi Liu, Jingchun Sun, and Yu Shyr. 2016. “Disrupted Cooperation between Transcription Factors across Diverse Cancer Types.” BMC Genomics 17. BioMed Central: 560. doi:10.1186/s12864-016-2842-8.

Wang, Maonan, Jingzhou Zhao, Lishen Zhang, Fang Wei, Yu Lian, Yingfeng Wu, Zhaojian Gong, et al. 2017. “Role of Tumor Microenvironment in Tumorigenesis.” Journal of Cancer 8 (5). Ivyspring International Publisher: 761–73. doi:10.7150/jca.17648.

Wang, Yifan, Jian Shi, Kequn Chai, Xuhua Ying, and Binhua P Zhou. 2013. “The Role of Snail in EMT and Tumorigenesis.” Current Cancer Drug Targets 13 (9). NIH Public Access: 963–72. http://www.ncbi.nlm.nih.gov/pubmed/24168186.

Wang, Yifan, Jingyi Liu, Xuhua Ying, Pengnian Charles Lin, and Binhua P. Zhou. 2016. “Twist-Mediated Epithelial-Mesenchymal Transition Promotes Breast Tumor Cell Invasion via Inhibition of Hippo Pathway.” Scientific Reports 6 (1). Nature Publishing Group: 24606. doi:10.1038/srep24606.

Warburg, O. 1956a. “Injuring of Respiration the Origin of Cancer Cells.” Science 123 (3191). American Association for the Advancement of Science: 309–14. doi:10.1126/science.123.3191.309.

Warburg. 1956b. On the Origin of Cancer Cells. Science (New York, N.Y.). Vol. 123. http://www.ncbi.nlm.nih.gov/pubmed/13298683.

Wheelock, Margaret J, Yasushi Shintani, Masato Maeda, Yuri Fukumoto, and Keith R Johnson. 2008. “Cadherin Switching.” Journal of Cell Science 121 (Pt 6). The Company of Biologists Ltd: 727–35. doi:10.1242/jcs.000455.

White, Eileen, and Robert S DiPaola. 2009. “The Double-Edged Sword of Autophagy Modulation in Cancer.” Clinical Cancer Research : An Official Journal of the American Association for Cancer Research 15 (17). NIH Public Access: 5308–16. doi:10.1158/1078-0432.CCR-07-5023.

WHO. 2014. “World Cancer Report 2014 [Online].”

Williams, Hannah, Padma-Sheela Jayaraman, and Kevin Gaston. 2008. “DNA Wrapping and Distortion by an Oligomeric Homeodomain Protein.” Journal of Molecular Biology 383 (1). Academic Press: 10–23. doi:10.1016/J.JMB.2008.08.004.

Wise HM, Hermida MA, Leslie NR. Prostate cancer, PI3K, PTEN and prognosis. Clin Sci (Lond). 2017 Feb 1;131(3):197-210. doi: 10.1042/CS20160026.

Witsch, Esther, Michael Sela, and Yosef Yarden. 2010. “Roles for Growth Factors in Cancer Progression.” Physiology 25 (2): 85–101. doi:10.1152/physiol.00045.2009.

Wrana, J L. 2000. “Crossing Smads.” Science’s STKE : Signal Transduction Knowledge Environment 2000 (23): re1. doi:10.1126/stke.2000.23.re1.

Wu, Jun, and Lewis L Lanier. 2003. “Natural Killer Cells and Cancer.” Advances in Cancer Research 90: 127–56. http://www.ncbi.nlm.nih.gov/pubmed/14710949.

Xiang, Wei, and Ludger Rensing. 1999. “Changes in Cell Morphology and Actin Organization during Heat Shock in Dictyostelium Discoideum : Does HSP70 Play a Role in Acquired Thermotolerance?” FEMS Microbiology Letters 178 (1). Oxford University Press: 95–107. doi:10.1111/j.1574-6968.1999.tb13764.x.

Xu, Yixiang, Dong-Kee Lee, Zhen Feng, Yan Xu, Wen Bu, Yi Li, Lan Liao, and Jianming Xu. 2017. “Breast Tumor Cell-Specific Knockout of *TWIST1* Inhibits Cancer Cell Plasticity, Dissemination, and Lung Metastasis in Mice.” Proceedings of the National Academy of Sciences of the United States of America 114 (43): 11494–99. doi:10.1073/pnas.1618091114.

Yang, A. D., E. Ramsay Camp, Fan Fan, Lanlan Shen, Michael J. Gray, Wenbiao Liu, Ray Somcio, et al. 2006. “Vascular Endothelial Growth Factor Receptor-1 Activation Mediates Epithelial to Mesenchymal Transition in Human Pancreatic Carcinoma Cells.” Cancer Research 66 (1): 46–51. doi:10.1158/0008-5472.CAN-05-3086.

Yang, Jing, and Robert A. Weinberg. 2008. “Epithelial-Mesenchymal Transition: At the Crossroads of Development and Tumor Metastasis.” Developmental Cell 14 (6). Cell Press: 818–29. doi:10.1016/J.DEVCEL.2008.05.009.

Yang, Li, Yanli Pang, and Harold L. Moses. 2010. “TGF-β and Immune Cells: An Important Regulatory Axis in the Tumor Microenvironment and Progression.” Trends in Immunology 31 (6): 220–27. doi:10.1016/j.it.2010.04.002.

Yatchenko Y, Horwitz A, Birk R. Endocrine and exocrine pancreas pathologies crosstalk: Insulin regulates the unfolded protein response in pancreatic exocrine acinar cells. Exp Cell Res. 2019 Jan 6. pii: S0014-4827(19)30002-3. doi: 10.1016/j.yexcr.2019.01.004.

Yesudhas, Dhanusha, Maria Batool, Muhammad Ayaz Anwar, Suresh Panneerselvam, and Sangdun Choi. 2017. “Proteins Recognizing DNA: Structural Uniqueness and Versatility of DNA-Binding Domains in Stem Cell Transcription Factors.” Genes 8 (8). Multidisciplinary Digital Publishing Institute (MDPI). doi:10.3390/genes8080192.

Yip, Jana, Yang Shen, Michael Berndt, and Robert Andrews. 2005. “Primary Platelet Adhesion Receptors.” IUBMB Life (International Union of Biochemistry and Molecular Biology: Life) 57 (2). Wiley-Blackwell: 103–8. doi:10.1080/15216540500078962.

Yuan, T L, and L C Cantley. 2008. “PI3K Pathway Alterations in Cancer: Variations on a Theme.” Oncogene 27 (41): 5497–5510. doi:10.1038/onc.2008.245.

Zakin L, De Robertis EM. Extracellular regulation of BMP signaling. Curr Biol. 2010 Feb 9;20(3):R89-92. doi: 10.1016/j.cub.2009.11.021.

Zeisberg, Michael, and Eric G Neilson. 2009. “Biomarkers for Epithelial-Mesenchymal Transitions.” The Journal of Clinical Investigation 119 (6). American Society for Clinical Investigation: 1429–37. doi:10.1172/JCI36183.

Zhang CZ, Leibowitz ML, Pellman D. Chromothripsis and beyond: rapid genome evolution from complex chromosomal rearrangements. Genes Dev. 2013 Dec 1;27(23):2513-30. doi: 10.1101/gad.229559.113.

Zhang, Fahao, Juwon Lee, Shan Lu, Curtis A Pettaway, and Zhongyun Dong. 2005. “Blockade of Transforming Growth Factor-Beta Signaling Suppresses Progression of Androgen-Independent Human Prostate Cancer in Nude Mice.” Clinical Cancer Research : An Official Journal of the American Association for Cancer Research 11 (12). American Association for Cancer Research: 4512–20. doi:10.1158/1078-0432.CCR-04-2571.

Zhang, Wenjun, Tatiana A Yatskievych, Robert K Baker, and Parker B Antin. 2004. “Regulation of Hex Gene Expression and Initial Stages of Avian Hepatogenesis by Bmp and Fgf Signaling.” Developmental Biology 268 (2): 312–26. doi:10.1016/j.ydbio.2004.01.019.

Zhang, Wenjun, Tatiana A. Yatskievych, Xu Cao, and Parker B. Antin. 2002. “Regulation of Hex Gene Expression by a Smads-Dependent Signaling Pathway.” Journal of Biological Chemistry 277 (47): 45435–41. doi:10.1074/jbc.M208056200.

Zheng, Lei, and Wen-Hwa Lee. 2001. “The Retinoblastoma Gene: A Prototypic and Multifunctional Tumor Suppressor.” Experimental Cell Research 264 (1): 2–18. doi:10.1006/excr.2000.5129.

Zhou, Beiyun, Yixin Liu, Michael Kahn, David K Ann, Arum Han, Hongjun Wang, Cu Nguyen, et al. 2012. “Interactions between β-Catenin and Transforming Growth Factor-β Signaling Pathways Mediate Epithelial-Mesenchymal Transition and Are Dependent on the Transcriptional Co-Activator cAMP-Response Element-Binding Protein (CREB)-Binding Protein (CBP).” The Journal of Biological Chemistry 287 (10). American Society for Biochemistry and Molecular Biology: 7026–38. doi:10.1074/jbc.M111.276311.

Zhu ML, Kyprianou N. Role of androgens and the androgen receptor in epithelial-mesenchymal transition and invasion of prostate cancer cells. FASEB J. 2010 Mar;24(3):769-77. doi: 10.1096/fj.09-136994.

Zieglschmid, Veit, Christiane Hollmann, Bertha Gutierrez, Andreas Krehan, Sepp Kaul, and Oliver Böcher. 2007. “Heterogeneous Expression of Tumor-Associated Genes in Disseminated Breast Cancer Cells.” In Anticancer Research, 27:1769–76. http://www.ncbi.nlm.nih.gov/pubmed/17649771.

Zorn, Aaron M, Karen Butler, and J.B Gurdon. 1999. “Anterior Endomesoderm Specification inXenopusby Wnt/β-Catenin and TGF-β Signalling Pathways.” Developmental Biology 209 (2): 282–97. doi:10.1006/dbio.1999.9257.

Annex

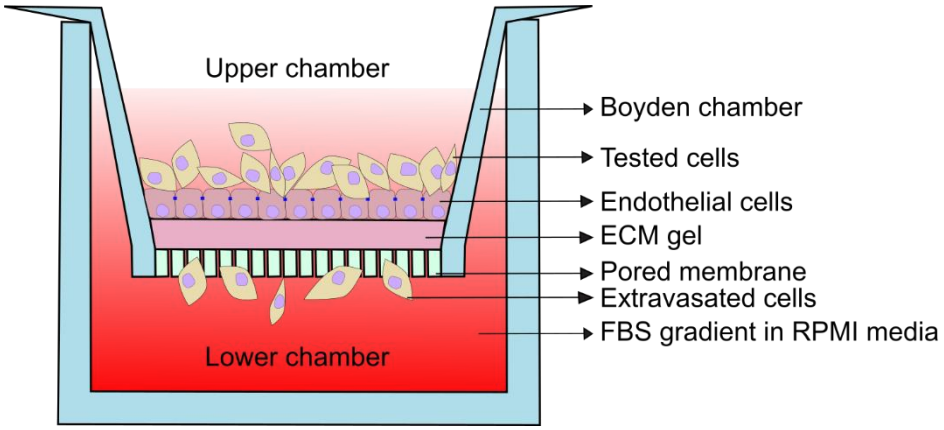

Annex 1. Extravasation assay. A Boyden chamber was placed in a 24-wells plate, EMC gel was then plated on top of the pored membrane and left to set at 37°C degrees for 1 hour. HUVEC cells were seeded in the upper chamber with Endothelial cell media (Promega) and left in a tissue culture incubator until a confluent monolayer was formed. Once the monolayer was formed, the tested cells were seeded in the upper chamber in 2% FBS RPMI media and 10% FBS RPMI media was added to the lower chamber to create an FBS gradient. The plate was incubated for 48h at 37°C in 5% CO_2.

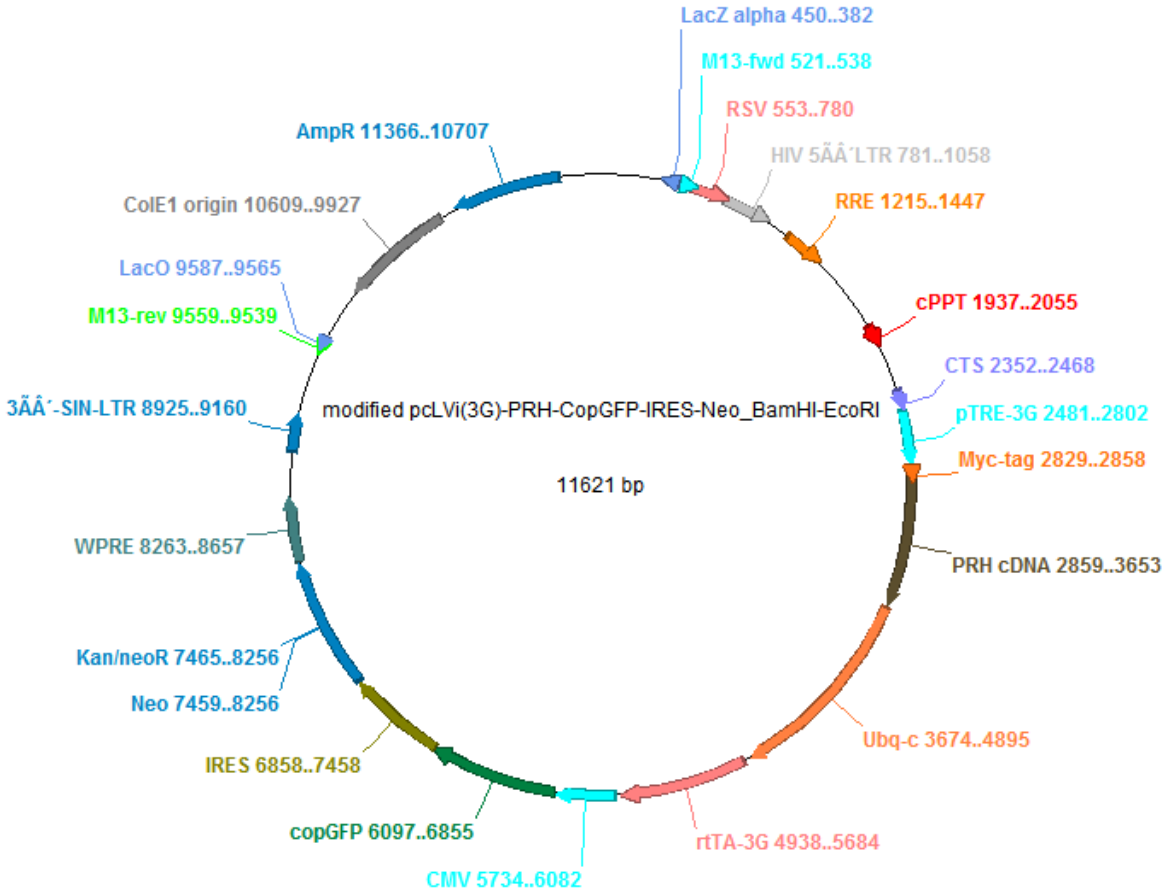

Annex 2. pCLVi(3G)-PRH-CopGFP-IRES-Neo_BamHI-EcoRI plasmid map.